ALMA MATER STUDIORUM

UNIVERSITÀ DEGLI STUDI DI BOLOGNA

Dottorato Di Ricerca in Geofisica

CICLO XXV

Settore Concorsuale di afferenza: 04/A4

Settore Scientifico disciplinare: GEO/11

PALEOSECULAR VARIATION OF THE MAGNETIC FIELD RECORDED IN PLEISTOCENE-HOLOCENE VOLCANICS FROM PANTELLERIA (ITALY) AND AZORES ARCHIPELAGO (PORTUGAL): IMPLICATIONS FOR LOCAL VOLCANIC HISTORY

Ph.D .Thesis by:

Anita Di Chiara

Tutor .

Dr. Fabio Speranza

Coordinator

Prof. Michele Dragoni

A. 2013

INDEX

PART I – INTRODUCTION AND AIM OF THE RESEARCH

1. Introduction

Reconstructing the eruptive history of active volcanoes is a primary goal of volcanological studies, in order to depict a future scenario, and determine the volcanic hazard of an area. However, the lack of outcrops, the deposit variability and discontinuity make such aim challenging. Recently, paleomagnetism, a branch of Geophysics studying the remanent magnetization preserved in rocks, has been increasingly used, combined with classical tools, to solve two volcanological problems: the correlation and dating of volcanic units. Indeed, volcanic rocks record instantaneously the magnetic field of the Earth while cooling down (below the blocking temperature), and so coeval units are expected to share similar values of the directions and intensities of the magnetization. This is the tenet for correlating volcanic units. Paleomagnetism has been successfully used as a correlating tool in several papers (Jones and McElhinny, 1966, Grommè et al., 1972, Bogue and Coe, 1981, Prévot and McWilliams, 1989, Hagstrum and Champion, 1994, Jurado - Chichay et al., 1996, Hayashida et al., 1996, Màrton et al., 2007, Finn et al., 2011).

In this study, I have first used paleomagnetic directions to correlate ignimbrites, pyroclastic density current deposits which are highly variable in volumes and diagnostic features, at the volcanic island of Pantelleria (Italy).

Furthermore, I correlated and dated volcanic cones and contemporaneous lava flows exposed at the island of Faial (Azores, Portugal).

Besides helping to correlate volcanic, paleomagnetism has been already used with success as a dating tool of Holocene volcanic units (Rutten and Wensink, 1960; Doell and Cox, 1963; Soler et al., 1984; Rolph et al., 1987; Carlut et al., 2000; Tanguy et al., 2003; Incoronato et al., 2002; Speranza et al., 2006; 2008; 2010; among many others). The "paleomagnetic dating method" relies upon the comparison between magnetic directions recorded by the studied units with the expected directional values from references Paleo-Secular Variation curves (PSV, i.e. the variation of the geomagnetic field along time, ranging from years to centuries). Therefore, the assumption behind the application of the paleomagnetism as a dating tool relies on the availability of paleomagnetic and archeomagnetic data which allow to depict the pattern of the geomagnetic field variations in a given age window. Indeed, the magnetic field of the Earth continuously changes direction and intensity, with secular swings, geomagnetic excursion (the field direction depart from the GAD - the geocentric axial dipole - direction), and abrupt intensity variations (called "spikes"). These behaviors are explained with the contribution of the non-dipole component (about 5 %) of the geomagnetic field, which can be approximated to an axial dipole for its 95% (Merrill et al., 1996; McElhinny and McFadden, 2000; and Merrill, 2010). Owing to its non-axial dipole contribution, secular variations have regional validity. Thereby, patterns of secular variation are similar over sub-continental regions, but very different from one continent to another, reflecting size and distribution of the non-

dipole sources of geomagnetic field within the Earth's core. Moreover, secular variation is not cyclic and so unpredictable, and so one of the early objectives of paleomagnetic investigations is to obtain records of geomagnetic secular variation, from the paleomagnetism of archeological artifacts (archaeomagnetism), volcanic rocks, and marine and lake sediments. Materials suitable for paleomagnetic directional studies are every material that record permanently a snapshot of magnetic field at the moment of the formation: archeological materials (e.g., ovens, pottery), sedimentary (e.g., from lakes and seas) and volcanic rocks, can be mentioned above all.

Several global datasets are available, especially for the last 10,000 years (Donadini et al., 2009; Korte et al., 2009; Korte et al., 2011), derived from archeomagnetic, sedimentary and volcanic data. Historical measurements of the geomagnetic field began around the 1,600 AD (Jackson et al., 2000), while reliable paleointensity data are available after the mathematical basis provided by Gauss, in 1835 AD. Europe and North America are well-studied areas and many PSV data exist. However, in many other regions, data distribution is uneven, scattered, or lacking entirely, especially in the Southern hemisphere and Oceans. Paleointensity data are much less difficult to obtain, therefore less paleointensity estimate are available in literature.

To this respect, one of the aims of this thesis is to fill these gaps by gathering new data, both directions and intensities, from the Atlantic Ocean, where data are sparse and scarce. Therefore, I focused on the island of São Miguel (Azores). These Islands of the Azorean Archipelago (in the middle of the Atlantic Ocean) are a suitable target since radiocarbon ages constraining the ages of several lava flows of the last 3 ka, are available. Thereby I obtained new paleodirection and paleointensity data from these well-dated lava flows and tried to reconstruct the pattern of the PSV of the paleomagnetic field of the Atlantic Ocean.

1.1 Objectives of the research

The work presented in this thesis is the result of a three year study (from January 2010 to December 2012), of which, three months were spent in the field collecting samples and mapping volcanic features and eight months were spent making laboratory measurements in the paleomagnetic laboratory of INGV, Rome. Furthermore, four months (from January to May 2011) were spent during an internship at the Scripps Institution of Oceanography (SIO, a department of the University of San Diego, California, US). The aim of the internship was to learn the laboratory techniques necessary for measuring the paleointensity of lavas and transmit these to the paleomagnetic laboratory of Rome, at INGV.

The research focused on the Pleistocene ignimbrites from Pantelleria Island, and on the basaltic plateau of lavas from São Miguel and Faial, which belong to the Azores Archipelago, located in the middle of the central-northern Atlantic Ocean.

The two main goals of this thesis are: (1) the correlation and dating of volcanic units using paleomagnetic data, and (2) to provide new PSV data for the Atlantic Ocean, where reference data are lacking.

(1) First goal concerns the application of paleomagnetism to solve volcanological problems of correlation and dating of volcanic units. Indeed, volcanic units are often difficult to correlate, because of the variability of deposits, and because different eruptive events can produce rocks with similar petrographic characteristics, and conversely rocks with different characteristic within the same eruptive event. This thesis deals two different kinds of deposits (produced by two different volcanic environments): ignimbrites, and basaltic lava flows and scoria cones.

A high-explosive volcanic environment produces several volcanic deposits, as pumice fall, pyroclastic flows, lahar deposits, to mention some of the most common. Ignimbrite is a welded pyroclastic density current deposit, characterized by a high variability of features within a same deposit, depending on several factors (e.g., distance from the eruptive center, intensity, volume, percentage of fluids versus solid particles, fragmentation of solid particles, temperature, chemistry and rheology of magma). Discontinuous geometries, volumes, and variability of facies within the same deposit strongly complicate the issue of the correlation.

I studied ignimbrites emplaced during middle-upper Pleistocene at the island of Pantelleria (in the Strait of Sicily, 36° N, 12° E) (Chapter 10). The volcanic history of the island is marked by two calderas: the youngest is well constrained in age (at 45 ka, the age of the emplacement of the Green Tuff unit), whereas the oldest, the pre-45 ka, (Caldera La Vecchia) is loosely constrained in age and the eruptive history between the two catastrophic events is still unclear. In this study, paleomagnetism was used to correlate ignimbrites from Pantelleria (Italy). The studied ignimbrites are scattered on the sea cliffs and neither well constrained in volumes nor in ages. Geochronological dating of studied ignimbrites are available, but age error bars amount to centuries and partially overlap. The overall goal of this study is to contribute to unravel the volcanic history of the island and to constrain the caldera-formation event. The study is published in the Bulletin of Volcanology (Speranza et al., 2012)

A low-explosive volcanic environment is typical of basaltic volcanoes, which encompass a broad array of explosive and eruptive processes. In terms of eruptions (driven by magmatic volatiles) explosive styles include Hawaiian to Strombolian eruptions. Any given basaltic volcano may exhibit one to the two styles at various times in its lifetime. Typically, basaltic plateaus of inter-fingered lava flows are dotted by scoria cones, and the determination of the relative and absolute chronology of events are difficult.

This volcanological setting characterizes the two further areas I studied, at islands of São Miguel (Chapter 14) and Faial (Chapter 15); the two volcanic islands are active and belong to the Archipelago of the Azores, located between a Latitude of 36 - 39° N and a Longitude of 25 - 30° W in the Atlantic Ocean.

Faial recoded historical eruptions but the rest of the Holocene history is unraveled, thus, no age-constraints nor a relative eruptive chronology had been documented so far. The aim of the part of my doctoral thesis dedicated to Faial is specifically to use paleomagnetism to reconstruct the Holocene volcanic history of the Island at the Capelo Peninsula, where the two historical eruptions took place during 1957-58 (the Capelinhos eruption) and 1672-73 (the Fogo eruption). Firstly, I attempted to use paleomagnetic technique for correlating scoria cones and lava flows, and afterwards for dating Holocene volcanic units. Keeping in mind that the use of paleomagnetism as a dating tool is limited to the availability of PSV curves valid for the studied region, and being aware that paleosecular variation curves are poorly constrained for the studied area, I focused on the island of São Miguel. The western part of the Island is a plateau of well-dated (radiocarbon dating, Moore 1990, 1991; Moore and Rubin 1991) lava flows which represent the ideal target for the paleomagnetic investigation. Therefore, I paleomagnetic sampled lava flows well-age constrained to the last 3 ka, with the purpose to reconstruct the secular variation pattern for the Azores area for this age interval.

(2) Hence, the second aim of the research is to provide new PSV data from lava flow deposits, for areas where no data are available (e.g., Oceans), and in particular from São Miguel for an age interval of the last 3 ka. The aim is to recover the paleomagnetic field pattern, both in directions and intensities (Chapters 13 and 14). Paleodirections of well-dated volcanic materials are rather easy to obtain, whereas recovering the strength of the magnetic field in the past, the paleointensity, is still a challenging matter for the low rate of success of the analyses. Many factors can bias or even invalidate analysis. For this reason much less paleointensity data exist, compared with the paleodirectional data. In order to contribute with new paleointensity data from a region where data are lacking, the Atlantic Ocean, several paleointensity experiments were run on rock samples collected at São Miguel during July 2010, and already investigated to gather paleomagnetic directions (Chapter 14). I applied a new variation of the classical methods by pre-selecting carefully suitable samples, so minimizing effects of bias. Paleointensity results had an higher success rate and represented the first paleointensity set of data for the central-northern Atlantic Ocean.

PSV data from São Miguel are published in the Journal of Geophysical Research as Di Chiara et al.(2012) and were useful for this thesis, as at Faial dating of Holocene volcanic deposits was also obtained by comparing paleomagnetic directions with expected values from the new reference curves relocated from São Miguel).

1.2 A guide to this thesis

The research presented in this Doctoral Thesis is divided in six Parts and sixteen Chapters.

Part I includes two chapters. The first Chapter contains a brief introduction to the aim of the research presented in this thesis. In Chapter 2, are resumed current challenges of Volcanology which are tackled. In Part II, the third and fourth Chapters include a brief overview of the matter of Paleomagnetism, and the methods used for gathering paleomagnetic directions (Chapter 3.3) and intensity (Chapter 4) data.

In the Part III, Chapters 5 to 7 include a brief description on how the paleomagnetic method is applied as a tool to address volcanological problems of correlating and dating volcanic deposits. The Chapter 7 is dedicated to an overview of past studies which similarly apply the paleosecular variation of the Earth's magnetic field to correlate (Chapter 6.1) and date (Chapter 7) volcanic units. In Chapter 8 the paleosecular variation curves for the Atlantic Ocean matter is faced, including an overview of the paleomagnetic data available so far.

In Part IV, Chapter 11 is dedicated to the presentation of the results from the investigation of Pleistocene ignimbrites from the island of Pantelleria (Italy), published on the Bulletin of Volcanology as Speranza et al., 2012. After an introduction to the problem faced in the chapter and a description of the geological setting of Pantelleria, follows a description of the sampling, paleomagnetic and mineralogical analyses performed, and finally the results obtained.

Part V includes four chapters. The first three, Chapter 12 to 15, focused on the new paleomagnetic data provided from the Azores Archipelago (Portugal), located in the central-northern Atlantic Ocean, where few paleomagnetic data were available before my research. The São Miguel volcanic island is the focus of this part of the investigation, where previous comprehensive geological study and radiocarbon dating allowed the paleomagnetic study of well-dated lava flows emplaced during the last 3,000 years. Analysis of the paleomagnetic directions detailed in Chapter 13 yielded the first paleosecular variation curve for the Atlantic Ocean, published on the Journal of Geophysical Research (Di Chiara et al., 2012). Chapter 14 is dedicated to the study of paleointensities performed on the same rock samples collected at São Miguel (Chapter 13). After a brief introduction to the controversial topic of recovering reliable data on the strength of the geomagnetic field, methods and experiments performed are described. Finally, new data are compared with the few available data and the first paleointensity dataset available for the region is presented. The forth Chapter of the Part IV reports on the study performed at the Capelo Peninsula (Faial, Azores, Portugal). A brief introductive part includes a discussion on the matter of correlating scoria cones and lava flows emplaced during the same eruptive events. Firstly, I used paleomagnetism to correlate scoria cones and lava flows and to unravel the number and relative chronostatigraphy of volcanic events; secondly, I provided ages to these events. The implications of this study are important for volcanic hazard estimates of this area highly populated and volcanically (and seismically) active.

Finally, in Part VI, I will conjointly discuss the main results of this thesis and making concluding remarks.

2. Studied volcanic deposits

Volcanology is a comprehensive matter that studies volcanoes, eruptive styles, volcanic products (classified for origin and emplacement characteristics), and related geological, geophysical and geochemical aspects. Efforts are focused on identifying volcano-stratigraphic units, calculate erupted volumes, infer the energy of eruptions, constrain the age and frequency of eruptive events, and finally determine the volcanic hazard of a given area. Active volcanoes are monitored continuously, by remote sensing, network of instruments for geophysical measurements, like seismographs, GPS stations for ground deformation, geochemical parameters from gases and water. The aim of monitoring is to assess whether an eruption is imminent, define the alert level (e.g., from "green" and "yellow" to "red alert" for imminent unrest; http://volcanoes.usgs.gov), and eventually plan the evacuation.

Natural disasters are never solely acts of nature (Hewitt, 1997). They are the result of natural events interacting with human lives and artificial structures. The risk of a volcanic area (Fournier d'Albe, 1979, Crandell et al., 1984) is based on the hazard evaluation (probability of an eruption occurrence), the vulnerability (the percentage of human lives exposed to a disaster), and the worth of elements exposed to risk (valuable structures and human lives). It is remarkable that direct consequences of volcanic events, as famine and tsunamis, can be more deathly events than the volcanic events itself. Therefore, a systematic assessment of volcanic hazard is vital. The first studies on the issue started only in the 1960s (Tilling, 1989), followed by the preparation of volcanic hazard maps in subsequent decades (Crandell et al., 1979 and references therein; Crandell et al., 1984, Tilling, 1989), and development of methodologies to assess volcanic hazards (Crandell and Mullineaux, 1975, Crandell et al., 1984).

The evaluation of the volcanic hazard is the product of the absolute probability of eruption occurrence, and relative probability that an area nearby the volcano is affected by the volcanic event. Criteria for calculating the relative probability are different relying on the intensity of the eruption and characteristics, morphology and the past history of the volcano. The forecasting of future eruptive scenario, recovering the intensity, the frequency of expected volcanic events, and the affected area remains the primary goal.

The basis of reconstructing the eruptive history of a volcano is to correlate past deposits, recognizing the eruption types, maximum extent of deposits, volumes, and dating eruptive episodes. Yet, this is often difficult, owing to the complexity of geometries (relation with paleo-topography, area and volumes), the variability of diagnostic characteristics, and the lack of chronological data from exposed volcanic. And it is on the chronological matter that paleomagnetism can give an invaluable contribution for both correlating deposits and yielding absolute ages.

As this work deals with correlating welded pyroclastic density currents (ignimbrites) at Pantelleria Island (Chapt. 10) and correlating scoria cones and lava flows at Faial Island (Azores Archipelago, Chapt. 14), I will briefly introduce the main features of studied deposits in the following two chapters.

2.1 Pyroclastic density current deposits

Pyroclastic density currents (Sparks et al., 1973; Walker et al., 1980; 1981; Wilson, 1986; Branney and Kookelaar, 2002) are fast-moving currents of super-heated gas and rock (collectively known as tephra), which reaches speeds moving away from a volcano of up to 230 m/s (e.g. St Helens eruption in 1980 AD, Branney and Kookelaar, 2002). The origin is typically the collapsing eruptive column during a high explosive eruption (e.g., sub-plinian, plinian). Depending on volumes involved and energy, pyroclastic flows can be valley-confined, or they may have the ability to overcome topographic barriers (up to 1,000 m high). For instance, this is the case of the Ito ignimbrite (Japan, Yokohama, 1974), or the Campanian Ignimbrite (Barberi et al., 1978), and the widely studied Taupo Ignimbrite in New Zealand (e.g., Wilson 1993).

The destructive power damages lands, demolishes towns and killed population (e.g., 1902 AD, Pelèe eruption, 29,000 victims). Pyroclastic flows deposits with complex distribution fans around vent and change aspect by veering from the vent. Thus, deposits from a same eruptive event can vary from highly dense and poorly sorted debris to well organized, sorted and less dense, similar to surges. A common feature of all ignimbrites is to form flat-topped ponds in topographic lows.

Fig. 1 – Overview of spectacular sequence of ignimbrites exposed at Cala delle Capre (Pantelleria Island, Italy).

Typical welded deposits are ignimbrites, commonly with large volumes discharged during caldera-forming eruptive events. Two different types of ignimbrite are distinguished relating to the caldera-forming event, intracaldera and extracaldera. The intracaldera ignimbrites are confined and thicker and occur during caldera's collapse; the extracaldera ignimbrites successions are characterized by a wider thickness variability and higher difference of facies (particular features). In some cases the valley ponds are connected by thin veneer ignimbrites veneers and drape interfluves (e.g., Walker et al., 1981).

Correlating welded ignimbrites is difficult, since they exhibit a wide spectrum of variability of deposit types, facies and volumes from the proximal to distal deposit from the vent within a same pyroclastic flow deposits. The pyroclastic flow tends to unload coarser particle in the proximal zone and dilute while departing from the eruptive center, changing drastically aspect and diagnostic features (e.g., particle size and type, internal structure, and subdivision of sub-units). Lithic-rich "Breccia" deposits are also variable for genesis and features; some are the basal layer of pyroclastic density current deposits, others are produced by a caldera-forming event (lag breccias, lithic-rich breccias). The correlation between breccias is also extremely difficult since different sections can show very different characteristics, as for instance the nature and dimensions of blocks and the degree of welding.

Difficulties in correlating volcanic deposits increase when eruptive frequency is high and the region has a climate favorable to the development of vegetation, which covers up field evidence and relative relations of units.

2.2 Volcanic cones and lava flows deposits

Volcanic cones are the most common volcanic landforms. Depending on the magma sources and the interaction with water, lava domes (from felsic lavas), cinder and scoria cones (from mafic lavas), and maar and tuff cones (from the interactions between magma and water) are recognized.

Briefly, cinder and scoria cones are the most common volcanic landform, formed by the accumulation of pyroclastic products, proximal to distal graded welded and/or non-welded pyroclastic fragments of different size (e.g. McGetchin et al., 1974; Valentine et al., 2005; Mannen and Ito, 2007). They accumulate around approximately circular or elongated vents, building up conical landform (truncated at the top), formed during strombolian, hawaiian, phreatomagmatic and sub-plinian eruption of low viscosity magma. The majority of the cones are monogenetic, results from a single eruptive event (Wood, 1980; Walker, 2000). Elongate monogenetic shapes can result from a single eruptive event occurring along a fissure (Breed, 1964, Wood 1980), when eruption does not rapidly localize to a single vent, or a few vents along a fissure (Riedel et al., 2003). Scoria cones are typically clustered in cone fields or distributed in a plateau (e.g. Michoacán–Guanajuato, Mexico, see Hasenaka and Carmichael, 1985), or as parasitic cones in the flank of a stratovolcano (e.g. Etna, see Corazzato and Tibaldi, 2006).

Fig. 2 – Scoria cone and lava flow field at São Miguel (Azores Islands, Portugal).

Geomorphological studies on scoria cones are based on morphometric parameter analysis from topographic maps (Wood 1980; Hooper 1995), high-resolution digital terrain models (DTM, Parrot 2007), satellite images where available (e.g. Wood, 1980, b; Thouret, 1999; Dóniz et al., 2008; Favalli et al., 2009a), and analogic models (e.g., Kervyn et al., 2012)

Geomorphological studies (including morphology and geometry) can help to determine the relative ages of cinder cones (Wood, 1980; Hasenaka and Carmichael, 1985; Hooper, 1995; Inbar and Risso, 2001; Parrot, 2007; Kervyn et al., 2012); hence, for longer period of exposure to erosional processes we expect a decreasing of aspect ratio value. Nonetheless, Insbar et al., (2011) studied the Tolbachik cinder cone field (Kamchatka, Russia), and reported that the average aspect ratio is 0.21 for recent cones and 0.16 for older cones. Those values are influenced by climatic conditions (Insbar and Risso, 2001), then they must be considered as not fully reliable.

It can be argued that the slope angle of scoria cones flanks decreases along the time, and so a steeper angle indicates a relatively younger cone and conversely a flatter slope indicates an older cone. Surprisingly, angles decreases rapidly in the first years after the eruption (e.g. Wood 1980 refers that recent cones slope on Mt Etna decreased of 10° in only 450 years).

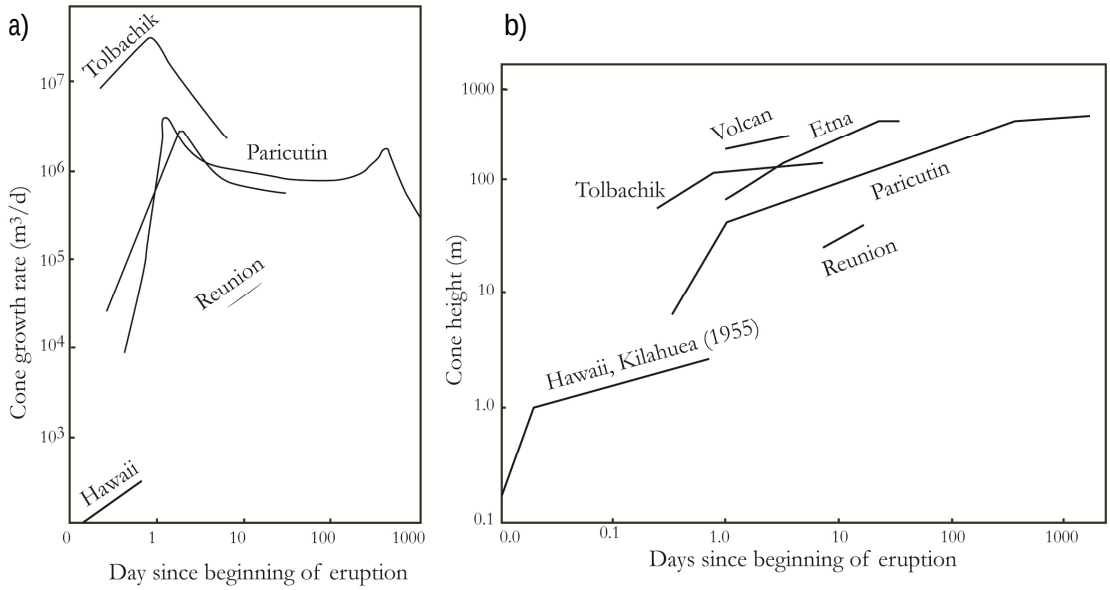

Fig. 3 - Modified from Wood (1980). a) Cone growth versus day since the beginning of eruption; b) Changes in cone height thorough an eruption, based on data from various sources. Each segment connect different stages of single eruptions

The average slope for recent cones is of 31.9°, while the old cone group has an average slope of 26°. Results are similar to the values calculated for instance in Paricutin volcano (Mexico, Wood 1980). Geomorphologic analysis of landform can be untrustworthy as some cones are of scoriae and some of spatter and some both. Those differences include eruptive styles and volumes that affect analysis.

Typically, during strombolian to hawaiian eruptions cinder cones form and lava flows extrude. Thus, cones lacking lava flows originating at their bases occur rarely (Wood 1980b). Comparison of the volumes of 35 cinder cones (CV) and associated lava flows (FV) from six different volcanic regions (San Francisco volcanic field, unpublished measurements; Etna, Italy, Wadge, 1977; Piton de la Fournaise, Reunion, Krafft and Gerente, 1977; Tolbachik, Kamchatka, Fedotov et al., 1977; Paricutin, Mexico, Fries, 1953; and Eldfell, Iceland, Self et al., 1974) reveals a strong correlation, with lava fields extending over six orders of magnitude with respect to the cone volume (Wood 1980) (Fig. 4).

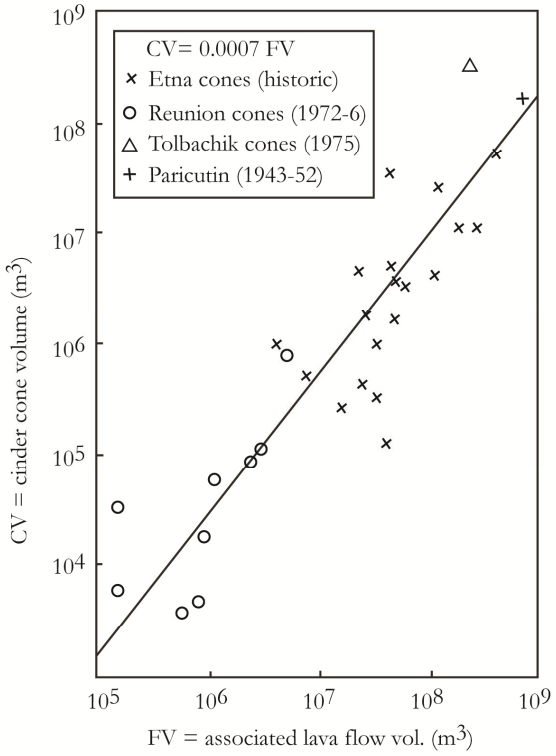

Fig. 4 - Modified from Wood (1980). Least squares relationship between volumes of the cinder cones (CV) and associated lava flows (FV), from Etna (Wadge, 1977); Reunion, Piton de la Fournaise (Krafft and Gerente, 1977), Tolbachik (Fedotov et al., 1976), and Paricutin, Mexico (Fries, 1953).

During effusive eruption frequently basaltic-like lava flows emplace; eruptions producing lava flows with different compositions, such as ultramafic and felsic lavas also occur but are less frequent (in these cases lava flows are less extended and more viscous).

Several factors influence the lava flow morphology, although the exact relations remain uncertain (Crisp and Baloga, 1990), and so the width behavior and area of extension remains difficult to predict. Some factors are topography, thermal history, rheology, and emplacement conditions, the effects of changes in volatile inventory (degassing and/or inflation) and volume, lost of inactive regions of the flow (e.g., Fink and Zimbelman, 1986; Wadge and Lopes, 1991; Griffiths and Fink, 1992; Baloga et al., 1998; Peitersen and Crown, 2000). Another important factor is the viscosity, which depends on composition, width, aspect ratio, internal structure, crystals and fluids contents. Typically, lava units overlap and inter-finger, hiding the relative chronology and change the relief, thus making more difficult the correlation issue.

Petrographic features (e.g. mineral content percentages, type and size of phenocrysts, groundmass composition, xenolite and relict mineral occurrence) are commonly used in volcanology for characterization and correlation tools. However, in the case of lava flows, slight petrographic differences may exist also in the same lava sampled at different locations from the vent (reflecting variations in effusion rate, thermal history, mechanical

fractionation, oxygen fugacity), or in different flows emplaced during a single long-lasting eruption, reflecting probably magmatic zonation (Blake, 1981). It is well known that products of individual large silicic eruptions often show chemical zonation, in which element concentrations and isotopic ratios in the magma vary over the course of the eruption. Much less documentation exists for chemical variations within basaltic systems over the duration of a single eruption or closely spaced eruptive events. For instance, during the 1733– 1736 Lanzarote eruption, the lavas changed from alkali basalts to olivine tholeiites over a period as short as two weeks (Carracedo et al., 1992). Moreover chemical characterization may not to be univocal. Monogenetic scoria cones (basaltic to andesitic) from the southern Cascades Range (North-western America) studied by Strong and Wolff (2003) exhibited large chemical variations within the products of single eruptions. Two types of chemical variations occur within cones. First, there are several cases where the chemistry of the late-stage lava flow is significantly different from that of the scoria. Second, chemical variations occur within the scoriae. The consequence is that other independent evidences are generally needed to corroborate the correlation between cinder and scoria cones with the lava flows extruded during the same eruption. Nonetheless, in terms of volcanic hazard eruptions, scoria cones and lava flows emplacements are less "dangerous" than the pyroclastic density currents. Indeed infrequently lava flow eruptions cause deaths; one notable case was the eruption of the 1977 AD events of Nyiragongo (Africa) during which lavas flew up to 80 Km/h (e.g., Tazieff, 1977, Demant et al., 1994).

PART II – METHODS

3. Introduction

The following chapter is addressed to readers who are not experienced on the use of paleomagnetism for solving volcanological problems. After a brief introduction to the matter of the Paleomagnetism, I overview methods to recover paleomagnetic directions and intensities of the past magnetic field of the Earth from magnetized rocks.

3.1 Brief introduction to Paleomagnetism

Paleomagnetism (Tarling, 1983; Tauxe, 1998; 2009; and Butler, 2004) is branch of Geophysics that studies the geomagnetic field behavior of the geological past.

The Earth's magnetic field is approximately a dipolar field (95% of the field component), resulting from an internal source (the dynamo in Earth's core mantle and crustal field) and external source (atmospheric field, and crustal induced field; Merrill et al., 1996). The non-dipolar field is that part of internal geomagnetic field, remaining after that dipole contribution has been removed. A fundamental tenet of paleomagnetism, embodied in the geocentric axial dipole (GAD) hypothesis, is that when the geomagnetic field is averaged over long time scales (at least 10 ka) only the axial-dipole contribution can be considered important when investigating sedimentary rocks with sufficiently slow sedimentation rates. On the contrary, the aim of this thesis is the study of the geomagnetic field variation on smaller timescales, i.e. paleosecular variations, recorded on magnetized volcanic rocks where the geomagnetic field is locked instantaneously at the time of cooling.

Paleomagnetism has widespread applications for a variety of disciplines: the study of atmosphere and biosphere interactions, the study of the early history of the Earth (e.g., Tarduno et al., 2006), the physics of the Earth's interior (e.g., Christensen and Wicht, 2007), tectonics (e.g., Torsvik et al., 2008), geologic applications from magnetostratigraphy, biostratigraphy (e.g., Opdyke and Channell, 1996), and archaeomagnetic dating (e.g., Lanos, 2004; Pavòn-Carrasco et al., 2011). Our understanding of the geomagnetic field is based on data obtained from historical measurements (e.g., Jackson et al., 2000; Jackson, 2003), archaeological and geological samples (e.g., Korte and Constable, 2011) and numerical simulations (e.g., Glatzmaier and Roberts, 1996).

Paleomagnetism entails the assumption that the magnetization "frozen" during rocks formation is parallel to the contemporaneous geomagnetic field. The original magnetization can be stable along geological times, although may be exposed to other magnetic field, and undergo thermal, chemical processes that can overprint or even

remove the primary magnetization, secondary remagnetizations. Secondary magnetizations can be partial or total, deleting completely the original magnetization.

The essential paleomagnetism theory was presented by the Noble prize winner Louis Néel (1949, 1955), who explained how the ancient magnetic field (B_{anc}) might be preserved in rock's magnetic memory.

The Néel relaxation theory (1949) defines the relaxation time (τ) by equation which relates τ to volume of single domain grains (v), the anisotropy constant (k), the absolute temperature (T), the microscopic coercitive force in single domain grains (h_c) and the saturation magnetization of the ferromagnetic material (j_s):

$$\tau = \frac{1}{\mathrm{C}} \exp\left(\frac{v\, h_c\, j_s}{2\mathrm{k}T} \right)$$

The Nèel theory is valid for the single domain grains (SD, i.e. of ~ 0.03 μm with a single and stable domain). Depending on the Temperature, the relaxation time can overcome the geological time or be unstable over minutes (as the T closes in the unblocking temperature of magnetic grains the relaxation time decrease exponentially).

The capability of rocks to record a stable remanent magnetization depends on the relaxation time, as stated by the Néel theory (1949, 1955), depending in turn from temperature, and volume of magnetic grains (Butler, 2004; Tauxe, 2009). A primary magnetization is imparted during rock formation (consolidation, diagenesis, cooling, etc) by means of several acquisition mechanisms (detrital, thermal, chemical magnetization), based on the assumption that the original magnetization is parallel to the Earth's Magnetic field at the time of the formation. Nevertheless, rocks can acquire secondary magnetizations or be remagnetized entirely after acquisition for primary magnetization. The Natural Remanent Magnetization (NRM) is the remanent magnetization present in a rock sample prior to laboratory treatment, and depends on the geomagnetic field and the geological processes during rock formation. NRM is typically composed of different component; a primary component is the component acquired during the rock formation, and secondary components are acquired subsequently, altering or even obscure the primary NRM. The main forms in which the NRM is recorded are the TRM, DRM and CRM. The Thermo Remanent Magnetization (TRM) acquired during cooling from high temperatures above Curie Temperatures (temperature above which the magnetic material retain a remanent magnetization; it changes with respect to magnetic minerals). The Detrital Remanent Magnetization (DRM) is acquired during the accumulation of magnetic minerals during sedimentation. The Chemical Remanent Magnetization (CRM) is acquired during the formation (precipitation of ferromagnetic minerals from a solution) of magnetic minerals within a rock, or the alteration of pre-existent magnetic minerals.

Secondary component of remanent magnetization should be detected and rejected (as the Isothermal and Viscous Remanent Magnetizations - IRM and VRM).

For the interpretation it is critical to isolate the primary and secondary magnetizations and eventually their post-depositional tilting, or folding and other geological processes overprinting the original component of remanent magnetization. For further details, see reference books by Butler (2004) and Tauxe (2009).

3.2 Paleomagnetic sampling

This thesis deals with the study of volcanic rocks. In fact, sediments tend to average out secular variation, depending on sedimentation rate and post-depositional processes, which is at odds with the aims of this work. The most suitable materials for paleosecular variations studies are those recording a TRM, as volcanic rocks and archeomagnetic artifacts.

It is worth to briefly explain the sampling procedure (standard in many paleomagnetic studies), and the laboratory protocols used in this thesis.

Samples were drilled from outcrops using a petrol-powered drill cooled by water, diamond tipped, one-inch internal diameter drill bits. Cores were spaced widely through the outcrop and only fresh surfaces, where evidence of alteration was absent, were drilled.

The total number of samples usually collected for each site is 15 to 20. Cores were oriented (Fig. 5, 6) in-situ with a standard paleomagnetic orienting tool fitted with a magnetic compass. To overcome the magnetic deviation caused by the magnetization of the sampled volcanic body itself or other anomalies (i.e. strongly magnetized volcanic, metamorphic or intrusive rocks), a sun compass was also systematically used for core orientation. Indeed, it has been largely demonstrated that a magnetic compass can deviate up to 10-15° from the real orientation value because of the presence of a strongly magnetized rocks (i.e., magnetic declination, see discussion in paragraph “source of bias” (Chapt. 7.2) (Baag et al., 1995; Valet and Soler, 1999; Tanguy and Le Goff, 2003; Lanza and Zanella, 2006; Speranza et al., 2006).


b)


c)

Fig. 5 – During sampling paleomagnetic cores in São Miguel with the colleague Massimiliano P., site Sml03 (a) and the dangerous but worthwhile site Sml26 (b); Fabio S. sampling the first site at Fayal, Fay01 (c) with Adriano P. and J.Pacheco.

The total number of samples usually collected for each site is 15 to 20. Cores were oriented (Fig. 6) in-situ with a standard paleomagnetic orienting tool fitted with a magnetic compass. To overcome the magnetic deviation caused by the magnetization of the sampled volcanic body itself or other anomalies (i.e. strongly magnetized volcanic, metamorphic or intrusive rocks), a sun compass was also systematically used for core orientation. Indeed, it has been largely demonstrated that a magnetic compass can deviate up to 10-15° from the real orientation value because of the presence of a strongly magnetized rocks (i.e., magnetic declination, see discussion in paragraph "source of bias" (Chapt. 7.2) (Baag et al., 1995; Valet and Soler, 1999; Tanguy and Le Goff, 2003; Lanza and Zanella, 2006; Speranza et al., 2006).

Fig. 6 - a) Orienting in-situ the core using magnetic and sun compasses; b) mark the azimuth of the core; c) extract the core; d) mark the azimuth and the direction; and e) an example of paleomagnetic samples extracted from one paleomagnetic site and marked with the name and the in situ orientation.

3.3 Recovering paleomagnetic directions from samples

Sampled cores were cut into standard two-centimeter long samples. All the paleomagnetic analyses were conducted inside a magnetically shielded laboratory, to avoid influences of the geomagnetic field. All the analysis presented in this study were performed in the Laboratory of Paleomagnetism of the INGV- Rome (Italy), except for the paleointensity analyses, which were conducted at SIO (La Jolla, CA, US). To recover paleomagnetic directions, samples were progressively demagnetized by Thermal (TH) or Alternating Field (AF) demagnetization techniques. The TH demagnetization process consists of heating sample at progressively higher temperature steps (from room temperature to 600°C), and measuring at each step the vector of the magnetization (direction and module) after cooling at zero field. The magnetization is gradually removed and the NRM is vectorially investigated. In this process, magnetic minerals with lower blocking temperatures that usually hold magnetic overprints are demagnetized at lower temperatures leaving only a remanence contribution from magnetic minerals with higher unblocking temperatures. In other words, the contribution of low unblocking temperature magnetic grains is eliminated by increasing the temperature to overcome the blocking temperature of the magnetic materials. The limitation of the TH-cleaning demagnetization is that the heating and cooling process may cause the alteration of magnetic minerals and the creation of new magnetic minerals through thermochemical alteration of unstable phases. Similarly, in AF- demagnetization technique, a sample is subjected to progressively higher alternating magnetic fields (from 0 to 120 μT) and the magnetization vector is measured at every step after demagnetization (as in the TH method). Magnetization eliminated in the 10 – 20 μT coercivity range is usually related to the long-lasting overprint of the normal-polarity field activity during the Bhunes Chron (the viscous components). Higher coercivity magnetization components are generally related to magnetizations imparted on the rock at the time of formation; typically, this component is more stable and called characteristic remanent magnetization (ChRM).

4. Recovering paleomagnetic intensity, the theory

Paleomagnetic measurements have shown that along geological time, ranging from a few years to millions of years, the geomagnetic field has undergone continuous changes both in direction and intensity. Although at present we have an accurate assessment of the geomagnetic field's variability with time, yet, the information on the strength of the field in geological past, the paleointensity, is relatively sparse and imprecise. Compared to the paleo-direction information, determining the paleointensity is more difficult because of complicated theory and experimental procedure.

In principle, the technique to recover information about past intensities of the geomagnetic field is straightforward. Hence, it is possible to determinate the intensity of the ancient magnetic field assuming that the intensity of the thermoremanence acquired by a rock (M_{TRM}) is linearly correlated with the magnitude of ancient field (B_{anc}).

The Nèel' s equation describes the dependence of TRM on various parameters including H (the strength of the magnetizing field) in the limited case of Single Domain grains (at room temperatures):

$TRM\ (20°C) = N\ (T_B) \nu\ J_s(20°C)\ \tanh(b)$

where T_B is the blocking Temperature of the magnetic grain; N is a term that describe the shape distribution; ν is the volume of the SD grains; J_s is the saturation magnetization of the ferromagnetic materials; kT= thermal energy; and $b = \nu\ J_s(T_B)H\ /\ k\ T_B$

For typical values of parameters, b is << 1. This provides a useful simplification because tanH (b) >> b for b << 1, and the equation above can be simplified

$TRM(20°C) \sim N(T_B)\ \nu\ j_s(20°C)\ H(b)$

Thus, TRM depends linearly on the strength of the magnetic field present during cooling through the blocking temperature (T_B).

The magnetic field dependence can be explicated by combining terms depending on grain-size (v) and shape distribution (N), blocking temperature (Tb), and ferromagnetic properties (e.g., N(TB), $j_s(T_B)$,etc.) into a proportionality constant, α.

$\alpha = \nu\ j_s(20°C)(\nu\ j_s(20°C)H(b)/\ kT_B$ and the equation (8.2) becomes:

$TRM = \alpha H$

This relation states that exists a linear correlation between the TRM acquired during cooling in the geomagnetic field and the intensity of the field H.

In principle, it is possible to determine the ancient intensity of the field (H_{paleo}), if the linear correlation exists: $TRM_{paleo}=\alpha_{paleo}B_{paleo}$

Indeed all the parameters involved in the formula, are measurable.

In theory, it is possible to reproduce in a laboratory the acquisition of a TRM_{lab} by heating and cooling a sample under a known H_{lab}. If the linear relation exists the TRM_{lab} acquired is related with the H_{lab} by a constant α_{lab}. More the H_{lab} is similar to H_{paleo}, more the TRMs acquired are similar, and the proportionality constants α_{lab} and α_{paleo} are expected to be similar. Indeed, for $\alpha_{lab} \cong \alpha_{paleo}$ and the TRM_{paleo} and TRM_{lab} are known , the H_{paleo} can be easily determined.

$H_{paleo}= (TRM_{paleo}/TRM_{lab})H_{lab}$

The theory outlined is relatively simple. Unfortunately, in practice, many causes of concern occur in the attempt of recovering paleointensity (Tauxe, 2009):

1. The proportionality constant α may not be constant when the NRM acquisition is not linear.
2. Weathering, chemical alterations, post-depositional processes, and alteration during laboratory procedure may cause alteration of the capacity of the specimen to acquire remanence (during lab experiments).
3. The multi domain (MD) and Pseudo Single Domain (PSD) grains behavior is not fully predictable, and so the original NRM is difficult to reproduce. Hence blocking (T_b) and unblocking (T_{ub}) temperatures may not be the same (reciprocity of the T_b and T_{ub}).
4. If the remanence is anisotropic and the field laboratory is not parallel to the paleofield direction, the α_{lab} and α_{paleo} are different. Indeed the proportionality constant is a tensor and in this case the scalar approximation fails.
5. The TRM is the only remanent magnetization that is suitable for paleointensity experiments since it can be reproduced in laboratory (thus excluding all the others natural magnetization, as DRM and CRM).
6. The cooling rate of a specimen can be unduly large and it cannot be reproduced in the laboratory, raising differences between the α_{lab} and α_{paleo}.

All these factors invalidate the theory and laboratory experiments are demanded to evaluate the changes of the capability of a rock to acquire remanent magnetization.

The suitable rocks for the paleointensity experiments are those that can acquire a stable TRM during cooling under Curie Temperatures, even under low geomagnetic field (not lower than 1 μT); and therefore the only candidates for absolute paleointensity measurements are igneous and metamorphic rocks, baked sediments, and heated archeomagnetic artifacts (potteries, bricks, ceramics…).

Hence, most absolute paleointensity studies have been carried out on basalt lavas (Pan et al., 2002) because their magnetization processes are relatively well understood, as well as on archeomagnetic materials. Basaltic glass has been recently proven as an excellent material in recording the magnetic field as it quenches very rapidly (e.g., Ferk et al., 2008). Also the quenched part of a lava flow deposit has yielded excellent results (Cromwell et al., 2011).

As a magnetic grain size increases (Carlut and Kent, 2002), and/or MD grains are predominant carrier of the remanent magnetization (Levi, 1977; Fabian 2001; Riisager and Riisager 2001; Leonardht et al., 2004; Selkin et al., 2007), the TRM shows a non-linear behavior (Kletetschka et al., 2006; Yu et al., 2004; Yu and Tauxe, 2005; Shaar et al., 2011). To detect changes in capacity of the specimen to acquire a TRM, and therefore to verify the assumption of the linearity, several experiments have been proposed.

The aims of the experiments are to test:

- if the TRM has a linear function with the H_{lab};
- whether the NRM has a single component;
- if mineralogical changes had occurred during the laboratory experiments (in the case of TT family);
- if the reciprocity of blocking and unblocking temperature is verified;

The basic idea of the experiments is to progressively replace a TRM in laboratory to the natural TRM and at each step of Temperature to check whether the capability of the rock to record the magnetic field at the given T step has changed or not.

4.1 Absolute paleointensity experiments: the Thellier family

The absolute paleointensity experiments can be ascribed to three families of experiments:

(i) the Thellier and Thellier protocol (Konigsberger, 1938; Thellier and Thellier, 1959), afterwards improved by adding a pTRM checks that have been introduced to monitor the presence of non-ideal magnetic grain sizes (Shcherbakova and Shcherbakov, 2000; Riisager and Riisager, 2001; Krasa et al., 2003). Correction for fabric and/or shape anisotropy and cooling rate effects can be carried out (Fox and Aitken, 1980).

(iii) Shaw techniques (Shaw 1974),

(iv) other approaches: Microwave (Walton et al., 1992) and (e.g., multispecimen approach by Dekker and Böhnel 2003)

Additional description of paleointensity methods has been given by Selkin and Tauxe (2000), Valet (2003), Donadini et al. (2007) among many others. In Donadini et al. (2007) are listed altogether 17 different classifications (Fig.7.), that comprise all the several subtypes of the three main groups of pi experiments. Since the most accepted and widely used methods to recover paleointensity is the Thellier method, it was used in this thesis and described in the following paragraph, skipping the other methods.

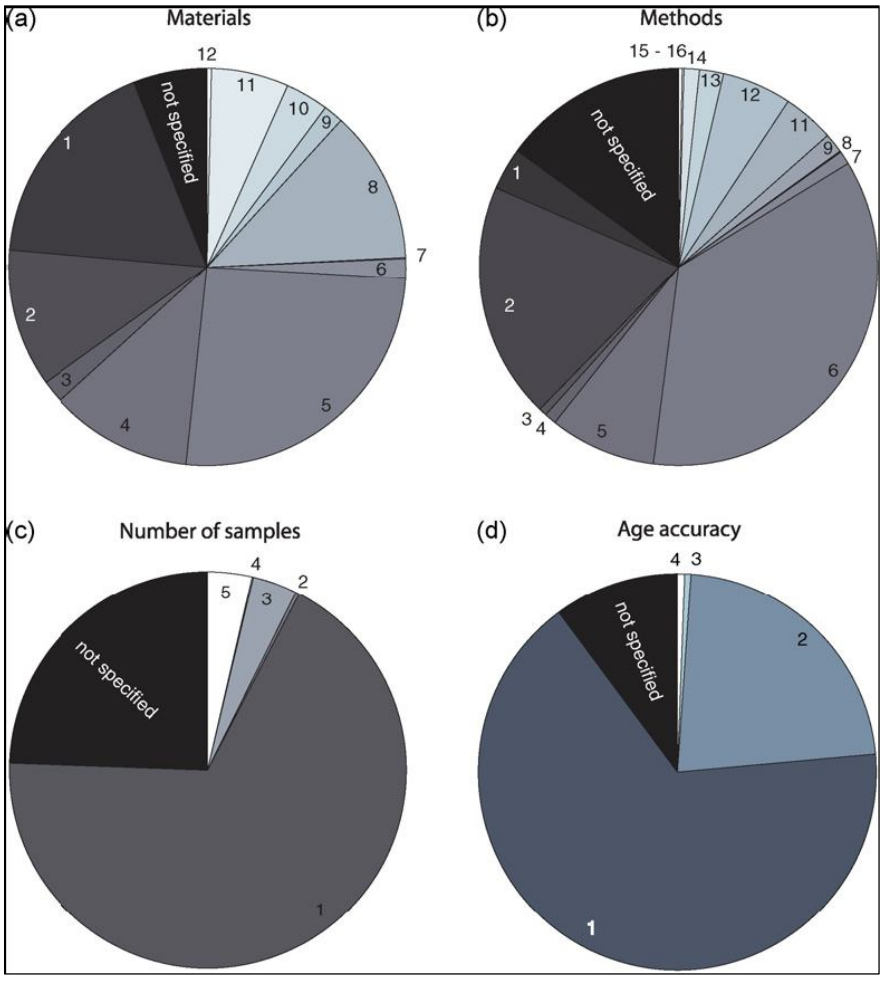

Fig. 7 - Figure from Donadini et al., (2007) (a) The distribution of materials during the last 12,000 years: 1 = bricks, 2 = clay, 3 = tiles, 4 = lava, 5 = pottery, 6 = sun-dried objects, 7 = porcelain, 8 = ceramic, 9 = kiln, 10 = oven or hearth, 11 = miscellaneous archaeological objects, 12 = iron slag, 13 = baked rocks. (b) The percentage of methodologies used for determining paleointensities on materials younger than 12,000 years. 1 = Thellier/Coe, pTRM check, anisotropy and cooling rate corrections; 2 = Thellier/Coe, pTRM check, anisotropy or cooling rate correction, 3 = Thellier/Coe, pTRM check, NRM oriented along laboratory field (*B*lab), cooling rate correction, 4 = Thellier/Coe, pTRM check, NRM oriented along B_{lab}, no cooling rate correction, 5 = Thellier with pTRM checks, no corrections, 6 = Thellier without checks, no corrections, 7 = Shaw, cooling rate correction and anisotropy correction, 8 = Shaw, anisotropy or cooling rate correction, 9 = Shaw, NRM oriented along B_{lab}, cooling rate correction, 10 = Shaw, NRM oriented along B_{lab}, no cooling rate correction, 11 = Shaw, no corrections, 12 = other techniques, 13 = microwave, pTRM checks, 14 = microwave, no pTRM checks, 15 = Thellier/Coe, alteration correction, no cooling and no anisotropy correction, 16 = Thellier without checks, NRM parallel to B_{lab}. (c) Distribution of the amount of samples per intensity determination: 1 = only one sample measured, 2 = two samples and standard deviation higher than 10%, 3 = two samples and standard deviation lower than 10%, 4 = at least three samples with standard deviation higher than 10%, 5 = at least three samples with standard deviation lower than 10%. (d) Age dating error distribution related to the intensity determinations: 1 = accuracy between ±100 years, 2 = accuracy between ±500 years, 3 = accuracy between ±1000 years, 4 = accuracy worse than 1000 years.

By far, the Thellier family of experiments is the most accepted and widely used method to recover paleointensities. The first attempt of progressively replace the NRM with a laboratory TRM has been proposed by Konigsberger, (1938). The laboratory protocol was introduced by Thellier and Thellier (1959) and involves a double-heating process:

1. Firstly the samples are heated to a Temperature T_i (> T (20°C), and below the Curie Temperature, Tc); after cooling to room temperature (at Zero field) the remaining TRM is measured. The difference between the two TRMs (the TRM_{paleo} and the $pTRM_i$ measured) represents the amount of TRM ($pTRM_i$) carried by with a blocking Temperature minor to T_i.
2. Secondly the samples are re-heated to a Temperature T_i and cooled down in a known magnetic field. The pTRM acquired is measured.
3. The two steps above are repeated until the T_c is reached and the magnetic remanence is virtually annulled.

Behind the double-heating experiment, three laws are assumed to be verified for this method to work (e.g., Yu et al., 2004):

i) "The law of independence of the pTRMs" states that each pTRM acquired in a single heating step is independent to those acquired in others pTRMs acquired at different temperatures.

ii) "The law of additivity of the pTRMs" states that the sum of all the pTRMs acquired during different T intervals (below the Tc) is equal to a single pTRM acquired in the union of these temperature intervals.

iii) "Linearity of TRM" says that the TRM acquired must be linearly proportional to the field within which it is acquired.

Many modifications has been developed to improve and to reduce the drawbacks of the original Thellier method. Indeed, there are several derivatives the Thellier experimental protocol (see reviews by e.g., Valet, 2003; Yu et al., 2004, and Tauxe and Yamazaki, 2007), all are based on similar basic assumptions and analyzed using Arai plots.

The paleointensity results are plotted as TRM remained vs. pTRM gained in the Arai plot (Nagata et al., 1963).

Tauxe and Staudigel (2004; see also Ben-Yosef et al., 2008) and then Yu et al., (2004) proposed a new laboratory protocol called "IZZI", by combining the Aitken (1988; in-field, zero-field; IZ) and Coe (1967; zero-field, in-field; ZI) techniques and pTRM tail check methods. The IZZI protocol of paleointensity method was experimentally tested by Yu and Tauxe (2005) and Shaar et al., (2010). The advantages are that it can easily detect the angular dependence resulting from the undemagnetized portions of partial thermoremanent magnetization (pTRM) tails; it provides a quantitative estimate for the consistency of the outcome between IZ and ZI step; and it is quicker because the extra "pTRM tail check" step becomes unnecessary, minimizing the number of heating steps IZZI.In the Fig 8 the magnitude of the NRM remaining after each step is plotted versus the pTRM gained at each temperature step. Closed symbols are zero-field first followed by in-field steps (ZI) while open symbols are in-field first followed by zero field (IZ). Triangles are pTRM checks

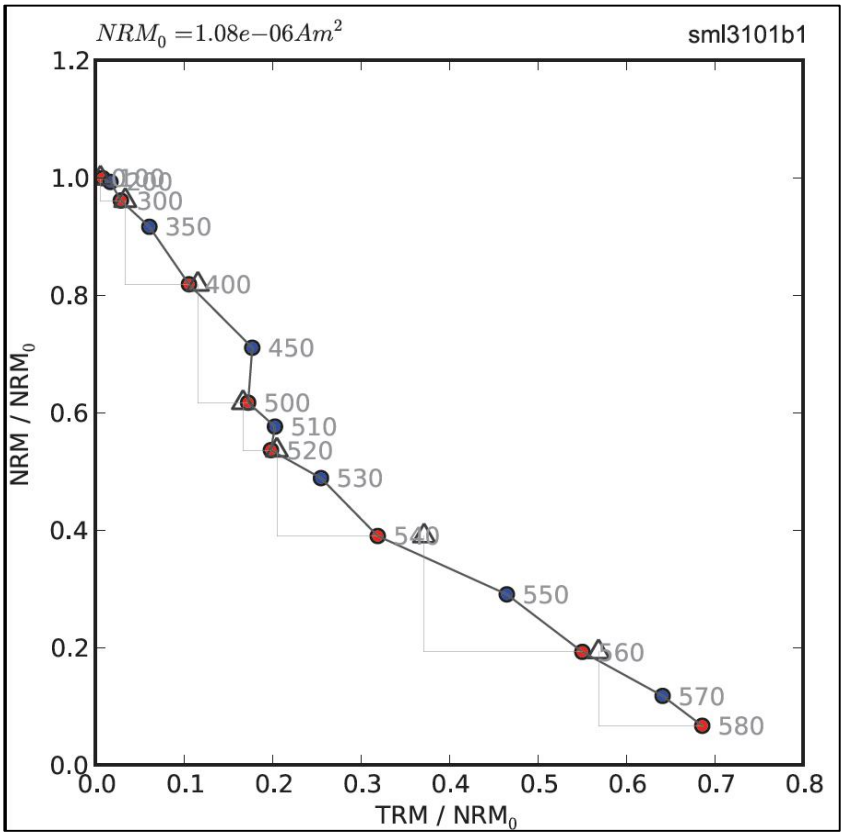

Fig. 8 - An example of Arai plot (specimen Sml3101b1 from São Miguel (Azores Islands) where the magnitude NRM remaining/the intial NRM is plotted versus the TRM gained/the initial NRM. Blue dots are the in-field step (IZ), red dots are the zero-field step (ZI) and triangles are the pTRM check steps.

In this research project, among the great number of methods available, the IZZI protocol was chosen for paleointensity experiments.

Beyond the matter of choosing a reliable method, it is critical to include a test of the reliability of the data.

4.2 Source of bias in paleointensity results

The paleointensity is commonly computed as the best fit line slope of all points in Arai plots (York, 1966).

The majority of paleointensity experiments result in curved Arai plots rather than straight lines.
The presence of MD grains is considered the main responsible of the different Arai plot shapes: concave or convex and 'S-shaped' curves (see Levi 1977; Xu and Dunlop, 1995, 2004; Biggin and Thomas, 2003; Coe et al., 2004; Fabian, 2001; Leonhardt et al., 2004), and also zigzagged (e.g. Ben-Yosef et al., 2008a; Tauxe and Staudigel, 2004; Yu et al., 2004; Yu and Tauxe, 2005).
According to Tauxe and Staudigel (2004), the different shapes in Arai plots (S-shaped, Zig-Zagged, concave or convex) depend both on the MD grains effect (of 4% or greater) and on the difference of direction between the NRM with respect to the laboratory field applied during Thellier experiments (creating the zig-zagging shape). When the NRM is perpendicular to the laboratory field the deviation is high.
Shaar et al. (2011) suggested (in agreement with Tauxe and Staudigel 2004) that the curvature of the Arai plot is systematically dependent on the angle between the field used in the paleointensity experiment and the field in which the NRM was acquired. According to Shaar et al., (2011) straight-line Arai plot occurs when the two fields are parallel and similar, and leads to a realistic result ("true slope"). Convex curves occur when the laboratory field is parallel but stronger than the NRM field. Concave curves occur randomly in all the other cases and yield different results, often far from the "true slopes". Zig-zagged patterns occur when the angle between B_{TRM} and B_{NRM} increases.
Moreover, they argued that MD grains occurrence is not the only source for non-straight lines in Arai plots. Low temperature steps tend to be overprinted by viscous remanent magnetization (VRM), and high-temperature steps are often biased by irreversible alterations of the magnetic mineralogy occurring during the repeated heating in the laboratory.
Additionally, secondary re-magnetizations can overprint the original NRM. For this reason NRM multi-components are discarded during the pre-selection of suitable data.
Magnetite with a very narrow range of unblocking temperatures appears to be the best situation to obtain suitable determinations of paleointensity with large success rate (Herrero-Bervera and Valet, 2009).

Depending on the source of bias, results can be corrected by the AARM correction, for the Anisotropy of the Anysteretic Remanent Magnetization (e.g. Aitken et al., 1981) and the Cooling rate correction (Fox and Aitken, 1980, McClelland-Brown, 1984; Bowles et al., 2005).

4.3 The quality of paleointensity estimates

Wealth of statistic parameters are currently used to test the reliability, and determinate the acceptance or discard paleonintensity results of experiments.

For the Thellier's protocol, Coe et al. (1978) have introduced results the first set of parameters. Subsequently, the issue has been readdressed by Selkin and Tauxe (2000) and Kissel and Laj (2004).

1. The Deviation of the Angle (DANG, Tauxe and Staudigel, 2004) is the angle between a component of the NRM and the line anchored to the origin. The more little is the angle, the more small is the parameter.
2. The Maximum Angle of Deviation (MAD, Kirschvink, 1980) represents the scatter of the NRM steps from the best-fit line.
3. The best-fit slope (b) for the data on the Arai plot, and its standard error σ (York, 1966; Coe et al. 1978), represent the best estimate of the pi.
4. The parameter β indicates the" scatter", the standard error of the slope σ (assuming uncertainty in both the pTRM and NRM data) over the absolute value of the best-fit slope |b| (Coe et al. 1978).
5. The remanence fraction (f) was defined by Coe et al. (1978) as the ratio of the NRM fraction and the component of the NRM intersection, which is the fraction of the NRM component used in the slope estimation: $f = \Delta y_T / y_0$, where ΔyT is the length of the NRM/TRM segment used in the slope calculation. This parameter works with the SD grains and also it can be misrepresented in the case of a multi-component NRM. So it has been modified by Tauxe and Staudigel (2004), and called f_{vds}. The parameter represents the fraction of the total NRM used for calculating the best-fit slope (b), estimated by vector difference sum (VDS, which stretch the different components of the NRM, if exist, by the sum of the vector difference at each demagnetization step). The f_{vds} is small when the NRM has different components.
6. The parameter δ_i expresses the difference between the original pTRM at a given temperature step and the pTRM check. It can result from experimental noise or from alteration during the experiment. Selkin and Tauxe (2000) normalized the maximum δi value within the region of interest by the length of the hypotenuse of the NRM/pTRM data used in the slope calculation.
7. In many cases, it is useful to consider the trend of the pTRM checks as well as their maximum deviations. Tauxe and Staudigel (2004) use the sum of these differences. This difference can be normalized by sum the pTRM acquired by cooling from the maximum temperature step used in the

slope calculation to room temperature. This parameter is called the Difference RATio Sum or DRATS. It results from the δ_i parameter normalized for the vector difference sum (VDS) of the NRM steps.

8. Cumulative DRAT (CDRAT), is defined as the sum of all the DRATs.
9. The Maximum Difference (MD) can be calculated if the pTRM tail check (when performed); it is the absolute value of the difference between the original NRM measured at a given temperature step and the second zero field step (the pTRM tail check). It is expressed as a percentage when normalized by the VDS of the NRM (MD%).
10. The Zig-Zag (Z) parameter explores the shape of the Arai plot when the IZZI protocol is adopted. The Zig-Zag (Yu et al., 2004) results from different slopes during the alternating of the IZ and ZI steps.
11. The "gap factor" g (Coe et al. 1978) penalizes uneven distribution of data points and it is: the weighted mean of the gap (Δy_i vertical component) and the number of data points N along the segment $g = 1 - \bar{\Delta}\bar{y}/\Delta y_T$, where $\Delta\bar{y}$ is given by : $\bar{\Delta}\bar{y} = \frac{1}{\Delta y_T} \sum_{i=1}^{i=N-1} \Delta y_i^2$,
12. The Coe quality index q (Coe et al. 1978) combines the standard error of the slope, the NRM fraction and the gap factors by: $q = \beta f g$. This parameter decreases when the spacing of the data is less uniform.
13. The γ parameter (Ben Yosef et al., 2009; Tauxe 2009) is used in the slope calculation. It is defined as the angle between the applied field and the best-fit line through the pTRM data at the maximum pTRM temperature. If this exceeds a few degrees, it is advisable to perform some test for the TRM (or ARM) anisotropy.
14. The "k" parameter recently proposed by Paterson (2010, abstr. AGU) to quantify the curvature of data points on an Arai plot, a feature commonly associated with MD behavior.

Kissel and Laj (2004) introduced a new set of paleointensity criteria (PICRIT-03) and listed threshold values of acceptability, or cut-off criteria. They pointed out that many parameters are more sensible to the laboratory noise and the laboratory field strength than expected. Before this study the choice of selection criteria was more arbitrary.

The cut-off values are chosen arbitrarily by authors depending on the purposes and the kind of materials used for pi experiments. Specimens passing all selection criteria are considered of grade "A", and fully trustworthy. In case of failure of any of the selection criteria (i.e. exceeding one or more cut-off values) the specimen results in grade "B"; and if two parameters overcome the cut-off criteria they results in grade "C" and so on.

The current process of selecting data and criteria is somewhat arbitrary. Also, there is no consensus about what criteria are appropriate and about the threshold values which provide the best exclusion of non-ideal or not-accurate paleointensity data.

PART III- THE USE OF THE PALEOSECULAR VARIATION OF THE GEOMAGNETIC FIELD AS A CORRELATING AND DATING TOOL OF VOLCANIC ROCKS

5. Introduction

The pioneering works of David (1910) and Chevallier (1925) at Etna drown the attention to lavas as potential recorders of past directions of Earth's Magnetic Field, and represent the first attempts to use paleomagnetism as dating tool. Since these pioneering works, the study of the Earth's magnetic field variations had a wide spread of application for a variety of disciplines (Chapter 3.1). Particularly, paleomagnetism has been used as a correlation and dating tool for volcanics, which may yield emplacement age clues, once the paleomagnetic directions obtained from loosely dated flows are compared to an independently obtained reference curve of the paleosecular variation (PSV) of the geomagnetic field. The paleomagnetic correlation is obtained by comparing paleomagnetic direction from different volcanic formation, considering as correlative those that share the similar values (see Chapter 6).

The "paleomagnetic dating tool" was successfully attempted on lavas from Vesuvio (Hoye, 1981), Etna (Tanguy et al., 1985; Rolph and Shaw, 1986), as well as in many other active and quiescent volcanoes (Chapter 2). It is remarkable that the amount of studies based on the use of PSV for correlating and dating volcanics has increased especially from the 80's and 90's. Contextually, the PSV reference curves has been better constrained with new paleomagnetic and archeomagnetic data, as well as extended to the past, allowing a greater widespread of the use of the "paleomagnetic method".

6. The PSV-based paleomagnetic correlation

Correlation between volcanic deposits is achieved by comparing paleomagnetic directions from different outcrops. Indeed, volcanics emplaced during the same eruption or eruptive event are expected to share the same paleomagnetic directions. Conversely, it is possible that, by chance, two different units may share the same directions, and so additional independent evidence, such as volcano - stratigraphic and petrographic observations are useful to corroborate paleomagnetic correlations. The method is independent on the petrography of the studied deposit, since magnetic minerals are ubiquitous in volcanic rocks; moreover paleomagnetic correlations can be applied over distances up to hundreds of kilometer far (e.g., pumice and ash fall deposits spread over large areas; Grommè et al., 1972).

The vicinity of paleomagnetic directions was classically used to infer on correlation of intrusive bodies (Jones and McHlhinny, 1966), of volcanic deposit as lava flows (Bogue and Coe, 1981; Hagstrum and Champion, 1994;

Jurado- Chichay et al., 1996), or ash-flow deposits (Prévot and McWilliams, 1989).. Hagstrum and Champion (1994) and Jurado-Chichay et al. (1996) paleomagnetically studied the Pohue Bay flow (Manua Loa Vulcan, Hawaii islands) with the associated cones, to determine the cone origin (primary or secondary processes).

In the cited examples, as also in many others, paleomagnetism is proven to represent a powerful correlative tool of volcanic products lacking univocal field correlation evidences.

6.1 Examples from literature of the use of PSV as a correlating tool

Jones and McHlhinny (1966) paleomagnetically investigated 20 sites of pre-Karroo age (1000 Ma) dolerites sampled in Bechuanaland (south-west border of Rhodesia) and the Transvaal shield (South Africa). They recognized two groups of direction of magnetization and inferred the correlation between the two dolerites, 1000 km far from each other, constraining the age of dolerites to a post-Waterberg sedimentary formation. Moreover, authors correlated the Waterberg formation to the Umkondo system. These two systems have an age comprised between 1420 +/-70 Ma (by the lead isotope method, Oosthuyzen, 1964) and 1950 +/-50 Ma (Nicolaysen et al., 1958).

Grommè et al., 1972) used paleomagnetism to correlate cooling units in the middle Tertiary ash-flow zone, in the Basin and Range province, between central and eastern Nevada and western Utah. The geochronological dating indicates an age interval of 0.8 Ma between different units. Paleosecular variation of geomagnetic field is used here to distinguish between all cooling units, over distances up to 200 km. These correlations are particularly useful when applied to stratigraphic sections of ash-flow sheets, and confined to mountain ranges that are separated by alluvium-filled valleys.

Bogue and Coe (1981) studied three sections (each of 8-10 lava flows) from the Columbia River Basalt Group, measuring the paleomagnetic direction from flows of Grande Ronde Basalt (southern-central Washington, US). The authors developed a statistical method for evaluating such correlations between pairs of sites. The analysis revealed that the same flow sequence is exposed at the three sites, which is interesting because for two of them the correlation was expected, but not for the third which is 180 km apart from the other two.

Prévot and McWilliams (1989) studied three Lower Jurassic volcanic sequences from three basins of eastern North America: Deerfield, Newark, and Hartford. The first two showed similar paleomagnetic directions both in a sedimentary and in intrusive Jurassic body. A volcanic sequence in Deerfield basalt showed anomalous different direction of 30° far from the expected values from Early Jurassic age, thus recording a peculiar secular variation event.

Hagstrum and Champion (1994) used paleomagnetism to correlate quaternary lava flows from the Lower East Rift Zone (LERZ) of Kilauea Volcano (Hawaii). Firstly, they used site mean direction from the flow 1970 AD as

a test, prooving that it was in good agreement with local geomagnetic field directions measured in 1970. Also, individual flows could be grouped by their paleomagnetic direction, indicating a different and perhaps more refined (in terms of age) eruptive history for the LERZ than implied by the geologic mapping by Moore and Trusdell (1991) alone.

Jurado- Chichay et al. (1996) similarly worked on lava flows from the Hawaii. They applied the paleomagnetic correlation tool to constrain the origin and temporal relationship of the Pohue Bay flow and its associated coastal cones, at the Mauna Loa volcano (Hawaii). Paleomagnetism helped to discriminate between cones originated from primary processes (volcanic eruption) or secondary processes (littoral cones, resulting of steam explosions that take place when lava flows into the ocean). A detailed paleomagnetic study of the Pohue Bay flow and associated cones emplaced along the coast allowed inferring the temporal relationship between cones and the main lava flow. Since the Pohue Bay flow eruptive center is upslope, cones had to form when the flow entered into the Ocean, therefore the similar paleomagnetic direction between the two contemporaneous volcanic units suggested a littoral origin. Moreover, the age of the Pohue Bay flow is constrained to 1300 years, from the vicinity of paleomagnetic directions from the studied flow with secular variation curves and age-dated flows.

Chenet et al. (2008 and 2009) study the Deccan flood basalt province (India) with a section of 3500 m and volumes up to 20.000 km^3, using an interdisciplinary approach, combining volcanology, petrology, geomorphology, absolute geochronological dating, and paleomagnetism. The paleomagnetic analyses shown that single eruptive events were able to emplace flows over distances from 100 to 800 km. The base assumption to recognize single eruptive events is that superimposed or nearby flows with statistically identical paleomagnetic directions (at the 95% confidence level) were erupted in too little time to have recorded significant secular variation (an order of decades). Depending on this assumption, groups of paleomagnetic directions were identified as single eruptive events erupted during few decades. The PSV correlation approach permits the unraveling of unsuspected complexities, using geomagnetic reversals and discriminating different pulses of activity.

7. The paleomagnetic dating

Absolute ages of volcanics are best determined through radiometric dating.

Radiometric dating is a technique used to date rocks (e.g., McRae, 1998) usually based on a comparison between the observed abundance of a naturally occurring radioactive isotope and its decay products, using known decay rates. The most common methods used for dating rocks are the potassium – argon (K/Ar), argon-argon ($^{39}Ar/^{40}Ar$), uranium - lead (Pb/U) and the radiocarbon dating using the ^{14}C content.

Nevertheless, in many situations radiometric dating is not possible, or difficult: in case of evident post-depositional alteration, or when the minerals content is not suitable (e.g., low K-content), or in case or rocks too young to let the isotopes decay. Yet both Ar/Ar and K/Ar method loose accuracy in young (Holocene) products, and cannot be used in K-poor volcanic rocks (i.e. basalts erupted in most intra-oceanic volcanoes). ^{14}C is, in turn, a powerful dating tool for the last millennia, and indeed it is the most suitable and commonly used for Holocene rocks, but organic material and/or soils are required, which can be uncommon at given climatic conditions.

For instance, when dealing with volcanic environments, only soils or lahars bear organic materials, which forms at favorable climatic conditions and when the eruption rate are low enough for a soil to develop. Therefore, in the case of active volcanoes with high frequency of eruptions, soils cannot form and the ^{14}C method cannot be used. As a consequence, there has been an increasing use of the PSV of the geomagnetic field recorded in volcanic rocks as an accurate correlating and dating tool of eruptions (Rutten and Wensink, 1960; Doell and Cox, 1963; Soler et al., 1984; Rolph et al., 1987; Carlut et al., 2000; Tanguy et al., 2003; Incoronato et al., 2002; Speranza et al., 2006; 2008; 2010; Chenet et al. 2009; Tanguy et al., 2009; among many others).

The advantage of the paleomagnetic dating method is that it can be used on whole rock samples, and does not need particular petrographic / chemical lava characteristics (magnetic remanence is generally carried by titamo-magnetite series of minerals, ubiquitous in volcanics).

Paleomagnetic dating is achieved by comparing the paleomagnetic directions "frozen" in lava flows and scoria cones (commonly derived with an accuracy of 2° - 3°) to a PSV reference curve, gathered in nearby regions by geomagnetic observations, archaeomagnetism, and paleomagnetism of sedimentary successions deposited at high rate. For instance, recent compilation of all European geomagnetic–archeomagnetic data sets (Speranza et al., 2008) revealed that during the Holocene, the field reached a maximum rate of change of ~ 7° per 100 years in the central Mediterranean region. (Fig. 9) Therefore, a paleomagnetic direction defined with an accuracy of 2°-4° can translate (after comparison with a PSV reference curve) into dating defined with an accuracy of ~100 years in the most favorable cases (see discussion in Speranza et al., 2006, and Lanza and Zanella, 2006).

Dating depends on the availability of Secular Variation curves available for the area, or nearby areas, within the 1000-2000 km, and on the accuracy of paleomagnetic determinations.

However, it has to be taken into account that volcanic units of different ages may share the same paleomagnetic direction by chance, because the geomagnetic field may reoccupy the same directions after a few centuries or

millennia. Thus, the paleomagnetic dating method is effective only when a (preferably small) input age window is provided by independent methods.

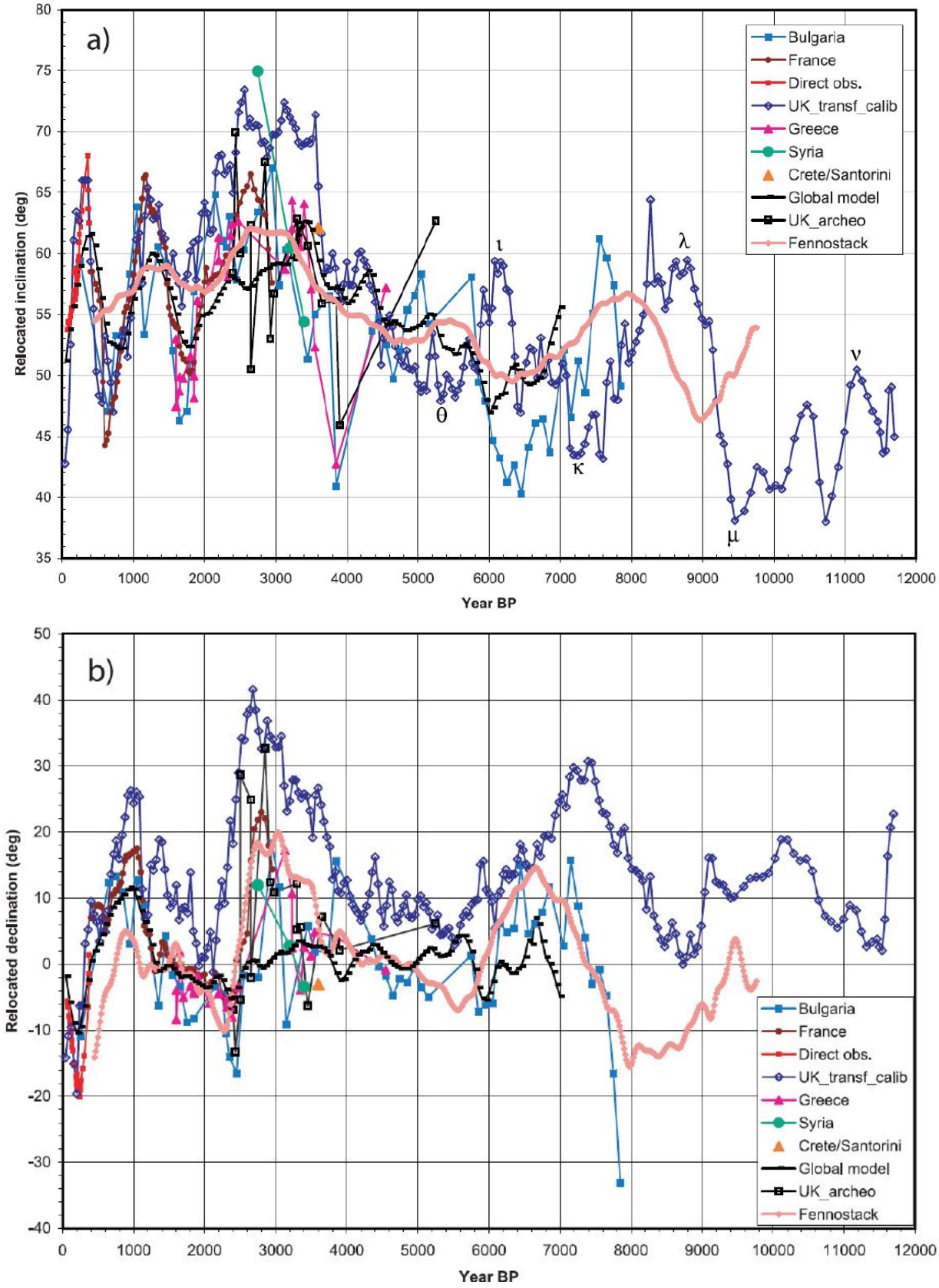

Fig. 9 - Reference PSV curves from Speranza et al. (2008) of declination (a) and inclination (b) relocated at Stromboli (38.8°N; 15.2°E) via pole method (Noel and Batt, 1990). All the PSV available are compared in this figure: Bulgaria curve by Kovacheva et al. (1998), French curve is by Bucur (1994) and Gallet et al. (2002), Greek curve is by Evans (2006), the UK archeomagnetic curve is by Zanarini et al. (2007), and the UK Holocene master curve is by Turner and Thompson (1981, 1982). The black PSV curve is derived from the Cals7k by Korte and Constable (2005).

Paleomagnetic dating has been successfully applied to several active volcanoes (mostly in Italy and islands of Hawaii) owing to PSV reference data provided by the rich European archeomagnetic data set and radiometrically dated local lava flows at Hawaii, respectively. The method has provided high-resolution dating, and has proven fundamental to constrain the timing of local volcanic history, supporting hazard scenarios for future eruptive activity (e.g., Soler et al., 1984; Rolph and Shaw ,1986; Rolph et al., 1987; Hagstrum and Champion, 1994; Jurado-Chichay et al., 1996; Carlut et al., 2000; Incoronato et al., 2002; Tanguy et al., 2003; Speranza et al., 2004, 2006, 2008, 2010; Pressling et al., 2009; Vezzoli et al., 2009; Tanguy et al., 2009; Chenet et al. 2009; among many others).

A Matlab code (archeo_dating) has been developed by Pavòn-Carrasco et al., (2011) for archeomagnetic/paleomagnetic dating volcanics of unknown ages. This dating tool is based on the methodology describe by Lanos (2004), using the probability density functions of the three geomagnetic field elements: declination, inclination and intensity). The pre-requisite is that a well-dated reference paleosecular variation curve (master PSVc) is available. Since for Europe the paleomagnetic reference data are densely distributed for the last 10 kyrs., the archaeo_dating method can be safely used. An important factor in the dating process is related to the behavior of the geomagnetic field itself, which is reflected by the PSV curves. Data from periods of rapid changes would provide more precise dates than those from slowly changing epochs. In addition, similar direction/intensity can be observed for different periods. This can generate non-unique problems. In these cases, additional information should be considered (archaeological information, stratigraphy, context, and typology) to select between alternative ages.

7.1 Examples in literature of the use of PSV as a dating tool

Many papers had been published on the issue of dating volcanic rocks using PSV so far. I have attempted to mention the majority of them. Since the availability of regional PSV curve for a studied area, the reconstruction of regional PSV reference curve is the tenet for applying the "paleomagnetic dating method". Many papers are based on this goal, and in many others the method is successfully applied to unravel the chronology of volcanic eruptions. Nonetheless, the method has been used since the last century several points are still debated (debate included in the following section 7.1.1, and Chapter 7.2). I divided the summary of papers mentioned in this chapter into three sections: Italy, Pacific and Atlantic Oceans.

7.1.1 Italy

In his pioneering work, Chevalier (1925) paleomagnetically investigated lava flows, from 1281 to the 1910 AD, erupted from Etna. He obtained the first PSV curve from lavas.

Hoye (1981) archeomagnetically investigated eleven lava flows produced by the historic eruption of the 79 AD of Vesuvius, Directions of the studied deposits are different from the present-day field, and well agree with the PSV the direction of which is significantly different from that of the present-day field, suggesting that the remanence is primary. The secular variation curve for Vesuvius agrees well with the Rome record and with other curves from Italy and London.

Tanguy et al. (1985) reconstructed a geomagnetic variation curve using archaeomagnetism during the past 1,000 years. The new reference curve was compared with previous results and leads to propose for older ages for numerous historically dated flows from Etna.

Rolph et al. (1987) studied the paleomagnetism forty historical lava flows from Mt Etna, with the purpose of determine the change of the magnetic field in Sicily through historic times. Authors constructed curves to show the local secular variation of the field in both direction and intensity. These curves were used to reconsider the ages attributed to a number of Etna lavas, and solve correlation and dating questions. They stressed that the paleosecular variation curves are powerful dating tools when compared with the NRM of rocks or materials that retain a paleomagnetic signal.

Carracedo et al. (1993) (as after Principe et al. 2004) studied the 1631 AD explosive eruption of Vesuvius. Paleomagnetism had been used to decide whether during the 1631 AD eruptive events were emplaced also lava flows, coming to the conclusion that the 1631 AD eruption lack in effusive events, which rather had been emplaced in a previous age than reported.

Incoronato et al., (2002) focused on the volcanoes of Etna and Vesuvius, and on Ischia Island, to retrieve the local PSV curve. Comparative paleomagnetic analyses of the three volcanoes proved that they share the same PSV pattern. This curve enabled a reassessment of the age of eruption of several lavas from these volcanoes: one Etna flow previously dated 81-1169 AD had been constrained as 1169 AD, and two flows has been dated 1536 and 1595 AD, respectively. They also dated flows from Vesuvius within the same time windows.

Lanza and Zanella (2003) derived the PSV curve of the geomagnetic field for the last 135 ka, investigating 121 sites of lava flow, scoria cone and pyroclastic rocks of Vulcano (Aeolian Islands). Volcanic units were previously isotopically dated using the K/Ar. The curve matches well with sedimentary records from Lago di Monticchio and Lago Grande di Mezzano (Brandt et al. 1999). Moreover, authors analyzed more than one hundred repeat stations of the Italian Magnetic Network to proposed the optimum reference point of relocating SV data.

Also Tanguy et al., (2003) applied the archeomagnetic dating method to the Mediterranean volcanoes Etna, Vesuvius and Ischia. Tanguy et al. (2003) collected large amount of samples to avoid local field distortions. Sixty-three lava flows and pyroclastic units had been paleomagnetically dated with a resolution increasing in younger ages from ± 100 to ± 40 years from 150 BC to 1,500 AD, owing to the accuracy of the determination of the paleosecular variation curve. According to authors, the method can be safely extended to the whole Europe to constraints eruption ages within the last 2 ka.

Principe et al. (2004) found that historical records available for the Vesuvius volcano help in constraining the timing of main eruptive events from 29 AD to 1631 AD , but some eruptions between 800 AD and 900 AD were unnoticed by historians. Moreover, it is often difficult to correlate historical accounts with deposits emplaced. Effusive eruption clustered in a short period between the 79 AD and the 1631 AD around 800 - 1000 AD, with lava flows and parasitic cones on the flank of the Vesuvio Mt. The method used by authors is the so-called "big sample plaster method" of Thellier (1981), and routinely applied at the Saint Maur Laboratories (France) which is based on collecting and analyzing altogether big oriented blocks (~ 1 kg) distributed over meters in the studied outcrop. According to authors, this method made possible to obtain errors very low (~α_{95} of 1°) and high time resolution (± 40 years).

Lanza and Zanella (2006) replied to Principe et al. (2004) about the chronology of Vesuvius activity from 79 to 1631 AD, and particularly discussing the high accuracy that it can be reached using paleomagnetic dating. Lanza and Zanella (2006) argue that the reference curve using for Etna is poorly constrained (with nine lava flows, dated by comparing them with the French curve) and not clearly indicated. Moreover, they use a procedure for dating based on a statistical approach (giving an age interval and an associated probability level, which quantifies the agreement between the direction to be dated and the reference curve, and is thus used to evaluate the reliability of the dating) without defining the parameters. The high accuracy (±40 years) of paleomagnetic dating was rather achieved by disregarding errors which have the same magnitude that the results.

The volcanic activity of the Stromboli Island (Aeolian Archipelago, Italy) is typically characterized by low-explosive lava fountain rhythmic activity, interrupted by paroxysms, mid-high explosive events. During the last century paroxisms occurred twelve times (e.g., Barberi et al., 1993). Since the age of these events preceeding the last two centuries is not well constrained, Speranza et al. (2004) sampled 17 paleomagnetic spatter lavas spread over the northern and western flanks of Sciara del Fuoco. By comparing paleomagnetic directions with the relocated paleosecular variation curve for the last 2,000 years, Speranza et al., (2004) suggested that most of the sampled spatters in the north flank emplaced during eruptive events between 1400 and 1600 AD, while they do not find evidences of highly explosive events before and after this period. Proceeding with the same successful method, Speranza et al. (2008) extend the investigation to the Holocene history of the Island, the Neostroboli phase. Sampling and analysis (paleomagnetic and petrographic) on 33 sites in lava flows allow to infer a detailed analysis of the Holocene data. Dating was obtained by comparing results with PSV curve relocated from the UK master curve (Turner and Thompson, 1981; 1982), and the French curve (Bucur 1994; Gallet et al., 2002), which are the most accurate and time-extended, based on several dataset from Europe. The eruptive crisis recovered during the previous study (Speranza et al., 2004) is confirmed.

Arrighi, et al. (2004) had adopted the same method of sampling of Principe et al. (2004) to study the recent eruptive history of Stromboli (Aeolian Islands, Italy) using archeomagnetic dating. To the lava flow at San Bartolo village was assigned an age of 100 ± 100 AD, predating the last sector collapse of the Stromboli volcano (with important implication of the volcanic hazard estimate). Authors remark that the method had been used successfully since the first studies on Italian volcanoes, but has significant discrepancies with respect to the widely accepted classical core-drilling methods. Differences were founded with results obtained by Speranza et al. (2004), which are also criticized for have used PSV not clearly defined. Concluding, Arrighi et al. (2004) conflict on the conclusion of Speranza et al. (2004) that a high energy eruption occurred between 1400 and 1600 AD, as also that no paroxysms are inferred to have occurred before 1,400 AD.

In a comment, Speranza et al. (2005) discussed each point of disagreement with Arrighi et al. (2004). With regard to the methodological problem, authors confirmed that the classical core-drilling method provides a more realistic estimate of dating and related uncertainties. Speranza et al. (2004) criticize the Sant Maurice laboratory (France) procedure (also called "blanket") which does not ensure a realistic average of the paleomagnetic field, and that the so accurate age-estimate is rather apparently obtained by a partial cleaning of the samples. Thus, considering the directions after 15-20 μT AF (instead the full stepwise demagnetization) can reflect a remanent magnetization different from the ChRM, and also unreliable since Arrighi et al. (2004) did not use the principal component analysis (PCA), nor analyzed the magnetic mineralogy of their samples. Speranza et al. (2005) concluded that the low α_{95} obtained by Arrighi et al. (2004) was obtained by rejecting sample arbitrarily or by an undersampling, and the bias can affect the PSV obtained, and that uncertainties of 2-4° reflects better the realistic values that can be obtained from volcanic rocks.

Arrighi et al. (2005) rebutted the critical points raised by Speranza et al. (2005), supporting the method used, the "big sample method", against the classical core-drilled method (which can cause, according to authors, a secondary drilling remanent magnetization, or DIRM), the criteria used to reject samples after paleomagnetic analyses, and the accuracy of paleomagnetic mean directions obtained.

Historical lava flows from Etna had been used by Speranza et al. (2006) as a test to address the dispute on how accurate can be the paleomagnetic dating method and codify the technique. Paleomagnetic directions retrieved from the 39 paleomagnetic sites sampled on 13 flows (four with known ages and nine loosely dated) were compared with the archeomagnetic data sets from the last 3 ka, from France, Unite Kingdom, Germany and Bulgaria relocated to Etna coordinates. Authors inferred new ages of the studied flows, compared with previous paleomagnetic results from the same Etna lavas, and faced the matter of the method, discussing the possible source of bias, and how accurate can be the paleomagnetic dating. Principe et al. (2004) argued that the paleomagnetic dating can achieve the accuracy of even 20 - 30°, whereas Lanza and Zanella (2006) and Speranza et al. (2005) questioned this conclusion arguing that many factors concur to raise the uncertainty (up to ~ 136–661 years, 307 years on average).

Lanza et al. (2005a) used to check paleomagnetic directions derived from Etna and Vesuvius direct measurement of the geomagnetic field in Italy. Other reference curves as also paleomagnetic data available for the two volcanic apparatus had been relocated to the same reference site (Viterbo town, central Italy), to be compared and discussed. The dispersion of the data is higher for Vesuvius than for Etna, and the possible reasons are largely discussed within their work. For instance source of bias are the undersampling of a studied flow, a TRM anisotropy and the effect of magnetized rocks underlying the studied flow.

Tanguy et al. (2005) comment on the work of Lanza et al. (2005a), arguing that the large dispersion obtained for Vesuvius are due to collecting data in a very restricted area, and the use of inadequate drilling tool which can produce a parasitic paramagnetization. Moreover, the compilation of data is criticized as inadequate, and Tanguy et al. (2005) pointed out that their paleomagnetic result from Vesuvius well match with French PSV curve; on the contrary the curve derived from Jackson's (2000) model is not consistent with Vesuvius' data. Tanguy et a. (2005) questioned the validity of the PSV by Incoronato et al. (2002), which resembled the Jackson's model for the 1600 , since it is based on a inaccurate or wrong dating of some flows to 1,631 AD and 1,697 AD eruptions.

Lanza et al. (2005b) replied to the comment by Tanguy et al (2005) defending their own work. Authors pointed out that a general agreement between the dataset published in Lanza et al. (2005a) and from previous authors (e.g., Rolph et al. 1987, Incoronato et al. 2002, and Tanguy et al. 2003) exits. The methodological problem is approached, stressing that the large sampling method used by French authors is useable only for arheological samples, that α_{95} mean (2-3°) obtained from lavas from Italian volcanoes have a reasonable level of accuracy. Archeomagnetic dating is based on two steps; the first yield TRM direction and the second consist in the

interpretation, based on the assumption that the directions correspond to the original NRM acquired originally during rocks formation. Therefore, the challenge has to be a better understating of magnetization processes.

Tanguy et al., (2009) revised the history of Etna and Vesuvius. Despite a wealth of previous works and historical accounts, the eruptive history for the past few millennia is not well known. In particular, the historical record has no valuable account at Etna from 252 to 1,062 AD, and is based on the work of pioneer geologists in the 80's.

Vezzoli et al., (2009) applied a high - precision archaeodating method to the products of 12 volcanic centers of the Ischia island (belonging to the Campanian magmatic province, central-south Italy). During the last 10 ka, Ischia experienced a caldera formation, uplift due to a resurgence within the caldera, and contemporaneously the formation along regional faults of lava domes, scoria and resurgence-related tuff ring cones. Results from 25 paleomagnetic sites are compared with regional PSV curves and new ages are obtained, from 4,100 BC to 355 AD, and three main periods of activity are documented: 1,800-1,000 BC, 650 BC-355 AD, and 1,302 AD. Vezzoli et al., (2009) concluded that the resurgence resulted from both the hydrostatic rebound and the rising of new batches of less evolved magma. The volcanic activity was more intense over the last 4,000 years.

At Pantelleria, the paleomagnetism of the most recent lavas and scoriae has been used to constrain the most recent silicic activity of the island to 5.9–6.8 ka (Speranza et al., 2010). By the comparison of paleomagnetic mean directions gathered from 10 sites from pumice fall and effusive deposits, Speranza et al. (2010) proved that they are consistent with reference geomagnetic field variation for the 5-10 ka interval. Cuddia del Gallo cone and Khaggiar lava flow directions indicate an age of 5.9 and 6.3 ka, in agreement with radiocarbon dating, whereas K/Ar dating indicates older ages of ~ the 30 %. Thus, last silicic volcanic activity at Pantelleria is tightly constrained around period around 6 ka. In contrast, no reliable PSV directional reference curves exist for pre-Holocene times implying that the paleomagnetism of ~80–130 ka ignimbrites from Pantelleria cannot yield absolute emplacement ages but can be used as a correlative tool.

7.1.2 Pacific Ocean

Hagstrum and Champion (1994) used paleomagnetism first to correlate quaternary lava flows in the Lower East Rift Zone (LERZ) of Kilauea Volcano (Hawaii), in agreement to the map by Moore and Trusdell (1991). Groups of individual flows refined in terms of age the eruptive history for the LERZ, than implied by the geologic mapping alone. Hence more precise dating is achieved in this work.

Jurado - Chichay et al. (1996) worked on lava flows at the Hawaii to constrain the origin and temporal relationship of the Pohue Bay flow and its associated coastal cones, at Mauna Loa volcano (Hawaii). The results show that lava from Pohue Bay and those pounded in the cones have similar paleomagnetic directions, thus they are close in ages. From the vicinity of paleomagnetic directions of the studied flow with secular variation curve

and age-dated flows, the age of the Pohue Bay flow is constrained to 1,300 years ago, thus younger than previously assigned.

7.1.3 Atlantic Ocean

Soler et al., (1984) recovered the secular variation of geomagnetic field in the **Canary Islands** during the last 400 years from paleomagnetic data from well-known historical lava flows. The age of historical lavas can be traced back to 1585 AD. The paleomagnetic directions of lavas allowed reconstructing the PSV curve that can be used as a dating tool for eruptions with unknown age. Authors used the PSV curve for assign an age to the last eruptive episode of Teide (Tenerife Island), which has not been dated by ^{14}C, as ~1,400-1,500 AD.
Pavón Carrasco and Villasante Marcos (2010) tried to reconstruct the last thousands of years of the volcanic history of Tenerife and La Palma (Canary Islands). They calculated a regional paleosecular variation curve and compared it with global geomagnetic models constructed from historical and instrumental geomagnetic observations for the last four centuries, e.g. the gufm1 model (Jackson et al., 2000; IGRF-11, IAGA, 2009) and from archeomagnetic and paleomagnetic data for the last 3 ka (ARCH3K.1 model, Korte et al., 2009). From the global ARCH3K.1 model and the regional European SCHA.DIF.3K model (Pavón-Carrasco et al., 2009) new PSV curve has been recovered and relocated at the Canary Islands, and then used to obtain paleomagnetic ages for both the historical lava flows, and two older lava-flows (Lavas Negras of the Teide, Tenerife Island; Montaña Quemada, La Palma Island). Paleomagnetic dating of older flows was compared with geochronological dating previously available, to confirm the reliability of results.

7.2 Source of bias

There are several possible sources of intra-flow variability, which can yield scatter of paleomagnetic directions. This topic has been discussed by Baag et al. (1995), Valet and Soler (1999), Urrutia-Fucuguachi et al. (2004), Lanza et al. (2005a), Lanza and Zanella (2006), and Speranza et al. (2006, 2008, 2012):

1) Local magnetic anomalies generated by the strongly magnetized underlying terrain and cooling lava flow (see Baag et al., 1995; Valet and Soler, 1999; Speranza et al., 2006). The comparison between sun and magnetic compass readings yields significant deviations of the magnetic needle. This is fully confirmed by field measurements carried out at Hawaii (Baag et al., 1995) and Canary islands (Valet and Soler, 1999), where field deflections up to 15° – 20° with respect to the expected values were observed, and subsequently modeled by Knudsen et al. (2003). Conversely, Tanguy and Le Goff (2004) documented much smaller (<3°) field deviations at a dozen measurement sites at Etna (Speranza et al., 2006; 2010; 2012).

2) Regional magnetic anomalies for large magnetic body at depth. However, it has been demonstrated for the island of Pantelleria (Zanella, 1998) that anomalies of 1500 – 2000 nT reported in the aeromagnetic map may cause a maximum field deviation of 1-2°.

3) magnetic mineralogy variability and magnetic anisotropy.

4) internal viscous deformation of lava flows and/or movement of blocks and lava during flow advance.

5) local tectonic effects and block tilting.

Al these factors have to be carefully evaluated as a possible source of bias of paleomagnetic results.

In order to minimize the problem discussed in point 2, regional magnetic anomaly maps are required and have to be evaluated. Effects of point 3 to 5, can be reduced by spacing cores as much as possible, sampling the studied units with two or more sites far from each other, at different localities, to evaluate carefully the local structural pattern and verify the inter-flow consistence of paleomagnetic results.

Undersampling may thus be reasonably assumed as the main cause for the differences between directions of the same age (Lanza et al., 2005a).

Taking into account all the listed source of bias, sites sampled within the same flow at different localities may share similar paleomagnetic directions, within an angular distance that normally can reach ~ 10°.

Speranza et al, (2006) deal with the issue of the age accuracy that can be obtained by using paleomagnetism for dating volcanic rocks. Authors studied lava flows from Etna volcano to address this issue, since several historical accounts are available, and the 85% of the edifice is made of lavas erupted during the last 15 kyrs.

Some authors suggested that a 20–30 years can be safely achieved (Tanguy et al., 2003; Arrighi et al., 2004; Principe et al., 2004), others observed a quite large scatter among paleomagnetic directions from the same flow, which may translate into significantly greater uncertainties on the age determinations (Hagstrum and Champion, 1994; Quidelleur et al., 2005; Lanza and Zanella, 2006). Speranza et al. (2006) used test flows with a known age and compared them with PSV valid for Italy, concluding that the average age accuracy that can be obtained is around 307 years.

8. Paleosecular variation curves for the Atlantic Ocean

Part of my Doctoral Thesis is aimed at reconstructing the Paleosecular Variation Curve (PSV) valid for the Atlantic Ocean area. The following Chapters 8 and 9 resumes the state of the art before my work, after a brief introduction to general features and problems relate to Global Models and PSV curves.

The geomagnetic secular variations are geomagnetic field changes with periodicity between 1 year and 10^5 yr. Even over the time of historic geomagnetic field records, directional changes are substantial.
A double contribution explains the origin of geomagnetic secular variations (Merrill et al., 1996; Butler, 2004; Tauxe, 2009): (1) non-dipole changes dominating the shorter periods (less than 3 kyrs) and (2) changes of the dipolar field with longer periods. Changes in the non-dipole field dominate periodicities less than 3,000 yr. Over historic time, there has been a tendency for some features of the non-dipole field to undergo westward drift, a longitudinal shift toward the west, at a rate of about 0.4° longitude per year. Other non-dipole features appear to be stationary.
The dipole portion of the geomagnetic field (90% of the surface field) also changes direction and amplitude.
To separate changes of the dipole and non-dipole fields, historic records as well as archeomagnetic records and paleomagnetic records from Holocene volcanic rocks have been analyzed.
Usually, paleomagnetic data from dated volcanic rocks and lacustrine sediments, and archeomagnetic data retrieved from heated archeological structures (ceramic or metallurgical kilns, heating chambers of baths, burnt houses and walls, ancient fire hearts, etc.) are used to unravel the geomagnetic field behavior during the last thousands of years, and yield the corresponding Paleosecular Variation Curve (PSV). These curves are of regional validity (Merrill et al. 1996), because of the non-dipolar character of the geomagnetic field, and therefore different curves need to be constructed for different regions. Once the PSV curve for a particular region is constructed, it can be used to date new lava flows by means of paleomagnetism. Additionally, PSV curves and well-dated paleomagnetic directions are fundamental to construct regional and global models of the geomagnetic field temporal variability and to investigate the physical processes behind it.
PSV curves have to be relocated to the studied area coordinate via pole method (Noel and Batt, 1990) for directions, and by Virtual Dipole Moment (VDM) or by Virtual Axial Dipole Moment (VADM) for intensities (Merrill et al., 1996), introducing an error negligible for distances that do not exceed the 1000-1500 km apart.

Our knowledge of the recent (Holocene) geomagnetic field evolution has been improved by the recent modeling work of Korte et al. (2011), with the model Cals10k.1b, realized using a comprehensive data compilation (both directions and intensities) and recently refined by new modeling strategies (Korte and Constable, 2011). More than 80% of data from global datasets (see Donadini et al., 2009; Korte and Constable, 2011) come from 0–3 ka data (subset of data used to build the model Cals3k.4, Korte and Constable, 2011).

The last available model for the last 3 ka (CALS3k.4, by Korte and Constable, 2011) was constructed using a new compilation of ~ 35,000 values (declination, inclination, and intensity) obtained from Holocene

lacustrine/marine sediments, archeological artifacts and historical lava flows (Korte and Constable, 2005; Genevey et al., 2008; Donadini et al., 2009). Recently, a new model extended to the last 10 ka had been published by Korte et al. (2011).

The IGRF-11 model (International Geomagnetic Reference Field, now at its eleventh version, Finlay et al., 2010) is available for the last century, and relies upon direct measurements.
Due to the uneven distribution of data, Holocene geomagnetic field evolution for some regions (oceans and most of the southern hemisphere) remains uncovered and so not well constrained; moreover, the paucity of data worsens when dealing with pre-Holocene deposits. This is indeed the case of the Azores area studied in this thesis, located in the central-northern Atlantic Ocean.
Indeed, for this area, the catalog of Donadini et al. (2009) yields only few data both directions and intensities from its eastern and northern margins.

8.1 Paleomagnetic data record for the Atlantic Ocean

The directional pattern of the geomagnetic field over the last 10 ka can be obtained from last updated global models: the Cas3k.4 by Korte and Constable (2011) and Cals10k.1b by Korte et al., (2011). Clearly global models tend to smooth maxima and minima, hiding peculiar features (such as magnetic "spikes"). On the contrary, paleosecular variation of the geomagnetic field recovered from real data (volcanic rocks, archeologic matters) faithfully reproduces real changes. For the studied area (Part V) of the Azores Archipelago, in the central-northern Atlantic Ocean, data are extremely scarce, especially with regard to the last 3 ka.

Johnson et al. (1998) reported on paleomagnetic results from 28 lava flows sampled at São Miguel, geochronological-dated with $^{40}Ar/^{39}Ar$ age raging from 878±45 ka to present ages. Other paleomagnetic studies are focused on reversals (Ellwood et al., 1973; Salgueiro, 1991; Silva et al., 2012).

Lund and Kleigwin (1994) published a paleosecular variation curve (PSV) from the Bermuda Rise, but the trend for the last 3 ka is almost anti-correlated with more recent global models. Moreover, Bermuda Rise is located at 3,000 km W to the Azores Archipelago.

From the Canary Archipelago, ~1,400 km far from the Azores Archipelago, volcanic islands in the Atlantic Ocean, paleomagnetic directions were gathered from fourteen 1585 – 1971 AD lava flows (Soler et al., 1984; Quidelleur et al. 2002), and a new PSV was presented by Pavon-Carrasco and Villasante Marcos, (2010) for the last 500 years. Other studies were focused on reversals of geomagnetic field (e.g., Tauxe et al., 2000).

Sedimentary paleomagnetic results from four Holocene cores drilled around Iceland and Greenland (Thompson and Turner, 1985; Channell et al., 1997; Stoner et al., 2000, 2007), and Cape Ghir, Morroco by Bleil and Dillon (2008) have been obtained so far. Iceland and Greenland records are between 2,500 km and 3,200 km away from

the Azores; western and central Europe data are closer, indeed the Cape Ghir record (Bleil and Dillon, 2008) is the closest and that is still ~1,600 km away.

For the last 400 years (1600 - 1900 AD) the gufm1 model Jackson et al., (2000) is available, based on direct measurement from ships of magnetic declination and inclination. Lacking PSV curves for the region for ages older than 1600 AD, the French archeomagnetic curve (Bucur, 1994; Gallet et al., 2002) for the last 3 ka, and the United Kindgom (UK) master curve (Turner and Thompson, 1981; 1982) for older Holocene times (see Tanguy et al., 2003; Speranza et al., 2004; 2008; 2010) can be relocated at Azores coordinated via pole method (Noel and Batt 1990). The UK master curve and French archeomagnetic curve fit reasonably well with the trend depicted by the global models despite of the distance of 2,500 km.

The paleodirection record for the Atlantic Ocean has been significantly increased by the new data presented in this thesis.

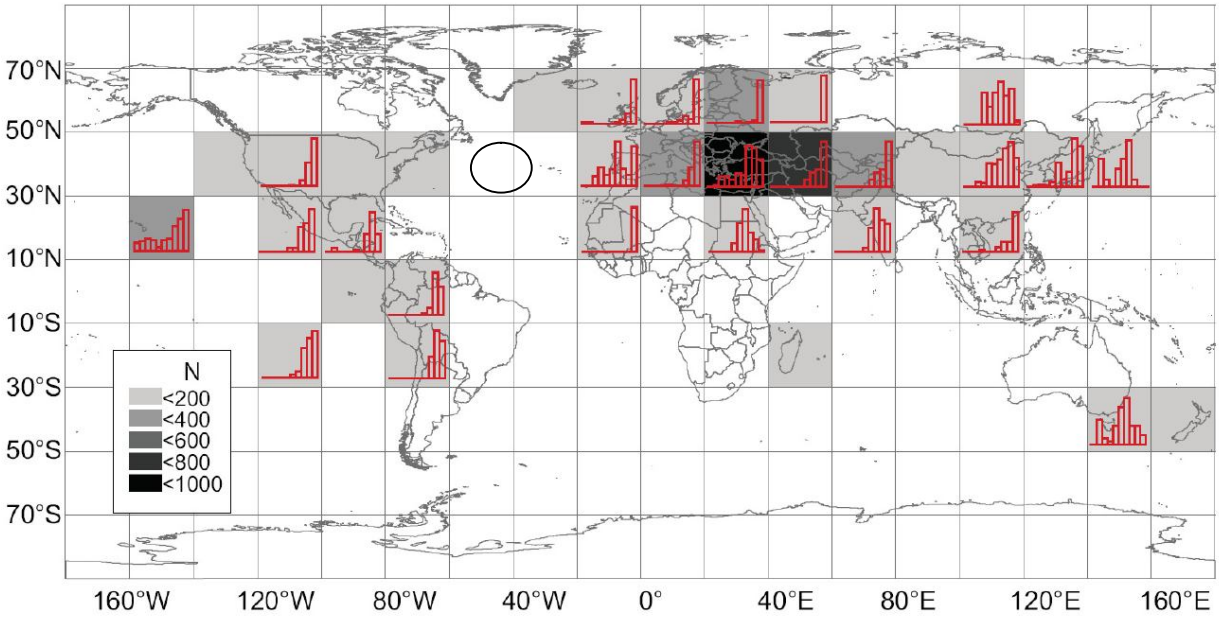

Fig. 10 - Mitra et al. (in press) show the spatial and temporal distribution of paleointensity data from the last 10 millennia available in the Archeoint database (Genevey et al. 2009). N indicates the number of paleointensity estimates and histograms indicate the distribution with time (each bar represents 1,000 years, older to the left). The circle indicates the location of the Azores Islands (PART V).

Paleointensity data from the Atlantic Ocean are very scarce. Paleointensity values were only reported from few historical (Michalk et al., 2008) and post-glacial (Schweitzer and Soffel, 1980; Stanton et al., 2011) lavas from Iceland.

9. Paleomagnetic databases

All the paleodirection and paleointensity data available are stored and described in different data sets developed since the early 1960s (e.g., Irving, 1964).

Seven databases sponsored by the International Association of Geomagnetism and Aeronomy (IAGA) were initiated by Tanaka et al. (1995), McElhinny and Lock (1996), McElhinny et al. (1997), and maintained by Perrin et al. (1998) and Perrin, M., and Schnepp, E., (2004), recently was updated with new data and published alongside a new queryable interface at http://earth.liv.ac.uk/pint/. There have been many compilations of paleointensity data over the last decade based on the so-called PINT database. In order to merge the several available IAGA databases (http://www.ngdc.noaa.gov/geomag/paleo.shtml) the MagIC database was created.

The MagIC (Magnetics Information Consortium) paleomagnetic database includes a wealth of paleodirections and paleointensity data records published. Geographic location, rock type and age of sampling sites, type of paleointensity experiments, summary statistics are information attached to the data of the database.

The GEOMAGIA50 database (Donadini et al., 2007; Korhonen et al., 2008) contains all published absolute paleointensity data for the past 50,000 years, including 8000 determination of paleodirections and paleointensity. The query form is available online at http://geomagia.ucsd.edu/geomagia/geomagiav2/query.php.

PART IV- CORRELATING IGNIMBRITES AT PANTELLERIA

10. Introduction

The Island of Pantelleria is located in the continental rift of the Strait of Sicily. The Island represents a unique case of study of a long-liver peralkaline volcanic complex, highly eruptive center, which had been active from ~300 ka. The understanding of the volcanic history is owed to the seminal paper of Mahood and Hildreth 1986, which inspired many other papers aimed to refine the current knowledge of the volcanological evolution. The volcanic history of the Island can be summarized in three major cycles, separated by two caldera collapses: the Cinque Denti Caldera dated between 45 and 50 ka, and the older Caldera La Vecchia, loosely dated between 175 and 106 ka.

In the following Chapter 11, I present 23 new paleomagnetic data used to correlate 5 of the pre-50 ka ignimbrite units (F, D, Z, Q, P) and two breccia units, and to propose a better age constrain for the oldest Caldera formation (130-160 ka), concluding that units D and Z coincide (dated 87 ka by La Felice et al., 2009), the two welded breccias are effectively correlatives (allowing to infer the Caldera La Vecchia formation around 130-160 ka). The current interest toward a more refined reconstruction of the Pantelleria volcanic history is proved by the recent papers by Scaillet et al. (2011), focused on the last 50 ka, and Rotolo et al. (2013) focused on the pre-50 ka volcanic history, both providing new geochronological dating. Particularly, Rotolo et al. (2013) conducted an extensive field-survey complemented by petrographic data and high-resolution $^{40}Ar/^{39}Ar$ dating. Author also discuss and confirm the finding obtained by Speranza et al. (2012), by new accurate $^{40}Ar/^{39}Ar$ dating.

Bull Volcanol (2012) 74:341–357
DOI 10.1007/s00445-011-0521-9

RESEARCH ARTICLE

Correlation of welded ignimbrites on Pantelleria (Strait of Sicily) using paleomagnetism

Fabio Speranza · Anita Di Chiara · Silvio G. Rotolo

Received: 4 November 2010 / Accepted: 28 June 2011 / Published online: 2 September 2011

Abstract Although the oldest volcanic rocks exposed at Pantelleria (Strait of Sicily) are older than 300 ka, most of the island is covered by the 45–50 ka Green Tuff ignimbrite, thought to be related to the Cinque Denti caldera, and younger lavas and scoria cones. Pre-50 ka rocks (predominantly rheomorphic ignimbrites) are exposed at isolated sea cliffs, and their stratigraphy and chronology are not completely resolved. Based on volcanic stratigraphy and K/Ar dating, it has been proposed that the older La Vecchia caldera is related to ignimbrite Q (114 ka), and that ignimbrites F, D, and Z (106, 94, and 79 ka, respectively) were erupted after caldera formation. We report here the paleomagnetic directions obtained from 23 sites in ignimbrite P (133 ka) and four younger ignimbrites, and from an uncorrelated (and loosely dated) welded lithic breccia thought to record a caldera-forming eruption. The paleosecular variation of the geomagnetic field recorded by ignimbrites is used as correlative tool, with an estimated time resolution in the order of 100 years. We find that ignimbrites D and Z correspond, in good agreement with recent Ar/Ar ages constraining the D/Z eruption to 87 ka. The welded lithic breccia correlates with a thinner breccia lying just below ignimbrite P at another locality, implying that collapse of the La Vecchia caldera took place at ~130–160 ka. This caldera was subsequently buried by ignimbrites P, Q, F, and D/Z. Paleomagnetic data also show that the northern caldera margin underwent a ~10° west–northwest (outwards) tilting after emplacement of ignimbrite P, possibly recording magma resurgence in the crust.

Keywords Pantelleria · Ignimbrite · Caldera formation · Paleomagnetism · Paleosecular variation of the geomagnetic field

Editorial responsibility: R. Cioni

F. Speranza (✉) · A. Di Chiara
Istituto Nazionale di Geofisica e Vulcanologia,
Sezione di Roma 2,
Via di Vigna Murata 605,
00143 Rome, Italy
e-mail: fabio.speranza@ingv.it

S. G. Rotolo
Dipartimento di Scienze della Terra e del Mare (DISTeM),
Università di Palermo,
Via Archirafi 36,
90123 Palermo, Italy

S. G. Rotolo
Istituto Nazionale di Geofisica e Vulcanologia,
Sezione di Palermo,
Via Ugo La Malfa 153,
90146 Palermo, Italy

Introduction

Pantelleria is a volcanic island at the northwest end of a continental rift that has been spreading since late Miocene times between Africa and Sicily (Rotolo et al. 2006; Civile et al. 2010). It has attracted the attention of volcanologists for over 130 years (Foerstner 1881), as it is the type locality for pantellerite, a strongly peralkaline Fe-rich rhyolite, which has unusual geochemistry, magma rheology, and associated volcanic features. Rock exposures on Pantelleria record a volcanic history exceeding 300,000 years (Mahood and Hildreth 1986), but much of the island is covered by the widespread 45–50 ka Green Tuff ignimbrite (thought to relate to the Cinque Denti caldera, Fig. 1), and younger, mostly silicic, and subordinate basaltic, lavas, and scoria cones (Civetta et al. 1988).

Rocks that document the pre-50 ka history of Pantelleria are mostly confined to cliff sections in isolated coves

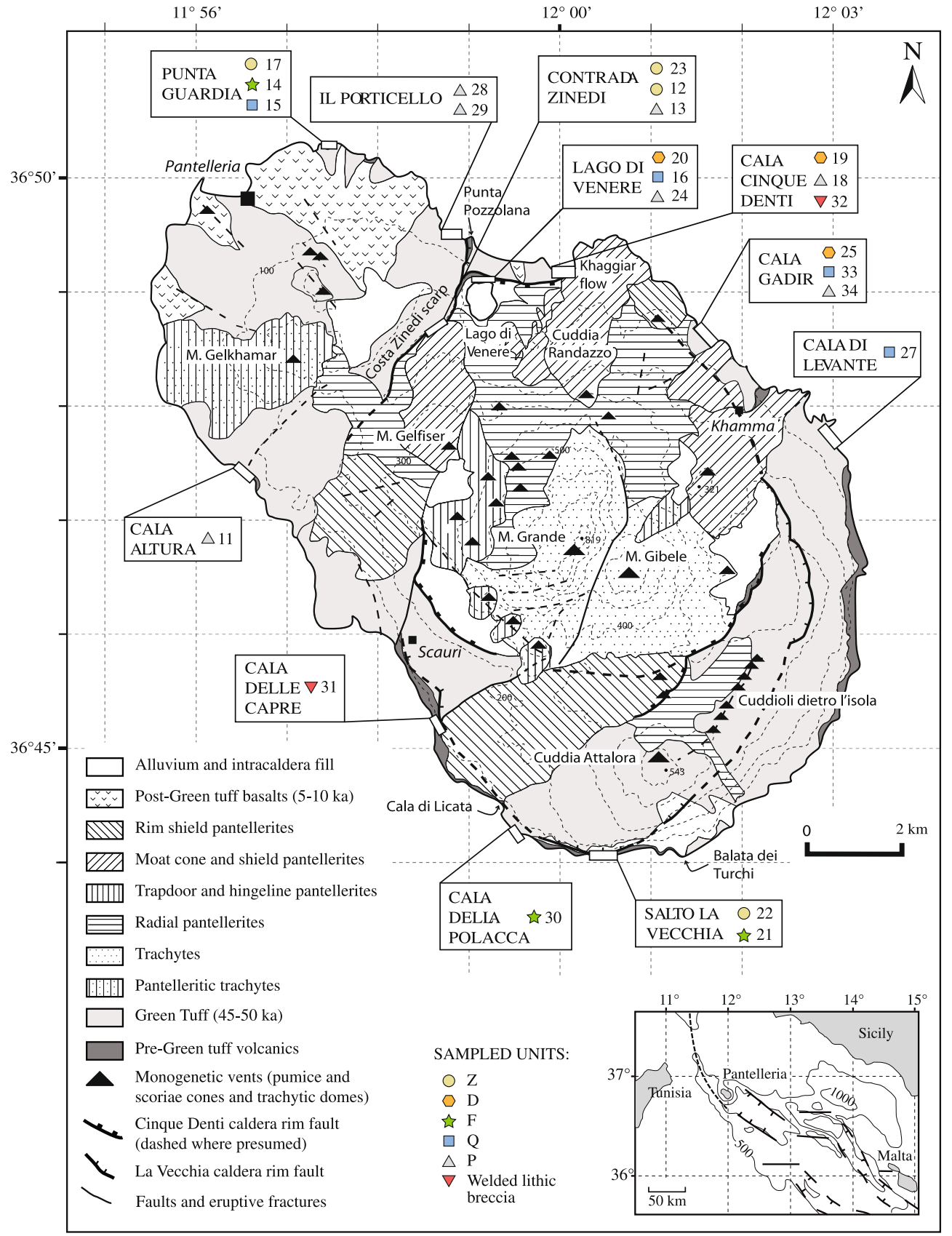

Fig. 1 Geological map of Pantelleria and location of the paleomagnetic sampling sites (the "Cos" suffix of each site, Table 1, is omitted). Caldera scarps and nomenclature of the sampled units are from Mahood and Hildreth (1986)

(Figs. 1 and 2) described in a seminal paper of Mahood and Hildreth (1986), who renamed and recorrelated some of the trachytic to pantelleritic ignimbrites previously studied by Wright (1980), and provided K/Ar ages. We use the stratigraphic nomenclature and ages of Mahood and Hildreth (1986) in this paper.

Along the southern coast, between Scauri and Balata dei Turchi (Fig. 1), there is evidence of an older caldera wall ("La Vecchia caldera" of Mahood and Hildreth 1986), splendidly exposed at and near Salto La Vecchia (Figs. 1 and 2g). The age of this caldera is bracketed between 175 ka (the age of the truncated welded tuff M), and 106 ka (the age of the well-dated ignimbrite F). Ignimbrite F, along with overlying ignimbrites D and Z, clearly laps the caldera wall (Figs. 2g and 3). Further west, at Cala delle Capre and Cala di Licata, a purplish-brown, lithic- and crystal-rich welded breccia located just below unit F (Fig. 2f) was considered by Mahood and Hildreth (1986) an obvious candidate for the eruptive unit related to caldera collapse. Unfortunately, the existence of low-precision K/Ar ages from welded lithic breccia at Cala delle Capre (127±37, 104±53 ka; Table 1) hampered accurate dating of the time of caldera formation.

Along the western and northern coast of Pantelleria, and around Lago di Venere, units P and Q, similarly densely welded, rheomorphic ignimbrites rich in anorthoclase crystals, crop out below units F, D, and Z, i.e., below tuffs lapping onto the La Vecchia caldera wall along the southern coast. Their K/Ar ages (133±3 and 114±4 ka, respectively) turn out to be intermediate to ages gathered from units M and F. Consequently, Mahood and Hildreth (1986) considered unit Q (exhibiting a more seriate size distribution of alkali feldspar and more crystal-rich lithic fragments than unit P) as potential equivalent of the lithic-rich breccia of Cala delle Capre. On this basis, they assigned a 114 ka age to the collapse that formed the La Vecchia caldera.

However, as Mahood and Hildreth (1986) themselves admit, correlation of pre-50 ka ignimbrites at Pantelleria is difficult, because (a) as a rule there is no exposure continuity between sea cliff sections and (b) primary features of ignimbrites (e.g., internal structures, presence of different flow units, proportion, and sizes of crystals/juvenile fragments) are strongly variable within the same unit, and not strictly in response of distal/proximal facies variation within a given pyroclastic density current (e.g., Sumner and Branney 2002; Andrews and Branney 2011). Consequently, the ignimbrite correlations put forward by Mahood and Hildreth (1986) essentially rely upon physical continuity and position within a recognizable sequence corroborated by the K/Ar ages.

These limits imply that both correlation along the island's cliffs of the five ignimbrites erupted since 133 ka (age of unit P), and identification of the La Vecchia caldera-forming ignimbrite (thus precisely dating caldera formation) await further verification. Radiometric dating can be useful for dating and have undoubtedly yielded the chronologic framework for the volcanic history of Pantelleria, yet there are some limits when used as a tool for correlating ignimbrite outcrops. Only a few outcrops can be dated, and Q–F and D–Z ignimbrites yielded K/Ar age differences (few thousand year (kyr)) that are comparable to their dating errors (Mahood and Hildreth 1986; Fig. 3 and Table 1). Recently, La Felice et al. (2009) have reported new $^{40}Ar/^{39}Ar$ ages for units D and Z which narrow considerably the age errors to less than 2 kyr (Fig. 3 and Table 1). Thus new Ar/Ar data have the potential to resolve the pre-50 ka volcanic history of Pantelleria, but again few outcrops can be dated (two ages were reported by La Felice et al. (2009), additional ages will be reported in a forthcoming paper; Stéphane Scaillet, personal communication).

In this paper, we demonstrate how paleomagnetic directions of ignimbrites can be a useful correlative tool, providing important constraints for interpretation of the pre-50 ka volcanic history of Pantelleria. When magmas are erupted and cool, they record an instantaneous snapshot of the characteristics of the local geomagnetic field, which undergoes continuous changes with time. The directional variation of the ancient geomagnetic field as witnessed by the paleomagnetic investigation of sedimentary sequences, volcanic rocks, and archeological archives, is called paleosecular variation (PSV) of the geomagnetic field. Although the geomagnetic field is predominantly dipolar, the nondipole component imparts a significant regional component to the geomagnetic field, such that PSV curves are region-specific (Merrill et al. 1996). The PSV curve for Europe is, perhaps, the best defined, given that the abundant archeological artifacts and geological sequences have yielded a wealth of paleomagnetic data. At the coordinates of southern Italy, PSV directional swings reaching ca. 40° in declination and 30° in inclination occurred during the Holocene (Speranza et al. 2008). A recent compilation of all European geomagnetic–archeomagnetic data sets (Pavón-Carrasco et al. 2009) has shown that during the last 3,000 years, the field reached a maximum rate of change of 7° per 100 years in the central Mediterranean domain.

If this rate of change is extrapolated to the geological past, a paleomagnetic direction defined with a precision of 2–4° (a value routinely obtained using classical paleomagnetic techniques on rapidly cooled volcanic rocks) should make it possible to ascertain whether two volcanic units formed within 100–200 years of one another and are synchronous or effectively so. It follows that for volcanic deposits formed some tens of kyr ago (as is the case of ignimbrites of Pantelleria), paleomagnetism can represent a correlation tool even more precise than high-resolution

Fig. 2 Characteristics of the studied ignimbrites (see Fig. 1 and Table 1 for site locations). Pantelleritic lava in Fig. 2f was erupted from Cuddie Bellizzi at 19±5 ka. Attalora fall (Fig. 2g) was erupted from the nearby Attalora volcanic center at 69±9 ka (Mahood and Hildreth 1986)

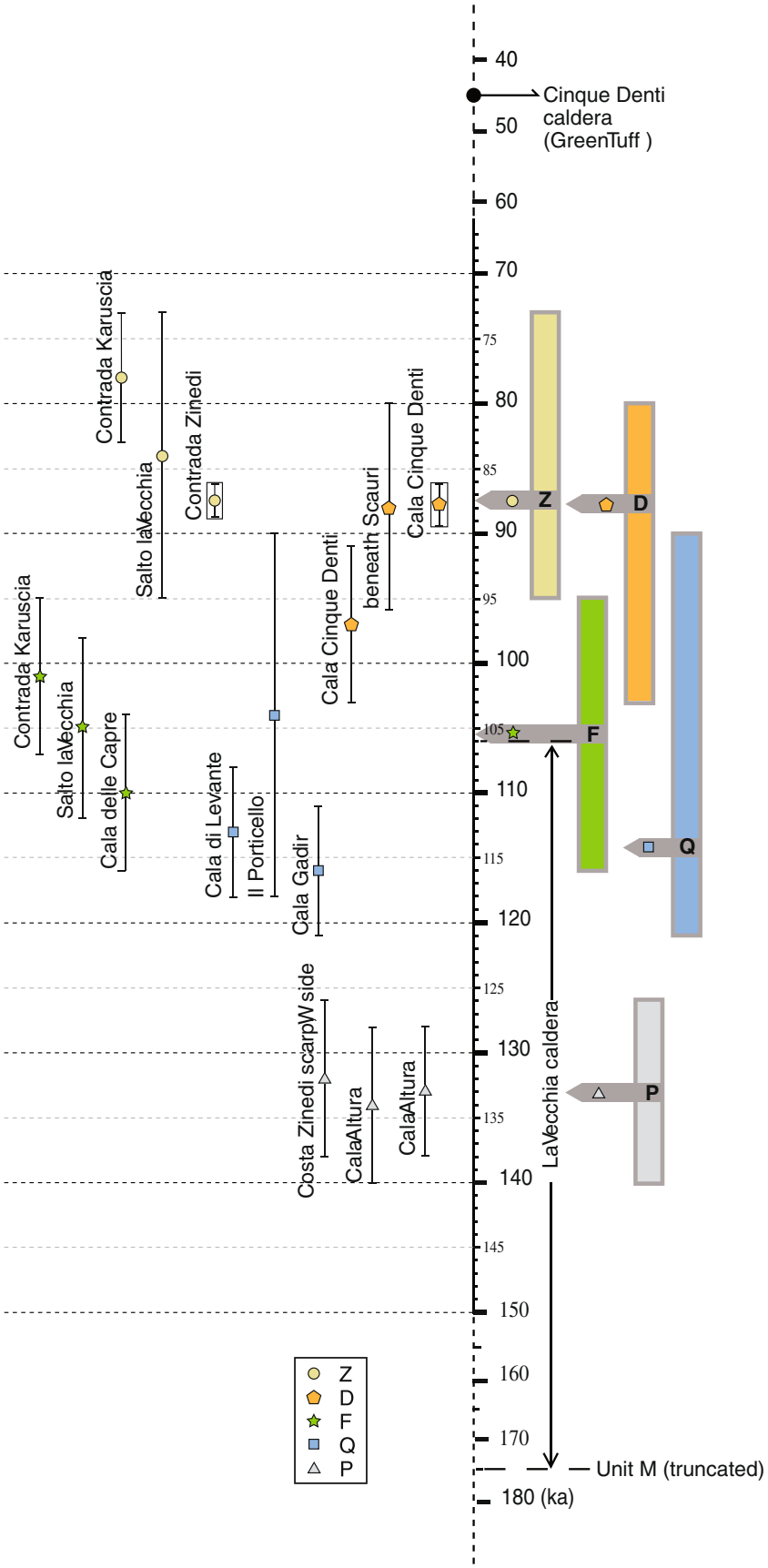

Fig. 3 K/Ar (*line error bars*, Mahood and Hildreth 1986) and Ar/Ar (*box error bars*, La Felice et al. 2009) ages reported for the studied ignimbrites. Indicated mean ages correspond to mean weighted K/Ar ages for units P, Q, and F (as reported by Mahood and Hildreth 1986), and are equated to Ar/Ar ages for units D and Z

Table 1 Location of sampling sites at Pantelleria and indipendent age constrains from geochronologic evidence

Site	Unit	Locality	Latitude °N	Longitude °E	Alt. (m asl)	K/Ar age (ka)	Ar/Ar age (ka)
Cos11	P	Cala Altura	36.7907	11.94393	10	133±5, 134±6	
Cos12	Z	Contrada Zinedi	36.81327	11.97812	212		
Cos13	P	Contrada Zinedi	36.81297	11.97767	204	132±6	
Cos14	F	Punta Guardia	36.83765	11.96305	18	101±6*	
Cos15	Q	Punta Guardia	36.8377	11.96285	11		
Cos16	Q	Lago di Venere	36.81907	11.98743	23		
Cos17	Z	Punta Guardia	36.8376	11.96315	22	78±5*	
Cos18	P	Cala Cinque Denti	36.8193	12.00122	15		
Cos19	D	Cala Cinque Denti	36.81955	12.00042	23	97±6	87.9±1.7
Cos20	D	Lago di Venere	36.81919	11.98776	26		
Cos21	F	Salto La Vecchia	36.73675	12.0113	262	105±7	
Cos22	Z	Salto La Vecchia	36.73675	12.0113	262	84±11	
Cos23	Z	Contrada Zinedi	36.81327	11.97812	212		87.5±1.3
Cos24	P	Lago di Venere	36.81871	11.98558	5		
Cos25	D	Cala Gadir	36.81063	12.02812	5		
Cos27	Q	Cala di Levante	36.79613	12.0498	2	113±5	
Cos28	P	Il Porticello	36.82561	11.98176	16		
Cos29	P	Il Porticello	36.82576	11.98169	3		
Cos30	F	Cala della Polacca	36.73835	11.99213	10		
Cos31	Br	Cala delle Capre	36.75307	11.97901	43	127±37, 104±53	
Cos32	Br	Cala Cinque Denti	36.81966	12.00042	8		
Cos33	Q	Cala Gadir	36.81046	12.02773	5	116±5	
Cos34	P	Cala Gadir	36.81046	12.02773	5		

Site coordinate and altitude were gathered by a Garmin GPS using WGS84 datum. References for geocronologic ages: K/Ar data (Mahood and Hildreth 1986); Ar/Ar data (La Felice et al. 2009). Unit names are after Mahood and Hildreth (1986), except for unit Br (Welded lithic breccia). *K/Ar data from Contrada Karuscia, 200 m south of Punta Guardia

Ar/Ar dating, which in the best cases may yield age error ranges of some centuries. However, it must be kept in mind that geochronologic data are necessary to provide a first-order age framework for investigated units because paleomagnetism cannot provide absolute ages for such old rocks. It is possible that two volcanic units of different age may share the same paleomagnetic direction by chance, because the geomagnetic field may reoccupy the same directions after a few centuries or millennia.

During the last two decades, paleomagnetic directions recorded by Holocene lavas at several active Italian volcanoes have been compared to independently available reference PSV curves of Europe, yielding an excellent chronologic framework of eruptions (Rolph and Shaw 1986; Tanguy et al. 2003; Speranza et al. 2006, 2008; Vezzoli et al. 2009). At Pantelleria, the paleomagnetism of the most recent lavas and scoriae has constrained the most recent silicic activity of the island to 5.9–6.8 ka (Speranza et al. 2010).

In contrast, no reliable PSV directional reference curves exist for pre-Holocene times implying that the paleomagnetism of ~80–130 ka ignimbrites from Pantelleria cannot yield absolute emplacement ages but can be used as a correlative tool. The use of PSV curves to this end has already been demonstrated for lavas from Hawaii (Hagstrum and Champion 1994), but not for ignimbrites to the best of our knowledge.

Volcanic history of Pantelleria

Volcanic rocks of Pantelleria comprise strongly peralkaline rhyolites (or pantellerites, as Pantelleria is their type locality) and trachytes, and subordinate (~5% of erupted volumes) mildly alkaline basalts (Cornette et al. 1983; Civetta et al. 1984, 1988; Mahood and Hildreth 1986; Rotolo et al. 2007).

The focus of sub-aerial volcanic activity apparently propagated northwestward with time. The oldest products (239–325 ka pantelleritic and trachytic lavas) are exposed along the S–SE coast of the island (Mahood and Hildreth 1986). An older alkali granite lithic clast

(500±17 ka) from ignimbrite Z has also been documented by Ar/Ar dating (Rotolo and Villa 2001). Subsequent explosive activity yielded several ignimbrites (with subordinate lavas and pumice fall deposits), that dominated Pantelleria's history from 175 ka (unit M) to 45–50 ka (Green Tuff; Villari 1969; Cornette et al. 1983; Mahood and Hildreth 1986). Synchronous with ignimbrite emplacement, two overlapping calderas formed: the older La Vecchia caldera is poorly bracketed by ages of ignimbrite M and F (175 and 106 ka, respectively), while the Cinque Denti caldera (called Monastero caldera by Cornette et al. 1983) is constrained to have formed at 45–50 ka by the K/Ar age of the widespread Green Tuff, thought to record the caldera-forming eruption (Mahood and Hildreth 1983, 1986; Civetta et al. 1988). The Costa Zinedi scarp in the NW of the Island (Fig. 1) is mantled by ignimbrite P and younger ignimbrites, and it is thought to be the remnant of a caldera rim that is older than La Vecchia caldera, reactivated during more recent collapses (Mahood and Hildreth 1986).

According to Civetta et al. (1988, 1998) the post-50 ka silicic activity can be grouped in six eruptive cycles (the first being represented by the Green Tuff eruption), each separated by several kyr of quiescence. The most recent silicic activity was characterized by emplacement of pumice cones, associated lava domes, and the voluminous ~6.0 ka pantelleritic Khaggiar lava (Speranza et al. 2010). A submarine basaltic eruption ~4 km NW of Pantelleria in 1891 AD was the most recent activity (Washington 1909).

Characteristics of the studied ignimbrites

This paper adopts the nomenclature, K/Ar ages and descriptions of ignimbrites given in Mahood and Hildreth (1986; Figs. 1, 2 and 3, Table 1). We have integrated our field observations and petrographic analyses with these. Whole rock chemistry of individual pyroclastic units shows some variations from place to place.

The studied ignimbrites are frequently characterized by rheomorphism, i.e., the ductile deformation that affects the hot and welded pyroclastic material, during and soon after deposition (e.g., Sumner and Branney 2002; Branney et al. 2004; Andrews and Branney 2011, and references therein). Ignimbrites of peralkaline magmas are intrinsically prone to rheomorphism due to the alkali excess over alumina in pantellerite that, coupled to halogen abundance, strongly reduce melt viscosity (Mahood 1984).

According to Macdonald's (1974) classification scheme for peralkaline rocks, unit F is a pantellerite, units D and Z straddle the pantellerite/comendite boundary, whereas units P and Q are less peralkaline comendites. Their principal features are briefly outlined below, from the oldest to the youngest deposit.

At Cala Cinque Denti we sampled a ≥4 m thick trachy-comenditic welded lithic breccia, neither dated nor correlated so far, lying just below (older than) ignimbrite P (Fig. 2c). The lithic breccia is a heterolithic and chaotic assemblage of poorly sorted lithic blocks (sometimes imbricated and welded), with abundant lumps of juvenile spatter. On the opposite (SW) side of the island, at Cala delle Capre (Fig. 1), a similar purple–brown, lithic- and crystal-rich comenditic welded lithic breccia up to 20 m thick with abundant juvenile spattered bombs, crops out below ignimbrite F (Fig. 2f). The lithic breccia from Cala delle Capre yielded low-precision 127±37 and 104±53 ka K/Ar ages (Mahood and Hildreth 1986).

Unit P is a welded comenditic ignimbrite with rheomorphic folds (Fig. 2d), and is exposed along the northern coast and the Costa Zinedi scarp. It is characterized by a light gray glassy heterolithic matrix, bearing seriate and tabular crystals of 1 cm alkali feldspar (~30% of the matrix), and rare and subrounded lithics. Its thickness varies from 3 up to 10 m across palaeotopography. Three K/Ar ages from Cala Altura and Costa Zinedi constrain ignimbrite P to 133.1±3.3 ka.

Similarly, rheomorphic comenditic ignimbrite Q (Branney et al. 2004) varies in thickness from 8 to more than 13 m (Fig. 2b). It is characterized by a brown vesicular matrix of glassy tuff with seriate and elongate crystals of 5 mm alkali feldspar, brown, black and gray subrounded aphyric lithics, and pumice lapilli. Mahood and Hildreth (1986) interpreted unit Q as having formed during formation of La Vecchia caldera, and they correlated it with the welded breccia of Cala delle Capre. Because unit Q is K/Ar dated at 113.9±3.6 ka (ages were gathered from three localities), Mahood and Hildreth (1986) place at 114 ka the formation of La Vecchia caldera.

Ignimbrite F varies with palaeotopography from 0.8 to 7 m at Cala delle Capre (Fig. 2f) and commonly has a 5 cm thick basal vitrophyre. It is massive to laminated. The lower and upper parts of the flow contain ca. 5% of 2 mm long and 15–20% of 3–4 mm long (respectively) alkali feldspar crystals. The upper portion also grades into a 30–40 cm thick welded breccia, very rich in fine-grained material. Three K/Ar ages constrain ignimbrite F to 105.7±3.5 ka.

Ignimbrite D, mostly exposed along the NE cliffs of Pantelleria (Fig. 2c, e), is a 5–12 m thick generally massive ignimbrite characterized by a fine heterolithic matrix containing rare black–red lithics and ca. 20 vol.% of alkali feldspar crystals. Two K/Ar determinations yielded a mean 93.9±4.7 ka age (Mahood and Hildreth 1986) and 87.9±1.7 ka $^{40}Ar/^{39}Ar$ age has been reported from Cala Cinque Denti (Figs. 1, 2, and 3 and Table 1; La Felice et al. 2009).

Unit Z crops out along the S–SW and northern cliffs of Pantelleria, and along the Costa Zinedi scarp (Figs. 1 and 2). It is a 2–6 m thick ignimbrite comprising at least three

sub-units, recognizable only along the northern coast of the island. Above the basal glassy vitrophyre (up to 10 cm thick), a peculiar layer with abundant rounded pumice lapilli (up to 5 cm in length), is variably scavenged out by strong seawater alteration. Upper layers of the ignimbrite become laminated to massive, and increasingly fine-grained upwards. The average alkali feldspar content is up to 15 vol.%. Potassium–argon ages (two determinations) yielded a 79.3±4.2 ka age (Mahood and Hildreth 1986) and an Ar/Ar 87.5±1.3 ka age was obtained at Contrada Zinedi (La Felice et al. 2009).

Sampling and methods

During 2009 and 2010, we sampled 23 sites (from 11 different stratigraphic sections) in the ignimbrites of Pantelleria (Figs. 1 and 2; Table 1). Four and five sections are located along the southern and northern coast (respectively), and two sections are subaerial scarps of Costa Zinedi and the Cinque Denti caldera rim at Lago di Venere (Fig. 1).

One site was sampled in the welded lithic breccia of Cala delle Capre (Fig. 2f), and an additional site was sampled in the thinner and uncorrelated welded breccia of Cala Cinque Denti (Fig. 2c). Seven and four sites were sampled in rheomorphic units P and Q, respectively, predominantly from the northern coast and the scarps around Lago di Venere. Three, three, and four sites were collected in younger ignimbrites F, D, and Z (respectively), from both sea cliffs and internal tectonic scarps (Fig. 2). Sites Cos12–23 and 28–29 were sampled at different stratigraphic levels of units Z and P exposed at Contrada Zinedi and Il Porticello (respectively, Fig. 1), in order to test the reliability of the paleomagnetic method as proxy for ignimbrite correlation.

At each site we drilled 10–19 (15 on average) 2.5-cm diameter cores using a petrol-powered portable drill cooled by water. We spaced the cores as much as possible in the studied ignimbrites in an attempt to gather a well-averaged, representative paleomagnetic direction for each volcanic unit. Cores were systematically drilled in the ignimbrite matrix and subordinately in juvenile clasts. Visible lithic clasts were rigorously avoided. All cores were oriented by both a magnetic and a sun compass. The local field declination values (i.e., the difference between the magnetic and sun compass readings) are generally $\leq|5°|$, similar to evidence gathered by Speranza et al. (2010) from the most recent silicic products of the island.

The sampled cores were cut into standard cylindrical specimens, and the remanent magnetization of one specimen per core was measured in the shielded room of the paleomagnetic laboratory of the Istituto Nazionale di Geofisica e Vulcanologia (Roma) using a 2G Enterprises DC-SQUID cryogenic magnetometer. For all specimens, alternating field (AF) cleaning was carried out by translating the specimens through three perpendicular coils in-line with the magnetometer, using 14 demagnetization steps per specimen, up to a maximum peak field of 150 mT. In addition, two twin specimens per site were thermally cleaned in 11 demagnetization steps up to a maximum temperature of 600°C, using a Pyrox shielded oven. Alternating field and thermal demagnetization data were plotted on orthogonal demagnetization diagrams (Zijderveld 1967), and the magnetization components were isolated by principal component analysis (Kirschvink 1980). Site mean paleomagnetic directions were computed using Fisher's (1953) statistics.

Additional magnetic analyses were carried out on 30 specimens from 15 representative sites to characterize the magnetic mineralogy. Hysteresis properties were measured using a Princeton Measurement Corporation MicroMag alternating gradient magnetometer (model 2900) with a maximum applied field of 1 T. The measured hysteresis parameters include saturation magnetization (M_s), saturation remanent magnetization (M_{rs}), and coercive force (B_c). Acquisition of an isothermal remanent magnetization (IRM) and subsequent back-field DC remagnetization (both in a succession of fields up to 1 T), were also carried out on the same specimens. Data were also used to compute the coercivity of remanence (B_{cr}).

For 15 selected specimens, we also measured the variation of the low-field magnetic susceptibility during a heating and cooling cycle performed in air, from room temperature up to 700°C, using an AGICO KLY-3 kappa-bridge coupled with a CS-3 furnace. The Curie point of the magnetic minerals present in the samples was determined from the thermomagnetic curves as the temperature, or range of temperatures, at which paramagnetic behavior starts to dominate.

Results

All investigated specimens show low coercivity values (B_c is between 8 and 40 mT) and reach saturation at ca. 0.3 T (Fig. 4). The hysteresis parameters were plotted in a Day plot (Day et al. 1977; Dunlop 2002) of ratio M_{rs}/M_s against the ratio of remanent coercive force to coercive force (B_{cr}/B_c). Most of the samples follow the theoretical mixing curve for single domain (SD) and multidomain magnetite, although three specimens are located on the SD–superparamagnetic mixing curve (Fig. 4). Samples from the same ignimbrite frequently yield different hysteresis parameters, implying that magnetic properties show a large range of variation within the same lithofacies and cannot be used as correlative tool for volcanic rocks.

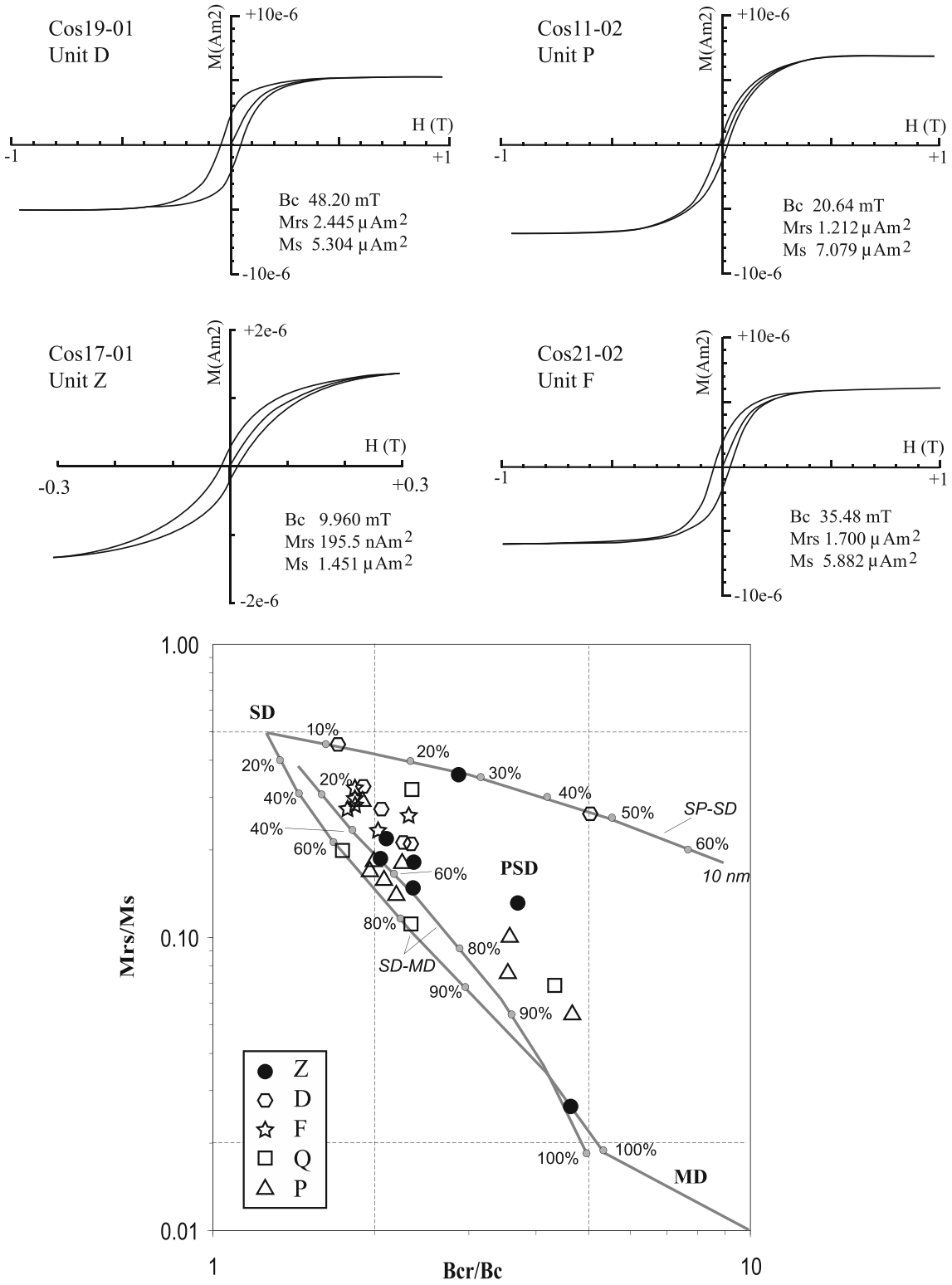

Fig. 4 Representative hysteresis data and plot of hysteresis ratios (M_{rs}/M_s versus B_{cr}/B_c, after Day et al. 1977) for the collection of specimens measured

Thermomagnetic curves predominantly indicate almost pure magnetite only, with a single Curie temperature at ~580–600°C (Fig. 5a–b). For some of these samples, the additional presence of a minor amount of hematite is suggested by magnetic susceptibility values clearly higher than zero at T>600°C. Only four out of 15 specimens (two from ignimbrite P and two from Z) show multiple Curie temperatures (in the range 200–600°C), suggesting variable

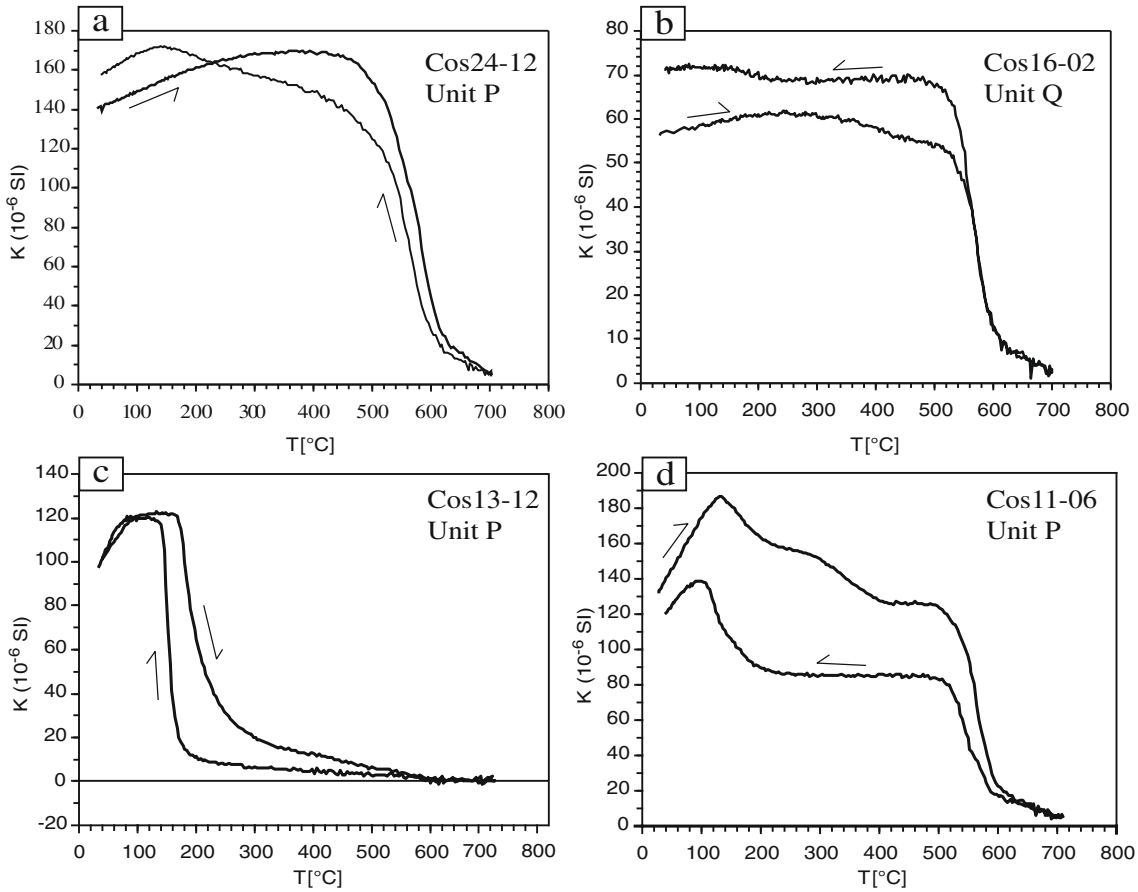

Fig. 5 Representative thermomagnetic cycles

composition in the titanomagnetite series (Fig. 5c–d). We note that the reported predominant ferromagnetic mineral in comendites is Ti-rich magnetite, being gradually substituted by ilmenite and aenigmatite in the more evolved pantellerite rocks (White et al. 2005; Rotolo et al. 2007; Di Carlo et al. 2010). The apparent inconsistency with our rock magnetic results, which point to nearly pure magnetite as dominant magnetic mineral, can be resolved considering our scanning electron microscope observations of comendites, showing that Ti-rich magnetite underwent oxy-exsolution processes, unmixing trellis-type lamellae of ilmenite and magnetite.

A well-defined characteristic remanent magnetization (ChRM) was isolated in the 20–150 mT field interval (Fig. 6) for all AF-cleaned specimens, except those from ignimbrite F and Z at Salto La Vecchia (sites Cos21–22). Here, aberrant components were observed up to variable AF fields and for seven specimens up to the maximum available AF peak field of 150 mT. As sites of Salto La Vecchia are located on top of a 260 m high sea cliff (Fig. 2g), they may have been struck by lightning, inducing a relatively hard IRM in the exposed rocks. Thermally cleaned specimens systematically yielded a ChRM in the 250–600°C temperature interval (Fig. 6). Twin specimens of samples from Salto La Vecchia revealing aberrant ChRMs after AF cleaning, yielded again aberrant ChRMs in the 300–600°C temperature interval (Fig. 6).

None of the ignimbrites studied by us had been paleomagnetically investigated before. Zanella (1998) collected from several sites products of eruptions younger than 150 ka, but only rhyolite and basalt lavas and the Green Tuff ignimbrite were sampled.

Discussion

Petrological data indicate that the pre-eruptive magmatic temperatures of the ignimbrites were in the 750–920°C range (White et al. 2009; Di Carlo et al. 2010). Higher temperatures characterize the less evolved comenditic ignimbrites P and Q, whereas lower temperatures characterize the more evolved ignimbrites. Ignimbrite emplacement temperatures were well above the 580°C Curie temperature of magnetite, the predominant ferromagnetic mineral according to our rock magnetic results. Therefore, the studied rocks are expected to have thoroughly recorded the local PSV during cooling.

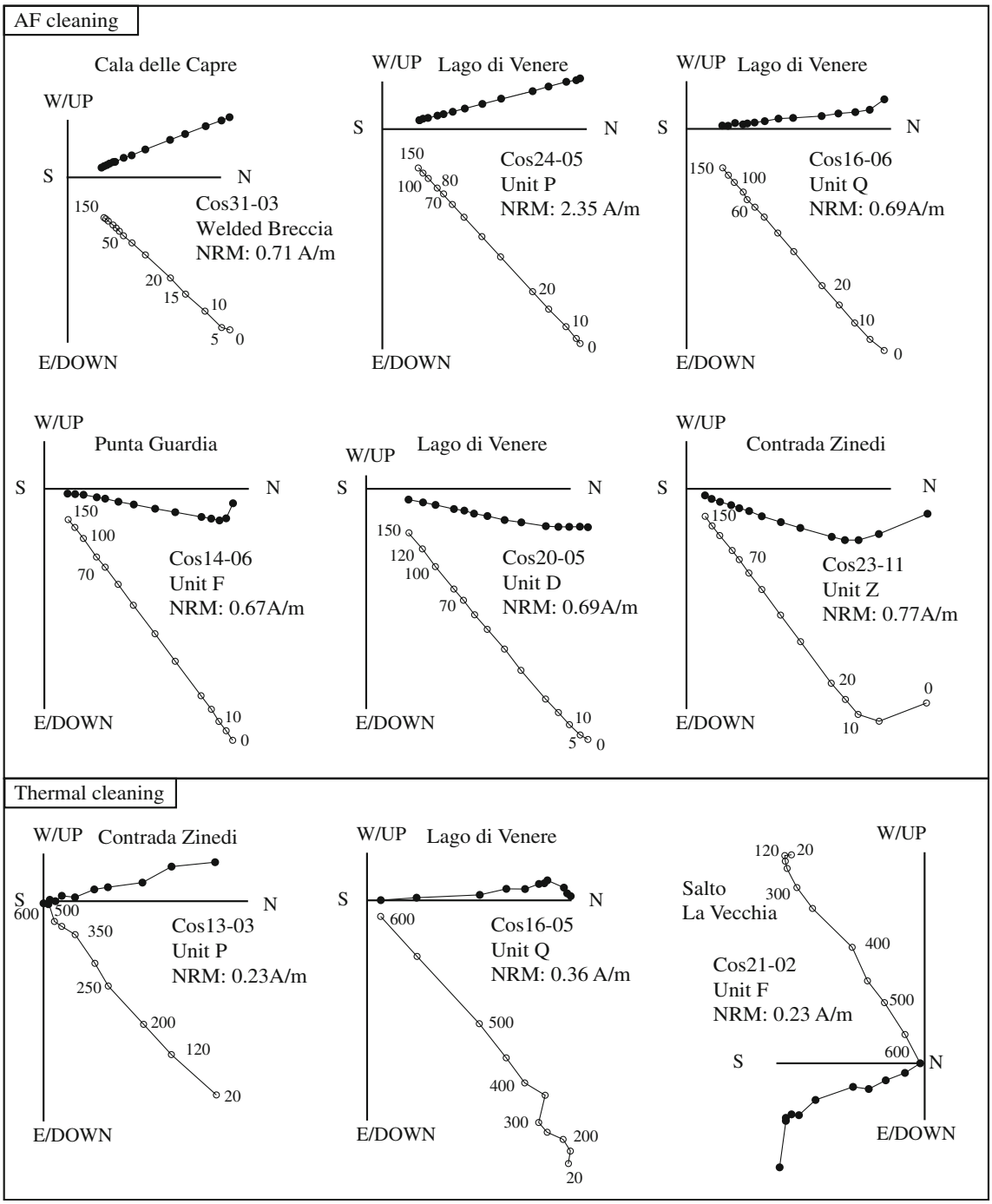

Fig. 6 Orthogonal vector diagrams of typical demagnetization data, in situ coordinates. *Open and solid dots* represent projections on the vertical and horizontal planes, respectively. Demagnetization step values are in mT and °C for the AF and thermal cleaning data, respectively

Accordingly, demagnetization diagrams systematically reveal from 250 to 600°C a unique magnetization component, generally less than 20° away from the geocentric axial dipole field direction (D=0°, I=56.2°) expected at Pantelleria (Figs. 6 and 7; Table 2). Moreover, although mean paleomagnetic declinations exhibit a considerable ~50° scatter (from −22° to 29°, Fig. 7), paleomagnetic directions from a single volcanic unit are generally similar. The paleomagnetic scatter, therefore, should predominantly reflect PSV of the geomagnetic field recorded by the studied volcanics.

The mean α_{95} value of our data set is 2.1° (from 1.5° to 2.7°, excluding sites Cos21–22 from Salto La Vecchia, where statistics are biased by the IRM induced by lightning,

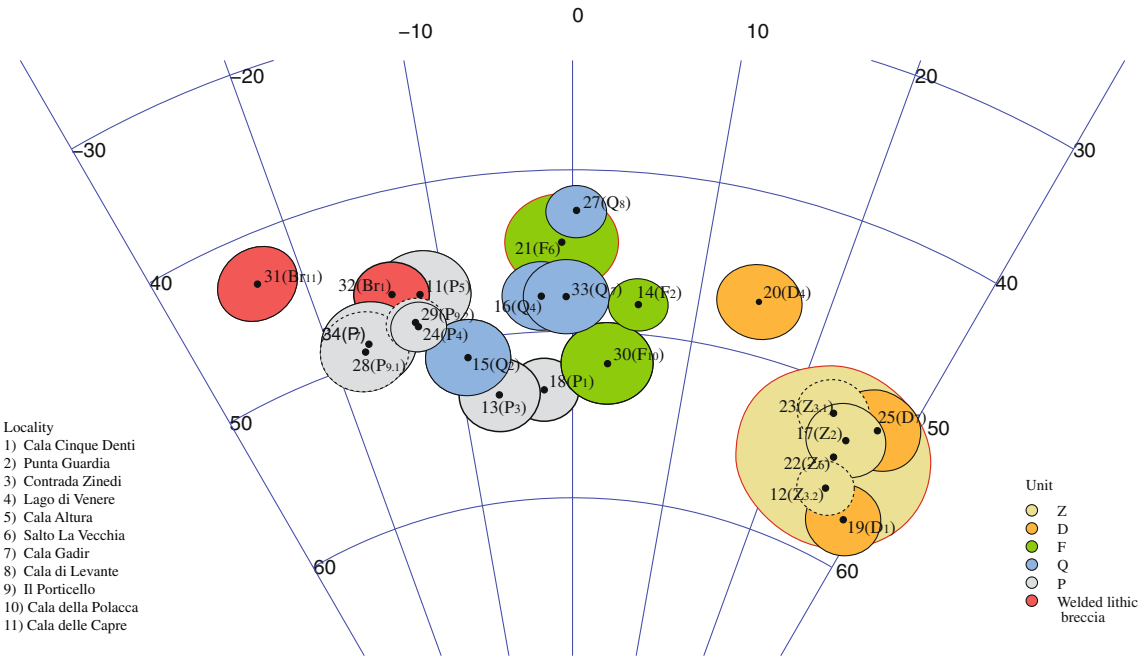

Fig. 7 Equal-area projection (lower hemisphere) of mean paleomagnetic directions from ignimbrites of Pantelleria (the "Cos" suffix of each site is omitted). Units are in parentheses, unit subscripts correspond to locality numbers detailed on the left. Ellipses about the paleomagnetic directions are the projections of the relative α_{95} cones. Ellipse margins of directions from Breccia and units P from Cala Cinque Denti and Contrada Zinedi (sites Cos13, Cos18, and Cos32) are in bold (see text). Ellipse margins of Z–F sites from Salto La Vecchia (biased by lightning) are in red. Ellipse margins of Z and P test sites from Contrada Zinedi and Il Porticello (respectively) are *dashed*. All paleomagnetic directions are listed in Table 2

Table 2 Mean paleomagnetic directions from Pantelleria and paleomagnetically inferred units

Site	n/N	*D* (°)	*I* (°)	*k*	α_{95}(°)	Locality	Unit
Cos11	14/15	348.1	46.8	218	2.7	Cala Altura	P
Cos12	15/15	25.6	56.0	597	1.6	Contrada Zinedi	**Z=D**
Cos13	15/15	353.3	53.6	290	2.2	Contrada Zinedi	P
Cos14	15/15	5.3	48.2	559	1.6	Punta Guardia	F
Cos15	15/15	351.0	51.1	280	2.3	Punta Guardia	**P**
Cos16	15/15	357.5	47.8	332	2.1	Lago di Venere	Q
Cos17	16/16	25.4	52.9	287	2.2	Punta Guardia	**Z=D**
Cos18	13/15	357.4	53.5	484	1.9	Cala Cinque Denti	P
Cos19	14/15	28.6	57.2	355	2.1	Cala Cinque Denti	**D=Z**
Cos20	17/17	14.8	46.8	234	2.3	Lago di Venere	**F? D/Z?**
Cos21	9/15	359.2	44.5	292	3.0	Salto La Vecchia	F
Cos22	15/16	25.0	54.1	60	5.4	Salto La Vecchia	**Z=D**
Cos23	13/15	23.4	51.7	421	2.0	Contrada Zinedi	**Z=D**
Cos24	15/15	347.4	48.7	656	1.5	Lago di Venere	P
Cos25	14/15	27.5	51.5	276	2.4	Cala Gadir	**D=Z**
Cos27	18/18	0.2	42.6	459	1.6	Cala di Levante	Q
Cos28	18/18	342.6	49.3	251	2.4	Il Porticello	P
Cos29	12/12	347.2	48.5	732	1.6	Il Porticello	P
Cos30	15/16	3.0	51.9	233	2.5	Cala della Polacca	F
Cos31	19/19	336.7	43.1	241	2.2	Cala delle Capre	Br
Cos32	17/18	345.9	46.4	307	2.0	Cala Cinque Denti	Br
Cos33	10/10	359.5	47.9	437	2.3	Cala Gadir	Q
Cos34	10/11	343.1	49.0	396	2.6	Cala Gadir	P

n/*N* is the number of samples yielding interpretable demagnetization data/total number of cores drilled at a site; *D* and *I* are paleomagnetic declination and inclination, respectively; *k* and α_{95} are statistical parameters after Fisher (1953). Units in bold are inferred after this study

Table 2). This value is smaller than that derived (using identical methods, instruments, and paleomagnetic laboratory), after investigating lavas and scoriae from Stromboli (3.0–3.4°), Etna (4.5°), and Pantelleria (3.7°; Speranza et al. 2004, 2006, 2008, 2010). Thus it seems that welded ignimbrites yield paleomagnetic directions that provide even better constraints than lavas, opening significant perspectives for future PSV investigation of such pyroclastic successions. Correlative ignimbrites are expected to yield similar paleomagnetic directions. To evaluate similarity using statistical methods, Lanza and Zanella (2003) and Speranza et al. (2010) used the McFadden and Lowes (1981) test to verify whether volcanic units (predominantly lavas) share a common true mean paleomagnetic direction, and can therefore be regarded as synchronous and correlative. We have used the McFadden and Lowes (1981) test for sites Cos12 vs. Cos23 and Cos28 vs. Cos29, sampled at different stratigraphic levels of ignimbrites Z and P, respectively (Figs. 1 and 7; Tables 1 and 2). Surprisingly, we find that in both cases the two adjacent sites, though yielding very similar paleomagnetic directions (angular distance is 4.5° and 3.1°, respectively), and in one case showing overlapping confidence cones, do not share a common true mean direction. We conclude that the McFadden and Lowes (1981) test is unsuitable to address correlations of ignimbrite outcrops, at least on Pantelleria, probably because the α_{95} values are very low, compared to sites sampled in sediments.

Most likely causes for the observed recording bias in ignimbrites are local magnetic anomalies (due to the underlying terrain and/or to already magnetized parts of the cooling volcanic unit), and/or variations in magnetic mineralogy (see Lanza and Zanella (2006), Urrutia-Fucugauchi et al. (2004) and Speranza et al. (2006) for an exhaustive discussion on factors affecting the fidelity of paleomagnetic recording in volcanic rocks). In any case, we stress that paleomagnetic direction variability along different stratigraphic levels of ignimbrites is very small (less than 5°) if compared to PSV variability as apparent in our data set (ca. 50° in declination, Fig. 7). Thus vicinity of paleomagnetic directions (i.e., angular distance <10°) can still be used to infer ignimbrite correlations, particularly when peculiar (i.e., low/high) inclinations/declinations are observed.

All ignimbrites D and Z (except ignimbrite D at site Cos20, Lago Di Venere) yield strongly positive (23–29°) declination values, and 51–57° inclination values (Fig. 7, Table 2). Thus ignimbrites D and Z are inferred to be the same unit, supporting an inference made by Mahood and Hildreth (1986) and recent evidence from Ar/Ar dating gathered by La Felice et al. (2009), placing the D/Z ignimbrite eruption at 87 ka. The direction of site Cos20 (D=14.8°, I=46.8°) is ca. 10° away from both directions of units D/Z and F, the latter being characterized by barely positive declination values and ~50° inclination values (we do not consider site Cos21, inferred to have been affected by lightning). Thus ignimbrite D sampled at Lago di Venere is an outlier that could equally correspond to unit F or D/Z, unless it records a different eruption than the eruption of ignimbrite F, and to ignimbrite D elsewhere, which seems unlikely.

Three out of the four Q sites yield declinations near zero and inclination values of 43–48°. Conversely, the direction of Q site Cos15 (Punta Guardia) is defined by D=351.0°, I=51.1°, being close to directions from ignimbrite P, mostly characterized by 343–348° declination values and 47–49° inclination values. Accordingly, we suggest that strongly rheomorphic ignimbrite exposed at Punta Guardia (Fig. 2b) and along the northern coast of Pantelleria corresponds to ignimbrite P instead of ignimbrite Q. The welded lithic breccia sampled at Cala delle Capre yields a strongly negative declination value (D=336.7°), whereas the thinner welded lithic breccia that lies below ignimbrite P at Cala Cinque Denti (Fig. 2c) is characterized by a direction very similar to typical P directions. However, analyzing P and Breccia directions of Fig. 7, we note that: (1) P directions from Cala Cinque Denti and Contrada Zinedi (sites Cos18 and 13) are ca. 10° away from the other five P directions from other localities; (2) such an angular distance turns out to be very similar to the angular distance between directions from the two Breccia sites. This suggests that the sites at Cala Cinque Denti and Contrada Zinedi have been tilted towards the WNW. The tilting must have occurred before emplacement of ignimbrite D/Z, because these ignimbrites have very similar paleomagnetic directions at all localities (except ignimbrite D at Lago di Venere).

The average direction of units P from Cala Cinque Denti and Contrada Zinedi (D=357.4°, I=53.5°) overlaps the average direction of the remaining five P sites (D=345.7°, I=48.5°) if tilted by 11° towards the ESE (N110°, towards the caldera). If also the breccia site from Cala Cinque Denti is tilted by the same amount and in the same direction, the two breccia sites from Cala Cinque Denti and Cala delle Capre strikingly overlap (Fig. 8), suggesting that the two welded breccias exposed at the northern and SW edge of the island are synchronous. We stress that paleomagnetic directions from the two welded lithic breccias overlap only after applying a tilt of 11° to N110° calculated from the sole unit P directions, thus strengthening both hypotheses of locality tilting and breccia correlation.

In principle, tilting at Contrada Zinedi and Cala Cinque Denti might be related to both isostatic adjustment in the footwall of a listric normal fault parallel to caldera scarp (e.g., Branney 1995) and to magma resurgence after caldera collapse. In the past, regional tilting associated with caldera collapse has been constrained by paleomagnetic studies of ignimbrites from the English Lake District (Channell and McCabe 1992; Piper et al. 1997).

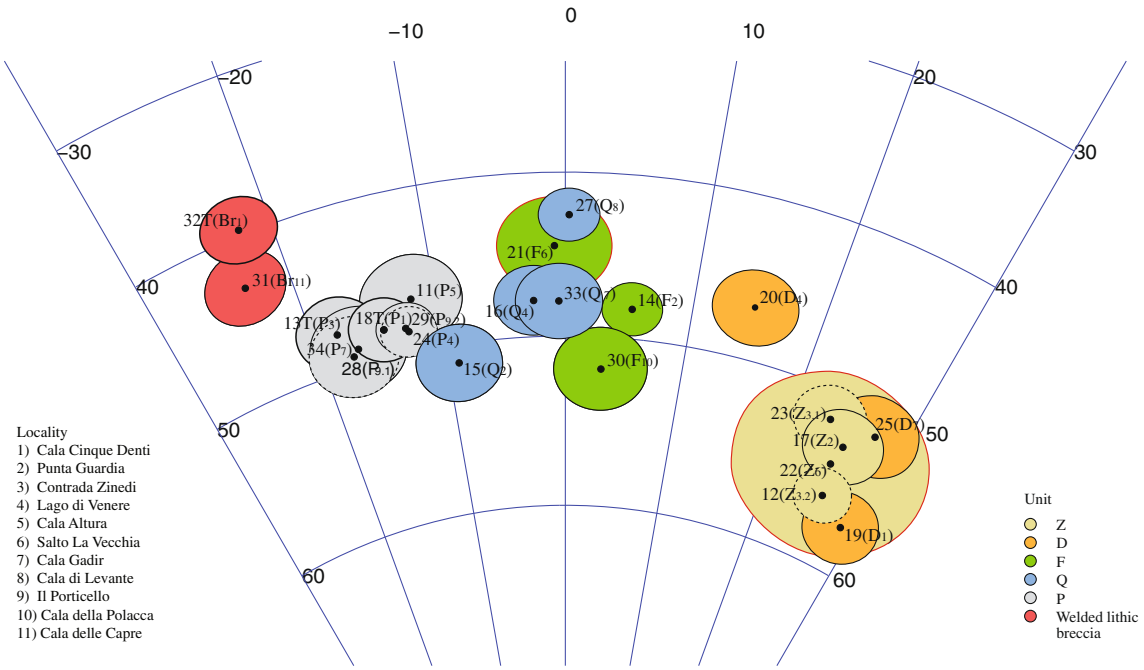

Fig. 8 Same figure as Fig. 7, but changed by tilting by 11° towards the ESE (N110°) the directions from Breccia and unit P from Cala Cinque Denti and Contrada Zinedi (sites Cos13, Cos18, and Cos32; see text). Their confidence ellipses are in *bold*

Isostatic adjustment due to faulting can hardly explain our tilting data, as at Pantelleria faults are never observed along caldera scarps, and scarp orientation at Cala Cinque Denti and Costa Zinedi is different (E–W and SW–NE, respectively), whereas tilting is the same. Resurgence of magma in the crust occurring after emplacement of voluminous ignimbrite P (overlying D/Z units show no tilting), and roughly beneath the eastern margin of the Khaggiar flow (Fig. 1), could account for the observed tilting. However, it is remarkable that tilting is not observed in units P and Q from Lago di Venere (sites Cos24 and 16, Figs. 1 and 7), located between the tilted Costa Zinedi and Cala Cinque Denti outcrops. We conclude that our explanation for tilt remains weak and more paleomagnetic data from additional adjacent localities would be needed to properly understand it.

The welded lithic breccia of Cala delle Capre was considered by Mahood and Hildreth (1986) the best candidate to represent products of a caldera forming eruption, but was only loosely dated using K/Ar methods, and not correlated to ignimbrites P and Q. Mahood and Hildreth (1986) suggested on petrographic grounds a correlation with ignimbrite Q, thus inferring that the collapse of La Vecchia caldera occurred at 114 ka (the age of ignimbrite Q). Our paleomagnetic data support a correlation of the welded lithic breccia of Cala delle Capre with the similar deposit just below (and older than) ignimbrite P at Cala Cinque Denti (Fig. 2c and f).

The petrographic features of the juvenile material contained in the welded breccia show significant differences at the two localities: juvenile clasts of Cala Cinque Denti contain an olivine forsterite 18–22 mol% and a clinopyroxene ferrosilite 28–30 mol%; at Cala delle Capre they contain much more abundant and Fe-richer olivines and clinopyroxenes (forsterite 7–8 mol% and ferrosilite 42–44 mol%, respectively), and also accessory phases (ilmenite, apatite, and pyrrothite) absent in the welded lithic breccia at Cala Cinque Denti. However, these petrographic differences do not necessarily imply that ignimbrite at the two localities is not the same because: (1) the two localities are ca. 8 km apart (Fig. 1); (2) the sampled stratigraphic levels are probably different (at Cala delle Capre we sampled the bottom of a 20 m thick breccia, whereas at Cala Cinque Denti we sampled the top of a 4 m thick breccia because the lowermost parts were not exposed, Fig. 2); (3) our sampling of juvenile clasts was scattered and nonsystematic; and (4) if they represent ignimbrites of different ages their sharing by chance the same low paleomagnetic inclination of ca. 40°, and the same (very peculiar) strongly negative declination exceeding −20° (Fig. 8) would seem unlikely.

As a consequence, we conclude that petrographic differences between breccias from Cala Cinque Denti and Cala delle Capre can be simply related to the contribution of heterogeneous magma batches to the same ignimbrite. Our correlation implies that the La Vecchia caldera must definitely have formed before 133 ka (K/Ar age of ignimbrite P), and after unit M, which is truncated by the La Vecchia caldera scarp around Salto La Vecchia (175 ka,

Fig. 2g). By also considering the low-precision K/Ar ages gathered from welded breccia of Cala delle Capre (127±37, 104±53 ka), we suggest that collapse of the La Vecchia caldera took place between ~130 and 160 ka. This is in good agreement with the inference of Mahood and Hildreth (1986) that the Costa Zinedi scarp had formed prior to the eruptions of units P and Q, as indicated by unit thickness variations occurring across the scarp (see their Fig. 10). We regard the Costa Zinedi scarp as the NW wall of the La Vecchia caldera, reaching the north coast at Punta Pozzolana and connected to the younger Cinque Denti caldera scarp at Lago di Venere (Fig. 1).

Our thermal demagnetization data (Fig. 6) provide information about the cooling history of the deposits, and the temperature at which rheomorphism of comenditic ignimbrites P and Q occurred. Rheomorphic ignimbrites have been paleomagnetically investigated in the past (Pioli et al. 2008) but not to address the rheomorphism temperature issue.

The majority of the P and Q ignimbrite sites sampled by us are characterized by strong rheomorphic folds (e.g., Branney et al. 2004) most evident at Punta Guardia and Lago di Venere (Fig. 2b, d). Thermal demagnetization data from these sites systematically reveal a unique magnetization component (ChRM) between 250°C and 600°C (Fig. 6). ChRMs are very well-grouped (very small α_{95} values are observed, Table 2), and reflect local PSV directions, implying a primary magnetization postdating rheomorphic folding. Thus our data indicate that ignimbrites P and Q were hotter than 600°C when rheomorphic flow stopped, and this is consistent with proposed high glass transition temperatures (Tg) of trachyte and similarly mildly peralkaline magmas (Tg≥700°C; Giordano et al. 2005).

Conclusions

The paleomagnetism of 23 ignimbrite outcrops from Pantelleria has shown that rheomorphic ignimbrites, emplaced at high (>500–600°C) temperature, are excellent recorders of the PSV of the geomagnetic field. Mean paleomagnetic directions from individual ignimbrites are similar (normally no more than 7–8° apart), and considering all studied units, the range varies from −25° to 30° in declination and 40° to 60° in inclination.

By considering similarity of paleomagnetic directions (within 10° of each other) as supporting ignimbrite correlation, the following conclusions can be made:

1. Ignimbrite Z coincides with unit D exposed along the NE island cliffs, confirming a conclusion reached by La Felice et al. (2009) based on new high-precision Ar/Ar ages. Thus, a voluminous D/Z ignimbrite was erupted at Pantelleria at 87 ka, ca. 40 kyr before the Green Tuff eruption.
2. Ignimbrite D from Lago di Venere (site Cos20) is a paleomagnetic outlier that could be associated with either unit F or D/Z. Alternatively, it represents a single lobe of an otherwise unrepresented pyroclastic flow, which seems unlikely.
3. Strongly rheomorphic ignimbrite Q from Punta Guardia (site Cos15) belongs in fact to ignimbrite P.
4. Welded lithic breccia of Cala delle Capre, considered by Mahood and Hildreth (1986) as the best candidate for deposits of La Vecchia caldera-forming eruption, correlates with a thinner welded lithic breccia lying below unit P at Cala Cinque Denti, at the opposite side of the island. Therefore, the collapse of the La Vecchia caldera, previously considered by Mahood and Hildreth (1986) as synchronous with unit Q (114±4 ka), is now inferred to have taken place before emplacement of unit P (133±3 ka).
5. Welded breccia and ignimbrite P from Cala Cinque Denti and Contrada Zinedi were tilted by ~10° towards the WNW (N290°, outwards from the caldera), prior to emplacement of ignimbrite D/Z, which shows no tilting. Such tilting might be due to magma resurgence occurring east of both localities after emplacement of ignimbrite P, although no tilting is observed at Lago Di Venere, located between Cala Cinque Denti and Contrada Zinedi.

Our paleomagnetic data allow a refinement of the pre-50 ka geologic history of Pantelleria depicted by Mahood and Hildreth (1986). We propose that the formation of the La Vecchia caldera was associated with the eruption that formed the welded lithic breccia at Cala delle Capre, during the 133–175 ka time window (bracketing ignimbrites P and M). By considering the low precision K/Ar ages gathered from the welded breccia by Mahood and Hildreth (1986; 127±37, 104±53 ka), a ~130–160 ka age for La Vecchia caldera formation seems reasonable. Mahood and Hildreth (1986) inferred that the collapse of La Vecchia caldera occurred at 114 ka, and that the Costa Zinedi scarp, predating unit P, was possibly related to an older caldera related to ignimbrites P, S, or M. Our work supports the stratigraphic evidence reported by Mahood and Hildreth (1986) for the age of the Costa Zinedi scarp, which can be now considered a proper segment of the La Vecchia caldera scarp.

The ~100 kyr period bracketing formation of La Vecchia caldera and eruption of Green Tuff and collapse of Cinque Denti caldera (45–50 ka) was punctuated by eruptions of ignimbrites P (K/Ar 133.1±3.3 ka; Mahood and Hildreth 1986), Q (K/Ar 113.9±3.6 ka), F (K/Ar 105.7±3.5 ka), and

D/Z (Ar/Ar 87 ka; La Felice et al. 2009), older and younger events yielding the most voluminous ignimbrites, relying also on our new paleomagnetically derived correlations. In particular, ignimbrite D/Z is exposed both along the S–SW and NE Pantelleria coast, in the latter showing considerable thickness (up to 12 m). We also correlate >10 m thick rheomorphic ignimbrite exposed along the northern coast around Punta Guardia with ignimbrite P.

The well-grouped characteristic magnetization components isolated at 250–600°C from strongly rheomorphic comenditic units P and Q, prove that these peralkaline ignimbrites underwent rheomorphic deformation at temperatures higher than 600°C, confirming the high (≥700°C) glass transition temperature estimated for trachyte and similar mildly peralkaline magmas.

Our work highlights the benefit of PSV analysis in volcanic rocks: it allows one to make (or rule out) correlations of units that cannot be traced in outcrop and are so close in age that their radiometric ages might not be resolvable. It is not a stand-alone method because the paleomagnetic directions can be re-occupied over time, but it can be used as a powerful correlative tool to accompany mapping, stratigraphic studies, and radiometric age determinations.

Acknowledgments Many thanks to S. La Felice for helpful discussions on the volcanic evidence from Pantelleria. FS expresses his gratitude to P. Landi for introducing him to the spectacular geology of Pantelleria. ADC thanks F. Salvini and M. Mattei for their support. Part of the 2009 field work was done along with unforgotten university degree students from Palermo and Madrid. The authoritative review by "The Lord of the Ignimbrites" Mike Branney provided us with a rigorous guide on terminology and interpretation of welded and rheomorphic ignimbrites. We are also grateful to Gail Mahood and Conall Mac Niocaill for providing careful reviews of our manuscript, as well as to BV Editor Raffaello Cioni and Executive Editor James D. L. White for carefully evaluating our paper. FS wishes to remind that this was the last work he could discuss with the late Maestro and friend Renato Funiciello.

References

Andrews GDM, Branney MJ (2011) Emplacement and rheomorphic deformation of a large, lava-like rhyolitic ignimbrite: Grey's Landing, southern Idaho. Geol Soc Am Bull 123:725–743

Branney MJ (1995) Downsag and extension at calderas: new perspectives on collapse geometries from ice-melt, mining, and volcanic subsidence. Bull Volcanol 57:303–318

Branney MJ, Barry TL, Godchaux M (2004) Sheathfolds in rheomorphic ignimbrites. Bull Volcanol 66:485–491. doi:10.1007/s00445-003-0332-8

Channell JET, McCabe C (1992) Paleomagnetic data from the Borrowdale Volcanic Group: volcano–tectonics and Late Ordovician palaeolatitudes. J Geol Soc London 149:881–888

Civetta L, Cornette Y, Crisci G, Gillot PY, Orsi G, Requejo CS (1984) Geology, geochronology and chemical evolution of the island of Pantelleria. Geol Mag 121:541–562

Civetta L, Cornette Y, Gillot PY, Orsi G (1988) The eruptive history of Pantelleria (Sicily Channel) in the last 50 ka. Bull Volcanol 50:47–57

Civetta L, D'Antonio M, Orsi G, Tilton GR (1998) The geochemistry of volcanic rocks from Pantelleria island, Sicily channel: petrogenesis and characteristics of the mantle source region. J Petrol 39:1453–1491

Civile D, Lodolo E, Accettella D, Geletti R, Ben-Avraham Z, Deponte M, Facchin L, Ramella R, Romeo R (2010) The Pantelleria graben (Sicily Channel, Central Mediterranean): an example of intraplate "passive" rift. Tectonophys 490:173–183

Cornette Y, Crisci GM, Gillot PY, Orsi G (1983) The recent volcanic history of Pantelleria: a new interpretation. In: Sheridan MF and Barberi F (eds). Explosive volcanism. J Volcanol Geother Res 17:361–373

Day R, Fuller M, Schmidt VA (1977) Hysteresis properties of titanomagnetites: grain size and compositional dependance. Phys Earth Planet Int 13:260–277

Di Carlo I, Rotolo SG, Scaillet B, Buccheri V, Pichavant M (2010) Phase equilibrium constraints on pre-eruptive conditions of recent felsic explosive volcanism at Pantelleria Island, Italy. J Petrol 51:2245–2276

Dunlop DJ (2002) Theory and application of the Day plot (M_{rs}/M_s versus Hcr/Hc): 1. Theoretical curves and tests using titanomagnetite data J Geophys Res. doi:10.1029/2001JB000486

Fisher RA (1953) Dispersion on a sphere. Proc R Soc Lond 217:195–305

Foerstner H (1881) Nota preliminare sulla geologia dell'isola di Pantelleria secondo gli studi fatti negli anni 1874 e 1881. Boll R Comit Geol It 12:523–556

Giordano D, Nichols ARL, Dingwell DB (2005) Glass transition temperature of natural hydrous melts: a relationship with shear viscosity and implications for the welding process. J Volcanol Geotherm Res 142:105–118

Hagstrum JT, Champion DE (1994) Paleomagnetic correlation of Late Quaternary lava flows in the lower east rift zone of Kilauea Volcano, Hawaii. J Geophys Res 99:21,679–21,690

Kirschvink JL (1980) The least-square line and plane and the analysis of paleomagnetic data. Geophys J R Astron Soc 62:699–718

La Felice S, Rotolo SG, Scaillet S, Vita G (2009) Tephrostratigraphy, petrochemistry and ^{40}Ar-^{39}Ar age data on pre-Green Tuff sequences, Pantelleria. In: Conferenza A. Rittman "La vulcanologia italiana: stato dell'arte e prospettive future" (abstract), pp. 61–62, Nicolosi (Catania, Italy), June 11–13, 2009

Lanza R, Zanella E (2003) Paleomagnetic secular variation at Vulcano (Aeolian Islands) during the last 135 kyr. Earth Planet Sci Lett 213:321–336

Lanza R, Zanella E (2006) Comments on "Chronology of Vesuvius' activity from A.D. 79 to 1631 based on archeomagnetism of lavas and historical sources" by C. Principe et al. Bull Volcanol 68:394–396

Macdonald R (1974) Nomenclature and petrochemistry of the peralkaline oversaturated extrusive rocks. Bull Volcanol 38:498–516

Mahood GA (1984) Pyroclastic rocks and calderas associated with strongly peralkaline magmatism. J Geophys Res 89 (B10):8540–8552

Mahood GA, Hildreth W (1983) Nested calderas and trapdoor uplift at Pantelleria, Strait of Sicily. Geology 11:103–106

Mahood GA, Hildreth W (1986) Geology of the peralkaline volcano at Pantelleria, Strait of Sicily. Bull Volcanol 48:143–172

McFadden PL, Lowes FJ (1981) The discrimination of mean directions drawn from Fisher distributions. Geophys J R Astr Soc 67:19–33

Merrill RT, McElhinny MW, McFadden PL (1996) The magnetic field of the earth: paleomagnetism, the core, and the deep mantle. Elsevier, New York

Pavón-Carrasco FJ, Osete ML, Torta JM, Gaya-Piqué LR (2009) A regional archeomagnetic model for Europe for the last 3,000 years, SCHA.DIF.3K: applications to archeomagnetic dating. Geochem Geophys Geosyst. doi:10.1029/2008GC002244

Pioli L, Lanza R, Ort M, Rosi M (2008) Magnetic fabric, welding texture and strain fabric in the Nuraxi Tuff, Sardinia, Italy. Bull Volcanol 70:1123–1137

Piper JDA, Stephen JC, Branney MJ (1997) Palaeomagnetism of the Borrowdale and Eycott volcanic groups, English Lake District: primary and secondary magnetization during a single late Ordovician polarity chron. Geol Magazine 134:481–506

Rolph TC, Shaw J (1986) Variations of the geomagnetic field in Sicily. J Geomagn Geoelectr 38:1269–1277

Rotolo SG, Villa IM (2001) $^{40}Ar/^{39}Ar$ dating of an alkali-granite enclave from Pantelleria island. Periodico Mineral 70:269–275

Rotolo SG, Castorina F, Cellura D, Pompilio M (2006) Petrology and geochemistry of submarine volcanism in the Sicily Channel Rift. J Geol 114:355–365

Rotolo SG, La Felice S, Mangalaviti A, Landi P (2007) Geology and petrochemistry of the recent (<25 ka) silicic volcanism at Pantelleria Island. Boll Soc Geol It 126:191–208

Speranza F, Pompilio M, Sagnotti L (2004) Paleomagnetism of spatter lavas from Stromboli volcano (Aeolian Islands, Italy): implications for the age of paroxysmal eruptions. Geophys Res Lett 31: L02607. doi:10.1029/2003GL018944

Speranza F, Branca S, Coltelli M, D'Ajello Caracciolo F, Vigliotti L (2006) How accurate is "paleomagnetic dating"? New evidence from historical lavas from Mount Etna. J Geophys Res 111: B12S33. doi:10.1029/2006JB004496

Speranza F, Pompilio M, D'Ajello Caracciolo F, Sagnotti L (2008) Holocene eruptive history of the Stromboli volcano: constraints from paleomagnetic dating. J Geophys Res 113:B09101. doi:10.1029/2007JB005139

Speranza F, Landi P, D'Ajello Caracciolo F, Pignatelli A (2010) Paleomagnetic dating of the most recent silicic eruptive activity at Pantelleria (Strait of Sicily). Bull Volcanol 72:847–858. doi:10.1007/s00445-010-0368-5

Sumner JM, Branney MJ (2002) The emplacement history of a remarkable heterogeneous, chemically zoned, rheomorphic and locally lava-like ignimbrite: 'TL' on Gran Canaria. J Volcanol Geotherm Res 115:109–138

Tanguy JC, Le Goff M, Principe C, Arrighi S, Chillemi V, Paiotti A, La Delfa S, Patanè G (2003) Archeomagnetic dating of Mediterranean volcanics of the last 2100 years: validity and limits. Earth and Planet Sci Lett 211:111–124

Urrutia-Fucugauchi J, Alva-Valdivia LM, Goguitchaichvili A, Rivas ML, Morales J (2004) Palaeomagnetic, rock-magnetic and microscopy studies of historic lava flows from the Paricutin volcano, Mexico: implications for the deflection of paleomagnetic directions. Geophys J Int 156:431–442

Vezzoli L, Principe C, Malfatti J, Arrighi S, Tanguy JC, Le Goff M (2009) Modes and times of caldera resurgence: the <10 ka evolution of Ischia Caldera, Italy, from high-precision archaeomagnetic dating. J Volcanol Geotherm Res 186:305–319

Villari L (1969) On particular ignimbrites of the island of Pantelleria (Channel of Sicily). Bull Volcanol 33:828–839

Washington HS (1909) The submarine eruptions of 1831 and 1891 near Pantelleria. Am J Sci 27:131–150

White JC, Ren M, Parker DF (2005) Variation in mineralogy, temperature, and oxygen fugacity in a suite of strongly peralkaline lavas and tuffs, Pantelleria, Italy. Canad Mineral 43:1331–1347

White JC, Parker DF, Ren M (2009) The origin of trachyte and pantellerite from Pantelleria, Italy: insights from major element, trace element, and thermodynamic modelling. J Volcanol Geotherm Res 179:33–55

Wright JV (1980) Stratigraphy and geology of the welded air-fall tuffs of Pantelleria, Italy. Geol Rundsch 69:263–291

Zanella E (1998) Paleomagnetism of Pleistocene volcanic rocks from Pantelleria Island (Sicily Channel), Italy. Phys Earth Planet Int 108:291–303

Zijderveld JDA (1967) AC demagnetization of rocks: analysis of results. In: Runcorn SK, Creer KM, Collinson DW (eds) Methods in palaeomagnetism. Elsevier, Amsterdam, pp 254–286

PART V– PALEOSECULAR VARIATION AT THE AZORES

12. Introduction

Part IV is dedicated to present results obtained after the two last year of the PhD (2011 - 2012). Efforts had been focused firstly to collect new samples from well-dated lava flows from the island of São Miguel, which is the largest island of the Azores Archipelago (straggling the Middle - Atlantic – Ridge, in the triple junction where the European, Nubian and North-American plates meet), since paleomagnetic data from this area lack in literature.

In Chapter 13 are presented results from paleomagnetic analysis of directions obtained from 35 sites sampled on 16 flows emplaced in the last 3 ka. Results have been interpolated with a cubic spline interpolation and the first PSV curve has been obtained.

In Chapter 14 are shown results of paleointensity experiments. The protocol applied for recovering paleointensities is the IZZI method, an embellishment of the classical Thellier and Thellier technique. Some improvements had been proposed in this section, such as a rigorous pre-selection of suitable samples (i.e., displaying a unique NRM component, any alteration evidences during experiments, a Single Domain predominant component of grains, bearing remanent magnetization). The experiments had been carried out in the laboratory of paleomagnetism, hosted by the Scripps Institution of Oceanography (La Jolla, California) and headed by Prof. Lisa Tauxe, obtaining the first reliable dataset of paleointensity data for this region.

Paleomagnetic secular variation at the Azores during the last 3 ka

Anita Di Chiara,[1] Fabio Speranza,[1] and Massimiliano Porreca[2]

Received 5 March 2012; revised 22 May 2012; accepted 25 May 2012; published 12 July 2012.

[1] We report on 33 new paleomagnetic directions obtained from 16 lava flows emplaced in the last 3 ka on São Miguel, the largest island of the Azores. The data provide 27 well-dated directions from historical or ^{14}C dated flows which, together with 6 directions previously gathered from the same flows by Johnson et al. (1998), yield the first paleomagnetic directional record of the last 3 ka from the Atlantic Ocean. Within-flow directions are consistent, suggesting that inclination swings from 60° to 25° and declination changes between −10° to 20° reflect variations in the geomagnetic field over the last 3 ka. To a first approximation, the declination record is consistent with predictions from CALS3k.4 and gufm1 global field models. Conversely, inclination values are lower than model predictions at two different ages: 1) four sites from the 1652 AD flow yield I = 48° instead of I = 63° predicted by gufm1; 2) data from several flows nicely mimic the inclination minimum of 800–1400 AD, but inclination values are lower by ∼10° than CALS3k.4 model predictions. By interpolating a cubic spline fit on declination / inclination versus age data, we tentatively infer the directional evolution of the geomagnetic field at the Azores from 1000 BC to 1600 AD. The obtained curve shows three tracks in virtual overlap during the 1000–800 BC, 800–500 BC, and 400–700 AD time spans.

Citation: Di Chiara, A., F. Speranza, and M. Porreca (2012), Paleomagnetic secular variation at the Azores during the last 3 ka, *J. Geophys. Res.*, *117*, B07101, doi:10.1029/2012JB009285.

1. Introduction

[2] Our knowledge of the recent (Holocene) geomagnetic field evolution has been improved by the recent modeling work of *Korte et al.* [2011]. The modeling studies are essential in improving our understanding of geodynamo processes and core-mantle boundary (CMB) interactions. However, the paucity of paleomagnetic data (both direction and intensity) does not allow a full understanding of dynamic features for modeling CMB field over the last 10 ka [*Korte and Holme*, 2010], and therefore new data should be acquired in support of this aim.

[3] The last available model for the last 3 ka (CALS3k.4) [*Korte and Constable*, 2011] was constructed using a new compilation of ∼35,000 values (declination, inclination, and intensity) obtained from Holocene lacustrine/marine sediments, archeological artifacts and historical lava flows [*Korte and Constable*, 2005; *Genevey et al.*, 2008; *Donadini et al.*, 2009]. However, data distribution is uneven, and if the Holocene geomagnetic field evolution for some areas (such as Europe) is well constrained, other regions (oceans and most of the southern hemisphere) still lack significant Holocene geomagnetic information to consider the local field evolution retrievable by global models as fully reliable.

[4] This is indeed the case of the central-northern Atlantic Ocean, for which the catalog of *Donadini et al.* [2009] yields only few data from its eastern and northern margins. *Lund and Kleigwin* [1994] also published a paleosecular variation curve (PSV) from the Bermuda Rise, but the trend for the last 3 ka is almost anti-correlated with more recent global models. From islands in the Atlantic Ocean, paleomagnetic directions were gathered from fourteen 1585–1971 AD lava flows from the Canary Islands [*Soler et al.*, 1984]. Paleointensity values were reported from few historical [*Michalk et al.*, 2008] and post-glacial [*Schweitzer and Soffel*, 1980; *Stanton et al.*, 2011] lavas from Iceland. Sedimentary paleomagnetic results from four Holocene cores drilled around Iceland and Greenland [*Thompson and Turner*, 1985; *Channell et al.*, 1997; *Stoner et al.*, 2000, 2007], and Cape Ghir, Morroco by *Bleil and Dillon* [2008] have been obtained so far. Iceland and Greenland records are between 2500 km and 3200 km away from the Azores; western and central Europe data are closer, indeed the Cape Ghir record is the closest and that is still ∼1600 km away. All the mentioned sites are located slightly more distant or within the 30° of the Azores. Therefore more data are required to define the evolution of the geomagnetic field in this area, which is the final aim of this work.

[5] Comparison of local PSV curves of the geomagnetic field for the Holocene is often used as a dating tool for a given volcanic complex [*Rutten and Wensink*, 1960; *Doell and Cox*, 1963; *Carlut et al.*, 2000]. Loosely dated Holocene volcanics can be precisely constrained in age (with an accuracy of ∼100 years in some cases; see discussion in

[1]Istituto Nazionale di Geofisica e Vulcanologia, Rome, Italy.
[2]Centro de Vulcanologia e Avaliação de Riscos Geológicos, Universidade dos Açores, Ponta Delgada, Portugal.

Corresponding author: A. Di Chiara, Istituto Nazionale di Geofisica e Vulcanologia, Via di Vigna Murata 605, Roma I-00143, Italy. (anita.dichiara@ingv.it)

0148-0227/12/2012JB009285

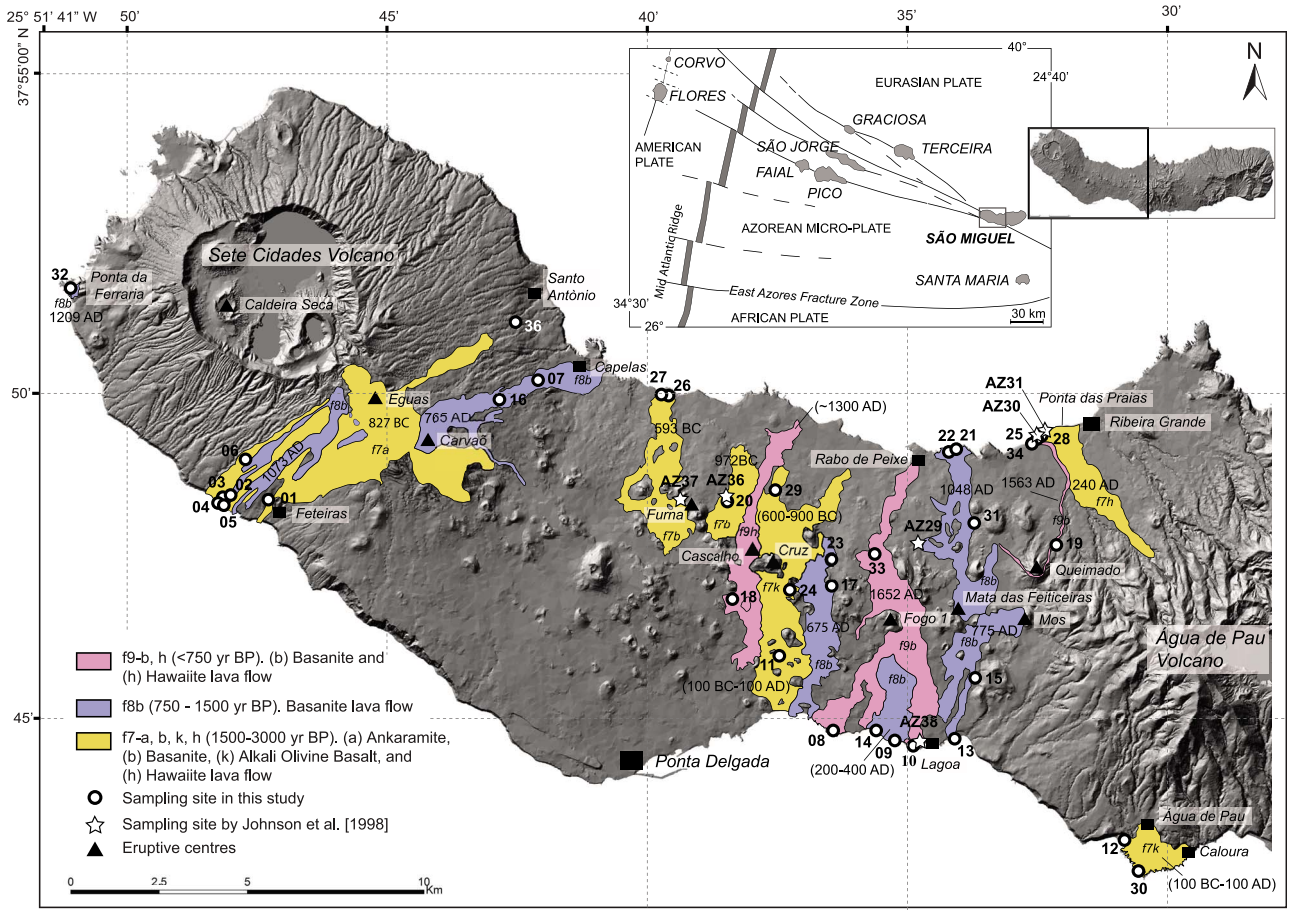

Figure 1. Digital elevation model of São Miguel, and location of the studied flows and paleomagnetic sampling sites from this study (the "Sml" prefix of each site is omitted), and *Johnson et al.* [1998], labeled with prefix "AZ-." Flow geometry, characteristics, and ages are after *Moore* [1990, 1991]. 1563 and 1652 AD flows are historic. Calendar ages of the other lava flows were calibrated by us using CALIB6.0 [http://calib.qub.ac.uk/calib/calib.html] from original ^{14}C ages reported by *Moore and Rubin* [1991]. Flow ages between parentheses are paleomagnetically inferred.

Speranza et al. [2006]) by comparing their paleomagnetic directions to PSV reference data, independently available from the same area, or relocated from nearby (maximum 1000–2000 km far) sites. Paleomagnetic dating has been successfully applied to several active volcanoes in Italy and on the island of Hawaii, owing to PSV reference data provided by the rich European archeomagnetic data set and radiometrically dated local lava flows. In such cases paleomagnetism has provided high-resolution dating, and has proven fundamental to constrain the timing of local volcanic history, thus supporting hazard scenarios for future eruptive activity [e.g., *Rolph et al.*, 1987; *Hagstrum and Champion*, 1994; *Jurado-Chichay et al.*, 1996; *Lanza and Zanella*, 2003; *Tanguy et al.*, 2003; *Speranza et al.*, 2004, 2008, 2010; *Pressling et al.*, 2009; *Vezzoli et al.*, 2009].

[6] We are able to calibrate the PSV of the Azores, straddling the Mid-Atlantic ridge at 23°–32°W (Figure 1), by using the detailed geological maps of São Miguel island from *Moore* [1990, 1991], coupled with radiocarbon dating of most of the volcanic products emplaced in the last tens of ky reported by *Moore and Rubin* [1991]. In this paper we report 33 new paleomagnetic directions obtained from 16 different lava flows of the last 3 ka exposed at São Miguel, the largest island in the Azores (Figure 1). Two of the studied lava flows were emplaced in the last five centuries and are described in historical chronicles [*Mitchell-Thomè*, 1981; *Booth et al.*, 1978], while the ages of eleven flows are tightly constrained by radiocarbon ages of charcoals or paleosols lying below the flows themselves. Our data, along with six paleomagnetic directions previously gathered from the same lavas by *Johnson et al.* [1998], allow reconstruction of the evolution of geomagnetic field directions for the Azores during the last 3 ka.

2. Volcanic History of São Miguel and Characteristics of the Studied Lavas

[7] São Miguel is the largest (760 km^2) of the nine volcanic islands of the Azores Archipelago, straddling the Mid-Atlantic Ridge at the triple junction of the North American, Eurasian and African plates (Figure 1). The emerged part of the Azores developed from at least 8.1 Ma [*Abdel-Monem et al.*, 1975; *Feraud et al.*, 1980] to present-day.

[8] Extensive geological mapping [*Booth et al.*, 1978; *Moore*, 1990, 1991], ^{14}C [*Moore and Rubin*, 1991], K/Ar [*Abdel-Monem et al.*, 1975; *McKee and Moore*, 1992], and $^{40}Ar/^{39}Ar$ [*Johnson et al.*, 1998] radiometric dating were carried out on the São Miguel island. The island consists of four large trachytic stratovolcanoes, which have been active over the last 100 kyr (Sete Cidades, Agua de Pau, Furnas and Nordeste), although the Nordeste volcanic complex in the eastern border of the island is significantly eroded and appears to be extinct [*Abdel-Monem et al.*, 1975; *Feraud et al.*, 1980; *Fernandez*, 1980; *Johnson et al.*, 1998; *Queiroz et al.*, 2008].

[9] In the western part of the island, between the Sete Cidades and Agua de Pau stratovolcanoes (Figure 1), a relatively flat region with numerous alkali basaltic eruption cones up to 200 m high and lava flows younger than 30 ka, was termed the "Waist Zone" [*Booth et al.*, 1978], "Zone 2", or "Região dos Picos" [*Moore*, 1990, 1991]. This is also the most populated area of the island, where some of most recent lava flows were emplaced during the first settlement of the island (eruptions of 1563 AD Pico Queimado and 1652 AD Fogo 1 [*Booth et al.*, 1978; *Moore*, 1990; *Ferreira*, 2000]).

[10] Eruptive styles and related products at São Miguel have a typical bimodal nature. Stratovolcanoes are generally characterized by trachytic explosive eruptions with the emplacement of pyroclastic fallout and flow deposits. By contrast in Zone 2 and the peripheral volcanic centers a predominant effusive and Strombolian volcanic activity is recorded with the emplacement of alkali basaltic lava flows. These involved a wide range of lavas, from ankaramites, basanites, alkaline olivine basalts, hawaiites, mugearites and benmoreites [*Moore*, 1990].

[11] Our paleomagnetic investigation focused on 16 basaltic-like lava flows from the last 3 ka (mostly exposed in Zone 2 and reaching the ocean) evidenced in Figure 1. We systematically refer to *Moore* [1990, 1991], and *Moore and Rubin* [1991] for flow descriptions and relative radiocarbon dating. We studied eleven basanite, two hawaiite, one ankaramite, and two alkali olivine basalt flows. Two basanite lavas are historic: the thin 1563 AD flow which erupted from the Pico Queimado cone on the west-mountainside of Agua de Pau Volcano, and the extensive 1652 AD lava flow, which erupted from the Fogo 1 cone and reached the northern coast next to Rabo de Peixe village, and the southern coast between Popùlo and Lagoa villages.

3. Sampling and Methods

[12] During July 2010, we collected paleomagnetic samples from 35 sites in 16 flows at São Miguel (Figure 1 and Table 1), mostly located within Zone 2 and the southwestern coast-side of Sete Cidades volcano. Six sites (prefixed AZ) from the same flows had been already paleomagnetically investigated by *Johnson et al.* [1998].

[13] Pre-historical flow ages were inferred from radiocarbon ages reported by *Moore and Rubin* [1991], which were recalibrated by us with the latest version of Stuiver's program [http://calib.qub.ac.uk/calib]. The age ranges with their probability distribution (1σ and 2σ) are reported in Table 1.

[14] In Zone 2 we sampled the historical flows of 1652 AD and 1563 AD, as well as the Pico do Cascalho flow (site Sml18), which can be dated about to ~1300–1500 AD. Although the latter flow lacks historical accounts, according to *Moore* [1991], it is younger than Caldeira Seca eruption of Sete Cidades Volcano (Figure 1), dated at 1314 ± 71 AD by *Shotton and Williams* [1971] and 1432 ± 100 AD by *Moore and Rubin* [1991]. The oldest well-dated sampled lavas are the Eguas ankaramite (827 ± 305 BC; site Sml36) and Aflitos basanite (972 ± 142 BC; site Sml20 and AZ36). In the western part of the island, we extensively sampled the Feteiras (Sml01 to 06) lava flow, which according to our field data crops out more widely with respect to geological limits given by *Moore* [1991] (Figure 1). Furthermore, we sampled two flows in the age range 750–1500 BP (Lagoa flow) and four between 1500 and 3000 BP (Cruz and Caloura flows). Two out of 35 sampled sites are poorly constrained in regard to the flow attribution and age (Sml27 and 31, Table 1).

[15] At each site we drilled 10–24 (15 on average) 2.5-cm diameter cores using a petrol-powered portable drill cooled by water. We spaced the cores as much as possible in the studied lavas in an attempt to gather a well-averaged, representative paleomagnetic direction for each lava flow. All cores were oriented by a magnetic and a sun compass. The local field declination values, i.e., the magnetic deviation (the difference between the magnetic and sun compass readings), are mostly between −20° and −1° (Table 1). The average local field declination value calculated from all sites is D = −9.5° ± 5.8°, which indeed compares well with the declination yielded by the IGRF-11 model [http://omniweb.gsfc.nasa.gov/vitmo/igrf_vitmo.html] for São Miguel at 37.8°N, 25.5°W (D = −9.5°). The sampled cores were cut into standard cylindrical specimens, and the natural remanent magnetization (NRM) of one specimen per core was first measured in a 2G Enterprises DC-SQUID cryogenic magnetometer, hosted in the shielded room of the paleomagnetic laboratory of the Istituto Nazionale di Geofisica e Vulcanologia (Roma). Specimens with NRM <10 A/m were measured on a 2G magnetometer while those exceeding this threshold were measured on an AGICO JR6 spinner magnetometer. Stepwise thermal demagnetization was carried out in seven demagnetization steps up to maximum temperatures of 600°C, using a Pyrox shielded oven. Thermal demagnetization data were plotted on orthogonal vector component diagrams [*Zijderveld*, 1967], and the magnetization components were isolated by principal component analysis [*Kirschvink*, 1980]. Site mean paleomagnetic directions were computed using *Fisher* [1953] statistics.

[16] Additional magnetic analyses were carried out on a specimen from each site to characterize the magnetic mineralogy. Hysteresis properties were measured using a Princeton Measurements Corporation MicroMag alternating gradient magnetometer (AGM, model 2900) with a maximum applied field of 1 T. The measured hysteresis parameters included saturation magnetization (Ms), saturation remanent magnetization (Mrs) and coercive force (Bc). Acquisition of an isothermal remanent magnetization (IRM) and subsequent back-field DC remagnetization (both in a succession of fields up to 1 T) were also carried out on the same specimens to determine the coercivity of remanence (Bcr). For the same specimens, we also measured the low-field magnetic susceptibility during a heating and cooling cycle performed in air, from room temperature up to 700°C, using an AGICO KLY-3 kappabridge coupled with a CS-3 furnace. The Curie temperature (T_c) of the magnetic minerals present in the

Table 1. Location of Sampling Sites at São Miguel (This Work and From *Johnson et al.* [1998]) and Independent Age Constraints From Historic or Geochronologic Evidence[a]

Site	Unit - Flow	Locality	Latitude (°N)	Longitude (°W)	Alt. (m.a.s.l.)	d (deg)	^{14}C Age (years BP)	Calendar Age 1σ (68.3%)	Calendar Age 2σ (95.4%)
Sml11	f7k - Cruz	Estadio PDL	37°45′53″	25°37′30″	64	−6.7 ± 2.5	1500–3000*		
Sml29	f7k - Cruz	Aflitos- Batalha	37°48′26″	25°37′35″	91	−5.1 ± 2.9	1500–3000*		
Sml12	f7k - Caloura	Praia de Caloura	37°42′58″	25°30′59″	7	−12.0 ± 5.3	1500–3000*		
Sml30	f7k - Caloura	Caloura Hotel	37°42′29″	25°30′40″	3	−10.8 ± 3.7	1500–3000*		
Sml09	f8b - Lagoa	Lagoa-OVGA	37°44′32″	25°35′18″	3	−15.9 ± 2.6	750–1500*		
Sml14	f8b - Lagoa	Atalhada- Restaurant	37°44′40″	25°35′41″	3	−12.0 ± 4.5	750–1500*		
Sml20	f7b - Aflitos	Batalha	37°48′15″	25°38′30″	151	−7.7 ± 2.3	2800 ± 120	1114–830 BC	1316–774 BC
AZ36	f7b - Aflitos	Batalha	37°48′24″	25°31′26″	151		2800 ± 120	1114–830 BC	1316–774 BC
Sml36	f7a - Eguas	Santo Antonio	37°50′58″	25°42′35″	252	−19.3 ± 2.4	2700 ± 250	1132–522 BC	1456–350 BC
Sml26	f7b - Furna	Capelas (Poços E)	37°49′57″	25°39′42″	11	0.6 ± 2.5	2460 ± 220	829–357 BC	1091–37 BC
Sml27	f7b - Furna (?)	Capelas (Poços E)	37°49′57″	25°39′33″	10	−6.7 ± 2.8	2460 ± 220 (?)	829–357 BC	1091–37 BC
AZ37	f7b - Furna	Arrenquinha	37°48′25″	25°39′45″	223		2460 ± 220	829–357 BC	1091–37 BC
Sml25	f7h - Ponta das Praias	Ponta das Praias	37°49′11″	25°32′26″	3	−14.5 ± 8.6	1790 ± 150	72–408 AD	107 BC–577 AD
Sml28	f7h - Ponta das Praias	Ponta das Praias	37°49′11″	25°32′24″	4	−1.2 ± 6.9	1790 ± 150	72–408 AD	107 BC–577 AD
AZ31	f7h - Ponta das Praias	Ponta das Praias	37°49′22″	25°32′34″	4		1790 ± 150	72–408 AD	107 BC–577 AD
Sml17	f8b - Caldeirão	Pinhal de Paz fork	37°46′56″	25°36′30″	197	−8.6 ± 3.0	1350 ± 120	568–782 AD	504–900 AD
Sml23	f8b - Caldeirão	Giestas – cross road R31	37°47′21″	25°36′34″	155	0.3 ± 3.4	1350 ± 120	568–782 AD	504–900 AD
Sml24	f8b - Caldeirão	Geothermal plant	37°46′51″	25°37′18″	229	−18.3 ± 6.9	1350 ± 120	568–782 AD	504–900 AD
Sml07	f8b - Carvão	Marranhão	37°50′07″	25°42′08″	202	−11 ± 3.8	1280 ± 150	633–897 AD	504–1029 AD
Sml16	f8b - Carvão	Marranhão - trough	37°49′46″	25°42′51″	382	−4.0 ± 3.4	1280 ± 150	633–897 AD	504–1029 AD
Sml13	f8b - Mos	Santa Cruz de Lagoa	37°44′34″	25°34′10″	3	−15.0 ± 3.7	1250 ± 150	652–899 AD	533–1048 AD
Sml15	f8b - Mos	Cabouco	37°45′31″	25°33′42″	143	−13.0 ± 4.9	1250 ± 150	652–899 AD	533–1048 AD
Sml21	f8b - Mata das Feiticeiras	Rabo de Peixe- range	37°49′03″	25°34′03″	6	−10.4 ± 6.4	1010 ± 120	936–1161 AD	775–1259 AD
Sml22	f8b - Mata das Feiticeiras	Rabo de Peixe- sport facilities	37°48′59″	25°34′10″	6	−9.5 ± 3.5	1010 ± 120	936–1161 AD	775–1259 AD
AZ29	f8b - Mata das Feiticeiras	Alminhas	37°47′53″	25°35′81″	133		1010 ± 120	936–1161 AD	775–1259 AD
Sml01	f8b - Feteiras	Feteiras	37°48′20″	25°47′19″	146	−19.3 ± 2.4	980 ± 90	983–1163 AD	887–1252 AD
Sml02	f8b - Feteiras	Feteiras	37°48′25″	25°48′04″	110	−10.7 ± 6.7	980 ± 90	983–1163 AD	887–1252 AD
Sml03	f8b - Feteiras	Feteiras harbor	37°48′17″	25°48′15″	34	−15.1 ± 3.5	980 ± 90	983–1163 AD	887–1252 AD
Sml04	f8b - Feteiras	Feteiras arc	37°48′18″	25°48′19″	3	−9.3 ± 3.0	980 ± 90	983–1163 AD	887–1252 AD
Sml05	f8b - Feteiras	Feteiras harbor	37°48′13″	25°48′11″	5	−8.4 ± 2.9	980 ± 90	983–1163 AD	887–1252 AD
Sml06	f8b - Feteiras	Escalinha –wheat field	37°48′57″	25°47′43″	265	−25.3 ± 28.2	980 ± 90	983–1163 AD	887–1252 AD
Sml32	f8b - Ponta da Ferraria	Ferraria -Thermae	37°51′40″	25°51′15″	7	−8.7 ± 3.7	840 ± 60	1155–1264 AD	1117–1276 AD
Sml18	f9h - Cascalho	Pico de Roma	37°46′45″	25°38′25″	190	−7.5 ± 2.6	Less than 500 ± 100 and 663 ± 105 AD	~1300–1500 AD	
Sml19	f9b - Queimado	St Barbara-biscoito	37°47′32″	25°32′07″	119	−2.3 ± 2.3		**1563 AD**	
Sml34	f9b - Queimado	Praia Santa Barbara	37°49′08″	25°32′32″	5	−9.1 ± 1.0		**1563 AD**	
Sml31	f9b - Queimado (?)	Ribeira Grande-Oficina	37°47′54″	25°33′45″	114	−1.8 ± 5.7		**1563 AD (?)**	
AZ30	f9b - Queimado	Ponta das Praias	37°49′15″	25°32′55″	5			**1563 AD**	
Sml08	f9b - Fogo 1	Popùlo	37°44′42″	25°36′32″	5	−12.4 ± 2.3		**1652 AD**	
Sml10	f9b - Fogo 1	Lagoa – sport facilities	37°44′26″	25°34′58″	4	−1.3 ± 2.9		**1652 AD**	
Sml33	f9b - Fogo 1	R31- Pit	37°47′26″	25°35′40″	143	−11.6 ± 1.6		**1652 AD**	
AZ38	f9b - Fogo 1	Lagoa	37°47′26″	25°35′40″	5			**1652 AD**	

[a]Sites from *Johnson et al.* [1998] are prefixed "AZ." Site coordinates and altitude were gathered by a Garmin GPS using WGS84 datum. d = Site-mean magnetic deviation (and standard deviation) calculated by comparison between magnetic and sun compass readings of the paleomagnetic core orientations. Units and uncalibrated ^{14}C ages with an error of 1σ are from *Moore* [1990, 1991] and *Moore and Rubin* [1991]. Question mark indicates doubtful flow attribution. Historic ages are in bold. *Flows whose age is defined by an age interval. Calendar ages were calibrated using the Stuiver's program CALIB6.0 Online [http://calib.qub.ac.uk/calib/calib.html]. The second letter in Unit name gives petrography characterization: a, Ankaramite; b, Basanite; h, Hawaiite; k, Alkaline Olivine Basalt.

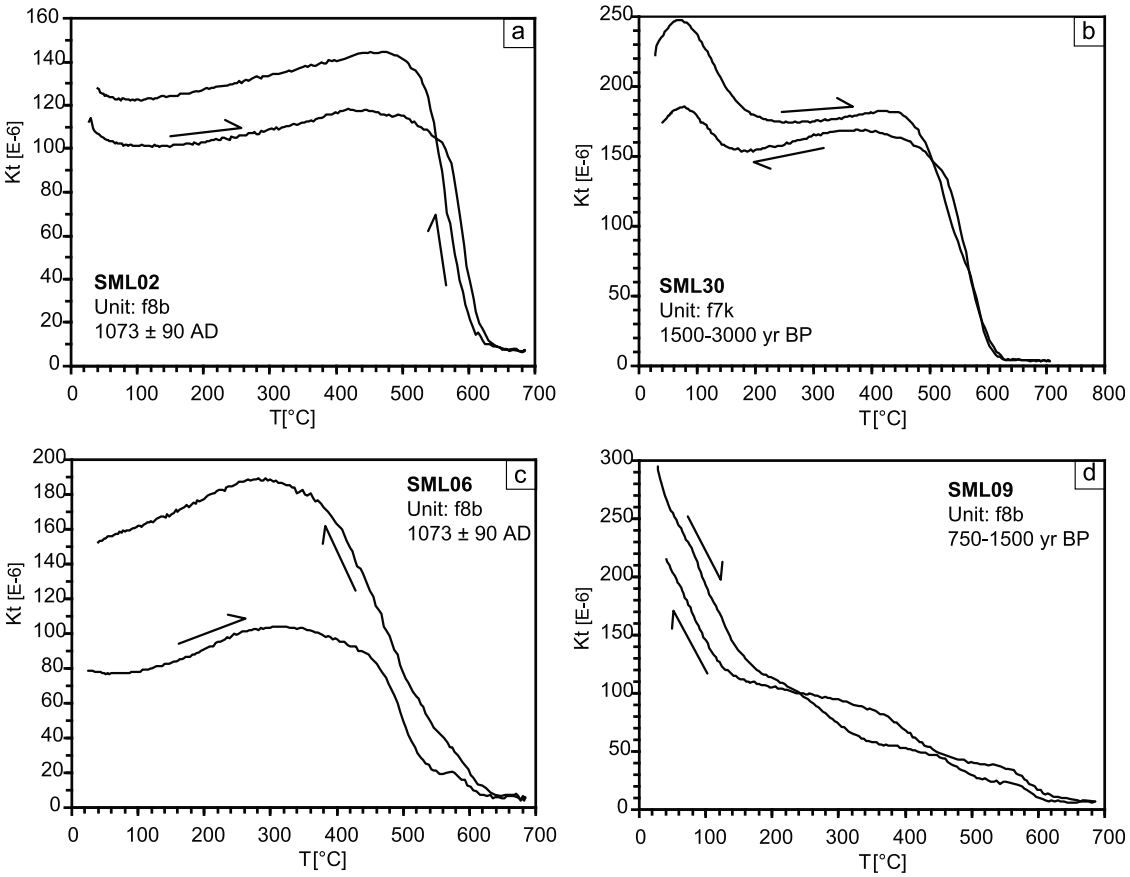

Figure 2. (a–d) Representative susceptibility-temperature cycles.

samples was determined from the susceptibility-T curves as the temperature (or range of temperatures) at which paramagnetic behavior starts to dominate, or abrupt susceptibility drops occur.

[17] In addition, we have carried out petrographic observations on six thin sections of the sampled lavas. Thin sections are from sites Sml01 and Sml04, (likely both from Feteiras flow, 1073 AD), Sml17, Sml23, Sml24 (Caldeirão flow), and Sml29 (probably Cruz flow). Microscopic observations were performed with transmitted light using a polarizing microscope.

4. Results

4.1. Magnetic Mineralogy

[18] Susceptibility-T curves reveal four main behaviors: 35% of the analyzed samples show an almost reversible variation trend in the heating-cooling cycle, with a distinct T_c at about 585° and a reduction in T_c on cooling at 575°C. There are slight differences in the susceptibility values of the heating and cooling curves, with the cooling curve displaying susceptibility values which are 20–25% higher than in the heating curve (Figure 2a). Similarly, 23% of the samples reveal almost reversible curves, but lower susceptibility values on cooling below 500°C (Figure 2b). For these samples there is no marked difference in the T_c at about 580°C between heating and cooling. These samples show also a peak in susceptibility at 70°C and an additional T_c between 100°C and 200°C, seen in both heating and cooling curves, which is indicative of the presence of high-Ti titanomagnetite phase besides magnetite. 21% show an irreversible trend, with two T_cs at about 500°C and 580°C, and the formation of new magnetic phases during heating, which resulted in markedly increased susceptibility values during cooling (Figure 2c). 21% of the samples yield an almost reversible variation trend and multiple Curie temperatures in the 250–600°C range (four different T_cs), indicating a complex and variable composition in the titanomagnetite series (Figure 2d).

[19] Hysteresis analyses show a predominance of low-coercivity values, with Bc comprised between 4.72 and 25.21 mT. Hysteresis parameters, ratios of saturation remanence to saturation magnetization (Mrs/Ms) and remanent coercive force to coercive force (Bcr/Bc), were plotted in a Day Plot [*Day et al.*, 1977]. Most of the specimens are spread on the theoretical mixing curve [*Dunlop*, 2002] between single domain (SD) and multi domain (MD) magnetite grains (Figure 3). We attempted to correlate flows based on their magnetic mineralogy characteristics, but this was not possible because sites from the same lava flow yielded different hysteresis parameters. Therefore we conclude that magnetic mineralogy cannot be used as a volcanological correlation tool in our study.

4.2. Petrographic Characterization

[20] In general, we observed largely crystallized porphyritic lava in all the samples (Figure 4). The main phenocrysts are olivine and clinopyroxene, representing about 5–20%

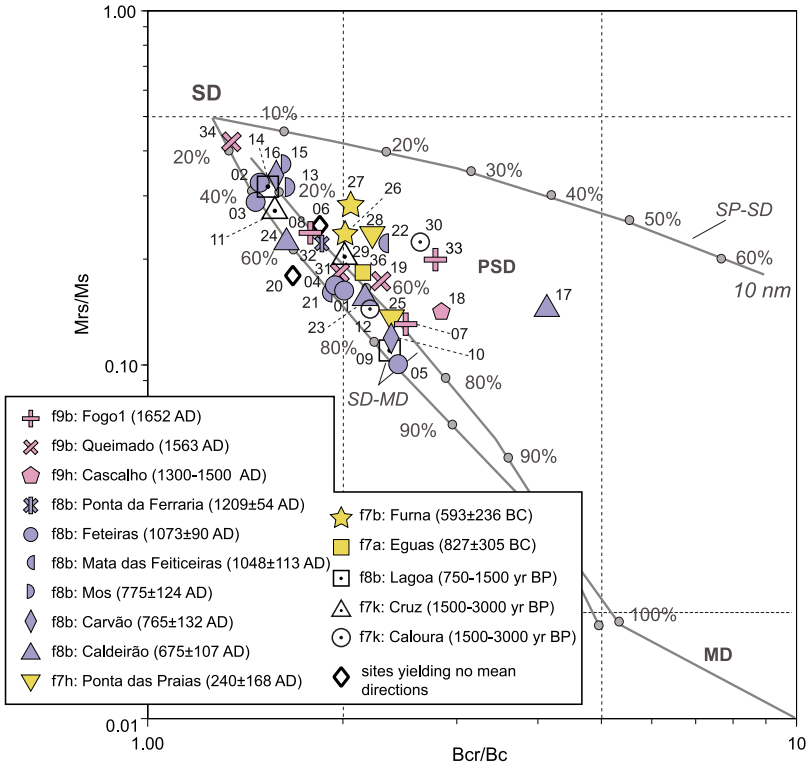

Figure 3. Plot of hysteresis ratios (Mrs/Ms versus Bcr/Bc, after *Day et al.* [1977]) for one representative specimen from each site. The number adjacent to each specimen indicates the site number.

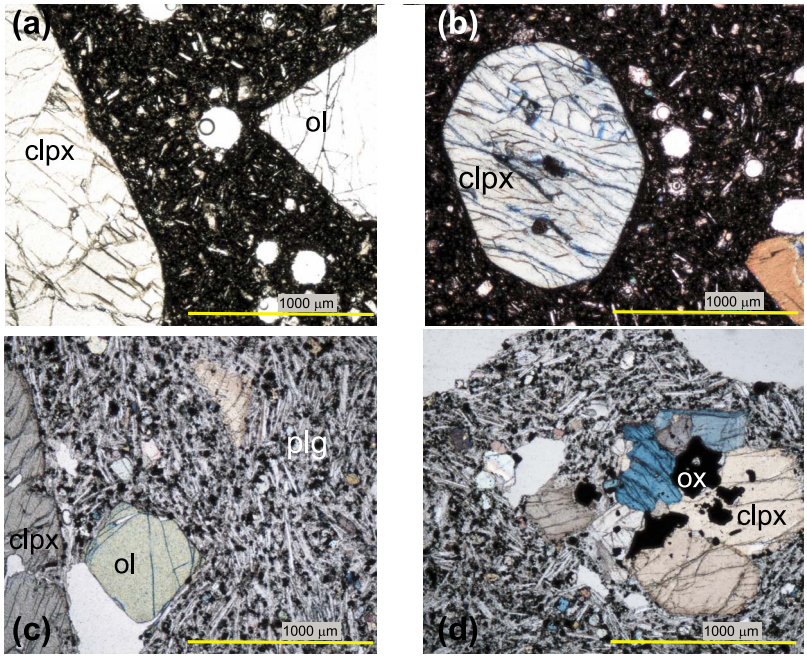

Figure 4. Polarized microscopy images (crossed-polarized light) from four different sites sampled in Feteiras (Figures 4a and 4b) and Caldeirão (Figures 4c and 4d) lava flows, erupted at different times (1073 and 675 AD respectively) and giving different paleomagnetic directions (Table 2 and Figure 6). (a) Sample Sml01-A1: millimeter-size phenocrysts of clinopyroxene (clpx) and olivine (ol) with subeuhedral and prismatic shape in a very-fine grain groundmass; (b) sample Sml04-A1: subeuhedral and prismatic clinopyroxene (clpx); (c) sample Sml17-A1: typical trachytic texture with aligned microcrystals of plagioclase (plg) in the groundmass; (d) sample Sml23-A1: example of glomeroporphyritic texture. Note the occurrence of the Fe-Ti oxides (ox) both in the groundmass and in the aggregate. Scale bar equals 1 mm.

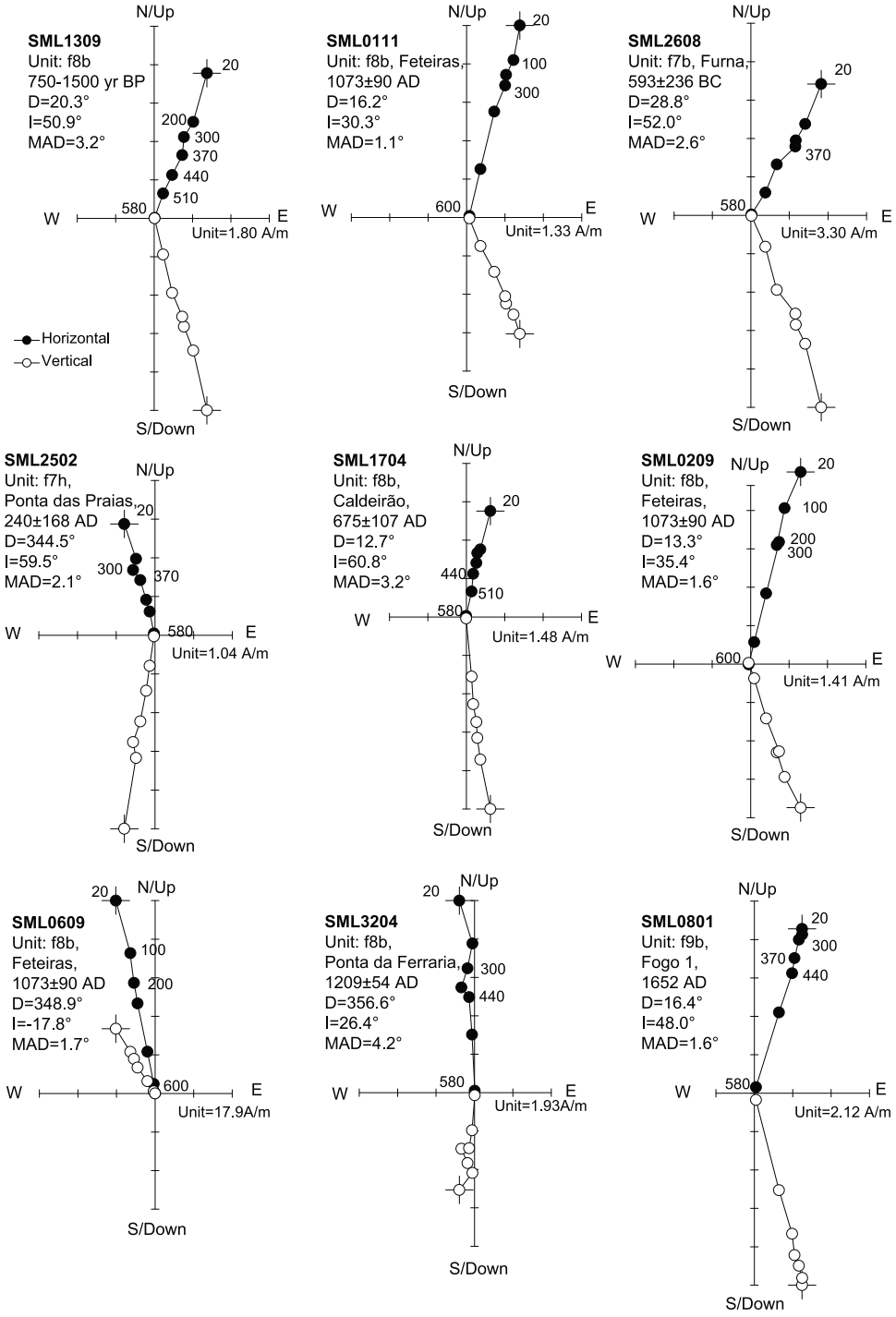

Figure 5. Orthogonal vector diagrams of typical thermal demagnetization data, in situ coordinates. Demagnetization step values are in °C.

of rock, whereas the plagioclase grains are less common. In particular, the samples from the Feteiras flows (Sml01-A1, Sml04-A1) have similar petrographic features (Figures 4a and 4b). Indeed they are characterized by porphyritic texture with sub- to millimeter-sized phenocrysts of olivine and clinopyroxene. Plagioclases are particularly rare. Olivine show subeuhedral to euhedral habits (Figure 4a), whereas clinopyroxene represents generally the largest grain with prismatic or subeuhedral habit. The groundmass is very fine (Figures 4a and 4b) and partially glass in both samples, with microcrysts of olivine, clinopyroxene, plagioclase and Fe-Ti oxides (in order of abundance). The four thin sections from Caldeirão and Cruz (Sml17-A1, 23-A1, 24-A1, and 29-A1) flows have different petrographic features with respect to Feteiras lava samples, showing an enrichment in plagioclase both as phenocrysts and microcrysts in groundmass, that is typical of a trachytic texture (Figures 4c and 4d). In all cases, sub- and millimeter-sized plagioclase are very abundant

Table 2. Mean Paleomagnetic Directions of Sites and Flows From São Miguel[a]

Site	Mean Calendar Age ($\pm 1\sigma$)	n/N	Declination (deg)	Inclination (deg)	k	α_{95} (deg)
Flow f7b - Aflitos						
Sml20	972 ± 142 BC	0/15	(-)	(-)	(-)	(-)
AZ36		7/7	10.0	54.9	347	3.2
Flow f7a - Eguas						
Sml36	827 ± 305 BC	7/12	3.4	59.2	246	3.9
Flow f7k - Cruz N						
Sml29	**1000–500 BC**	10/14	8.7	57.5	357	2.6
Flow f7b - Furna						
Sml26	593 ± 236 BC	09/14	19.2	55.4	165	3.4
Sml27		12/15	7.8	60.8	199	3.1
AZ37		9/9	359.9	49.2	1046	1.6
*Sample Mean**		*24/29*	*13.0*	*58.0*	*122*	*2.7*
*Site Mean***		*2/3*	*13.9*	*58.2*		
Flow f7b - Cruz S						
Sml11	**100 BC-100 AD**	14/15	349.1	49.4	330	2.2
Flow f7b - Caloura						
Sml12	**100 BC-100 AD**	10/15	347.5	46.9	317	2.7
Sml30		09/14	353.5	51.2	167	4.0
*Sample Mean**		*19/29*	*352.0*	*48.0*	*158*	*2.5*
*Site Mean***		*2/2*	*350.4*	*49.1*		
Flow f8b - Lagoa						
Sml09	**200–400 AD**	14/15	358.4	55.9	224	2.7
Sml14		14/15	1.0	54.3	102	4.1
*Sample Mean**		*28/30*	*1.0*	*55.9*	*265*	*1.8*
*Site Mean***		*2/2*	*359.7*	*55.1*		
Flow f7h - Ponta das Praias						
Sml25	240 ± 168 AD	15/15	351.7	57.8	467	1.8
Sml28		10/14	356.6	53.9	199	3.4
AZ31		5/5	352.8	57.3	253	4.8
*Sample Mean**		*25/29*	*356.0*	*56.0*	*215*	*2.0*
*Site Mean***		*3/3*	*353.8*	*56.4*	*997*	*3.9*
Flow f8b - Caldeirão						
Sml17	675 ± 107 AD	10/14	13.3	53.5	236	3.0
Sml23		10/14	12.6	57.3	110	4.6
Sml24		9/11	11.4	53.5	315	2.9
*Sample Mean**		*29/39*	*11.9*	*56.6*	*152*	*1.9*
*Site Mean***		*3/3*	*12.4*	*54.8*	*1280*	*3.4*
Flow f8b - Carvão						
Sml07	765 ± 132 AD	15/16	13.8	42.8	424	1.9
Sml16		14/15	9.8	44.2	200	2.8
*Sample Mean**		*30/31*	*16.6*	*43.3*	*252*	*1.7*
*Site Mean***		*2/2*	*11.8*	*43.5*		
Flow f8b - Mos						
Sml13	775 ± 124 AD	14/15	10.3	50.9	143	3.3
Sml15		10/15	12.2	48.0	231	3.2
*Sample Mean**		*24/30*	*10.2*	*48.5*	*163*	*2.3*
*Site Mean***		*2/2*	*11.3*	*49.5*		
Flow f8b - Mata das Feiticeiras						
Sml21	1048 ± 113 AD	13/13	5.2	37.3	76	4.8
Sml22		10/14	358.5	32.9	229	3.2
AZ29		5/5	5.6	35.0	271	4.7
*Sample Mean**		*23/27*	*1.1*	*34.2*	*154*	*2.5*
*Site Mean***		*3/3*	*3.0*	*35.1*	*420*	*6.0*
Flow f8b - Feteiras						
Sml01	1073 ± 90 AD	08/10	3.6	28.7	345	3.0
Sml02		15/15	5.6	34.4	279	2.3
Sml03		13/15	9.5	33.3	452	2.0
Sml04		12/14	7.3	30.7	363	2.3
Sml05		14/14	6.8	23.6	610	1.6
Sml06		0/15	(−)	(−)	(−)	(−)
*Sample Mean**		*62/68*	*6.4*	*32.7*	*267*	*1.1*
*Site Mean***		*5/5*	*6.5*	*30.2*	*301*	*4.4*
Flow f8b - Ponta da Ferraria						
Sml32	1209 + 54/−53 AD	11/15	355.4	32.4	377	2.4
Flow f9h - Cascalho						
Sml18	**1300 AD**	10/15	355.9	29.7	450	2.3
Flow f9b - Queimado						
Sml19	1563 AD	11/16	5.1	54.7	513	2.0
Sml34		11/15	1.6	57.0	216	3.1

Table 2. (continued)

Site	Mean Calendar Age ($\pm1\sigma$)	n/N	Declination (deg)	Inclination (deg)	k	α_{95} (deg)
Sml31	**1563 AD**	10/15	1.9	57.0	314	2.7
AZ30		5/6	0.7	58.2	246	4.9
*Sample Mean**		*32/46*	*0.5*	*55.5*	*231*	*1.5*
*Site Mean***		*4/4*	*2.4*	*56.7*	*2002*	*2.1*
Flow f9b - Fogo 1						
Sml08	1652 AD	14/15	14.4	50.9	304	2.3
Sml10		12/14	7.0	43.8	249	2.8
Sml33		20/24	11.4	47.1	308	1.9
AZ38		5/9	15.0	48.4	728	2.8
*Sample Mean**		*46/53*	*11.1*	*47.7*	*197*	*1.5*
*Site Mean***		*4/4*	*11.8*	*47.6*	*438*	*4.4*

[a]Flow names and ages are defined as in Table 1. Ages in bold are paleomagnetically inferred. n/N is the number of paleomagnetic directions used to calculate the mean direction/total number of samples/sites. k and α_{95} are statistical parameters after *Fisher* [1953]. When only two sites per flow are available, k and α_{95} values are not reported. Flow-mean paleomagnetic directions are calculated both averaging sample-mean (*) and site-mean (**) directions. Paleomagnetic mean for the Furna flow is calculated averaging sites Sml26 and 27, since site AZ37 is possibly located on a different flow (see text).

(20 to 50% of total rock). Slight differences are found between Sml17-A1, 23-A1, 24-A1 and the Sml29-A1. The Sml29-A1 is characterized by a large amount of millimeter-sized plagioclase, which represents the main phase. In Sml17-A1, 23-A1 and 24-A1 clinopyroxene is the predominant phenocryst, whereas olivine and plagioclase are less frequent (Figure 4c). Phenocryst shapes range from subeuhedral to euhedral, and large millimeter-sized policrystal aggregates occur. The latter are composed by clinopyroxene, plagioclase and opaque grains (in order of abundance) with a typical glomeroporphyritic texture (Figure 4d). The groundmass is composed by microcrysts of plagioclase (60–85% of the groundmass) and Fe-Ti oxides (10–20%), whereas olivine and clinopyroxene are rare (Figures 4c and 4d). In conclusion, the Feteiras and Caldeirão-Cruz groups are clearly distinct, and are characterized by plagioclase-poor and plagioclase-rich modal composition, respectively. In the Caldeirão-Cruz flows, petrographic variations are negligible within the single group of Caldeirão lava (Sml17-A1, 23-A1, 2-A14), whereas slight differences exist when compared with the Sml29-A1 (Cruz flow). Petrographic features (e.g., mineral content percentages, type and size of phenocrysts, groundmass composition, xenolite and relict mineral occurrence) are commonly used in volcanology as characterization and correlation tools. However, in the case of lava flows, slight petrographic differences may exist also in the same lava sampled at different locations from the vent (reflecting variations in effusion rate, thermal history, mechanical fractionation, oxygen fugacity), or in different flows emplaced during a single long-lasting eruption, reflecting probably magmatic zonation [*Blake*, 1981]. The consequence of this is that other independent evidence is generally needed to corroborate petrographic correlation.

4.3. Paleomagnetic Directions

[21] A well-defined characteristic remanent magnetization (ChRM) was isolated for nearly all lava samples in the 300–600°C temperature interval (Figure 5). A few specimens (particularly from sites Sml06 and Sml20) yielded aberrant ChRMs up to 600°C (sample Sml0609 in Figure 5). The same specimens also showed very high NRM values (~30–100 A/m), and the highest magnetic deviation values (up to −25°), calculated from magnetic and sun compass readings of core orientation. Thus we concluded that the aberrant (more than 50° from the GAD field direction expected at São Miguel) components in such specimens are due to a relatively hard isothermal remanent magnetization caused by lightning strikes. Results from these sites were rejected from any further analyses. The α_{95} values relative to the mean paleomagnetic directions evaluated for 33 sites vary from 1.6° to 4.8° (average 2.8°, Table 2). For the old Aflitos flow (972 ± 142 BC, Table 1) we have the sole paleomagnetic direction of site AZ36 by *Johnson et al.* [1998], because our site Sml20 was rejected.

[22] Site-mean paleomagnetic directions from São Miguel, (Table 2), vary between ~−10° to 20° in declination, and 60° to 25° in inclination values (Table 2 and Figure 6). Importantly, directions from the same flow are consistent: angular distances of directions between sites from the same flow are systematically <9°. The paleomagnetic scatter within Feteiras flow (five sites) is within 10°, and similar to that observed for the 1652 AD event. There are several possible sources of intraflow variability, which can yield scatter of paleomagnetic directions (see comprehensive discussions by *Urrutia-Fucuguachi et al.* [2004], *Lanza and Zanella* [2006], and *Speranza et al.* [2006, 2008, 2012]): 1) local magnetic anomalies generated by the strongly magnetized underlying terrain and cooling lava flow [see *Baag et al.*, 1995; *Valet and Soler*, 1999; *Speranza et al.*, 2006]; 2) magnetic mineralogy variability and magnetic anisotropy; 3) internal viscous deformation of lava flows and/or movement of blocks and lava during flow advance; 4) local tectonic effects and block tilting. Despite all these possible sources of bias in geomagnetic field recording, our results seem to be reliable. In fact, sites from different localities, sampled within the same flow, share similar paleomagnetic directions (within an angular distance of ~10°).

[23] Our directions generally agree with those of *Johnson et al.* [1998] who determined six paleomagnetic directions from the flows we studied (Figure 1). In the case of Furna flow, the angular distance between directions of our sites Sml26 and 27 is 8°. However, the angular distance between site AZ37 and Sml26 and 27 is 13° and 12°(respectively), whereas it has been observed in this and other studies [*Speranza et al.*, 2008, 2012] that intraflow variability is mostly within 10°. Thus we cannot exclude that sites Sml26–27 and AZ37 do not come from the same flow. Eleven flow-mean directions are calculated with *Fisher* [1953] statistic, where more than one site-mean direction per flow is available (Table 2). Intraflow consistency (within a tolerance

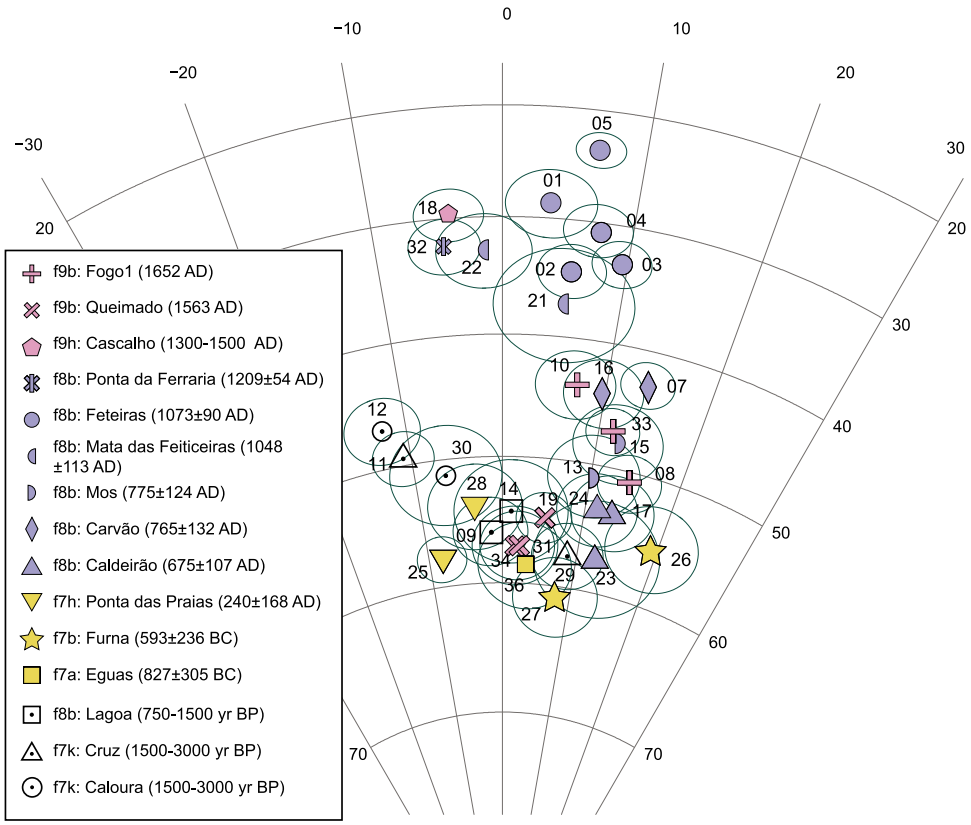

Figure 6. Equal-area projection (lower hemisphere) of site-mean paleomagnetic directions from the studied lavas of São Miguel (the "Sml" prefix of each site is omitted). The ellipses around the paleomagnetic directions are the projections of the relative α_{95} cones. All paleomagnetic directions are listed in Table 2. Colored groups denote three different age ranges (yellow for 1500–3000 yr BP; light-blue for 750–1500 yr BP; and pink for <750 yr BP), colored symbols indicate different flows, and empty symbols mark age-uncertain flows.

of 10°) implies that the observed swing in paleomagnetic declination values of 30° and inclination of 35° is not due to scatter, but reflects the behavior of the geomagnetic field over the last 3 ka.

5. Discussion

5.1. Paleosecular Variations at the Azores During the Last 3 ka

[24] In Figure 7 we have superimposed the 33 well-dated paleomagnetic directions from São Miguel (27 from us, 6 from *Johnson et al.* [1998]), on the geomagnetic directions predicted for São Miguel (37.8°N, 25.5°W) by the most recent global field models. We have considered the gufm1 historical model for 1600–2000 AD [*Jackson et al.*, 2000], as well as the recently issued 0–3 ka CALS3k.4 model [*Korte and Constable*, 2011]. In Figure 7 we also show the French archeomagnetic curve [*Bucur*, 1994; *Gallet et al.*, 2002] (Figure 7), relocated to São Miguel via pole method. Paleomagnetic declination values from São Miguel are at first glance consistent with those predicted by the global field models. The main difference concerns the historical 1652 AD lava flow, for which the gufm1 model predicts D = 1.3°, while the average paleomagnetic declination from four sites (three from us, one from *Johnson et al.* [1998]) is 11.8° ± 6.6°. For older ages, our data basically confirm declination swings predicted by the CALS3k.4 model, although the 200 AD declination minimum seems to be smoothed by few degrees in the model. The agreement with the French curve is remarkable and in some cases even better than the archaeomagnetic field models. For instance the minimum in declination around 200 AD is perfectly reproduced. It seems that the errors introduced by the transfer of the French curve to the Azores using a GAD are less than the uncertainties of the global field models.

[25] Larger discrepancies with respect to the global models are apparent when inclinations are considered (Figure 7). Gufm1 predicts I = 63° for the 1652 AD flow, while the four paleomagnetic sites yield an average inclination of 47.6° ± 4.4°. Considering the 56.7° ± 2.6° inclination that are consistent with models, obtained from the four sites sampled in the 1563 AD flow, we document relatively low inclinations in the North Atlantic Ocean during the 17th century AD. This suggests that a rapid inclination drop occurred at least 150 years before the 1760s, as indicated by gufm1.

[26] We note that inclinations were measured in the Atlantic Ocean much later than declinations, and according to *Jackson et al.* [2000] no inclination values were measured

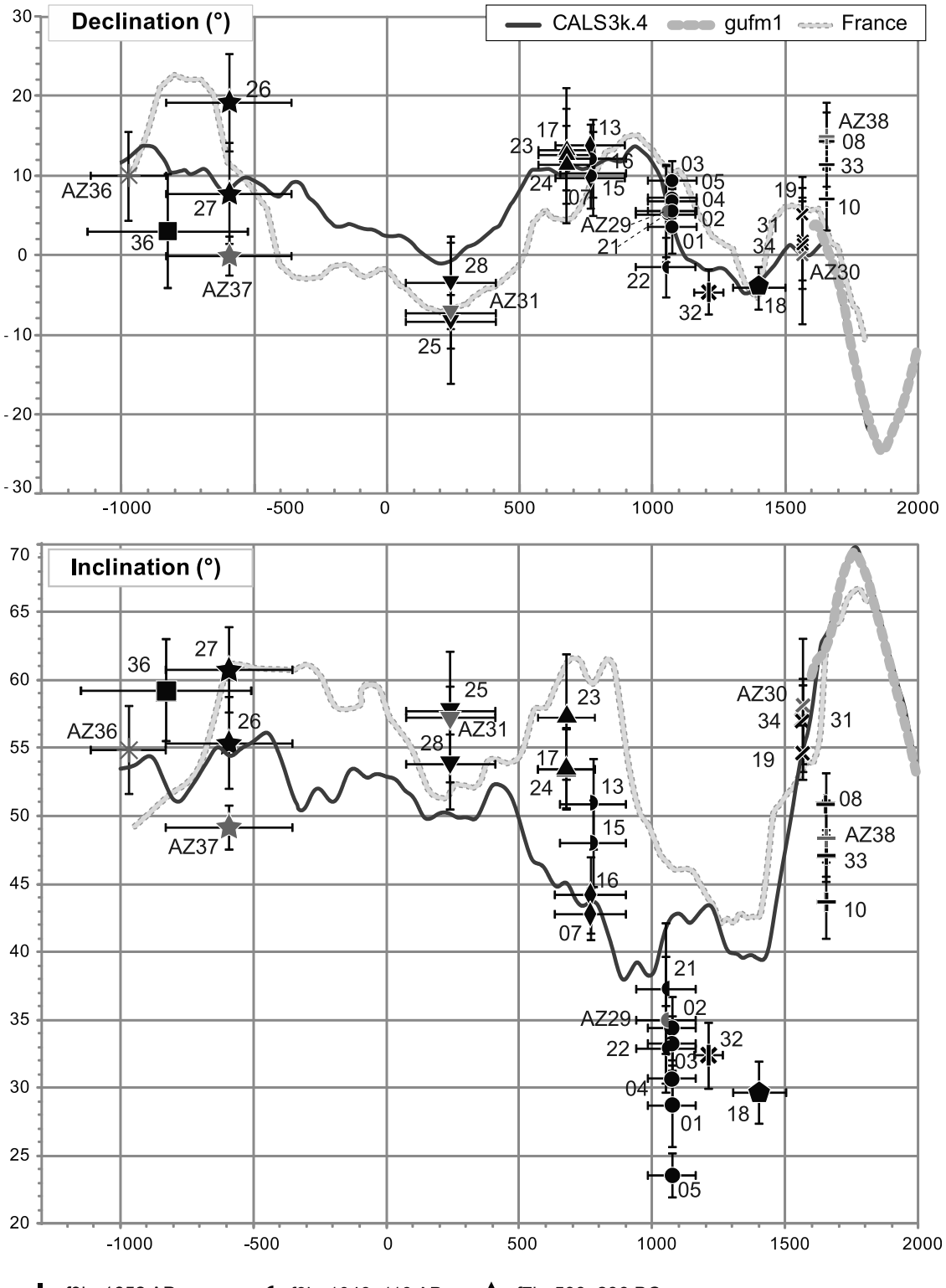
Declination (°)
CALS3k.4
gufm1
France
Inclination (°)
AZ36
AZ37
AZ31
AZ29
AZ30
AZ38
f9b: 1652 AD
f9b: 1563 AD
f9h: 1300 AD
f8b: 1209±54 AD
f8b: 1073±90 AD
f8b: 1048±113 AD
f8b: 775±124 AD
f8b: 765±132 AD
f8b: 675±107 AD
f7h: 240±168 AD
f7b: 593±236 BC
f7a: 827±305 BC
AZ- Sites by Johnson et al. [1998]

Figure 7

aboard ships before the 18th century. In order to verify whether some non-dipole field effect has occurred at the Azores region during the last 400 years, the contribution of the dipole and non-dipole components to the total field has been calculated using the *GUFMfield.for* program (http://jupiter.ethz.ch/~cfinlay/gufm1.html). We find that discrepancies from our data and models could not be explained as a non-dipolar field effect because during the last 400 years the contribution of the non-dipolar component is very small ($1*10^{-4}$ versus $5*10^{-4}$ of intensity) when compared with the total intensity curve. Although those discrepancies are difficult to explain, the reliability of our data is upheld by both the paleomagnetic consistency of far sites from the same flow (Figure 1), and the agreement with the directions determined by *Johnson et al.* [1998].

[27] Our data confirm the pronounced inclination minimum predicted by CALS3k.4 model for the ~800–1400 AD time span, as well as documenting inclination values lower by ~10° with respect to predictions, and a trend much more similar to the relocated French curve than to CALS3k.4 model. The ~10° inclination difference seems to be related to non-dipolar field components, as it is also observed with respect to the French archeomagnetic curve relocated by pole method. For older ages, our inclination data roughly agree with both the reference model and French curve. It may be argued that our data suffer from a paleomagnetic recording bias, instead of reproducing true inclination features of the geomagnetic field in the Atlantic Ocean in the 1000–1400 AD and ~1600 AD periods. Biased too-low paleomagnetic inclinations with respect to geomagnetic observations were indeed observed in both historic lavas from Hawaii [*Castro and Brown*, 1987], and Paricutin volcano, Mexico [*Urrutia-Fucuguachi et al.*, 2004]. However, such documented cases represent a small percentage if compared with several other studies documenting faithful recordings of the geomagnetic field by lavas [e.g., *Rolph et al.*, 1987; *Hagstrum and Champion*, 1994; *Jurado-Chichay et al.*, 1996; *Lanza and Zanella*, 2003; *Tanguy et al.*, 2003; *Speranza et al.*, 2008, 2010]. There are several geomagnetic, tectonic, and magnetic mineralogy controls that in principle may result in biased recording of inclination in volcanic rocks. However, all these factors can be excluded from our data set because 1) paleomagnetic directions from the same lava flow are always consistent (Figure 6) also considering independently gathered directions by *Johnson et al.* [1998]; 2) low inclinations characterize only some flows at given ages, while many others yield inclination values consistent with model predictions (Figure 7); 3) local magnetic anomalies of ~1000 nT reported by *Blanco et al.* [1997] cannot be responsible for the great differences between our paleomagnetic inclinations and model predictions. In fact, *Zanella* [1998] has calculated that at Pantelleria (Italy), at latitude similar to that of Azores, even a high-intensity magnetic anomaly of 800 nT is unable to yield a field deflection exceeding 1°.

5.2. Implications for the Characteristics and Timing of Volcanic Eruptions at São Miguel

[28] The vicinity of paleomagnetic directions is classically used to infer on volcanic deposit correlation [*Jurado-Chichay et al.*, 1996; *Riisager et al.*, 2003; *Speranza et al.*, 2012]. However, additional independent evidence, such as volcano-stratigraphic and petrographic observations, may be useful to corroborate paleomagnetic correlations. Therefore, the observed vicinity of paleomagnetic directions from the same flow (Figure 6) along with field evidence, imply that site Sml31 effectively belongs to the 1563 AD basanitic lava (Figure 1), as also suggested by *Wallenstein et al.* [2007]. This confirms that the western branch of such thin low-viscosity flow erupted from Pico Queimado advanced 1–2 km farther north compared with the map of *Moore* [1990], and reached the 1048 ± 113 AD Mata das Feiticeiras flow.

[29] The age of the Pico do Cascalho hawaiite (site Sml18), initially constrained to the 1300–1500 AD time window, must be placed in the lower bound of the interval (~1300 AD), because of its very low inclination (29.7° ± 2.3°) compared with the 56.7° ± 2.1° value obtained from the 1563 AD flow (Figure 7). This implies that the last eruption of the Sete Cidades volcano (trachytic pumice deposit from Caldeira Seca), constrained by *Moore* [1991] and *Moore and Rubin* [1991] to be older than the Pico do Cascalho flow, must be similarly placed at ~1300 AD. Thus historical records indicating that eruption of Sete Cidades was occurring at the time of Portuguese discovery of the Azores at ~1444 AD [see *Moore and Rubin*, 1991] may be incorrect. The vicinity of paleomagnetic directions between sites Sml26 and 27, along with stratigraphic observations, allow us to confirm that Sml27 was effectively sampled in the Furna flow (829–357 BC).

[30] With regards to the four petrographically analyzed sites of Zone 2, their paleomagnetic directions are very similar, but petrographic features suggest that site Sml29 belongs to a different flow than sites Sml17, 23 and 24 (as indicated in the *Moore* [1991] map). In fact, site Sml29 has a larger amount of millimeter-sized plagioclase, while the main phase of Sml17, 23 and 24 is clinopyroxene.

5.3. Local Evolution of Geomagnetic Field at the Azores

[31] To determine the local evolution of the geomagnetic field at the Azores during the last 3 ka, we applied a cubic spline fit to the 13 well-dated flow-mean paleomagnetic directions shown in Table 2 (Figures 8a and 8b). Considering age error bars, and to avoid unrealistic fit oscillations (i.e., too fast changes in field values, which would result as improbable kinks), we assigned a common 770 AD age to sites from Carvão (765 AD) and Mos (775 AD) flows, a 1073 AD age (the age of Feteiras flow) to Mata das

Figure 7. Declination / inclination versus age plot for historical or ^{14}C dated paleomagnetic directions from this study (26 sites, the "Sml" prefix is omitted), and *Johnson et al.* [1998] (6 sites, labeled with prefix "AZ-"), compared with global field model predictions from gufm1 [*Jackson et al.*, 2000] and CALS3k.4 [*Korte and Constable*, 2011]. Sites of *Johnson et al.* [1998] are shown in gray. Ages (and relative error bars) are calendar ages (and relative errors) calibrated by us from radiocarbon ages by *Moore and Rubin* [1991]. Errors for site-mean declination and inclination values are α_{95} /cos(I) and α_{95} values, respectively (see Table 2). Cruz, Caloura and Lagoa flows are not included on this figure as the dating is uncertain.

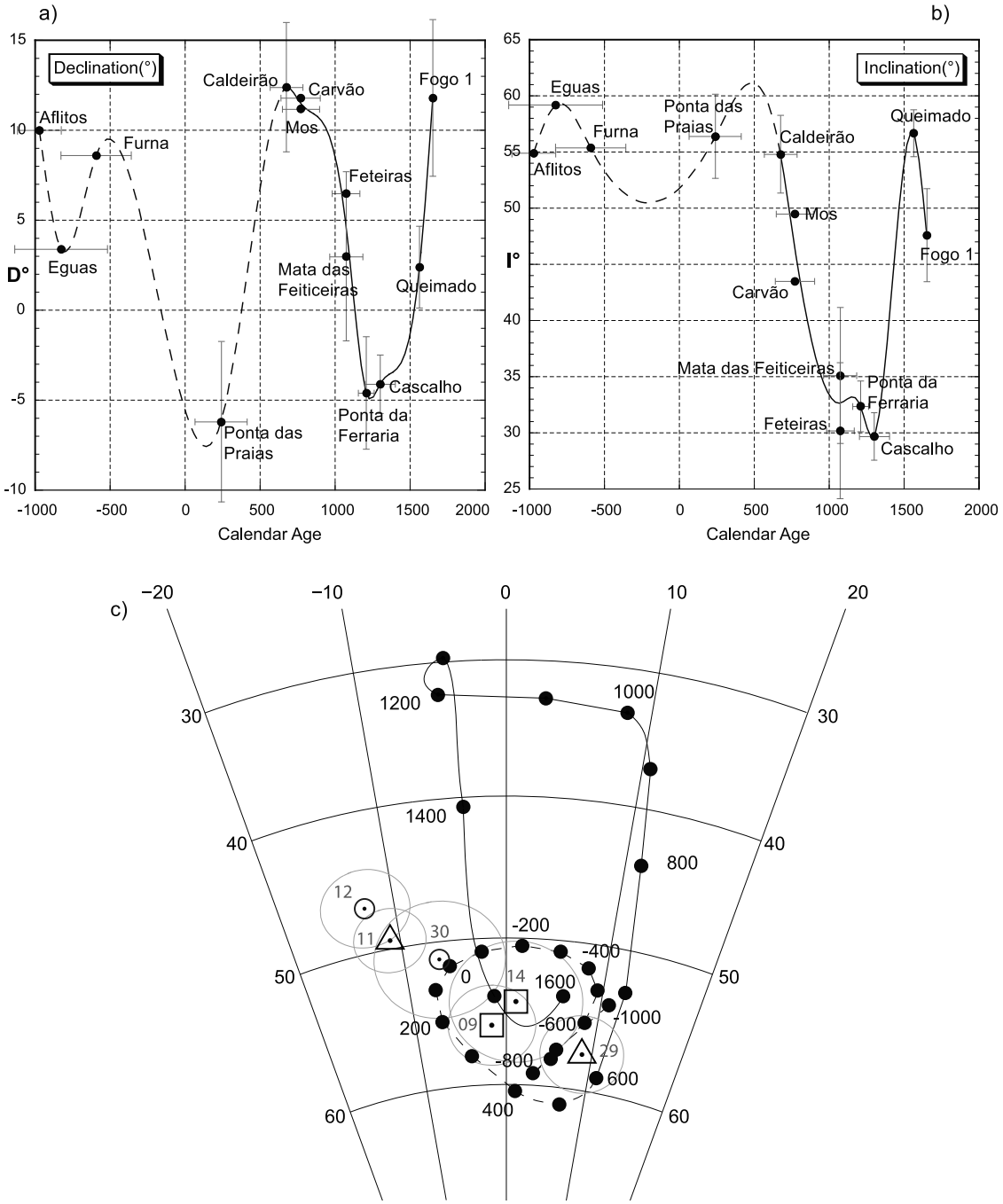

Figure 8. Cubic spline interpolation of flow mean (a) declinations and (b) inclinations versus respective calendar ages; (c) directions derived every 100 years from cubic spline interpolation, superimposed on paleomagnetic directions (and relative confidence cones) from three loosely dated flows (Figure 1 and Table 2). For ages older than 750 AD the fit line is dashed, as it is constrained by a limited number of data. Vertical error bars for declination and inclination data are α_{95} /cos(I) and α_{95} values, respectively (flow characterized by one or two sites have no α_{95} values, see Table 2).

Feiticeiras flow (sites Sml21–22 and AZ29), 1048 AD, and set to 1300 AD the age of the Pico do Cascalho flow (site Sml18). The directions from the 972 ± 142 BC Aflitos flow (site AZ36) and 827 ± 305 BC Eguas flow were also considered, although only one site direction per flow is available in both cases. Directions derived every 100 years from the cubic spline interpolation of paleomagnetic data are shown in Figure 8c. The evolution from 1000 to 800 BC is virtually overlapped by subsequent track from 800 to 500 BC, and very close to more recent track from 400 to 700 AD. This might represent a potential uncertainty problem for the use of paleomagnetic dating at the Azores. Conversely, the field evolution fingerprint between 700 and 1450 AD is univocal,

and characterized by a ~−5° declination / 30° inclination minimum centered at 1200–1300 AD.

[32] We point out that we used the spline fit interpolation since there are insufficient paleomagnetic data to use sliding age windows method to derive a PSV curve for the Azores with relative uncertainties on stepwise moving reference points, as this is routinely done when abundant archaeomagnetic data are available [e.g., *Bucur*, 1994]. Moreover, since for the flows older than Caldeirão (675 AD) the data density is low, an unconstrained behavior in the fit is introduced, allowing for a number of solutions including a flat line. Additional data are required to support the oscillation in the path before 750 AD (dashed curve in Figure 8).

5.4. Paleomagnetic Dating of Flows With Uncertain Age

[33] The local field evolution at São Miguel depicted in Figure 8 can be used to provide more accurate dating for the three loosely dated flows studied by us; Cruz (sites Sml11–29), Caloura (sites Sml12–30), and Lagoa (sites Sml09–14) flows (Figures 1, 6 and 8c). Dating is obtained by considering the overlap of the PSV curve with paleomagnetic directions (and relative confidence cones). We assume a 5° curve precision, and consider the small inter-flow paleomagnetic variability (mostly within 8°, Figure 6), as verified for our data set.

[34] With regards to the Cruz and Caloura flows, previously constrained in the 1500–3000 yr BP time window by *Moore* [1990, 1991], we first document that the northern and southern branch of the Cruz alkali olivine basalt flow (sites Sml11 and 29, Figure 1) yield very different paleomagnetic directions (Table 2). Thus they must represent two different age lavas, that we name Cruz N and Cruz S. The southern branch (Cruz S, site Sml11), together with the Caloura alkali olivine basalt (sites Sml12 and 30) yield ~−10° declination / 50° inclination values, and can be correlated with the PSV cusp of 100 BC-100 AD, probably smoothed in Figure 8. The 2220 ± 70 yr BP radiocarbon age (calibrated age 265 ± 61 BC) gathered by *Queiroz* [1997] for pyroclastic deposit P11, resting above lava of site Sml11, is in rough agreement with paleomagnetic dating, although at its older age bound.

[35] Conversely, the northern branch of the Cruz lava, (Cruz N, site Sml29), can be referred to the 1000–500 BC time window (Table 2). It is noteworthy that the direction from site Sml29 is virtually coincident with directions from sites Sml17, 23, and 24, sampled in the adjacent 675 AD Caldeirão basanite (Figure 6). As we have verified that the petrography of site Sml29 and 17-23-24 is distinctly different, we can confirm that the Cruz N and Caldeirão lavas are two different flows, and uphold the inferred 1000–500 BC age for the Cruz N flow.

[36] Finally, the Lagoa basanite (sites Sml09 and 14) is not consistent with paleomagnetic directions of the 750–1500 yr BP time window (as indicated by *Moore* [1991]), but is compatible with slightly older ages (~200–400 AD, Figure 8).

6. Conclusions

[37] Thirty-three paleomagnetic directions (27 from us, 6 from *Johnson et al.* [1998]) from thirteen historical or ^{14}C dated lava flows from São Miguel yield the first 0–3 ka PSV record for the Azores. Systematic consistency (angular distance <9°) of paleomagnetic directions from the same lava flow ensure that the observed 40° of inclination / 30° of declination swings reflect local paleofield evolution. While the paleodeclination record is at first approximation consistent with CALS3k.4 [*Korte and Constable*, 2011], and gufm1 [*Jackson et al.*, 2000] global models, the following significant discrepancies are observed when the inclinations are considered:

[38] 1. Four sites from the 1652 AD historical flow yield I = 47.6° ± 4.4° (compared with I = 63° predicted by gufm1), suggesting much lower inclinations in the Atlantic Ocean during the 17th century AD with respect to model predictions. Thus the rapid inclination drop might have occurred at the Azores at least 150 years before than the 1760s indicated by gufm1, and this discrepancy could be related to the lack of inclination values available from the Atlantic Ocean before the 18th century.

[39] 2. Our data support the inclination minimum predicted by CALS3k.4 for ~800–1400 AD, yet indicates that inclination values were lower by at least 10° with respect to model prediction. The ~10° discrepancy is also observed with respect to the French archeomagnetic curve relocated to the Azores via pole method, thus suggesting a significant contribution of the non-dipole field. We document that inclination values at the Azores were as low as ~30° during 1200–1300 AD. For older ages, our data support models within ~5°.

[40] The PSV curve for the last 3 ka gathered in this study, preferably associated with additional geological and geochronological constraints, will hopefully serve to provide paleomagnetic dating for volcanic products recently emplaced at both São Miguel and all other islands of the Azores archipelago. PSV directions from São Miguel can be safely relocated to other Azores island (within 500 km from São Miguel) via pole method [*Noel and Batt*, 1990], introducing for such small distances directional errors not exceeding 1°–2° [e.g., *Lanza et al.*, 2005]. The PSV curve of Azores shows three tracks (1000–800 BC, 800–500 BC and 400–700 AD) in virtual overlap, and this might indeed represent a problem (i.e., unequivocal dating) when trying to paleomagnetically date lava flows of the last 3 ka.

[41] **Acknowledgments.** A. Pimentel, V. Borgognoni, and A. Castelli helped for sampling some of the sites. We thank D. Predazzi and A. Gomes for useful discussions about lava flow distribution. We thank A. Jackson for kindly providing geomagnetic observations from the Atlantic Ocean as well as L. Sagnotti and L. Tauxe for discussions on paleomagnetic data. We are grateful to two anonymous reviewers for providing very thorough and constructive comments on our manuscript as well as to JGR Associate Editor S. Gilder and Editor T. Parsons for carefully evaluating our work. We are also grateful to Centro de Vulcanologia e Avaliação de Riscos Geológicos (CVARG) for access to the various facilities required to undertake this work. A.D.C. and F.S. were funded by INGV and FIRB MIUR C2 funds (responsible L. Sagnotti), while M.P. was financially supported by CVARG.

References

Abdel-Monem, A. A., L. A. Fernandez, and G. M. Boone (1975), K–Ar ages from the eastern Azores group (Santa Maria, São Miguel and the Formigas Islands), *Lithos*, *8*(4), 247–254, doi:10.1016/0024-4937(75)90008-0.

Baag, C., C. E. Helsley, S. Xu, and B. R. Lienert (1995), Deflection of paleomagnetic directions due to magnetization of the underlying terrain, *J. Geophys. Res.*, *100*(B6), 10,013–10,027.

Blake, S. (1981), Eruptions from zoned magma chambers, *J. Geol. Soc.*, *138*(3), 281–287, doi:10.1144/gsjgs.138.3.0281.

Blanco, I., A. Garcìa, and J. M. Torta (1997), Magnetic study of the Furna caldera (Azores), *Ann. Geofis.*, *15*(2), 341–359.

Bleil, U., and M. Dillon (2008), Holocene Earth's magnetic field variations recorded in marine sediments of the NW African continental margin, *Stud. Geophys. Geod.*, *52*(2), 133–155, doi:10.1007/s11200-008-0010-6.

Booth, B., R. Croasdale, and G. P. L. Walker (1978), A quantitative study of five thousand years of volcanism on São Miguel, Azores, *Philos. Trans. R. Soc. London, A*, *288*, 271–319, doi:10.1098/rsta.1978.0018.

Bucur, I. (1994), The direction of the terrestrial magnetic field in France during the last 21 centuries. Recent progress, *Phys. Earth Planet. Inter.*, *87*, 95–109, doi:10.1016/0031-9201(94)90024-8.

Carlut, J., X. Quidelleur, V. Courtillot, and G. Boudon (2000), Paleomagnetic directions and K/Ar dating of 0 to 1 Ma lava flows from La Guadeloupe Island (French West Indies): Implications for time-averaged field models, *J. Geophys. Res.*, *105*, 835–849, doi:10.1029/1999JB900238.

Castro, J., and L. Brown (1987), Shallow paleomagnetic direction from historic lava flows, Hawaii, *Geophys. Res. Lett.*, *14*(12), 1203–1206, doi:10.1029/GL014i012p01203.

Channell, J. E. T., D. A. Hodell, and B. Lehman (1997), Relative geomagnetic paleointensity and δ18O ad ODP Site 983(Gardar Drift, North Atlantic) since 350 ka, *Earth Planet. Sci. Lett.*, *153*, 103–118, doi:10.1016/S0012-821X(97)00164-7.

Day, R., M. Fuller, and V. A. Schmidt (1977), Hysteresis properties of titanomagnetites: Grain size and compositional dependence, *Phys. Earth Planet. Inter.*, *13*, 260–267, doi:10.1016/0031-9201(77)90108-X.

Doell, R. R., and A. Cox (1963), The accuracy of the paleomagnetic method as evaluated from historic Hawaiian lava flows, *J. Geophys. Res.*, *68*, 1997–2009, doi:10.1029/JZ068i007p01997.

Donadini, F., M. Korte, and C. G. Constable (2009), Geomagnetic field for 0–3 ka: 1. New data sets for global modeling, *Geochem. Geophys. Geosyst.*, *10*, Q06007, doi:10.1029/2008GC002295.

Dunlop, D. J. (2002), Theory and application of the Day plot (Mrs/Ms versus Hcr/Hc): 1. Theoretical curves and tests using titanomagnetite data, *J. Geophys. Res.*, *107*(B3), 2056, doi:10.1029/2001JB000486.

Feraud, G., I. Kaneoka, and C. J. Allègre (1980), K/Ar ages and stress pattern in the Azores: Geodynamic implications, *Earth Planet. Sci. Lett.*, *46*, 275–286, doi:10.1016/0012-821X(80)90013-8.

Fernandez, L. A. (1980), Geology and petrology of the Nordeste volcanic complex. São Miguel, Azores, *Geol. Soc. Am. Bull.*, *91*, 675–680, doi:10.1130/0016-7606(1980)91<675:GAPOTN>2.0.CO;2.

Ferreira, T. (2000), Caracterização da actividade vulcânica da ilha de S. Miguel (Açores): Vulcanismo basáltico recente e zonas de desgaseificação. Avaliação de riscos, PhD thesis, 248 pp., Dep. de Geoci., Univ. dos Açores, Ponta Delgada, Portugal.

Fisher, R. A. (1953), Dispersion on a sphere, *Proc. R. Soc. London, A*, *217*, 295–305, doi:10.1098/rspa.1953.0064.

Gallet, Y., A. Genevey, and M. Le Goff (2002), Three millennia of directional variation of the Earth's magnetic field in western Europe as revealed by archaeological artefacts, *Phys. Earth Planet. Inter.*, *131*, 81–89, doi:10.1016/S0031-9201(02)00030-4.

Genevey, A., Y. Gallet, C. G. Constable, M. Korte, and G. Hulot (2008), ArcheoInt: An upgraded compilation of geomagnetic field intensity data for the past ten millennia and its application to the recovery of the past dipole moment, *Geochem. Geophys. Geosyst.*, *9*, Q04038, doi:10.1029/2007GC001881.

Hagstrum, J. T., and D. E. Champion (1994), Paleomagnetic correlation of Late Quaternary lava flows in the lowest east rift zone of Kilauea Volcano, Hawaii, *J. Geophys. Res.*, *99*(B11), 21,679–21,690, doi:10.1029/94JB01852.

Jackson, A., A. R. T. Jonkers, and M. R. Walker (2000), Four centuries of geomagnetic secular variation from historical records, *Philos. Trans. R. Soc. London, A*, *358*, 957–990, doi:10.1098/rsta.2000.0569.

Johnson, C. L., J. R. Wijbrans, C. G. Constable, J. Gee, H. Staudigel, L. Tauxe, V. H. Forjaz, and M. Salgueiro (1998), $^{40}Ar/^{39}Ar$ ages and paleomagnetism of São Miguel lavas, Azores, *Earth Planet. Sci. Lett.*, *160*, 637–649, doi:10.1016/S0012-821X(98)00117-4.

Jurado-Chichay, Z., J. Urrutia-Fucugauchi, and S. K. Rowland (1996), A paleomagnetic study of the Pohue Bay flow and its associated coastal cones, Mauna Loa volcano, Hawaii: Constraints on their origin and temporal relationships, *Phys. Earth Planet. Inter.*, *97*(1–4), 269–277, doi:10.1016/0031-9201(95)03135-9.

Kirschvink, J. L. (1980), The least-squares line and plane and the analysis of palaeomagnetic data, *Geophys. J. R. Astron. Soc.*, *62*(3), 699–718, doi:10.1111/j.1365-246X.1980.tb02601.x.

Korte, M., and C. G. Constable (2005), Continuous geomagnetic field models for the past 7 millennia: 2. CALS7K, *Geochem. Geophys. Geosyst.*, *6*, Q02H16, doi:10.1029/2004GC000801.

Korte, M., and C. G. Constable (2011), Improving geomagnetic field reconstruction for 0–3 ka, *Phys. Earth Planet. Inter.*, *188*, 247–259, doi:10.1016/j.pepi.2011.06.017.

Korte, M., and R. Holme (2010), On the persistence of geomagnetic flux lobes in global Holocene field models, *Phys. Earth Planet. Inter.*, *182*(3–4), 179–186, doi:10.1016/j.pepi.2010.08.006.

Korte, M., C. G. Constable, and F. Donadini (2011), Reconstructing the Holocene geomagnetic field, *Earth Planet. Sci. Lett.*, *312*(3–4), 497–505, doi:10.1016/j.epsl.2011.10.031.

Lanza, R., and E. Zanella (2003), Paleomagnetic secular variation at Vulcano (Aeolian Islands) during the last 135 kyr, *Earth Planet. Sci. Lett.*, *213*, 321–336, doi:10.1016/S0012-821X(03)00326-1.

Lanza, R., and E. Zanella (2006), Comments on "Chronology of Vesuvius' activity from A. D. 79 to 1631 based on archeomagnetism of lavas and historical sources" by C. Principe et al., *Bull. Volcanol.*, *68*, 394–396.

Lanza, R., A. Meloni, and E. Tema (2005), Historical measurement of the Earth's magnetic field compared with the remanence directions from lava flows in Italy over the last four centuries, *Phys. Earth Planet. Inter.*, *148*, 97–107, doi:10.1016/j.pepi.2004.08.005.

Lund, S. P., and L. Kleigwin (1994), Measurement of the degree of smoothing in sediment paleomagnetic secular variation records: An example from late Quaternary deep-sea sediments of the Bermuda Rise, western North Atlantic Ocean, *Earth Planet. Sci. Lett.*, *122*, 317–330, doi:10.1016/0012-821X(94)90005-1.

McKee, E. H., and R. B. Moore (1992), Potassium–argon dates for trachytic rocks on São Miguel, Azores, *Isochron West*, *58*, 9–11.

Michalk, D. M., A. R. Muxworthy, H. N. Bohnel, J. MacLennan, and N. Nowczyk (2008), Evaluation of the multispecimen parallel differetial pTRM method: A test on historical lavas from Iceland and Mexico, *Geophys. J. Int.*, *173*, 409–420, doi:10.1111/j.1365-246X.2008.03740.x.

Mitchell-Thomè, R. C. (1981), Vulcanicity of historic times in the Middle Atlantic Islands, *Bull. Volcanol.*, *44*, 57–69.

Moore, R. B. (1990), Volcanic geology and eruption frequency, São Miguel, Azores, *Bull. Volcanol.*, *52*, 602–614, doi:10.1007/BF00301211.

Moore, R. B. (1991), Geologic map of São Miguel, Azores, *U.S. Geol. Surv. Misc. Invest. Map*, *I-2007*, scale 1:50,000.

Moore, R. B., and M. Rubin (1991), Radiocarbon dates for lava flows and pyroclastic deposits on São Miguel, Azores, *Radiocarbon*, *33*(1), 151–164.

Noel, M., and C. M. Batt (1990), A method for correcting geographically separated remanence directions for the purpose or archaeomagnetic dating, *Geophys. J. Int.*, *102*, 753–756, doi:10.1111/j.1365-246X.1990.tb04594.x.

Pressling, N., F. A. Trusdell, and D. Gubbins (2009), New and revised ^{14}C dates for Hawaiian surface lava flows: Paleomagnetic and geomagnetic implications, *Geophys. Res. Lett.*, *36*, L11306, doi:10.1029/2009GL037792.

Queiroz, G. (1997), Vulcão das Sete Cidades (S.Miguel, Açores), História Eruptiva e Avaliação do Hazard, PhD thesis, Univ. dos Açores, Ponta Delgada, Portugal.

Queiroz, G., J. M. Pacheco, J. L. Gaspar, W. P. Aspinall, J. E. Guest, and T. Ferreira (2008), The last 5000 years of activity at Sete Cidades volcano (São Miguel Island, Azores): Implications for hazard assessment, *J. Volcanol. Geotherm. Res.*, *178*, 562–573.

Riisager, J., P. Riisager, and A. K. Pedersen (2003), Paleomagnetism of large igneous provinces: Case-study from West Greenland, North Atlantic igneous province, *Earth Planet. Sci. Lett.*, *214*, 409–425, doi:10.1016/S0012-821X(03)00367-4.

Rolph, T., J. Shaw, and J. E. Guest (1987), Geomagnetic field variations as a dating tool: Application to Sicilian lavas, *J. Archaeol. Sci.*, *14*, 215–225, doi:10.1016/0305-4403(87)90008-2.

Rutten, M. G., and H. Wensink (1960), Paleomagnetic dating, glaciations and the chronology of the Plio-Pleistocene in Iceland, paper presented at XXI International Geology Congress, Copenhagen.

Schweitzer, C., and H. C. Soffel (1980), Paleointensity measurements on post-glacial lavas from Iceland, *J. Geophys.*, *47*, 57–60.

Shotton, F. W., and R. Williams (1971), Birmingham University radiocarbon dates II, *Radiocarbon*, *10*(2), 200–206.

Soler, V., J. C. Carracedo, and F. Heller (1984), Geomagnetic secular variation in historical lavas from the Canary Islands, *Geophys. J. R. Astron. Soc.*, *78*, 313–318, doi:10.1111/j.1365-246X.1984.tb06487.x.

Speranza, F., M. Pompilio, and L. Sagnotti (2004), Paleomagnetism of spatter lava from Stromboli volcano (Aeolian Islands, Italy): Implications for the age of paroxysmal eruption, *Geophys. Res. Lett.*, *31*, L02607, doi:10.1029/2003GL018944.

Speranza, F., S. Branca, M. Coltelli, F. D'Ajello Caracciolo, and L. Vigliotti (2006), How accurate is "paleomagnetic dating"? New evidence from historical lavas from Mount Etna, *J. Geophys. Res.*, *111*, B12S33, doi:10.1029/2006JB004496.

Speranza, F., M. Pompilio, F. D'Ajello Caracciolo, and L. Sagnotti (2008), Holocene eruptive history of the Stromboli volcano: Constraints from paleomagnetic dating, *J. Geophys. Res.*, *113*, B09101, doi:10.1029/2007JB005139.

Speranza, F., P. Landi, F. D'Ajello Caracciolo, and A. Pignatelli (2010), Paleomagnetic dating of the most recent silicic eruptive activity at Pantelleria (Strait of Sicily), *Bull. Volcanol.*, *72*, 847–858, doi:10.1007/s00445-010-0368-5.

Speranza, F., A. Di Chiara, and S. G. Rotolo (2012), Correlation of welded ignimbrites on Pantelleria (Strait of Sicily) using paleomagnetism, *Bull. Volcanol.*, *74*(2), 341–357, doi:10.1007/s00445-011-0521-9.

Stanton, T., P. Riisager, M. F. Knudsen, and T. Thoardrson (2011), New paleointensity data from Holocene Icelandic lavas, *Phys. Earth Planet. Inter.*, *186*(1–2), 1–10, doi:10.1016/j.pepi.2011.01.006.

Stoner, J. S., J. E. T. Channell, C. Hillaire-Marcel, and C. Kissel (2000), Geomagnetic paleointensity and environmental record from Labrador Sea core MD95-2024: Global marine sediment and ice core chronostratigraphy for the last 110 kyr, *Earth Planet. Sci. Lett.*, *183*, 161–177.

Stoner, J. S., A. Jennings, G. B. Kristjánsdóttir, G. Dunhill, J. T. Andrews, and J. Hardardottir (2007), A paleomagnetic approach toward refining Holocene radiocarbon-based chronologies: Paleoceanographic records from the north Iceland (MD99–2269) and the east Greenland (MD99–2322) margins, *Paleoceanography*, *22*, PA1209, doi:10.1029/2006PA001285.

Tanguy, J. C., M. Le Goff, C. Principe, S. Arrighi, V. Chillemi, A. Paiotti, S. La Delfa, and G. Patanè (2003), Archeomagnetic dating of Mediterranean volcanics of the last 2100 years: Validity and limits, *Earth Planet. Sci. Lett.*, *211*, 111–124, doi:10.1016/S0012-821X(03)00186-9.

Thompson, R., and G. M. Turner (1985), Icelandic Holocene paleomagnetism, *Phys. Earth Planet. Inter.*, *38*, 250–261, doi:10.1016/0031-9201(85)90072-X.

Urrutia-Fucuguachi, J., L. M. Alva-Valdivia, A. Goguitchaichvili, M. L. Rivas, and J. Morales (2004), Paleomagnetic, rock-magnetic and microscopy studies of historic lava flows from the Paricutin volcano, Mexico: Implication for the deflection of paleomagnetic directions, *Geophys. J. Int.*, *156*, 431–442, doi:10.1111/j.1365- 246X.2004.02166.x.

Valet, J. P., and V. Soler (1999), Magnetic anomalies of lava fields in the Canary Islands. Possible consequences for paleomagnetic records, *Phys. Earth Planet. Inter.*, *115*(2), 109–118.

Vezzoli, L., C. Principe, J. Malfatti, S. Arrighi, J. C. Tanguy, and M. Le Goff (2009), Modes and times of caldera resurgence: The <10 ka evolution of Ischia Caldera, Italy, from high-precision archaeomagnetic dating, *J. Volcanol. Geotherm. Res.*, *186*, 305–319, doi:10.1016/j.jvolgeores.2009.07.008.

Wallenstein, N., A. M. Duncan, D. Chester, and R. Marques (2007), Fogo Volcano (São Miguel, Azores): A hazardous edifice, *Géomorphol. Relief Processus Environ.*, *3*, 259–270.

Zanella, E. (1998), Paleomagnetism of Pleistocene volcanic rocks from Pantelleria Island (Sicily Channel), Italy, *Phys. Earth Planet. Inter.*, *108*, 291–303, doi:10.1016/S0031-9201(98)00108-3.

Zijderveld, J. D. A. (1967), AC demagnetization of rocks: Analysis of results, in *Methods in Palaeomagnetism*, edited by S. K. Runcorn, K. M. Creer, and D. W. Collinson, pp. 254–286, Elsevier, Amsterdam.

14. Paleointensity determination from São Miguel (Azores Archipelago) over the last 3 ka

Anita Di Chiara[1,2], Lisa Tauxe[3], Fabio Speranza[1]

[1] *Istituto Nazionale di Geofisica e Vulcanologia, Roma, Italy, anita.dichiara@ingv.it, fabio.speranza@ingv.it*

[2] *University of Bologna, Bologna, Italy, anita.dichiara@unibo.it*

[3] *Geosciences Research Division, Scripps Institution of Oceanography, La Jolla, CA USA,ltauxe@ucsd.edu*

14.1 Abstract

In the Atlantic Ocean paleointensity data are dramatically scarce. New paleointensity data São Miguel (Azores Islands, Portugal) from 24 paleomagnetic sites from 14 lava flows emplaced during the last 3,000 years are presented in this study. Ten lava flows are radiocarbon dated (Moore 1990, 1991; Moore and Rubin, 1991), whereas three flows were archeomagnetic dated by Di Chiara et al. (2012) and one site was dated using stratigraphic relations. All the samples, previously investigated to recover paleodirections (Di Chiara et al., 2012), were subjected to IZZI experiments. Importantly, new data are internally consistent, and agree with Moroccan, and European datasets, as well as with the Cals3k.4 predictions (Korte et al. 2011), varying from 63.29 ZAm^2 and 168.8 ZAm^2. The peak of intensity around 600 BC is well supported by two sites from the same flow (Furna), and is comparable to the "spike" of intensity founded in West Levant records, as well as in Western Europe and in Iceland. The Latitudinal gradient from lower to higher Latitudes observed by Mitra et al. (in prep.) between 100 to 1000 AD m is confirmed as well as the predominance of the axial-dipole component between 0 to 100 AD.

14.2 Introduction

The aim of this study is to provide reliable absolute paleointensity data which are urgently required for the central-northern Atlantic Ocean and demanded for support robust estimates of the geomagnetic field behavior. The geographical coverage of data is poor (mostly in Europe and very little in the Southern Hemisphere), and the temporal distribution of data is uneven. Measurement of intensities began in 1840 AD (when C. F. Gauss devised the first method to measure it), whereas measurement of directions (declination and inclination) are available since 1590 AD (Jackson et al., 2000). Gubbins et al., (2006) combined the global model directions with paleomagnetic intensity measurements to estimate the strength of the magnetic field for this earlier period, calculating the first Gauss coefficient. Results highlight that the strength of geomagnetic field had fallen

constantly during the period 1590-1840 AD. For ages older than the 1590 AD data distribution is discontinuous and based on the availability of archeomagnetic and paleomagnetic data.

The GEOMAGIA intensity database was created by Donadini et al. (2006), then expanded (Donadini et al., 2009) and constantly updated; it contains all archeointensity, paleointensity from sediments and volcanics, as well as directional data that are known. The temporal and geographical distribution of data is uneven: for the last 10 ka, a large amount of data had been obtained on continents (Europe and N-America), whereas for oceans a southern hemisphere less data exist. For the Atlantic Ocean area few data, from historical (Michalk et al., 2008) and post-glacial lavas from Iceland (Schweitzer and Soffel, 1980; Stanton et al., 2011; Tanaka et al., 2012), and direct measurements (Jackson et al., 2000) for the last 400 years are available.

Consequently, global models (e.g., CALSxk.x family) for the Atlantic Ocean area are barely supported with archeointensity and paleointensity data (Korte et al., 2009; Donadini et al., 2009; Korte and Constable, 2011), especially the Southern and Central areas. Similar limitation has the comprehensive compilation of paleointensity data for the last 10 ka (ArcheoInt), compiled by Genevey et al., 2008 (http://earthref.org/ERDA/887/); ArcheoInt includes 87% of archeointensity data (from archaeological artifacts) and the remaining 13% of data obtained from volcanic products.

On the contrary, a plenty of data from Europe exist. Particular features are well-depicted and reproduced by several different studies from different regions. Between 2500-2800 ka, a rapid change in intensity have been recorded in Europe (Gallet and Le Goff, 2006; Ben-Yosef et al., 2008a; Genevey et al., 2009), reaching the highest values in Southern Jordan area (Ben-Yosef et al., 2009) up to 213.1 ZAm^2 between 816±17 BC and 983±25 BC. High field values for the same period were obtained from the Western US (Champion, 1980; Hagstrum and Champion, 2002) (values up to 140 ZAm^2), and even higher values of almost 200 ZAm^2 from Hawaii (Pressling et al., 2006). These data suggest the possibility of a global spike, and encourage further investigation of the regional extent of this feature. Our data serve to verify this hypothesis.

The Azores Archipelago is an ideal location for gathering new paleointensity data, since historical and pre-historical lava flows are well exposed and geochronologically dated (e.g., Feraud et al., 1980, 1981; Moore 1990, 1991). A paleosecular variation curve (PSV) had been obtained from 16 lava flows emplaced in the last 3 ka on Sao Miguel (Di Chiara et al. 2012). The PSV was reconstructed using 27 radiocarbon dated sites from 16 lava flows, together with 6 directions gathered by Johnson et al. (1998). The same samples from sites investigated by Di Chiara et al. (2012) were analyzed in this study, in order to obtain new paleointensity data.

To achieve our purpose, we firstly tackled with the methodological issue of the identification of an optimal method to recover the paleointensity of the Earth's magnetic field. Indeed, during the past twenty years a large number of techniques have been proposed to improve the quality and reduce the time of experiments for absolute paleointensity (Shaw, 1974; Kono, 1978; Hoffman et al., 1989; Sherwood, 1991; Pick and Tauxe, 1993; Tsunakawa and Shaw, 1994; Tanaka et al., 1995; Merrill et al., 1996; Shaw et al., 1996; Cottrell and Tarduno,

2000; Dunlop and Özdemir, 2000; Scherbakova and Scherbakov, 2000; Valet and Herrero-Bervera, 2000; Riisager and Riisager, 2001; Tarduno et al., 2001; Smirnov et al., 2003; Yamamoto et al., 2003; Chauvin et al., 2005; Dekkers and Böhnel, 2006). Although the efforts, in many cases no consensus was be reached to decide the best method. Therefore, some procedures remain controversial and poorly tested.

By far, the Thellier family of experiments is the most accepted and widely used method to recover paleointensities. It is based on two main assumptions: 1) a linear relation between the geomagnetic field existing in the moment of rock formation and the TRM (verified for Single Domain magnetic grains, and a laboratory field close to the expected value); 2) that during the experiments no alteration of minerals occurs. Suitable materials are rare: it is required a unique original component of Natural Remanent Magnetization (Thermal Remanent Magnetization), carried by Single Domain ferromagnetic materials (Thellier and Thellier, 1959; Tauxe and Yamazaki et al., 2007), with no evidences of alteration during laboratory analysis (Dunlop and Özdemir, 1997 and Tauxe, 2009). Therefore, one of the best approaches for testing the validity of the absolute paleointensity determination is to deal with lava flow deposits (e.g. Pan et al., 2002) and basaltic glasses (Ferk et al., 2008; Cromwell et al., 2011). Many cross-tests of the different techniques on historical flows of measured intensity had been run, in order to test various techniques and embellishment and to unravel the best method. For instance, about eight studies have been focused on the 1960 lava from the Big Island of Hawaii (Abokodair, 1977; Tanaka and Kono, 1991 Tsunakawa and Shaw, 1994; Tanaka et al., 1995; McLelland and Briden, 1996; Valet and Herrero-Bervera, 2000; Hill and Shaw, 2000; Yamamoto et al., 2003; Herrero-Bervera and Valet, 2009); nonetheless, no agreement had been achieved.

Among the studies to recover paleointensity that adopted the Thellier and Thellier method, a success between 60% and 21% had been obtained so far. Carlut and Kent (2000) reach a 60 % of success from Juan de Fuca ridge and from East Pacific Rise South volcanic rocks, Thomas et al., (2004) a 61% from Tertiary Sydney basin rocks, Valet and Herrero-Barvera (2000) had succeed for a 38 % in determination paleointensity from the 1960 AD Hawaii flow, and Calvo et al., (2002) obtained a 21% of values from Etna lavas.

Between the several embellishments aimed to reduce the effect of the repeated heating (i.e., mineralogical alteration), the IZZI protocol (Tauxe and Staudigel 2004; and Yu et al., 2004) has been used in this study.

The IZZI protocol is a modified combination of two embellishment of the original method, proposed by Aitken (1988; in-field, zero-field; IZ) and Coe (1967; zero-field, in-field; ZI), thus it alternates the IZ and ZI steps, and adds the pTRM check steps at each Temperature step. The advantages of this technique is triple: 1) the angular dependence between the Natural Remanent Magnetization (NRM) and the Thermal Remanent Magnetization acquired during experiments under a know laboratory field (TRM_{lab}) can be easily detected, indicated as an angle θ; 2) it provides a quantitative estimate for the consistency outcome between IZ and ZI steps; 3) it is quicker because the "pTRM tail check" is unnecessary.

Results are classically displayed and analyzed through the Arai plot (Nagata et al., 1963), a scatter plot displaying residual NRMs ('NRM remaining') versus cumulative pTRMs. If the material fulfills the assumption underlying the Thellier method (i.e. NRM that is pure TRM carried exclusively by stable SD), then the Arai plot is a straight line, connecting the two (x, y) endpoints: (0, NRM), and (TRM, 0). The most common approach to calculate the true intensity of the paleomagnetic field is the best-fit line. Some authors proposed to use only the low-temperature slope; however, others showed that the low-temperature slope could significantly overestimate the true field (e.g. Biggin and Thomas, 2003; Calvo et al., 2002; Chauvin et al., 2005). Some authors suggested averaging the slope of the two segments (e.g. Hill and Shaw, 2000), and other recommended using large segment as possible even if it is curved (e.g. Levi, 1977; Biggin and Thomas, 2003; Chauvin et al., 2005). An alternative option is using only the two end-points of the Arai plots when specimens show little signs of alteration (e.g. Coe et al., 2004; Garcia et al., 2006).

The difficulty of the interpretation rise from the multiple causes of failure that can affect results, drifting away from ideal straight line: i) MD grains effect (from 4% of the whole magnetic grains content or greater) will cause concave or convex and 'S-shaped' curves (see Levi 1977; Xu and Dunlop, 1995, 2004; Biggin and Thomas, 2003; Coe et al., 2004; Fabian, 2001; Leonhardt et al., 2004) displayed in the Arai Plot (Nagata et al., 1963); and ii) the difference of direction between the NRM with respect to the laboratory field applied during Thellier experiments (Xu and Dunlop, 2004; Fabian, 2001, Leonardth et al., 2004; Biggin 2006; 2010; Biggin and Poidras, 2006; Shaar et al., 2011), expressed as an angle θ, which likely it is responsible of the zig-zagged shape (when the NRM is perpendicular to the laboratory field the deviation is high).

Zigzags are unique feature of the IZZI protocol (Tauxe and Staudigel, 2004; Yu et al., 2004; Yu and Tauxe, 2005; Shaar et al., 2011a), and they occur when the IZ and the ZI data points create two distinguishable curves. The dependence of the zigzag feature on θ and the ratio B_{TRM}/B_{NRM} have to be tested. Many attempts to quantify the zigzagging had been proposed (e.g. Granot et al., 2007; Tauxe, 2010). Following these findings, Shaar et al., (2011) performed experiments to demonstrate that experimental conditions can influence paleointensity experiments. In particular, factors that play an important role are the difference of the intensity of the field laboratory (B_{TRM}), and the original NRM of the sample (B_{NRM}), and the angle between B_{TRM} and B_{NRM} (θ). Linear curves occur when $\theta = 0°$ and $B_{TRM}/B_{NRM} = 1$, and semi-linear curves with a weak zigzag occur when $\theta = 0°$ and $B_{TRM}/B_{NRM} \leq 2$. Concave curves occur when $\theta = 180°$, regardless the ratio B_{TRM}/B_{NRM}. Convex curves occur when $\theta = 0°$ and $B_{TRM}/B_{NRM} = 4$. The two endpoints of a non-linear plot (concave or convex) connected together yields the ideal SD line. For the same B_{TRM}/B_{NRM} the zigzag is weak for $\theta = 0°$ and strong for $\theta = 180°$. Convex curves in the Arai plot result when the field in the paleointensity oven is stronger than the ancient field. Shaar et al., (2011) defined a new parameter, the "IZZI_MD", which calculates the total area bounded by the IZ and the ZI curves normalized by the length of the ZI curve, and stating that the degree of zigzag increases with B_{TRM}/B_{NRM} and as θ deviates from 90° toward 0° or 180°.–These effects are thought to be responsible of an underestimate or overestimate the paleointensity calculation.

Yet, another key problem is to adequately choose the selection criteria (e.g. Biggin and Thomas, 2003; Kissel and Laj, 2004; Selkin and Tauxe, 2000; Tauxe, 2006) and cut-off values of the quality parameters, to consider a result reliable.

Here, we tested the insights suggested to enhance the IZZI method (by Tauxe and Staudigel, 2004; Shaar et al., 2011a; and Tanaka et al., 2012), thus, to carefully screen all the samples in a preliminary step, rejecting all that do not fulfill the assumptions underlying the technique (a single-component TRM carried by SD magnetic particles that do not alter during experiments). Therefore, samples are pre-selected from Thermal demagnetization cleaning analyses, previously run to recover the paleomagnetic direction (Di Chiara et al., 2012).

Recently, it was suggested that paleointensity estimates can be used, in conjunction with geomagnetic field global models (e.g., Jackson et al., 2000; Korte and Constable, 2011), to determine eruptive ages for young lavas (Carlut and Kent, 2000; Gee et al., 2000; Carlut et al., 2004 Bowles et al 2005).

14.3 Geological setting and studied lava flow deposits

São Miguel is the largest (760 km^2) of the nine volcanic islands of the Azores Archipelago, straddling the Mid Atlantic Ridge at the triple junction of the North American, Eurasian and African plates (Fig. 11). Four large trachytic stratovolcanos developed from 8.1 Ma (Abdel-Monem et al., 1975; Feraud, 1980) to historical times. From E to W six volcano-stratigraphic units had been recognized: Nordeste, Furna, the plateau do Congro, Agua de Pau, Região dos Picos, and Sete Cidades Volcano. The "Waist Zone'' (Booth et al., 1978), or ''Zone 2'', or "Região dos Picos" (Moore, 1990, 1991), is the most populated area of the island. The Região dos Picos is a flat area of basaltic lava flows speckled of volcanic cones. Two historical eruptions occurred in the island, both located in the central part and the eastern part of the Região dos Picos: the Fogo eruption in 1563 AD, the latest high explosive (subplinian) eruption at Fogo (subplinian) inland occurred in 1563 AD at Fogo caldera, which also produced a thin lava flows from the monogenetic Queimado cone, nearby the Ponta das Praias locality (Fig.11). The most recent inland effusive eruption emplaced from the Fogo1 cone during 1652 AD, reaching both the N coast (at Rabo de Peixe town) and the S coast nearby the Lagoa town. The two historical flow are described in historical chronicles by Mitchell-Thomè (1981) and Booth et al., (1978). For older flows boundaries were delimited in the geological map of Moore (1990) based on field evidences, but hardly on satellite images since only small scoria cones dotting the area are evident but the lava flows limits are covered by vegetation and by human colonization.

During July 2010, we paleomagnetically sampled these two historical lava flows, as well as other 32 paleomagnetic sites, with at least 15 well-spaced cores at every site. Cores were oriented both by solar and magnetic compass. All the 16 flows sampled with 35 sites are described in Di Chiara et al., (2012) (Fig. 1 and

Table 1 in Di Chiara et al., 2012, Chapter 13), including an age range between the 3,000 ka and the 1652 AD. Seven sites from the same flows had been already paleomagnetically investigated by Johnson et al. (1998). All the pre-historical radiocarbon ages reported by Moore (1990; 1991) and Moore and Rubin (1991) were recalibrated by us with the Stuiver's Online program Calib6.0 (Stuiver et al., 2009). After Di Chiara et al., (2012) 31 sites yielded reliable paleomagnetic results. Furthermore 4 of the 16 sampled flows were dated using the comparison of the paleomagnetic directions (see Table 2 in Di Chiara et al., 2012, Chapter 13): Cruz N and S, Lagoa, and Caloura flows (marked in Table 1) with relocated reference curves.

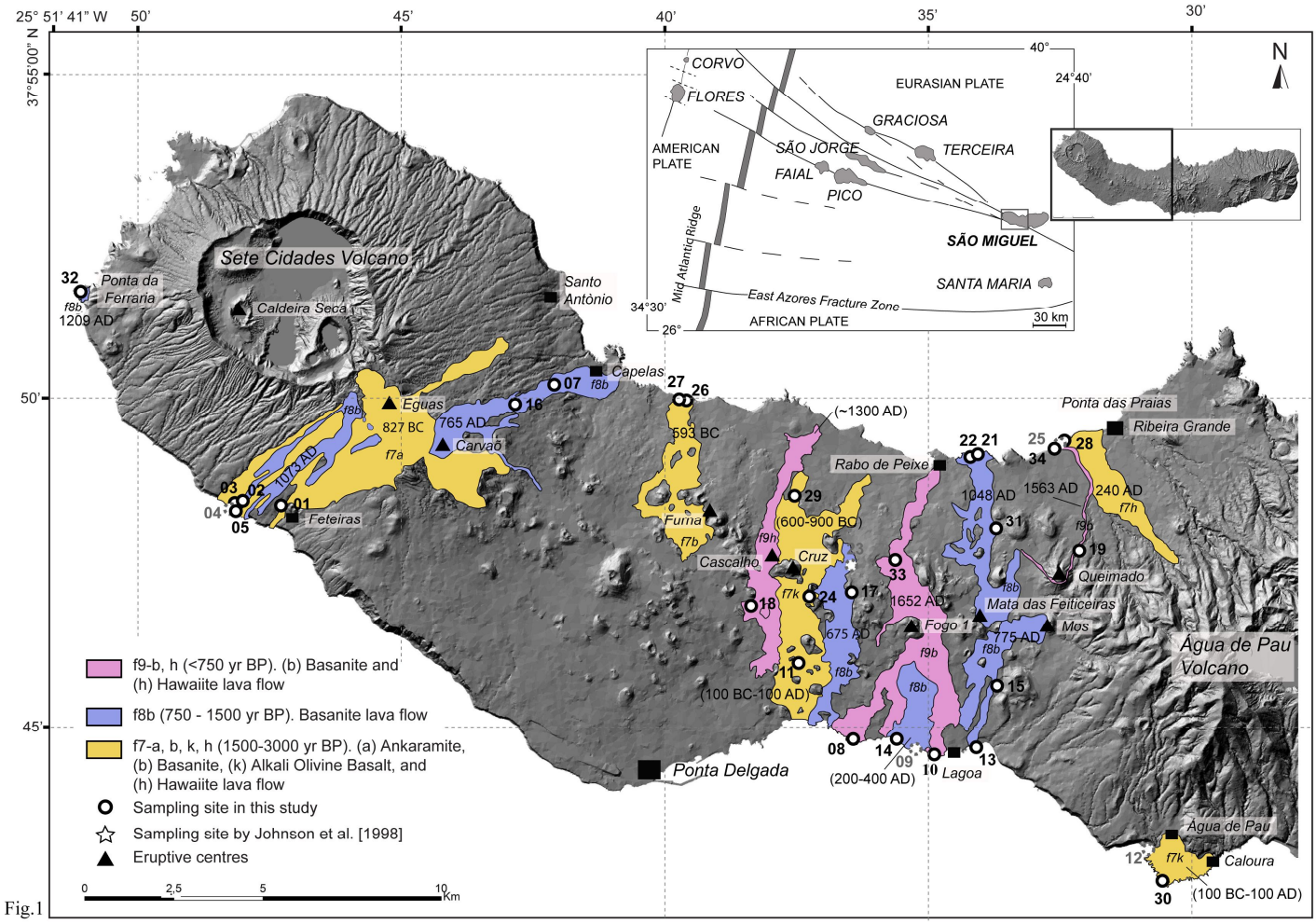

Fig.1

Fig. 11 - Digital elevation model of São Miguel, and location of the studied flows and paleomagnetic sampling sites from this study (the "Sml" prefix of each site is omitted). Flow geometry, characteristics, and ages are after Moore (1990, 1991). 1563 and 1652 AD flows are historic. Calendar ages of the other lava flows are calibrated using CALIB6.0 (http://calib.qub.ac.uk/calib/calib.html) from original ^{14}C ages reported by Moore and Rubin (1991). Flow ages between parentheses were paleomagnetically inferred (Chapter 13). Dashed circles indicate sites which fail in yielding paleointensity data.

14.4 Method

Here, we tested an insight suggested to enhance the IZZI method (by Tauxe and Staudigel, 2004; Shaar et al., 2011; and Tanaka et al., 2012): to carefully screen all the samples before start the paleointensity experiments, and select the most suitable. Thus, all the samples that do not fulfill the assumptions underlying the technique and diverge from an ideal behavior of a single-component of TRM, carried by SD magnetic particles that do not alter during experiments, are ruled out from paleointensity experiments. The aim is to minimize the source of bias affecting the success of paleointensity results, therefore samples that displayed evidences of no pure NRM (or rather multi-component). Hence, those samples (1) with no evidences of secondary remagnetizations, with the Zijderveld diagram pointing straight to the origin, (2) displaying square-shaped blocking temperature spectra (preferred to avoid the presence of MD grains), and (3) displaying a reversible features on the susceptibility-temperature curves (previously obtained from all the samples), as well as those revealing a single Curie Temperature have been selected. Indeed, as a particle size increases (Carlut and Kent, 2002) and MD grains are predominant carrier of the remanent magnetization (Levi, 1977; Fabian 2001; Riisager and Riisager 2001; Leonardht et al., 2004; Selkin et al., 2007) the TRM starts to have a non-linear behavior (Kletetschka et al., 2006; Yu et al., 2004; Yu and Tauxe, 2005; Shaar et al., 2011), and cause the failure of the experiments.
All the samples previously thermally-treated to recover paleomagnetic directions (Di Chiara et al., 2012) had been screened and samples displaying non-ideal behavior were rejected from any further analysis.

Between the 390 samples from 33 sites which yielded reliable paleodirections after the thermal demagnetization cleaning analyses (Di Chiara et al., 2012), only 64 samples from 28 sites passed the first rigorous pre-selection step, and were selected for the paleointensity experiments. From each lava sample 2 to 6 sister specimens were chosen. A total of 180 sister specimens were prepared for the paleointensity experiments. Individual chips were placed in clean glass vials and fixed into position with microfiber glass filters and Kasil "glue". The paleointensity experiments were carried out using the in-field, zero-field, zero-field, in-field (IZZI) protocol (Tauxe and Staudigel, 2004). All the 180 specimens were subjected to the IZZI procedure, but the "pTRM tail check" step was not performed here in order to reduce the number of steps. The protocol was run as follows: specimens placed in the glass vials were heated to 100°C and cooled in zero field (zero-field step); after measuring the NRM, specimens has been reheated to 100°C and cooled in laboratory field, direct along the Z axis and re-measured (In field step). The difference between the first NRM and the second step is the partial TRM (pTRM) gained by cooling from 100°C to room temperature. At following temperature step, the order of the double heating procedure is reversed such that specimens are cooled in-field (I) first, then in zero-field (Z) (Zero-field/In-field, ZI, and In-field/Zero-field, IZ). The so-called pTRM check step consist in go back to the previous Temperature step and repeat the in-field heating in order to check if the capability of the specimens are changed during the last heating step. The procedure was repeated in 43 steps alternating IZ and ZI and the pTRM checks, in 100 °C interval up to 300 °C, 50 °C up to 500°C and 10°C up to 600°C.

All the experiments were run in the shielded room of the paleomagnetic laboratory of The Scripps Institution of Oceanography (La Jolla, California, US), headed by L. Tauxe, using two shielded water-cooled ovens for paleointensities and the 2G cryogenic magnetometer.
In order to test whether the orientation of the NRM parallel to the laboratory field affects the robustness of the results (as suggested by Fabian, 2001; Leonhardt et al., 2004; Xu and Dunlop, 2004; Yu et al., 2004; Biggin, 2006; 2010; Biggin and Poidras, 2006; Shaar et al., 2011a) three batches of experiments had been performed. From two to four sister specimens from each sample have been analyzed in order to test the consistency of the results. The first 60 sister specimen were oriented by 'trials and errors' while placing the specimen in the vial, to have the NRM direction parallel to the applied field direction, thus with an angle between -70° and -89° (that is parallel to z-axis of the 2G cryogenic Magnetometer). In the second batch of experiments specimens were placed in vial randomly-oriented, whereas the third was carried out on 30 specimens oriented following the same procedure of the first batch of experiments, while other 30 specimens were placed in the vials randomly-oriented, selected from some specimens already analyzed (oriented) during the first batch of experiments.

Many authors stressed the importance of choosing a laboratory field equal or slightly lower than the expected paleofield (e.g., Shaar et al., 2011; Paterson et al., 2012). Since from the Korte et al., (2011) model the expected value of the field averaged for the different ages of our samples is ~40 μT, the same was the laboratory field used during the laboratory experiments.

The results of the experiments are classically displayed in the Arai plot (Nagata et al., 1963), where are plotted the residual NRMs versus the cumulative pTRMs, estimated trough vector subtraction. Acceptable paleointensity estimates have a linear Arai plot, but specimen with a nearly-ideal behavior could depart from the linearity. The acceptability limits are still a matter of discussion. Despite the plenty of parameters to quantify the quality of the data exist, the selection of the data remain subjective. Selection criteria chosen in this study are listed in Table 3.

Moreover, additional magnetic analyses were routinely carried out on 30 specimens (about one per site) to characterize the magnetic mineralogy. Hysteresis properties were measured using a Princeton Measurement Corporation MicroMag alternating gradient magnetometer (AGM, model 2900) with a maximum applied field of 1 T. The measured hysteresis parameters include saturation magnetization (Ms), saturation remanent magnetization (Mrs), coercive force (Bc) and the coercive force of the remanence (Bcr). Data were also to compute the ratios between Ms/Mrs and Bc/Bcr. The results were plotted in a Dayplot (Day et al., 1977; Dunlop, 2002).

Table1 -Location of sampling Sites at São Miguel

Flow name	Site	Lat (N)	Lon (W)	Age Uncalibrated (years BP)	Age (years±AD)
Furna	Sml26	37.832	25.661	2460±220	593±236 BC
	Sml27	37.832	25.659		
Cruz N	Sml29	37.807	25.626	1500–3000	400-700 BC*
Caloura	Sml30	37.708	25.511	1500–3000	0-200 AD*
Cruz S	Sml11	37.764	2.562		0-200 AD*
Lagoa	Sml14	37.744	25.594	750–1500	100-400 AD*
Ponta das Praias	Sml28	37.819	25.540	1790±150 AD	240±168 AD
Caldeirão	Sml17	37.782	25.608	1350±120 AD	675±107 AD
Caldeirão E	Sml23	37.789	25.609		
Caldeirão W	Sml24	37.780	25.621		
Carvão	Sml07	37.835	25.702	1280±150 AD	765±132 AD
	Sml16	37.829	25.714		
Mos	Sml13	37.742	25.569	1250 ±150 AD	775±124 AD
	Sml15	37.758	25.561		
Mata das Feiticeiras	Sml21	37.817	25.567	1010 ±120 AD	1048±113 AD
	Sml22	37.816	25.569		
Feteiras	Sml01	37.801	25.801		1073 ±90 AD
	Sml02	37.801	25.801		
	Sml03	37.804	25.804		
	Sml05	37.803	25.803		
Cascalho	Sml18	37.779	25.643	Less than 500±100and 663± 105 AD	1300±100 AD**
Ponta da Ferraria	Sml32	37.861	25.854	840 ±60 AD	1209±53 AD
Queimado	Sml19	37.792	25.535		1563 AD
	Sml31	37.798	25.562		
	Sml34	37.818	25.542		
Fogo 1	Sml10	37.740	25.582		1652 AD
	Sml33	37.790	25.594		
Fogo 1X	Sml08	37.740	25.608		

Site coordinated were gathered by a Garmin GPS using WGS84 datum. Units and uncalibrated 14C ages with an error of 1σ are from Moore [1990, 1991] and Moore and Rubin [1991].*Flows whose age is defined by an age interval. **Flose whose age was paleomagnetic dated by Di Chiara et al. (2012). Calendar ages were calibrated using the Stuiver's program CALIB6.0 Online [http://calib.qub.ac.uk/

14.5 Results

14.5.1 Magnetic mineralogy

Hysteresis property analyses show a predominance of low-coercivity values, with Bc comprised between 4.72 and 25.21 μT. Hysteresis parameters, ratios of saturation remanence to saturation magnetization (Mrs/Ms) and remanent coercive force to coercive force (Bcr/Bc), were plotted in a Day Plot (Day et al., 1977). Most of the specimens are spread on the theoretical (of pure Magnetite) mixing curve (Dunlop, 2002) between single domain (SD) and multi domain (MD) magnetite grains (Fig. 12).

Where magnetic mineralogy reveal the presence of PSD and MD grains as main carrier of remanent magnetization, effectively paleointensity results are unreliable and often fails (killed mostly by b, DANG and DRATS parameters). Nonetheless, magnetic mineralogy from different sites sampled from the same flow, as well as different samples collected from the same site, display different mineralogical characteristic. Thus we can conclude that mineralogical analyses are useful to foresee which a sample will give reliable results or not, but it has to be taken into account that specimen from the same sample and samples from the same sites show different (magnetic) mineralogical behaviors.

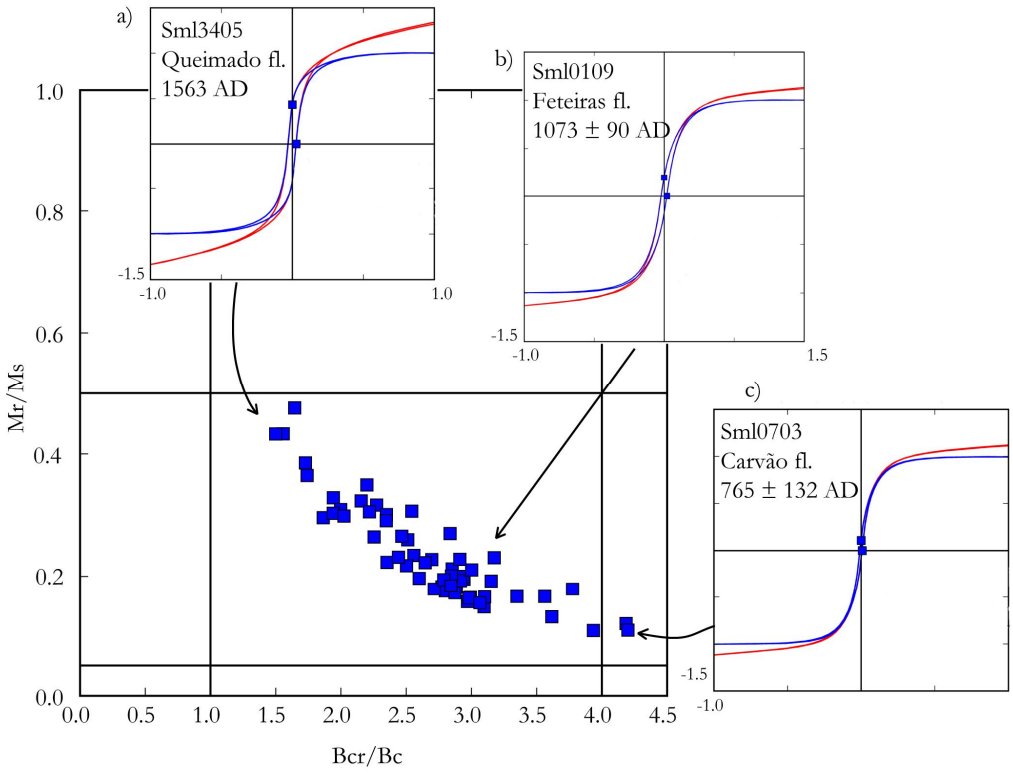

Fig. 12 - Plot of hysteresis ratios (Mrs/Ms versus Bcr/Bc, after Day et al., 1977) for one representative specimen from each site. Three representative hysteresi plots from samples Sml3405, Sml0109, and Sml0703. The first sample yielded relibla results, whereas the other two sites did not yield any reliable result.

14.5.2 Paleointensity results

The results of the experiment are presented and analyzed through the 'Arai plot' (Nagata et al., 1963), a scatter plot displaying residual NRMs ('NRM remaining') versus cumulative pTRMs, estimated through vector subtraction. The slope of the line multiplied by the laboratory field yields the intensity of the ancient field, assuming that the capacity to acquire TRM is a linear function that does not change over time or during the re-heating procedures. Here, we used all the data-points to calculate the best fit line, instead that only the low-temperature data, which could significantly overestimate the true field (e.g. Biggin and Thomas, 2003; Calvo et al., 2002; Chauvin et al., 2005). The paleointensity quality parameters adequately chosen (Coe et al., 1978; Selkin and Tauxe, 2000; Tauxe, 2010) are listed in Table 3. The fairly strict criteria chosen in this study ensure that only the most robust estimates are considered as reliable.

The MagIC.py program (version pmagpy-2.173, http://magician.ucsd.edu/Software/PmagPy) is used to process and display results of experiments.

The results display different and complicated patterns of Arai plots. Three types of shapes had been observed in Arai plots: the 13.8% have a segmented or concave shape (Fig. 12a, and d), the 8.3% has a ziz-zagged trend (Fig. 12h, and i), and the remaining 77.9% exhibits straight or nearly straight lines (Fig.12b, c, and e). In addition, a zigzagged pattern is superimposed on the curves, which varies in significance from barely detectable to extreme. Remarkably, we would obtain a 71.4 % of success (in terms of reliable paleointensity estimate) by slightly loosen the selection criteria. On the contrary, we prefer to keep a strict selection criteria, obtaining a lower percentage of success (46.1%) but more reliable (Table 2,this Chapter 14)At specimen level, only 83 of 180 samples succeeded. At site level four sites failed since no reliable estimates results (Sml01, 17, 30 and 33), whereas four sites are represented by only one paleointensity data (Sml07, 10, 21, and 23). The errors (sigma) are between 1.15 and 9 (5.0 of average). Paleointensity estimates for each flow are averaged and listed in Table 3. Paleointensity values range between ~ 35 μT (Cruz S flow) and ~95.22 μT (Furna flow, radiocarbon dated to 593±236 BC). Pointedly, sites from flows close in age (e.g., Caldeirão, 675±107 AD, Carvão 765±132 AD, and Mos 775±124 AD) share similar paleointensity values. Site Sml31 from Queimado flow (1563 AD) well agree with sites Sml34 and 19, thus confirming the paleomagnetic correlation proposed in Di Chiara et al. (2012). Two sites diverge from the flow mean: Sml08 (77.5±6.67 μT) is higher than the Sml10 (41.11 μT) from the historical flow of Fogo (1652 AD), and Sml24 (97.8±2.92 μT) is higher than Sml23 (58.3 μT), both from the Caldeirão flow (675±107 AD). Unfortunately all specimen from four sites failed (Sml01, 17, 30 and 33) since the Arai diagrams were erratic and no intensity values can be determined for these specimens.

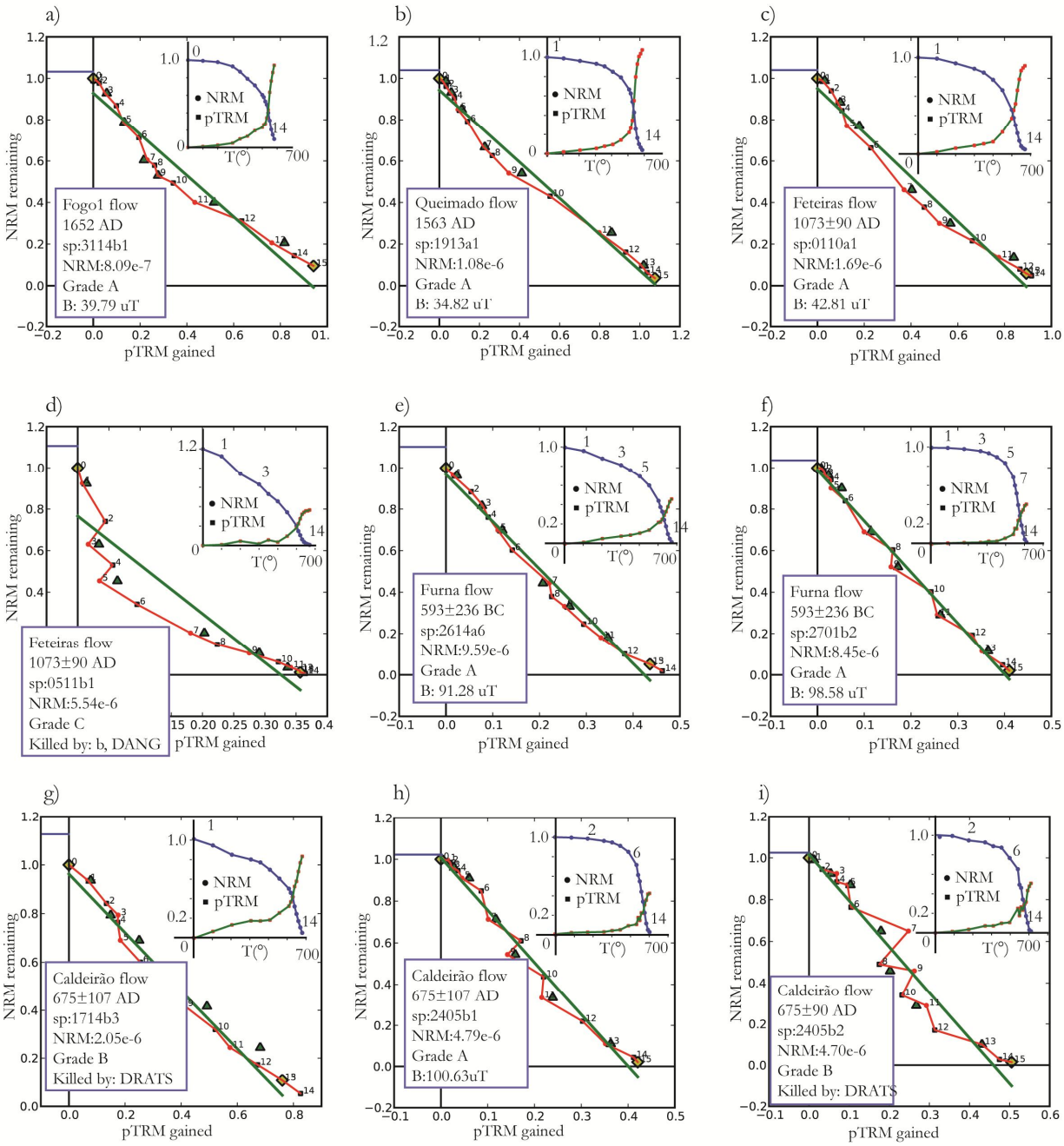

Fig. 13 - Representative IZZI experiment results displayed in Arai plots. a, b, c, e, f, h) Representative plots and susceptibility (χ)-T diagrams of six specimens that passed the selection criteria; d, g, i) Arai plots and χ - T diagrams of the specimens that failed to pass the selection criteria. The temperature interval used for isolating the characteristic remanence is marked with red line and squares.

Table 2 - Paleointensity results from sites and flows from São Miguel

Flow name	Sites	Lat (N)	Lon (W)	Age (years+/-)	σ (Age)	Dec(°)	Inc(°)	Intensity				VADM		
								N_B	B (μT)	σ	σ (%)	N_VADM	VADM	σ (VADM)
Furna	Sml26;27	37.832	25.661	-593	236	13.0	58.0	8	95.22	4.9	5.1	8	168.80	8.68
Cruz N	Sml29	37.807	25.626	*-750*	*250*	8.7	57.5	6	57.71	6.96	12.1	6	102.30	12.35
Cruz S	Sml11	37.764	25.625	*100*	*100*	349.1	49.4	1	35.68	0	0	0	63.29	0
Lagoa	Sml14	37.744	25.594	*300*	*100*	1.0	55.9	4	41.31	2.69	6.5	4	73.30	4.77
Ponta das Praias	Sml32	37.819	25.540	240	168	356.0	56.0	2	62.83	1.15	1.8	2	111.40	2.04
Caldeirão E	Sml23	37.782	25.608	675	107	12.6	57.3	1	58.3	0	0	0	103.00	0
Caldeirão W	Sml24	37.782	25.608	675	107	11.4	53.4	2	97.8	2.92	3	2	173.00	5.19
Carvão	Sml07;16	37.835	25.702	765	132	16.6	43.3	4	68.36	6.33	9.3	4	121.20	11.22
Mos	Sml13;15	37.742	25.569	775	124	10.2	48.5	12	69.22	9.21	13.3	12	122.80	16.34
Mata das Feiticeiras	Sml21;22	37.817	25.567	1048	113	1.1	34.2	4	48.61	4.78	10.3	4	82.70	8.47
Feteiras	Sml02;03;05	37.805	25.788	1073	90	6.4	32.7	10	55.85	6.11	10.9	10	99.02	10.83
Ponta da Ferraria	Sml28	37.861	25.854	1209	54	355.4	32.4	4	56.66	4.16	7.3	4	100.40	7.38
Cascalho	Sml18	37.779	25.643	*1300*	*0*	355.9	29.7	5	56.08	3.65	6.5	5	99.46	6.47
Queimado	Sml19;31;34	37.792	25.535	1563	0	0.5	55.5	11	39.91	5.68	14.2	11	79.10	14.20
Fogo 1	Sml10	37.745	25.608	1652	0	11.1	47.7	1	41.11	0	0	0	72.94	0
Fogo 1x	Sml08	37.745	25.608	**1652**	**0**	11.1	47.7	8	77.5	6.67	8.6	8	138.00	11.80

Flow names and ages are defined as in Table 1 (this Chapter 14). Age in bold are questioned in this study. Ages in italic character are age intervals "paleomagentically inferred" after Di Chiara et al. (2012). Declination and Inclination are from previous study. Mean intensity results are reported by flow (μT and VADM converted), after IZZI experiments and processed using the "pmagpy-2.173" by L. Tauxe.

14.6 Discussion

Among the studies to recover paleointensity (performed with the Thellier and Thellier method), a success between 60% and 21% had been obtained so far. The percentage of success of our paleointensity results is the 46.1 %. Perhaps most important, we find that the orientation of B_{TRM} and B_{NRM} can influence the degree of zig-zag (indeed tend to disappear when B_{TRM} and B_{NRM} directions are nearly parallel), but do not affect the reliability of results. On the contrary curved and segmented features dramatically influence the success rate. Indeed, the curved shape is due to magnetic mineralogical contents: when MD grains occur the behavior is erratic and experiments fail. Despite the carefulness in the pre-selection of suitable specimens some specimen eluded.

We conclude that the effort of orienting the specimen inside the vials and controlling the θ is not worthwhile, on the contrary is it well worth the investment of time spent to pre-select specimen by specimen from an original dataset, to avoid all the known sources of bias.
We used strict selection criteria that ensure the robustness of our paleointensities estimates, from 24 paleomagnetic sites sampled from 14 lava flows.

In Figure 14 we have superimposed the 14 paleointensity results on the geomagnetic intensities predicted for São Miguel (37.8°N, 25.5°W) by the most recent global field model, the Cals3k.4 by Korte and Constable (2011). Our mean-paleointensity data vary from 35.68 μT (63.29 VADM, Cruz S flow) and 95.22 ±4.9 μT (168.8 VADM, Furna flow, 593±236 BC). At a first glance, our results agree with the global model prediction. Indeed, mean intensities from the Queimado flow (1563 AD), Feteiras (1073±90 AD) and Mata das Feiticeiras (1048±113 AD), as well as the Caldeirão (675±107 AD) and Ponta das Praias (240±168 AD) flows have a maximum distance 9 μT.

Ten of the studied flows are radiocarbon dated by Moore (1990) and Moore and Rubin (1991). Three lava flows had been archeomagnetic dated by Di Chiara et al. (2012): Cruz N (400-700 BC), Cruz S (0-200 AD), and Lagoa (100-400 AD). Cruz S and Lagoa mean paleointensities diverge from the expected values of about 15 μT. We suggest that either the field was lower than predicted by the global model, or paleomagnetic directions in some cases are not sufficient for dating, or the inferred ages of the two sites were erroneously assigned by Di Chiara et al. (2012). Stressing that the global model is not supported by real data in the area of the Atlantic Ocean, we nonetheless noticed that predicted values roughly agree with our real data presented in this study. Additionally, the Ponta das Praias flow (~240 AD) has an intensity higher than the two inferred sites (Cruz S and Lagoa) emphasizing an ascendant trend for older ages (up to the maximum around ~600 BC of the Furna flow). Thus,

we suggest that the age of the two sites (Cruz S and Lagoa) dated using paleomagnetism was probably erroneous. Combining paleodirection (Declination and Inclination, Table 2) and paleointensity values and comparing them with the Cals3k.4 (from 0 to 3 ka) and Cals10k (from 3 to 10 ka, by Korte et al., 2011) we rather suggest that the two flows could be older. Effectively, similar low values of declination (359.57°), inclination (55.1°) and intensity (41.31 μT) of Lagoa flow are comparable with the minimum reported in the Cals10k (Korte et al., 2011) in D, I and intensity (359.7°, 52.0° and 40.8 μT , respectively) around 3,100 AD. Another possibility is that the site Sml14 of the Lagoa flow could be even historical, since it was sampled in a lava flow close to a branch of the 1563 AD Queimado flow (according to the geological map of Moore 1990). This second hypothesis cannot be discarded since the Queimado flow yielded similar values (D=0.5°, and I=55.5°).

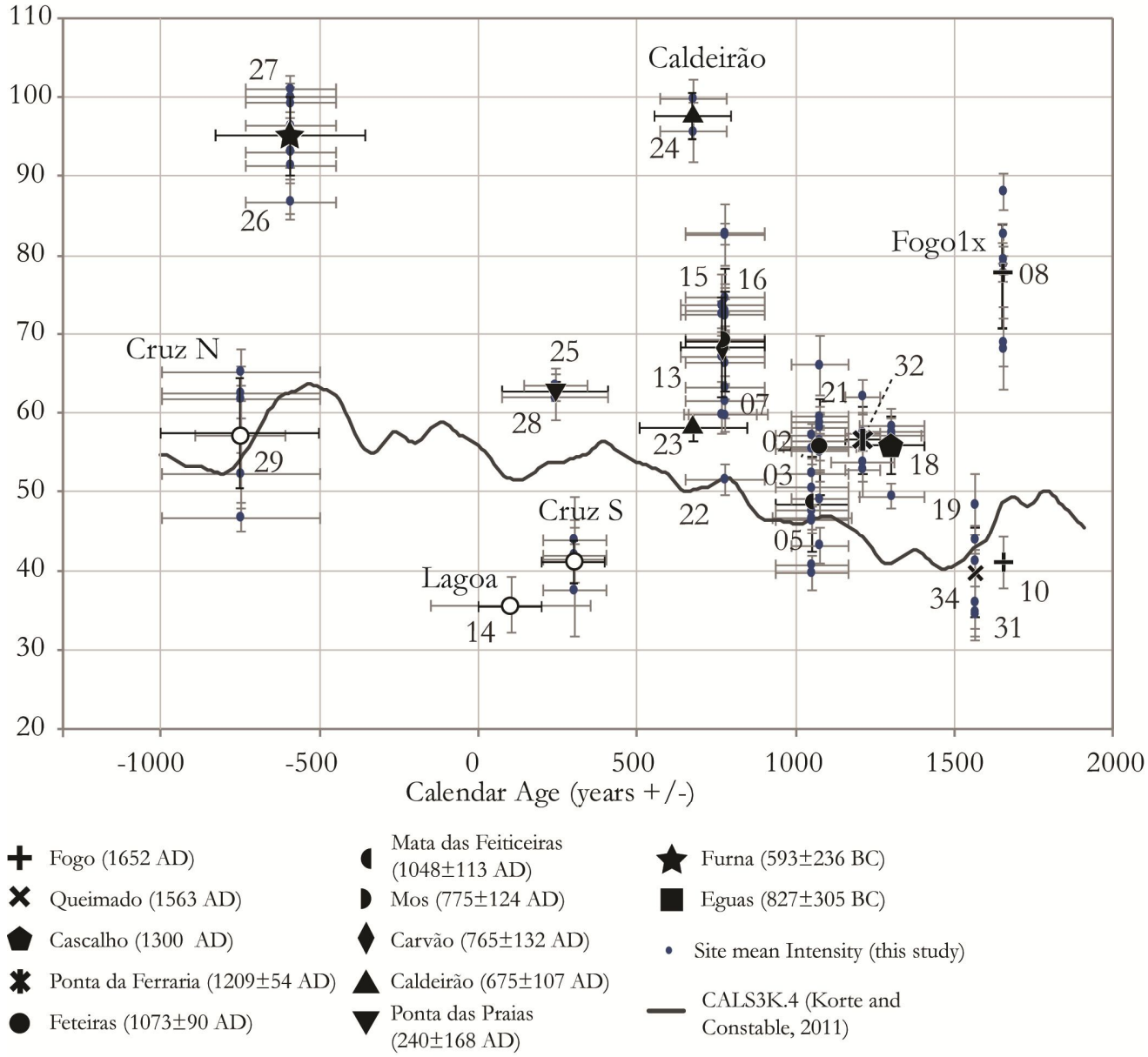

Fig. 14 - Flow mean intensity (μT) of historical, ^{14}C and paleomagnetically dated from this study (26 sites, the "Sml" prefix is omitted), and Di Chiara et al. (2012), plotted versus age plot, and compared with global field model predictions from CALS3k.4 (Korte and Constable, 2011). Ages (and relative error bars) are calendar ages (and relative errors) calibrated by us from radiocarbon ages by Moore and Rubin (1991), using Calib6.0 (Stuiver et al. 2009).

The age of the Cascalho flow was constrained using stratigraphic evidences and paleomagnetic directions. Indeed it was initially constrained to the 1300–1500 AD time window. Directions are much lower than the Queimado flow of 1563 AD, and so it has to be placed in the lower bound of the interval (~1300 AD). The intensity of 56.8 μT confirms this hypothesis since intensity well agree with those obtained for the 1000-1300 AD age interval (~55 μT), whereas it diverges from Queimado values that are lower (39.91 μT)

The other historical flow, Fogo, is characterized by a peculiar inclination (47.7°), which is discrepant with respect to the global models (e.g., gufm1 predicted an inclination of 63°), rising the suspect that either a rapid inclination drop occurred 150 years before the gufm1 prediction in the Atlantic area, or some problem in recording the paleomagnetic field occurred in the discussed flow. Paleointensity of Sml08 and Sml10 are clearly different, therefore we proposed that Sml08 (named here Fogo1x) is rather older than reported, and both direction and intensity suggest that it could be dated back to ~800 AD.

Paleomagnetic directions from Caldeirão flow well agree with global model predictions, whereas paleointensity reveal a discrepancy between sites Sml23 and 24, rather suggesting that the Sml24 (named Caldeirão W) could be older than 675 AD.

14.6.1 Paleointensities over the last 3 ka

We have calculated mean intensity values of paleomagnetic field and results are displayed in Table 2, and the VADM (Merrill et al., 1996). We emphasize three relative minima around 1563 AD, 1050 AD, and 400 AD, and three relative maxima around 1070 and 1300 AD, 700-800 AD and 593 BC. Rapid changes in archeointensity have been already noted in previous studies in Europe (Gallet and Le Goff, 2006; Ben-Yosef et al., 2008a; Genevey et al., 2009). We compared our data with European dataset (Fig. 15) from Morocco (Gomez-Paccard et al., 2012), Portugal (Nachasova et al., 2009; Hartmann et al., 2009; and Gomez-Paccard et al., 2012), Spain (Gomez-Paccard et al., 2006; 2008; 2012; Nachasova et al., 2007; Catanzariti et al., 2012; Beamud et al., 2012), and France (Chauvin et al., 2000; Genevey and Gallet 2002; Genevey et al., 2009; Gallet et al., 2009; Gomez-Paccard et al., 2012). Our data well agree with the entire dataset from Western Europe (Figure 16), particularly for the last 2,000 ka. European data trace a maximum around 600 AD which could be reproduced by our Caldeirão site Sml24 (97.8 μT), but more data are required to uphold this conclusion. The set of data from Portugal by Nachasova et al. (2009) is scattered, nonetheless suggesting an ascendant trend of paleointensities from 100 to 600 BC and a descendant trend from 600 BC and 1300 BC.

The maximum depicted is well reproduced by our Furna flow (593±236 BC) reaching the high value of 95.22 μT. Our Furna flow result is robust as it results from an average of **8** specimens from two flows (sampled 3 km

far from each other) belonging to the same volcanic event. Similar high field values around the same time interval are observed in the Western USA (Champion, 1980) with values up to 140 ZAm^2, and even higher values of 197.5 ZAm^2 from Hawaii (Pressling et al., 2006) around 840 BC. The high value recovered on the Hawaiian samples was belied after a re-measurement of the samples, obtaining a lower value (Pressling et al., 2007). A regional spike was also recorded in Europe (Genevey et al., 2003; Gallet et al., 2006; Gallet and Le Goff, 2006), in Syria (Genevey et al., 2003) and in Southern Jordan (213 ZAm^2, Ben-Yosef et al., 2008; 2009) around 800 and 1000 BC, but a slight disagreement exits between the Levant dataset and the Grecian master curve (De Marco et al., 2008), which highlights a peak of intensity ~600-500 BC with a VADM of 114 ZAm^2. Regardless the age discrepancy of the spike occurrence and the irregular distribution of datasets, European, Hawaiian and Azorean data suggest the possibility of a global spike, and encourage further investigation of the regional extent of this feature. Our paleointensity data from São Miguel roughly agrees also with the trend depicted from the global model Cals3k.4 (Korte et al, 2011), which is smoothed. Interesting insights result from the comparison (Figure 17) of our dataset and the data provided by Mitra et al. (in press). Seventeen archeointensity estimates from Senegal and Mali (West Africa) covering a time period between 1,000 BC and 1,000 AD. These data were compared with data from Morocco and Egypt, as also with European data, dividing data in three Latitude intervals: 0°-20°, 20°-40° and 40°-60° N. A Latitudinal gradient had been observed, especially in the time range between 100 and 1,000 AD, whereas from 0 to 1,000 BC both data from 20°-40° and 40°-60° reproduce a prominent feature culminating around 600 BC with a maximum (up to 120 VADM). The Latitudinal gradient is explained as a changing non-axial-dipole contribution and confirmed by the simulation ad core mantle boundary by Cals3k.4 model (Korte and Constable, 2011), whereas the structure of the field around 0-100 AD was more axial-dipolar. Our data (of a 38°N of Latitude) roughly agree with Mitra et al. (in press) conclusion, for the age interval between 400 and 1200 AD, whereas our values are higher than reported in the work of Mitra et al. (in press) especially for the peak of high intensity around 600 BC.

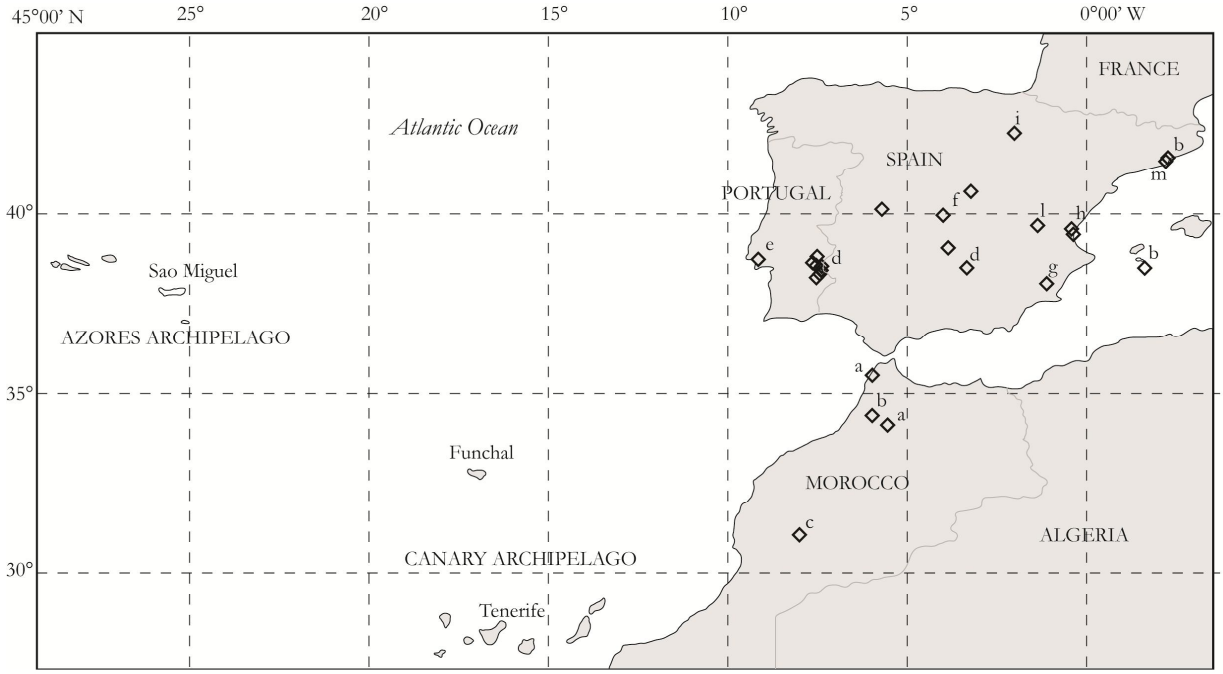

Spain:
f Catanzariti et al. (2012)
g Gomez-Paccard et al. (2006a)
h Gomez-Paccard et al. (2008) & Gomez-Paccard et al. (2006b)
i Kovacheva et al. (2009)
l Nachasova et al. (2007)
m Beamud et al., (2012)

Morocco:
a Kovacheva 1984, Kovacheva et al. (2009)
b Gómez-Paccard et al. (2012)
c Casas et al. (2008)

Portugal:
d Nachasova et al. (2009)
e Hartmann et al. (2009)

Fig. 15 - Location of paleointensity data compared with our data in Figure from Morocco, Portugal and Spain.

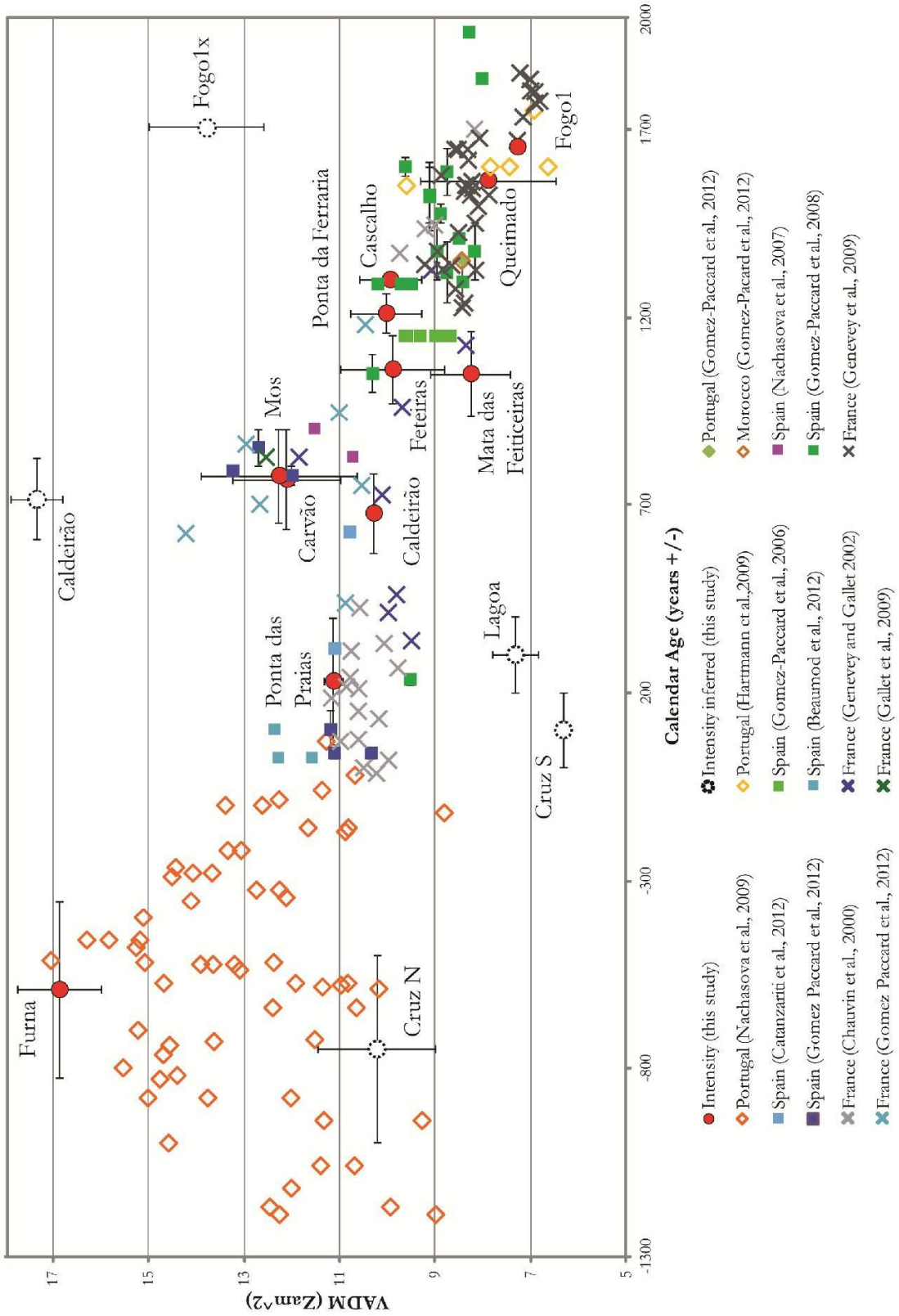

Fig. 16 - Comparison between paleointensity results from radiocarbon dated flows (this study) and data from Morocco (Kovacheva et al. 2009), Portugal (Nachasova et al., 2009, Gomez-Paccard et al., 2012, Hartmann et al., 2009), Spain (Gomez-Paccard et al., 2006,2008, 2012, Catanzariti et al., 2012, Beaumod et al., 2012) and France (Chauvin et al., 2000, Genevey and Gallet, 2002, Genevey et al., 2009, Gallet et al., 2009, Gomez-Paccard et al., 2012)

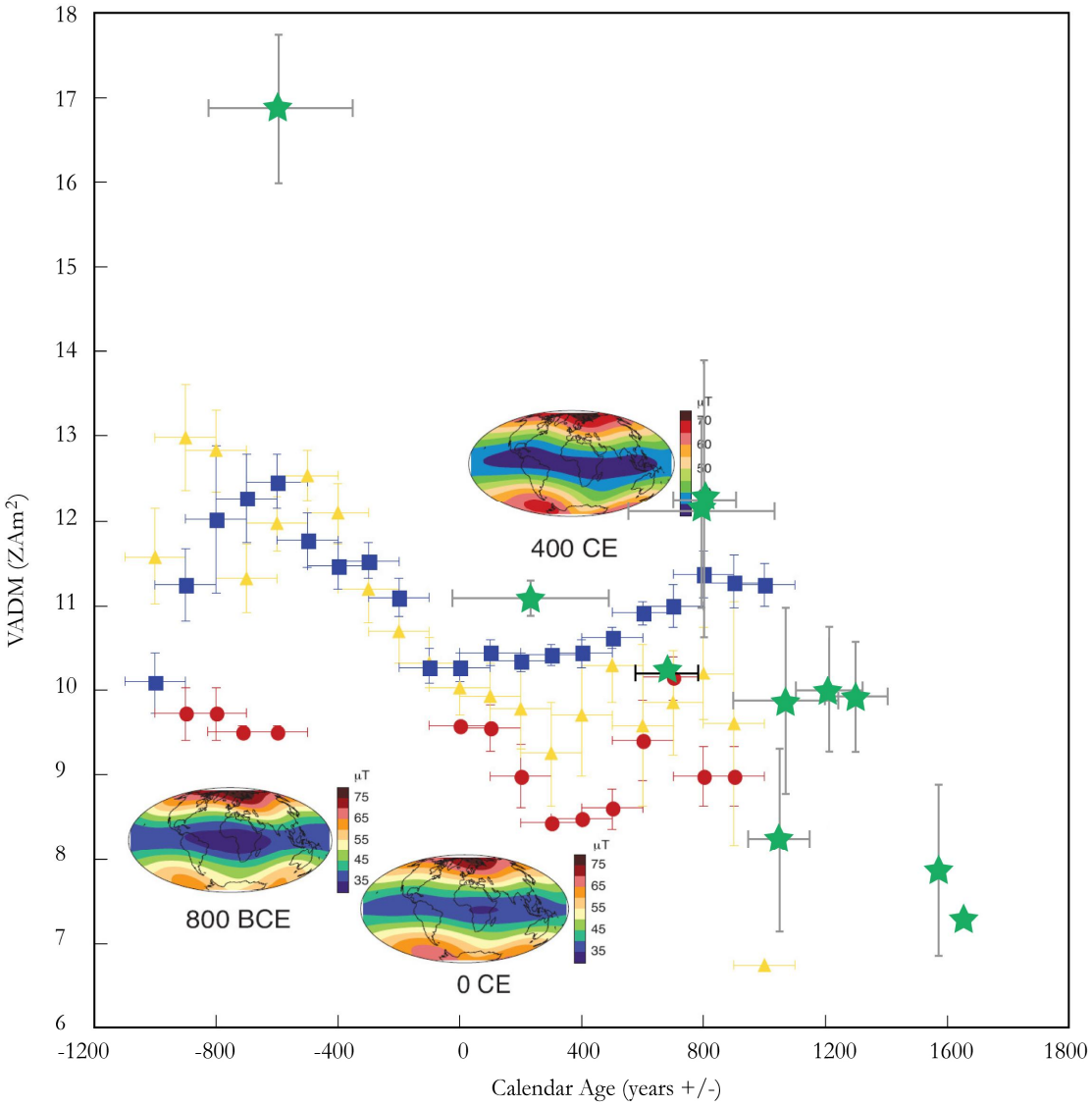

Fig. 17 - Modified after Mitra et al. (in press). Green stars are average VADM from this study (Lat 38°N), blue squares represent the average VADM for 60°N to 40°N, yellow triangles from 40°N to 20°N and red circles 20°N to 0°N. The longitudinal extent of the data from Mitra et al. (in press.) is between 20°W and 60°E. A 200 yrs moving window shifted by 100 yrs was used for the analysis. We used GEOMAGIA database (Korhonen et al., 2008; Donadini et al., 2009) and only paleointensity estimates obtained with a double-heating protocol were included in the analysis. The standard error is plotted on the y-axis and a fixed error of 100 yrs on the x-axis. The insets show the CALS3K.4 predictions at the surface for different periods in time.

14.7 Conclusion

New paleointensity data from lava flows well-age-constrained to the last 3,000 years (Moore 1990, 1991; and Moore and Rubin 1991) are presented in this study. All the samples previously investigated to recover paleodirections had been submitted to a strict pre-selection in order to choose the most suitable samples for paleointensity experiments. Although Shaar et al., (2011) suggested that the effort of orientate the specimen controlling the θ (trying to orientate parallel to the laboratory field) can be well worth the investment of time, after this study we rather disprove it; on the contrary is it worthwhile to pre-select specimen by specimen from an original dataset, to avoid all the known sources of bias (non ideal behaviors). The zigzag effect is superimposed on the curves, but is rather due to the experimental procedure and do not affect the reliability of the results, whereas a segmented pattern (concave or convex) effectively affect results leading to an over or underestimate of the intensity. Moreover, the choice of strict cut-off values of paleointensity selection criteria ensures the robustness of our paleointensity estimates.

We obtained from 24 new paleointensity estimates from 14 lava flows. Ten lava flows were radiocarbon dated, whereas three flows were archeomagnetic dated by Di Chiara et al. (2012) and one site was dated using stratigraphic relations.

Flows Cruz N and S, and Lagoa were dated using paleomagnetism. Nonetheless mean flow intensities may reveal a possible error during age assignment. Indeed these intensities are lower than expected, and so they could be older than previously stated. The Cals10k model (Korte et al. 2011) predicts declination of -3°, inclination of 52° and intensity of 39 μT around 3400 BC. There are other time when the field was low according to the model before 3,000 BC (inclination and declination also). The age of the Cascalho flow around 1300 AD is confirmed by the paleointensity.

The three sites from Caldeirão result in different values far from each other. Sml24 shows high value ~73 μT which is comparable with the European peak around 750 AD, whereas Sml23 is characterized by a lower intensity comparable with other flows almost coeval. More data are required to verify whether Sml24 belongs in fact to another flow or reflect the real pattern, which mean to admit that the strength of the field can change very fast.

The intensity of the site Sml08 assigned to the 1652 AD historical flow of Fogo 1 is effectively particularly high (77.5 μT) and far from Sml10 (~41 μT) of the same flow, as also from independently data gathered by Hartmann et al., (2009). Since also directions are different from the expected values for this age, we suggest that the flow sampled at Sml08 and 10 may be older.

The peak of intensity up to ~ 95 μT around 600 BC is well supported by two sites from the same flow (Furna). It is noteworthy that our results are comparable to the "spike" of intensity founded West Levant records, as well as in Western Europe.

Our data confirm the conclusion of Mitra et al. (in press.) of a predominance of the axial-dipole component between 0 to 100 AD, then a Latitudinal gradient from 100 to 1000 AD is observed from lower to higher Latitudes, and also a maximums around 500-600 BC is well reproduced and emphasized.

We conclude that:

- The archeomagnetic dating requires the three components of the geomagnetic field (declination, inclination and intensity) and a well determined global model (see Lanos 2004)
- Since some of the studied flows diverge from the predicted paleomagnetic behavior either some of earlier paper conclusions are inconsistent, or some of the flows mapped by Moore (1990) may be multiple flow so the geological map need to be improved
- Our data are consistent with conclusion mitra's concl that there is a high gradient at 500 BC, at 0 data ar consistent with data no field gradient and again aroud 800 AD the gradient rise
- Our data represent the first dataset of reliable paleointensity estimates for the central-northern Atlantic Ocean. The new data are internally consistent and radiocarbon dated, so they can be included in global geomagnetic datasets, and safely used to enhance the next global model of the geomagnetic field.

Acknowledgements

A.D.C. thanks Jason Steindorf for laboratory support, R. Mitra for useful discussions and helpfulness, and acknowledges a Marco Polo grant from the Bologna University. A.D.C. and F.S. were funded by INGV and FIRB MIUR C2 funds (responsible L. Sagnotti). This material is based on work founded by National Science Foundation grant EAR1141840 to L. T.

15. Constraining chronology and time-space evolution of Holocene volcanic activity on the Capelo Peninsula (Faial Island, Azores): a paleomagnetic contribution

Anita Di Chiara[1,2], Fabio Speranza[1], Massimiliano Porreca[2], Adriano Pimentel[2], Francesca D'Ajello Caracciolo[1], and José Pacheco[2]

[1]*Istituto Nazionale di Geofisica e Vulcanologia, Roma, Italy, anita.dichiara@ingv.it, fabio.speranza@ingv.it; francesca.caracciolo@ingv.it*

[2] *Università degli studi di Bologna, Italy*

[3] *Centro de Vulcanologia e Avaliação de Riscos Geológicos, University of the Azores, Ponta Delgada, Portugal , Massimiliano.Porreca@azores.gov.pt, Adriano.HG.Pimentel@azores.gov.pt, Jose.MR.Pacheco@azores.gov.pt*

15.1 Abstract

Faial is one of the most active volcanic islands of the Azores archipelago. The last historical eruptions occurred on the Capelo Peninsula (westernmost sector of the island) on 1672-73 AD and 1957-58 AD. The other exposed volcanic products of the peninsula are so far loosely dated within the Holocene. Here we present a successful attempt to correlate scoria cones and lava flows yielded by the same eruption on the Capelo Peninsula using paleomagnetic analyses in thirty-three sites (12 scoria cones, 21 basaltic lava flows). In the investigated products we recognized seven different pre-historical volcanic phases, whereas fifteen lavas were correlated with eight scoria cones. Dating was obtained by comparing our paleomagnetic directions with Holocene reference curves of the paleo-secular variation of the geomagnetic field from France and United Kingdom. We find that the volcanics exposed at the Capelo Peninsula are younger than previously believed, and entirely comprised in the last 4 ka. Our study confirms that paleomagnetism is a powerful tool for unraveling the chronology and characteristics of Holocene activity at volcanoes where geochronological age constraints are still few or lacking.

Keywords: Paleomagnetism; scoria cones; Holocene lava flows; paleomagnetic dating, paleosecular geomagnetic variation

15.2 Introduction

Faial is one of the most active volcanic islands of the Azores Archipelago (Fig. 18), however a detailed chronological framework of the recent volcanic eruptions on the island is lacking. Two historical eruptions

(1672-73 and 1957-58 AD) were witnessed in the Capelo Peninsula. The Peninsula, located in the westernmost sector of Faial, comprises a dextral en échelon alignment (WNW-ESE) of scoria cones, and minor tuff cones, with associated lava flows emplaced during the Holocene (Fig. 19; Quartau et al., 2012). The chronology of the pre-historical activity is poorly constrained and exclusively based on stratigraphic (Serralheiro et al., 1989) and geomorphological evidences (Quartau al., 2012). Clearly, constraining the age of Holocene eruptions and understanding the stratigraphic relations among cones and between cones and lava flows is fundamental, for both the statistical assessment of spatial and temporal volcanic patterns and their hazard implications.

Scoria cones are formed due to the accumulation of pyroclastic material around vents. Pyroclasts generally pile up around circular or elongated vents, building up conical landforms (truncated at the top) during hawaiian, strombolian, phreatomagmatic and/or sub-plinian eruption of low viscosity magma. The majority of scoria cones are monogenetic, resulting from a single eruptive event (e.g., Wood, 1980). Elongate monogenetic morphologies can result from a single eruptive vent, occurring along a fissure (Breed, 1964; Wood 1980), when the eruption does not rapidly become localized at a single vent, or from few vents along a fissure (Riedel et al., 2003). Scoria cones are typically clustered in cone fields or distributed on plateaus (e.g. Michoacán–Guanajuato, Mexico, see Hasenaka and Carmichael, 1985; San Francisco volcanic field, Arizona; Priest et al., 2001), or occur as parasitic cones along eruptive fractures along the flanks of stratovolcanos (e.g. Etna, see Corazzato and Tibaldi, 2006).

In the case of the Capelo Peninsula, scoria cones dominate the axial part, while lavas are exposed at the peninsula toe and close to the sea. As a rule, there are no clear field correlations between cones and lavas, mostly because of the exuberant vegetation that is widely spread in the Azores Islands. Wood (1980) argued that it is common that scoria cone eruptions produce lava flow deposits, while cones eruptions without lava flow extrusion rarely occur. Traditionally, the petrography of volcanic products has been used to study the source characteristics of lavas and scoria, and to correlate volcanic deposits (REF.) whenever the stratigraphic approach is not conclusive. However, changes in petrographic characteristics can occur during eruptive events (e.g., Strong and Wolff, 2003), making correlation of syn-depositional volcanic products questionable.

Elsewhere, scoria cones have also been dated and correlated through geomorphological studies based on morphometric and geometric characteristics using topographic maps (Wood, 1980; Hooper, 1995), high-resolution digital terrain models (Parrot, 2007; Fornaciai et al., 2012), and satellite images (Wood, 1980b; Hasenaka and Carmichael, 1985; Hooper, 1995; Inbar and Risso, 2001; Parrot, 2007). The criterion applied is based on the time of exposure to erosional processes; the longer the period of erosion, the smaller the aspect ratio of the cones. Surprisingly, the slope angle decreases rapidly in the first two years after the eruptive event (e.g. Wood, 1980b refers that recent cone slopes on Mt Etna decreased of 10° in only 450 years), while later the slope can be preserved with no significant changes when climatic conditions support the development of thriving vegetation. The alignment of cones generally suggests that they were formed during the same eruptive event. However, in regions where the tectonic processes control volcanic landform distribution over long periods of time, the repetition of similar elongation trends may complicate the interpretation.

To sum up, geomorphologic and/or petrographic studies may not be conclusive to correlate among scoria cones and/or with lavas flows exposed in the vicinities. In this paper we demonstrate how, conversely, paleomagnetic directions from scoria (or spatter) cones and underlying lava flows can be used as an accurate correlative and dating tool, thus providing significant constraints for the interpretation of the Holocene volcanic history of the Capelo Peninsula at Faial Island.

15.2.1 The use of the paleosecular variation of the geomagnetic field as a dating / correlating tool of volcanic rocks

Absolute ages of volcanics are best determined through radiometric dating. Yet both Ar/Ar and K/Ar methods loose accuracy when applied to young (Holocene) products, and can be hardly used in K-poor volcanic rocks (i.e. basalts erupted in most intra-oceanic volcanoes). ^{14}C is in turn a powerful dating tool for the last millennia, but needs carbon-rich soils, which can be uncommon at given climatic conditions and with high eruption frequency. As a consequence, during the last years there has been an increasing use of the paleosecular variation (PSV) of the geomagnetic field recorded in volcanic rocks as accurate dating / correlating tool of eruptions (Rutten and Wensink, 1960; Doell and Cox, 1965; Soler et al., 1984; Thompson and Turner, 1985; Rolph et al., 1987; Carlut et al., 2000; Incoronato et al., 2002; Lanza and Zanella, 2003; Tanguy et al., 2003; Speranza et al., 2008; 2010; Vezzoli et al., 2009 among many others). During cooling, volcanic rocks record an instantaneous snapshot of the local geomagnetic field direction, undergoing large swings with years (at least 40° in declination and 30° in inclination, at the latitude of Azores). The advantage of the paleomagnetic dating method is that it can be used on whole rock samples, and does not need particular petrographic / geochemical lava characteristics (magnetic remanence is generally carried by magnetite, ubiquitous in volcanics).

Paleomagnetic dating is achieved by comparing the paleomagnetic directions "frozen" in lava flows and scoria cones to a PSV reference curve, gathered in nearby regions by geomagnetic observations, archaeomagnetism, and paleomagnetism of sedimentary successions deposited at high rate, and relocated to the sampling site by pole method (Noel and Batt, 1990). Recent compilation of all European geomagnetic–archeomagnetic data sets (Speranza et al., 2008) revealed that during the Holocene, the field reached a maximum rate of change of ~ 7° per 100 years in the central Mediterranean region. Therefore, a paleomagnetic direction defined with an accuracy of 2°-4° can translate (after comparison with a PSV reference curve) into dating defined with an accuracy of ~ 100 years in the most favorable cases (see discussion in Speranza et al., 2006, and Lanza and Zanella, 2006). However, we stress that volcanic units of different ages may share the same paleomagnetic direction by chance, because the geomagnetic field may reoccupy the same directions after a few centuries or millennia. Thus, the paleomagnetic dating method is effective only when a input age window (preferably small) is provided by independent methods (e.g. radiometric dating). Moreover, although the geomagnetic field is predominantly dipolar, the non-dipole component imparts a significant regional component to the geomagnetic field, such that PSV reference curves do not have a global validity (Merrill et al. 1996), and cannot be safely relocated via pole method a distances greater than ~3000 km.

Besides yielding absolute dating (if appropriate PSV reference curves are available), paleomagnetism is always a powerful correlative tool of volcanic products lacking field correlation evidences. Hagstrum and Champion (1994) used the paleomagnetism as a correlative tool for scattered outcrops of late Quaternary lava flows in the lowest east rift zone of Kilauea Volcano (Hawaii). Jurado-Chichay et al. (1996) paleomagnetically studied the Pohue Bay flow (Manua Loa volcano, Hawaii islands) with the associated cones, to determine the cone origin (primary or secondary processes). Recently, Speranza et al. (2012) correlated several Pleistocene ignimbrite deposits spread on Pantelleria Island (Italy), relying on their paleomagnetic directions.

15.3 Faial Island

The island of Faial belongs to the central group of the Azores archipelago (Fig. 18). The nine volcanic islands of the Azores archipelago straddle the Mid Atlantic Ridge, where the Nubian, Eurasian and North-American plates meet. Tectonically, the Azores correspond to a transtensional regime as described by global GPS kinematic models, with a 4 mm/yr WNW relative motion of Eurasian plate relative to the Nubian plate (Sella et al., 2002; Fernandes et al., 2006).

The pentagonal shape of Faial (21 km long and 14 km wide) arises from a general WNW-ESE trend, the Pico-Faial ridge alignment, and a subordinate NW-SE fault system (Agostinho, 1937; Machado, 1955, 1982; Tazieff, 1959; Zbyszewski et al., 1959; Zbyszewski and Ferreira, 1959; Chovelon, 1982; Serralheiro et al., 1989; Madeira and Ribeiro, 1990; Madeira, 1998; Camacho et al., 2007; Trippanera et al., in press).

Pacheco (2001) provided an updated volcanic framework of Faial, previously described by Zbyszewski et al. (1959), Machado and Forjaz (1968), Forjaz (1977), Chovelon (1982), Serralheiro et al. (1989), and Madeira (1998). Four geomorphologic regions, which broadly correspond to four volcano-stratigraphic units, are recognized (Fig. 18): (i) The Ribeirinha volcanic complex located in the NE part of the island, which was emplaced from about 850 ka (Hildenbrand et al., 2012) to 580 ka, according to Feraud (1977) and Madeira (1998). The Ribeirinha Complex corresponds to shield-volcano mainly constituted by hawaiitic lava flows and later dislocated by the Pedro Miguel graben. Paleomagnetic results from Silva et al. (2010) proved that the onshore volcanic activity started during the Matuyama chron about 0.85 Ma ago, ~ 0.1 Myr older than age reported in previous works. (ii) The Caldeira Volcano, located in the central part of the island, is a stratovolcano constituted by the Cedros Complex (the Lower Group includes basaltic to benmoreitic lava flows, scoria cones and trachytic domes; while the Upper Group is made of trachytic pyroclastic deposits), which was emplaced from 470 ka (Feraud et al., 1980; Serralheiro et al., 1989) to present-day. About 1 ka ago, a 2 km wide summit caldera was formed during the last caldera forming eruption of the Caldeira Volcano. (iii) The Almoxarife Formation constitutes the Horta Platform, a plateau of basaltic lavas and scoria cones from fissural activity, located in the eastern part of the island, and dated between 30±20 ka (Feraud et al., 1980) and 10 ka (Madeira, 1998). (iv) The Capelo Formation includes the products of the most recent volcanic activity, favoring the growth of the homonymous peninsula in the westernmost part of the island. The Capelo Peninsula is thought to have

developed entirely during the Holocene (Madeira et al., 1995; Quartau et al., 2012), and is related to the settlement of scoria and tuff cones aligned along a WNW-ESE ridge. Two historical eruptions are recorded: the 1672-73 AD Cabeço do Fogo (Zbyszewski, 1960; Machado, 1958a; 1962; 1967), and the 1957-58 AD Capelinhos event (Machado, 1958a,b; Castello-Branco et al., 1959; Machado, 1959a,b; Machado et al., 1959; Zbyszewski and da Veiga Ferreira, 1959; Machado et al., 1962; Cole et al., 2001). A reconstruction of the temporal and spatial evolution of the volcanism and erupted volumes for the pre-historical (i.e. pre-1672 AD) activity at Capelo Peninsula has not been attempted so far.

15.4 The Capelo Peninsula: main features of scoria cones and lava flows

The Capelo Peninsula is a triangle-shaped 27 km² basaltic ridge forming the western part of Faial (Fig. 18), and entirely developed during the Holocene (Serralheiro et al., 1989), according to the analysis of its submerged insular shelf (Quartau et al., 2012). Predominantly sub-aerial low-explosivity (hawaiian to strombolian) basaltic eruptions yielded fifteen main scoriae cones (locally called Cabeços; we refer to Pacheco (2001) for cone nomenclature and characteristics). Half of the cones (from Trinta to Manuel Gato, Fig. 18) developed above the western mountainside of the Caldeira Volcano. The others rose from seafloor, with a phreatomagmatic episode followed by magmatic phase. On the western end of the peninsula, evidences of submarine/ hydromagmatic phases followed by magmatic activity are observed along paleo-sea cliffs at Costado da Nau volcano (Fig. 19), and witnessed during the historical eruption of Capelinhos in 1957-58 AD.

The fifteen cones of the Capelo Peninsula are aligned along WNW-ESE to NW-SE trending tectonic structures, en-echelon right oriented. Madeira (1998) suggested that the Capelo fracture zone may constitute the western extension of the Lomba do Meio fault corresponding, along with the Espalamaca fault (Fig.18), to the same tectonic structure as the Faial-Pico lineament. Recently, Trippanera et al. (in press) have estimated density values of up to 5 vents/km² for Capelo Peninsula. This represents a very high density concentration of eruptive vents, at which could correspond a high volcanic activity frequency in recent times (i.e. during the Holocene). The authors found that the vent clusters in Capelo are arranged in an overall left-stepping en-echelon configuration, implying a dextral component of shear in perfectly agreement with the kinematic data obtained by geodesy and seismology (Madeira and Brum da Silveira, 2003, Borges et al., 2007).

From E to W, fifteen main volcanic cones are observed and well exposed (Figs. 18 and 19): Cabeço dos Trinta (762 m a.s.l.), Lagoa (582 m), Cabeço Verde (571 m), Cabeço do Fogo (571 m), Cabeço do Garcia (582 m), the twin cones of Cabeço dos Caldeirões (310 m), Cabeço do Manuel Gato (287 m), Cabeço do Picarito (275 m), Cabeço Verde W or do Capelo (490 m), Caldeirão (360 m), Cabeço do Canto (340 m), Vigia (182 m), Costado da Nau (or Cabeço dos Concheiros, 181 m), and Capelinhos (140 m).

Following this order, we present a brief description of the main stratigraphic, geometrical and macroscopic petrographic observations performed during the field work.

On the western flank of the Caldeira Volcano lie the scoria cones of Cabeço dos Trinta, Lagoa and Verde. To the W, the Cabeço do Fogo cone rises (Fig. 19b).

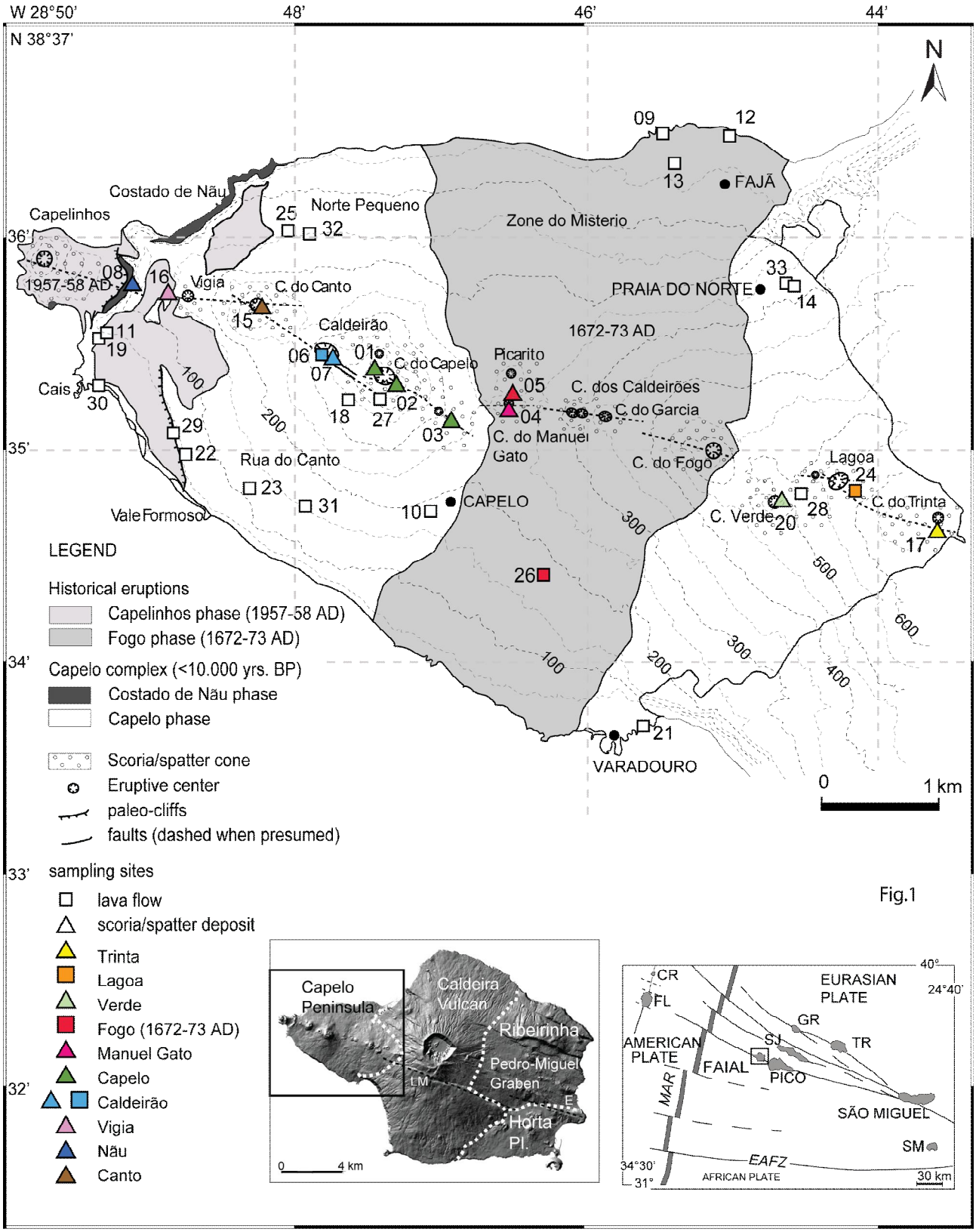

Fig. 18 - Geological Map of the Capelo Formation (modified from Serralheiro et al., 1959, and Madeira and Silveira, 2003) and location of paleomagnetic sampling sites (the "FAY" prefix is omitted). "C." is the abbreviation for Cabeço (= local name for volcanic cone). Digital elevation model interpretation of Faial Island is modified from Madeira, 1998 (LM= Lomba do Meio fault; E= Espalamaca fault). Schematic map of the Azores Archipelago is modified from Hildebrand et al., 2012 (CR=Corvo; FL= Flores; GR= Graciosa; TR= Terceira; SJ= Sao Jorge; SM= Santa Maria; MAR= Mid Atlantic Ridge; EAFZ= East Azores Fracture Zone).

The Cabeço do Fogo cone (Fig. 19f) was emplaced during the historical eruption of 1672-73 AD (Zbyszewski, 1960; Machado, 1967; Machado et al., 1962). The hawaian-strombolian volcanic event began on the 24th of April 1672 from the Cabeço do Fogo cone (Zbyszewski et al., 1959; 1960; Castelo Branco et al., 1959).

During the Cabeço do Fogo event, an eruptive fissure opened in E-W direction (Machado et al., 1962) and after spreading lavas both northward and southward that reached the coastline, the activity concentrated building a monogenetic scoriae cones Picarito (different from the "Picarito" referred by Castelo Branco et al., 1959 which is now recognized as Cabeço do Fogo, Zbyszewski et al., 1959). Lavas from Cabeço do Fogo covered the northern Capelo slope among Norte Pequeno, Fajã and Praia do Norte and to the south, lavas reached the coast, covering the area west of the Varadouro village. From E to W four cones elongated from East to West developed: Cabeço do Garcia, Cabeço dos Caldeiroes, Cabeço do Manuel Gato.

Cabeço do Capelo (Fig. 19a, c, e) with its two satellites cones (on the N and E flanks) is volumetrically the most important cone, arising from multi-stage, effusive and low-explosive volcanic activity. On its western flank rose the cone of Caldeirão (Fig. 19e), entirely made of basaltic lava flows. To the W, the perfect cone-shaped Cabeço do Canto (Fig. 19a) lies, and on its bottom-west side, the small monogenetic scoria cone of Vigia was emplaced. On the western tip of the Capelo Peninsula two multiphase cones rose up from the ocean: Costado da Nau (Water and Fisher, 1971; Camus et al., 1981) volcano is the product of a pre-historic eruption, located in the westernmost tip of Capelo Peninsula; the remnant of the volcano is exposed along a paleo-shore cliff (Fig. 19b), active before the 1957-58 Capelinhos eruption. The volcanic apparatus is similar to Capelinhos, since it results from alternating events of two hydromagmatic phases (phase 1 and 3, with layered welded and non- welded tuffs), alternated with two magmatic events; the lower magmatic phase (phase 2) is characterized by ~ 100 m thick lava flows, and the upper phase by spatter scoriae and bombs (phase 4, Fig. 19b). A network of dykes, exposed in the northern coast, feed these lava flows. In the geological map of Serralheiro et al. (1989), Costado da Nau is reported as an independent phase without any age indication.

The latest 1957-58 AD eruption took place on the western tip of the island, in the Capelinhos area. The historical Capelinhos eruption was described by Machado (1958a; 1959a; 1960a), Machado et al., (1962), Tazieff (1959), Castelo-Branco et al., (1959), Zbyszewski and Ferreira (1959), Zbyszewski (1960; 1963), Forjaz (1965), Machando and Forjaz (1968), Water and Fisher (1971), Camus et al. (1981), Cole et al. (1996; 2001), and an extensive photographic record is available.

Geochronological data available for the Capelo Peninsula are scarce, as they likely all refer to the 1672-73 AD historical event: Feraud et al. (1980) sampled in the area of Praia do Norte, an hawaiite lava (FA71 site) and obtained a 18th century age by K/Ar dating. Madeira et al. (1995) reported a ^{14}C age of 320±50 BP on charred wood (site FA2, Norte Pequeno locality) sampled from a mudflow deposit. By using the Stuiver's program, CALIB6.0 Online [http://calib.qub.ac.uk/calib/calib.html], we get 1455-1654 AD (1σ) calibrated age, again suggesting that the overlying flow is from the Cabeço do Fogo event.

A key stratigraphic marker to assess the age of Capelo volcanics is the so-named C11 pyroclastic deposit of the Upper Group of the Cedros Complex. The C11 is a key pyroclastic layer, well constrained from ^{14}C dates (Pacheco, 2001) to 980 ±50 years BP, which calibrated using the Online Stuiver's Progrwm CALIB6.0 [http://calib.qub.ac.uk/calib/calib.html] is 1076±103 years AD (2σ, 973- 1180 years AD). In the north-east side of Capelo Peninsula, stratigraphic relations between the C11 layer and lavas flows are frequently observed.

15.5 Sampling and methods

During July 2011, we paleomagnetically sampled 33 sites in the Capelo Peninsula, 11 in scoriae deposits from 8 different scoriae cones and one lava cone (FAY07 on the top of Caldeirão cone), and 23 in basaltic-like lava flows (Figs. 18 and 19, Table 1). Only five out of 23 lava sites show clear correlations in the field with four cones: FAY24 with Lagoa scoria cone, FAY06 with Caldeirão, FAY18 and 27, with the Capelo cone, and FAY26 with Cabeço do Fogo. At each site we drilled 15 (on average) 2.5-cm diameter cores using a water-cooled, petrol-powered portable drill. We spaced the cores as much as possible in the studied rocks to gather a well-averaged, representative paleomagnetic direction for each site. All cores were oriented using a magnetic and a sun compass, except site FAY33, for which we could only get magnetic orientation. The local field declination values (i.e. the differences between the magnetic and sun compass readings), are comprised between -20° and 1° (average -9.1°, Table 1), which compares well with the declination yielded by the IGRF-11 model (http://www.ngdc.noaa.gov/geomag-web/#declination) for Faial at 38.6°N, 28.8°W (D= -10° 33'). Some of the sites show clear stratigraphic relations with well-dated (1076 ± 103 AD) key pyroclastic layer C11: lava sites FAY14 and underlying FAY33 are both older than C11; at Fajã beach, a lava characterized by large xenolithes (up to 30 cm of diameter) of olivines and pyroxene sampled at sites FAY09 and FAY12 is mantled by C11, in turn lying below the 1672-73 AD lava. The sampled cores were cut into standard cylindrical specimens. The natural remanent magnetization (NRM) of all specimens was first measured by the 2G Enterprises DC-SQUID cryogenic magnetometer hosted in the shielded room of the paleomagnetic laboratory of the Istituto Nazionale di Geofisica e Vulcanologia (Roma). 187 specimens from 13 sites, characterized by a NRM lower than 10 A/m were further measured by the cryogenic magnetometer and demagnetized by on-line alternating field (AF), using 16 demagnetization steps, up to a maximum peak field of 120 μT. Conversely, the strong (>10 A/m) NRM of the remaining 242 specimens (20 sites) was measured by an AGICO JR6 spinner magnetometer, and thermal demagnetization (TH) was carried out in seven demagnetization steps up to maximum temperatures of 580°C, using a Pyrox shielded oven.

AF and TH demagnetization data were plotted on orthogonal vector component diagrams (Zijderveld, 1967), and the magnetization components were isolated by principal component analysis (Kirschvink, 1980). Site-mean paleomagnetic directions were computed using Fisher (1953) statistics (Table 2).

In addition, petrographic observations have been carried out on six thin sections from lavas and scoriae of sites FAY05, 06, 09, 13, 26, 30.

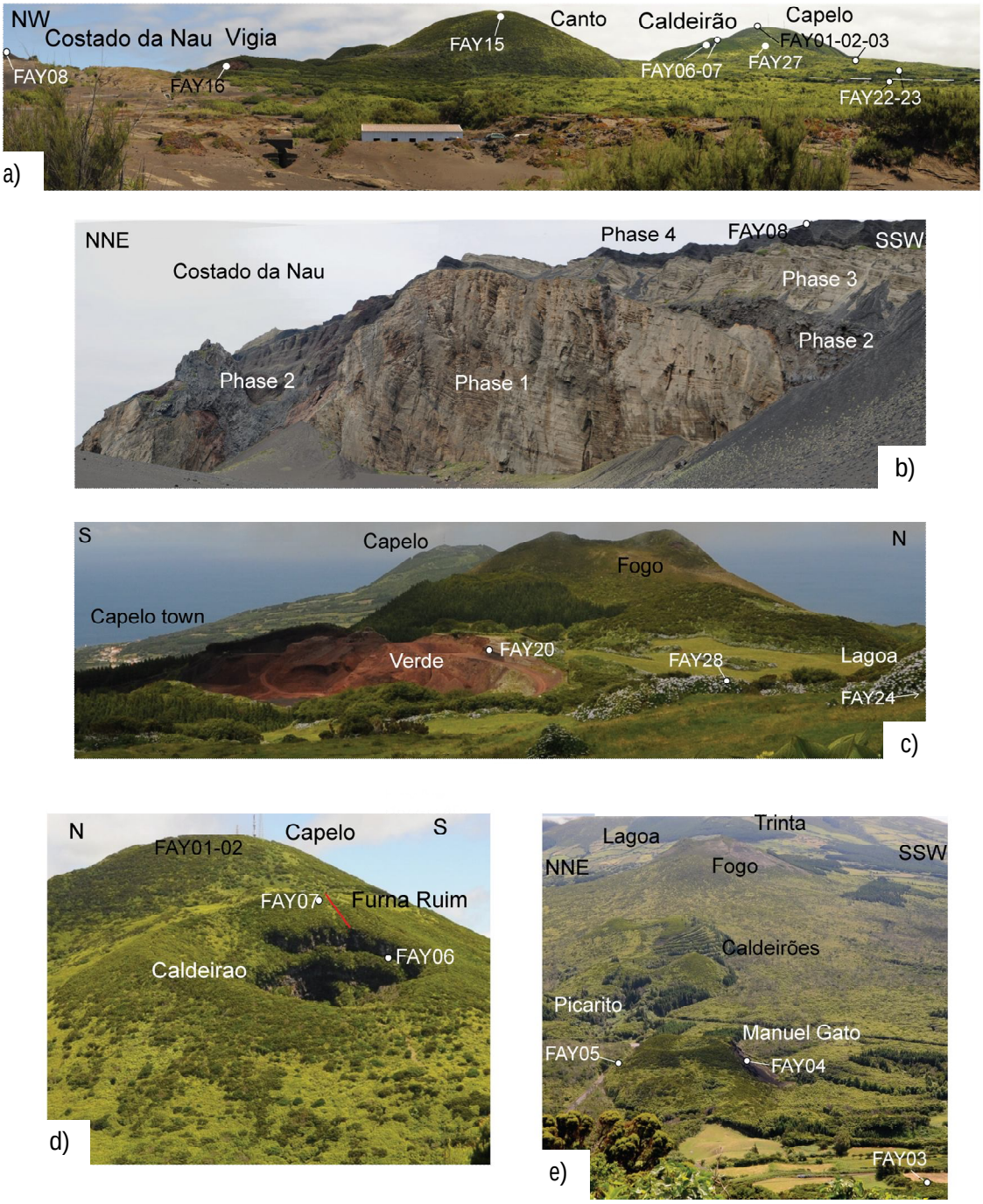

Fig. 19 - Photos from Capelo Peninsula; A) Overview from Cais harbor of NW-SE aligned scoria cones of Capelo (sampling sites FAY01, 02, 03 and 27), Caldeirão (FAY06 and 07), Canto (FAY15), Vigia (FAY16) and Costado da Nau (FAY08), as well as Costado da Nau paleo-cliff (FAY22 and 23). B) Costado da Nau cone section cut by marine erosion, showing the four magmatic / hydromagmatic phases. C) Landscape from the Trinta cone looking westward, and cones of Lagoa (site FAY24), Verde (FAY20), Fogo, and Capelo. D) Capelo (FAY01 and 02) and Caldeirão (FAY06 and 07) cones seen from Canto cone; the Furna Ruim fracture between the two cones is marked with the red line. E) Overview (from the top of the Capelo cone) of the aligned scoria cones of Picarito (FAY05), Manuel Gato (FAY04), the twin Caldeirões cones, Cabeço do Fogo 1672-73 AD (FAY26), and of the Lagoa and Trinta cones in the rear.

15.6 Results

15.6.1 Petrographic characterization

In all of the observed samples phenocrysts and microphenocrysts of olivine, plagioclase and clinopyroxene, occur in different proportions. The same mineral phases are found in the groundmass. (Fig. 20). Occasionally, Fe-Ti oxides are also present as microphenocrysts and in the groundmass.

FAY26, a lava flow from the historical eruption, contains plagioclase, olivine, and occasional clinopyroxene phenocrysts (Fig. 20a). Michel-Tomè (1981) refers that the 1672-73 AD eruption produced lavas of vesicular basanitoid type, occasionally trending more towards andesites, similarly to lavas from the 1957-58 Capelinhos eruption (Zbyszewski et al., 1959). Similar petrographic features are observed in FAY05, from the scoria cone of Picarito, but the texture is scoriaceous. The groundmass is vescicular, very glassy, and also hypocrystaline. Indeed, Zbyszewski et al., (1959) refers that Picarito cone was built during the same event of Cabeço do Fogo. Instead, lava from site FAY13 (Fig.20d) reveals a slight difference assemblages with respect to the Cabeço do Fogo characteristics (FAY26 and 05), since olivine and clinopyroxene are frequent, but plagioclase occurs occasionally as phenocrysts.

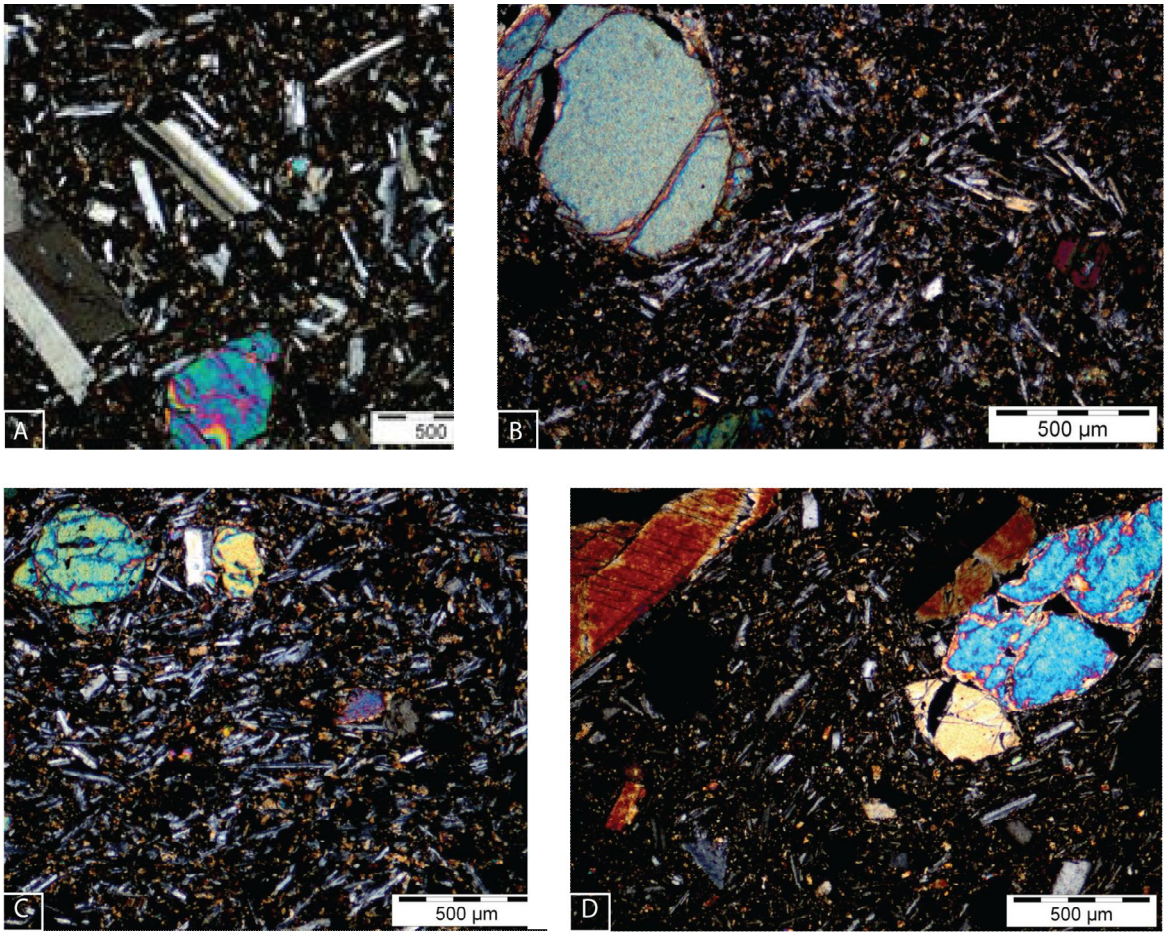

Fig. 20 - Thin sections images under crossed-polarized light from A) Historical (1672-73 AD) lava flow at FAY26; B) FAY09 from the Xenolith-rich lava sampled at Fajã beach; C) FAY06 from the Caldeirão lava; and D) FAY13 from the Fajã Quarry lava.

The same characteristics appear in the FAY06 (Fig.20c) thin section. FAY09 from xenolith-rich lava flow has mainly large olivine and clinopyroxene crystal, and plagioclase as phenocrysts, while the microphenocrysts include plagioclase, olivine, oxides, and occasional clinopyroxene.

Therefore, FAY13 has slightly different characteristics than FAY26 and FAY05, suggesting that they could be emplaced from different cones. However, it is known that slight petrographic differences may exist also in the same lava sampled at different locations from the vent (reflecting variations in effusion rate, thermal history, mechanical fractionation, oxygen fugacity, etc.) or in different flows emplaced during a single long-lasting eruption, reflecting probably magmatic zonation (e.g. Blake, 1981).

Much less documentation exists for chemical variations within basaltic systems over the duration of a single eruption or closely spaced eruptive events. For instance during the 1733– 1736 Lanzarote eruption, the lavas changed from alkali basalts to olivine tholeiites over a period no longer than two weeks (Carracedo et al., 1992). Moreover, chemical characterization may not to be univocal. For instance, monogenetic scoria cones (basaltic to andesitic) from the southern Cascades studied by Strong and Wolff (2003) exhibited large chemical variations within the products of single eruptions.

15.6.2 Paleomagnetic results

A well-defined characteristic remanent magnetization (ChRM) is isolated for nearly all lava and scoriae samples, in the 30 to 120 mT and 300° to 580°C intervals (Fig.21a). Predominantly low magnetic coercivities and complete demagnetization occurring between 550° and 580°C suggest that ChRMs are carried by magnetite. The α_{95} values relative to the mean paleomagnetic directions for 30 sites vary from 1.7° to 3.9° (2.9° and 2.8° on average for the AF- and TH- demagnetized sites, respectively), while three sites yielded scattered directions and were discarded by further consideration. Site-mean paleomagnetic declinations are mostly positive and vary from ≈ 30° to -20° values (Fig. 21b and Table 2), while inclinations are comprised between ≈ 50° and 70° (for comparison, the geocentric axial dipole field inclination expected at Capelo Peninsula is 57.9°).

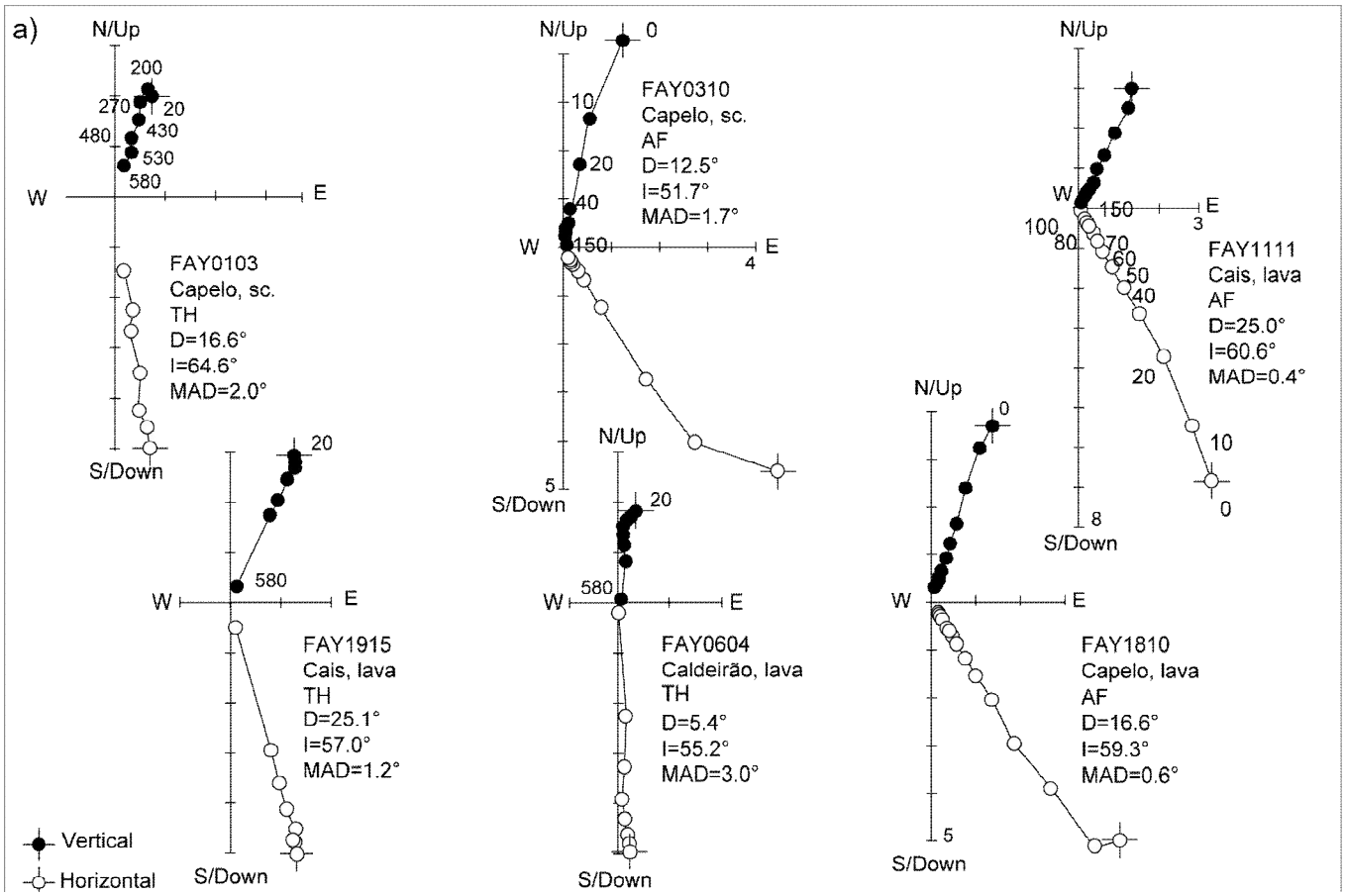

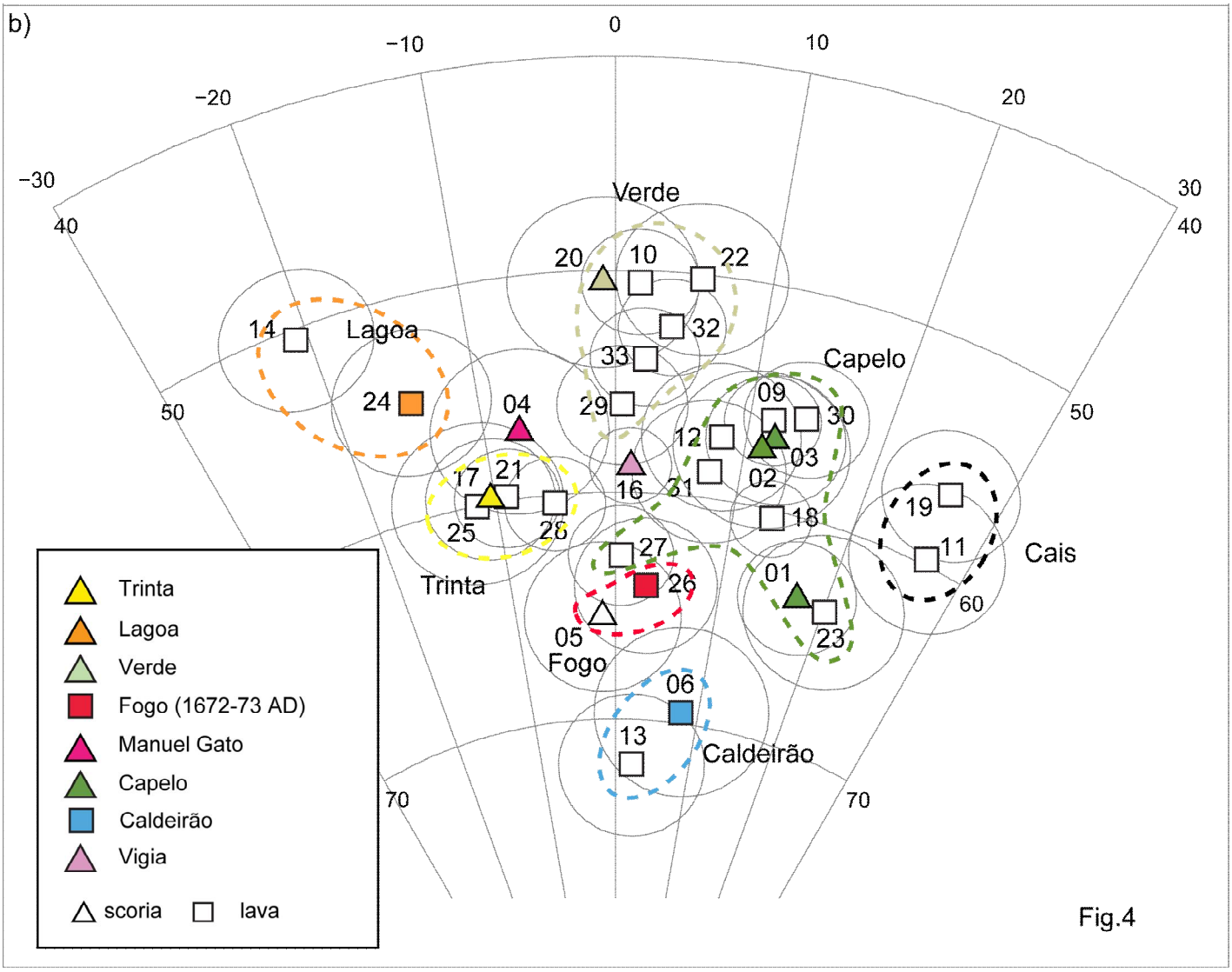

Fig.4

15.7 Discussion

15.7.1 Correlation of scoria cones and lava flows produced by the same eruption

Sites sampled in the same cone or in correlative cones (as the three sites from Capelo cone), or in correlative cone and flow (as sites from the 1672-73 AD eruption) yield similar paleomagnetic directions, comprised within a maximum angular distance of 8.8°. This is consistent with evidence gathered in other volcanoes, where paleomagnetic directions from the same volcanic unit (lava or ignimbrite) cluster within a ~ 10° spread (e.g., Hagstrum and Champion 1994; Speranza et al., 2010; 2012).

The paleomagnetic directions from Faial can be used firstly to correlate lava flows to given scoria cones, then to date volcanic activity after comparing paleomagnetic directions with geomagnetic directions expected from appropriate PSV reference curves. In the past, the vicinity of paleomagnetic directions has been used to correlate among them lava and ignimbrite outcrops (e.g. Rolph and Shaw, 1986; Jurado-Chichay et al., 1996; Tanguy et al.

2003; Riisager et al., 2003; Speranza et al. 2008; 2012; Vezzoli et al. 2009), but never (to the best of our knowledge) to correlate scoria cones with lava flows yielded by the same eruption.

The vicinity of paleomagnetic directions of sites FAY11 and 19 in Cais locality (Fig. 21b), along with common petrographic features and no paleosoil observed between the two lava flows, suggests that they emplaced contemporaneously (hereinafter referred as Cais phase).

A cluster of paleomagnetic directions concentrated between 0°-20° of declination and 56°-64° of inclination from ten sites sampled on the Capelo cone and along the peninsula flanks is recognized. In particular, directions from the two sites sampled in scoriae deposits on top of the Capelo (FAY02) cone and on the small satellite scoria cone on the flank (FAY03) overlap. Lava flows sampled on the southern flank of Capelo cone with sites FAY18, 23, 27 and 31 correlate with the Capelo cone mean direction, as well as FAY30 sampled in Cais locality. Field evidence indicates that sites FAY11-19 (Cais sites) overlie FAY30 and therefore are younger. In the northern coast of the Capelo Peninsula sites FAY09 and 12 collected from the thick xenolith-rich lava share a common paleomagnetic direction with sites from the Capelo cone, although they are located laterally with respect to it. Hereinafter we refer to this cluster of ten sites data as Capelo phase.

A third cluster of data, related to the so-called Verde phase, is characterized by -1° to 5° declination values, and 50° to 56° inclinations. It comprises data from two different zones, around Cabeço Verde (site FAY20 from the scoria cone and FAY33 lava from Praia do Norte), and in the lower slopes of the Capelo cone (lavas of sites FAY10, 22, 29, and 32).

Lavas from Lagoa cone (FAY24) and FAY14 sampled in Praia do Norte, show similar peculiarly western declinations (between -21° and -15°) and inclinations from 50° to 55°, thus can be safely correlated. Site FAY14 stratigraphically overlies the FAY33 lava of the Verde phase (and both are below the C11 pyroclastic deposit with date of about 1076 AD).

The other phase, called Trinta phase, is characterized by cluster paleomagnetic data with ~ -10° declinations and 60° inclinations includes FAY17 from Cabeço dos Trinta, the lava flow sampled at site FAY28, between Lagoa and Cabeço Verde, the lava flow of the Varadouro village (FAY21), and the far site FAY25, from Norte Pequeno.

Sites FAY06 (sampled inside the Caldeirão rim cone) and FAY13 (from the quarry of Fajã locality) share the same particularly high inclinations (≈ 70°), and a weakly positive declination. Site FAY26 from the 1672-73 AD flow yields a direction close to site FAY05 from Picarito, while site FAY04 from Cabeço do Manuel Gato yields a direction ~ 10° far. Finally, site FAY16 from the Vigia cone cannot be correlated with other sites.

15.7.2 Reference curves of the paleosecular variation of the geomagnetic field

Paleomagnetic dating of Holocene volcanics from Italy has been routinely done using the French archeomagnetic curve (Bucur, 1994; Gallet et al., 2002) for the last 3 ka, and the UK master curve (Turner and Thompson, 1981; 1982) for older Holocene times (see Tanguy et al., 2003; Speranza et al., 2004; 2008; 2010). Reference data were relocated to volcanic coordinates by pole method (Noel and Batt, 1990). Therefore we relocated the French archeomagnetic curve and the UK master curve to Faial Island (N 38,59 and W 28,80; Fig. 22, 23), although the distance with respect to source data (both ~ 2600 km) is at the upper bound level to use safely the pole relocation method. For ages older than 2500 yr BP, original ages of the UK master curve were recalibrated according to the new calibration points proposed by Snowball et al. (2007) relying on the comparison with the FENNOSTACK curve from Fennoscandia. Following Speranza et al. (2008), declinations of the UK master curve were lowered by 10° (before relocation), as a similar systematic error is apparent in the original data set when compared to other European archeomagnetic curves (the UK curve is gathered by sedimentary cores azimuthally non oriented).

In Fig. 23 we also show the recently issued PSV curve of the Azores (Di Chiara et al., 2012), gathered at São Miguel Island (Azores) by paleomagnetically studying a set of lava flows of the last 3 ka dated by ^{14}C method by Moore and Rubin (1991).

Curves relocated by pole method were also compared in Fig. 23 to global field models, gufm1 (Jackson et al., 2000) for the last four centuries, and CALS10k.b1 (Korte et al., 2011) for the whole Holocene. Global model of Korte et al. (2011) yields smoothed trends with respect to the French archeomagnetic curve and the UK master curve, yet the validity of the directions relocated from the French archeomagnetic curve and UK master curve has been clearly demonstrated by several studies made on Italian volcanoes, where again global models yielded too smoothed trends (see discussion in Speranza et al., 2008).

Fig. 22 - PSV reference curves from UK (Turner and Thompson, 1981,1982), France (Bucur, 1994, Gallet et al., 2002) and Sao Miguel (black curve, Di Chiara et al., 2012), and from global models gufm1 (Jackson et al. 2000) and CALS10k.1b (Korte et al., 2011). Age model of the UK master curve is according to Snowball et al. (2007), original declinations values of the UK master curve were lowered by 10° (see discussion in Speranza et al., 2008).

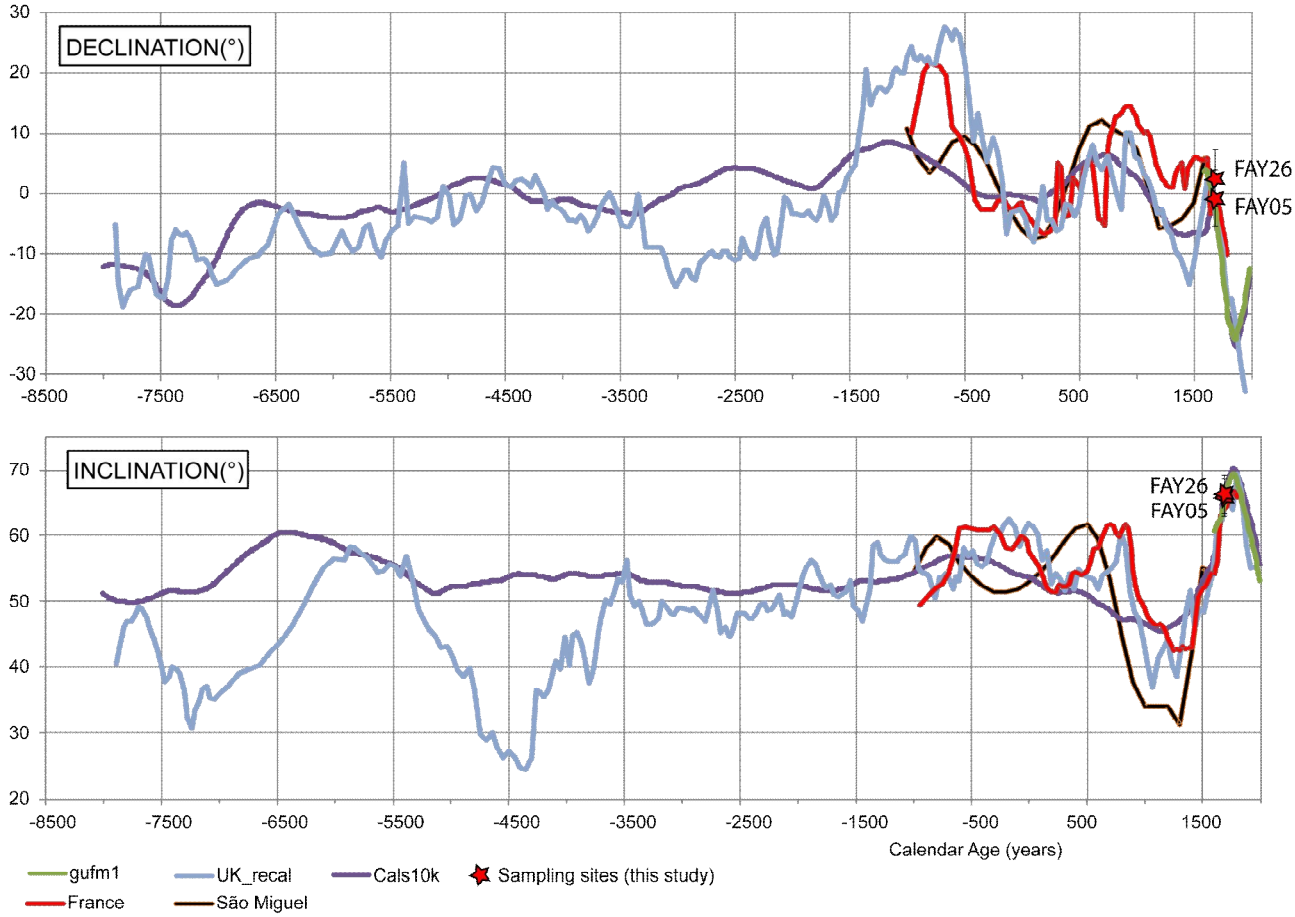

15.7.3 Dating volcanic activity at Capelo Peninsula

The paleomagnetic directions of site FAY26 (D=2.9°; I=64.1°) sampled in the 1672-73 AD historical flow, and FAY05 sampled in Picarito cone (D=358.7°; I=65.5°) are remarkably consistent with field direction predicted by gufm1 for 1673 (D=-0.5°; I=64.1°; Fig. 23), while the close Manuel Gato cone (FAY04) yields a direction ~ 10° far. Hence we confirm that Picarito cone was built during the Cabeço do Fogo historical eruption, whereas no definitive conclusion can be reached on the Manuel Gato cone origin (a 10° distance is in principle possible for sites from the same volcanic unit, e.g. Speranza et al., 2012; Di Chiara et al., 2012).

Our paleomagnetic data thus confirm the validity of the gufm1 model for the Azores in the late XVII century, while data from the 1652 AD flow at São Miguel had yielded an inclination ~ 15° lower than gufm1 predictions (Di Chiara et al., 2012). We put forward two hypotheses for this mismatch: 1) the 1652 AD flow of São Miguel did not faithfully record the local field direction (as it has been observed for the 1943–1952 AD eruption of Paricutin volcano (Mexico) by Urrutia-Fucugauchi et al., 2004), or 2) the flow assigned to 1652 AD in the geological map of Moore (1991) has in fact a different age (a 150 years older age would fit the expected

inclination). This last hypothesis is also supported by Ferreira (2000), which has strongly limited the areal distribution of the 1652 AD lava flow.

For dating the sites likely emplaced during the last 3 ka we used the archeomagnetic dating program archeo_dating, developed by Pavòn-Carasco et al., (2011) by following the procedure given by Lanos (2004). Arcaeo_dating program compares statistically the raw paleomagnetic data from a given locality with the expected directional values from the local PSV curve, relocated to the studied locality coordinates; in this study, the French Secular Variation master curve by Chauvin et al., 2002 and Gallet et al., 2002 (extending from 975 BC to 1830 AD) has been used.

Dating of older Holocene sites was done by observing the vicinity (up to ~ 10° of distance) of paleomagnetic directions with given tracks of the UK master curve. The 10° tolerance is chosen considering that a directional scatter of ~ 10° may characterize paleomagnetic directions (Speranza et al., 2012; Di Chiara et al., 2012), and that the pole relocation of the UK master curve from Britain to Azores may have added other error in the order of 2°-3° (e.g. Lanza et al., 2005). Therefore, accuracy of ages defined by comparison with the UK master curve must be considered in the order of ±200 years. Clearly, a possible better definition of reference PSV curves in the future will translate into more accurate ages derived by direct paleomagnetic data.

Cais lavas sampled at sites FAY11 and 19 correlate rather well with the declination maxima observed in the French curve between 650 and 850 BC (Fig. 23b) a 778-550 BC interval is obtained by archeo_dating. Cais lavas overlie site FAY30 from the Capelo phase, thus suggesting that Capelo phase is slightly older than Cais lavas, and can be constrained between 1000 and 1400 BC, after comparison with the UK master curve (Fig. 23c). Site distribution suggests that the Capelo phase, besides obviously being related to the Capelo cone and related lava flows, yielded also another cone feeding lavas of sites FAY09 and FAY12, and now buried below the Cabeço do Fogo products (Fig. 24a-b).

Lavas of sites FAY10, 22, 29, and 32 from the Verde phase are spread around the Capelo cone and seem thus to have similar ages. Therefore, we constrain the Verde phase to the 1400-2200 BC time span (Fig. 23c, significantly older age tracks of the UK curve are excluded as field evidence suggests quasi-continuity of the Capelo and Verde activity). Sites FAY22, 29 and 32 are located below the Canto cone, thus they are possibly related to it although this cannot be verified by data (site FAY15 from the Canto cone failed). Thus, similarly to the Capelo phase, magmas of the Verde phase were erupted by two different centers, by the Verde cone (yielding also lava flow of site FAY33), and by cone(s) virtually coinciding with the Capelo cone and now buried below it.

The declination minimum recorded by the sites from Lagoa cone (FAY14 and 24) can be necessarily dated to 2000-2200 BC, as FAY24 lava lies above FAY33 lava flow of the Verde phase.

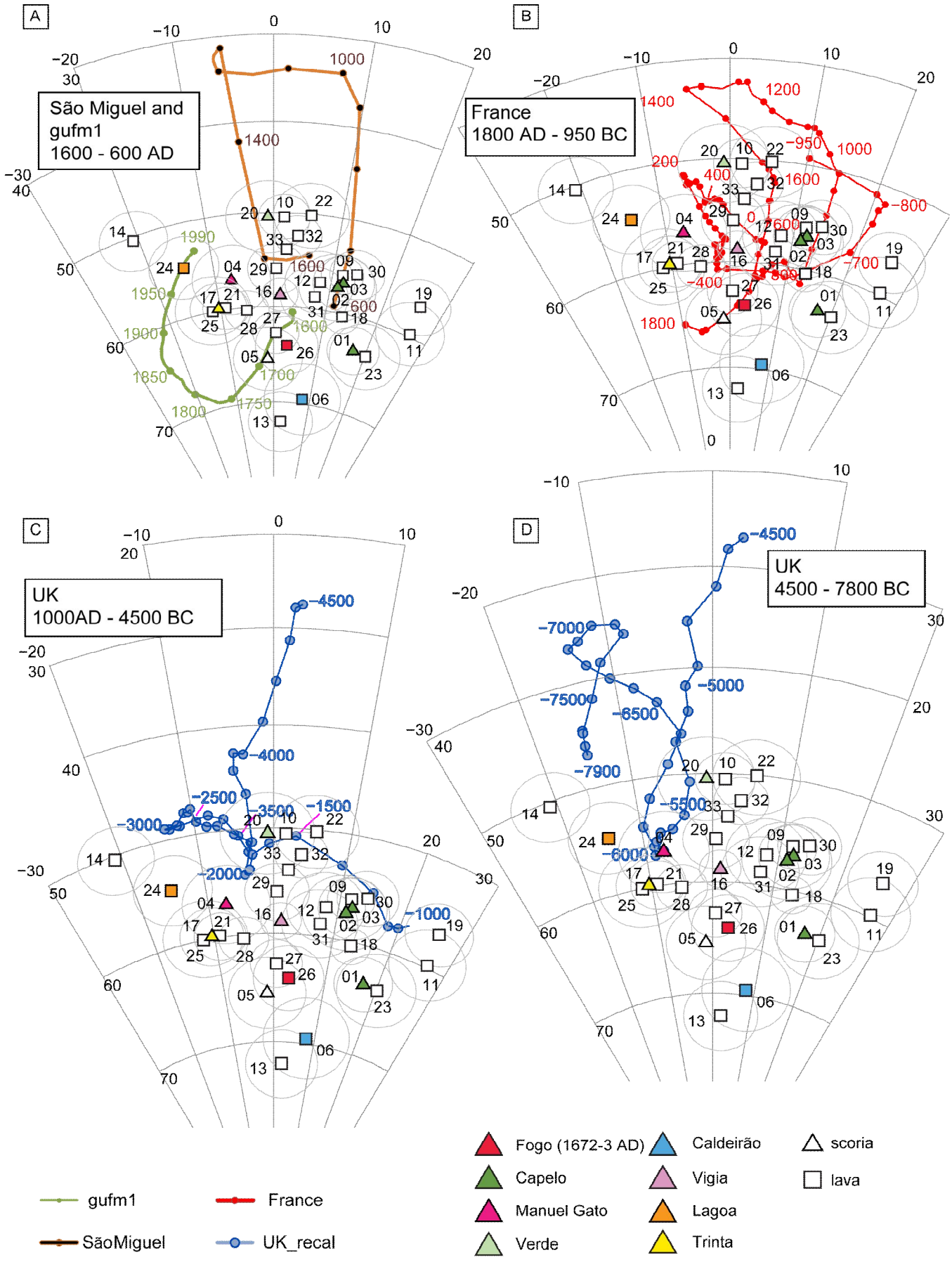
A
São Miguel and
gufm1
1600 - 600 AD
B
France
1800 AD - 950 BC
C
UK
1000AD - 4500 BC
D
UK
4500 - 7800 BC
gufm1
France
SãoMiguel
UK_recal
Fogo (1672-3 AD)
Caldeirão
scoria
Capelo
Vigia
lava
Manuel Gato
Lagoa
Verde
Trinta

Fig. 23 - Equal-area projection (lower hemisphere) of site-mean paleomagnetic directions from Capelo Volcanic Complex plotted with relocated reference directions shown in Figure 5. A) São Miguel curve (Di Chiara et al., 2012) and gufm1 (Jackson et al., 2000); B) French archeomagnetic curve (Bucur, 1994; Gallet et al., 2002); C) and D) modified UK master curve in the 1000-4500 BC (C) and 4500-7800 BC (D) age intervals.

The Trinta phase (FAY17, 28 and 21) can be similarly correlated with the cusp of 2000 BC, although it is also compatible with the 6000 BC cusp (Fig. 23d). However, the latter age is unlikely, as the Trinta cone is adjacent to the Lagoa and Verde cones, dated to 2000-2200 BC and 1400-2200 BC, respectively.

The Caldeirão site FAY06 and similar direction site FAY13 are ~ 10° far from the French directions in the 400-600 BC age window (Fig. 23b), while they are definitely more distant from all other reference curve points. We therefore tentatively assign a 400-600 BC age to the Caldeirão cone, and possibly to site FAY13, necessarily related to an additional cone located further east.

Vigia cone (FAY16) can be dated to three equally probable age intervals by arcaeo_dating: 342 BC-23 AD, 489-648 AD, and 1592-1654 AD, the latter age being excluded by lack of historical accounts. Vigia is mantled by volcanic deposits from Costado da Nau (phase 3 and 4), which is therefore slightly younger and can be reasonably constrained between the oldest possible Vigia age (342 BC) and the arrival of the first settlers in the island (~ 1470 AD) (Fig. 24b).

Fig. 24 - a) Re-interpreted geological map of the Capelo Peninsula and b) schematic plot of the paleomagnetically dated volcanic phases vs. emplacement longitudes. All flow directions and correlation with dated volcanic phases are paleomagnetically inferred, except for Cais and Vigia which are archeomagnetically dated (archaeo_dating program by Pavon-Carrasco et al., 2011)

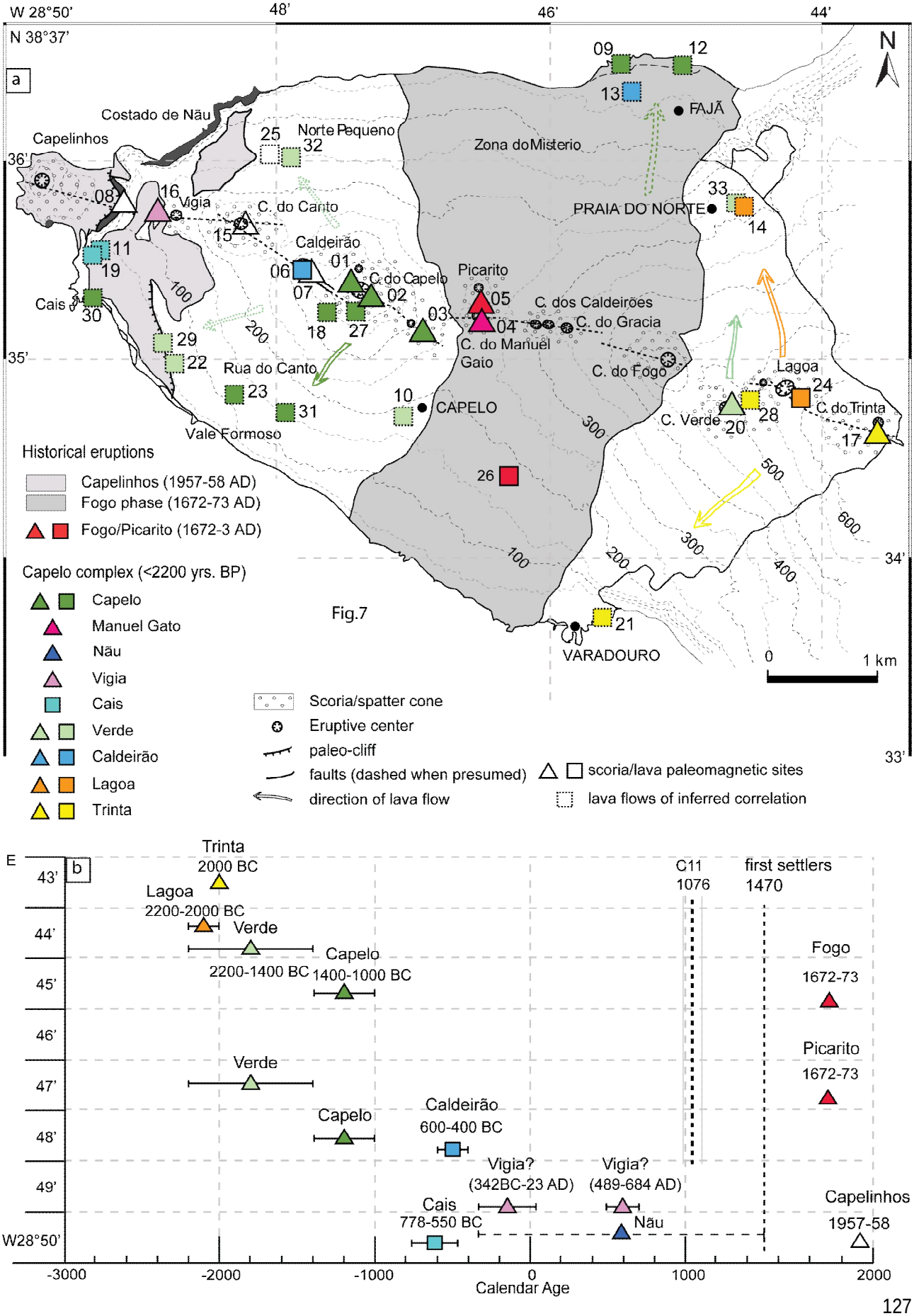
W 28°50'
48'
46'
44'
N 38°37'
36'
35'
34'
33'
N
a
Costado de Nāu
Capelinhos
Norte Pequeno
Zona do Misterio
FAJÃ
PRAIA DO NORTE
Vigia
C. do Canto
Caldeirão
C. do Capelo
Picarito
C. dos Caldeirões
C. do Gracia
C. do Manuel Gaio
C. do Fogo
Cais
Rua do Canto
Vale Formoso
CAPELO
Lagoa
C. do Trinta
C. Verde
VARADOURO
0
1 km
Historical eruptions
Capelinhos (1957-58 AD)
Fogo phase (1672-73 AD)
Fogo/Picarito (1672-3 AD)
Capelo complex (<2200 yrs. BP)
Capelo
Manuel Gato
Nāu
Vigia
Cais
Verde
Caldeirão
Lagoa
Trinta
Fig.7
Scoria/spatter cone
Eruptive center
paleo-cliff
faults (dashed when presumed)
direction of lava flow
scoria/lava paleomagnetic sites
lava flows of inferred correlation

E
b
43'
44'
45'
46'
47'
48'
49'
W28°50'
Trinta
2000 BC
Lagoa
2200-2000 BC
Verde
2200-1400 BC
Capelo
1400-1000 BC
Verde
Capelo
Caldeirão
600-400 BC
Vigia?
(342BC-23 AD)
Vigia?
(489-684 AD)
Cais
778-550 BC
Nāu
C11
1076
first settlers
1470
Fogo
1672-73
Picarito
1672-73
Capelinhos
1957-58
-3000
-2000
-1000
0
1000
2000
Calendar Age

15.8 Conclusion

By paleomagnetically studying the volcanics exposed in the Capelo Peninsula of Faial Island (Azores), we have documented the successful attempt to use paleomagnetism as a correlative tool between scoria cones and syn-eruptive lava flows. Correlations are inferred from the similarity of paleomagnetic directions, and supported by stratigraphic and petrographic evidence, when available. Our data support the correlation of seventeen lava flows with eight scoria cones.

Furthermore, paleomagnetic dating of volcanic events was attempted, relying on the comparison of our paleomagnetic directions and expected paleofield directions derived from relocated PSV reference curves from France and UK. We find that the volcanic products of the Capelo Peninsula, previously loosely constrained to the last 10 ka (Holocene), are in fact comprised in the last 4 ka. Volcanic activity of the Capelo Formation started ~ 4,000 years ago, with the emplacement of the Verde, Lagoa, and Trinta cones on the western mountainside of the Caldeira central volcano, within a narrow age window that we constrain between 2,200 and 1,400 BC (Fig. 24). Contemporaneously to the Verde activity, another huge cone rose further west, and is now buried below the Capelo cone and products. Subsequently, a rather continuous activity occurred between 1,400 BC and present-day, yielding the Capelo (1400-1000 BC), Cais (778-550 BC), Caldeirão (600-400 BC), Vigia (342 BC-23 AD or 489-684 AD), Costado da Nau (342 BC-1470 AD), Fogo-Picarito (1672-73 AD), and Capelinhos (1957-58 AD) cones and related products. At least the Capelo, and possibly the Caldeirão eruptions occurred along at least two different cones, or along multiple cones spread along the WNW-ESE eruptive fissure (as it was observed during the 1672-73 AD eruption). A general westward drift of the volcanic activity (Fig. 24) seems to be terminated ~ 2,500 years ago, with the emplacement of the Caldeirão and Cais lavas. Subsequently, volcanic activity remained confined at the western tip of the peninsula, although the huge 1672-73 AD eruption occurred again in the central-eastern part of the peninsula.

Our data demonstrate that paleomagnetism is a powerful tool for both correlating volcanic cones and lava flows, and dating Holocene volcanic products, if reliable PSV reference curves can be used for the studied area (best reference curves are available for Europe and neighbor regions). We confirm that paleomagnetism, coupled with field evidence, petrographic characterization, and geochronology (if available) allow unraveling the spatial and temporal behavior of Holocene volcanic activity with an accuracy that can be hardly attained by other tools, and this has important implications for a proper definition of recent volcanic activity and correct volcanic hazard assessment.

Acknowledgments

F. Mariani, D. D'Elia, and A. Pintòn helped for sampling. We thank J. Madeira for interesting discussion on Costado da Nau stratigraphy, as well as C. Onheiser for the English support. A.D.C. and F.S. were funded by INGV and FIRB MIUR C2 funds (responsible L. Sagnotti), while M.P., A.P. and J.P. were financially supported by CVARG.

PART VI – CONCLUSIONS

16. Main results

The first part of the thesis has dealt with the reconstruction of the pre – 50 ka geologic history (Green Tuff emplacement and Caldera Cinque Denti formation) at Pantelleria island (Strait of Sicily, Italy). Five ignimbrites emplaced during that period, dated by Mahood and Hildreth (1986) with K/Ar method. I addressed the study to refine correlations between units, unravel the volcanic history of the island, and constrain the age of the caldera-forming event using paleomagnetism. In fact, K/Ar age error bars amount to millennia and partially overlap, the outcrops were mostly confined in isolated sea-cliffs, and pyroclastic density currents (ignimbrites) are typically difficult to correlate, owing to the high variability in volumes and diagnostic features. I compared paleomagnetic directions obtained from studied ignimbrites, and considered the vicinity of paleomagnetic direction (within 10° of each other) as correlative proof. Results from the paleomagnetic study allowed a considerable refinement of the pre - 50 ka geologic history of Pantelleria depicted by Mahood and Hildreth (1986). Directions from two ignimbrites (Z and D) coincides, confirming a conclusion by La Felice et al. (2009) and Rotolo et al. (2013) based on new Ar/Ar ages; thus we document that a voluminous D/Z ignimbrite was erupted at Pantelleria at 87 ka. Welded-lithic breccia (Cala delle Capre section, south-west coast of Pantelleria), considered as the best candidate for deposits of La Vecchia caldera-forming eruption, well correlate with another lithic breccia (Cala Cinque Denti) exposed at the opposite coast of the island, helping to tightly constrain the formation of the Caldera La Vecchia collapse between ~130–160 ka. Rotolo et al. (in press) have recently confirmed and better constrain the age of the caldera collapse to 140-146 ka using Ar/Ar dating. Implications of our study are important to reassess the volcanic history of this quiescent volcano.

A second part of the thesis has been carried out in the Azores archipelago (Portugal), located in the central-northern Atlantic Ocean. I first focused the research on the São Miguel volcanic island, where previously available geological map and radiocarbon dating (Moore 1990, 1991; and Moore and Rubin 1991) allowed us to paleomagnetically sample 35 sites from eleven well-dated lava flows of the last 3,000 years. Paleomagnetic directions agree with results from six sites previously obtained by Johnson et al. (1998). The new data are consistent with directional values predicted by global field models (Cals3k.4 by Korte and Constable 2011, and gufm1 by Jackson et al. 2000), especially with respect to the declinations. Conversely, inclinations are lower than predicted values, emphasizing a minimum between 800 and 1,400 AD (with values lower by ~ 10° than models). The analysis of the paleomagnetic directions yielded the first paleosecular variation curve (PSV) for the Atlantic Ocean for the last 3,000 years. The new curve shows three tracks in virtual overlap during the 1000–800 BC, 800–500 BC, and 400–700 AD time spans.

In the third study, I carried out experiments to reveal the paleointensity of the geomagnetic field on the same eleven flows collected and studied from São Miguel, applying a new variation of the classical Thellier and Thellier

method. Values of the geomagnetic field intensity range from 39 and 69 μT, with a decreasing trend during the last 2,000 years. The new paleointensity data agree with values predicted by global field models (Cals3k.4 and Cals10k.1b by Korte et al. 2011), and with data relocated from Morocco, Portugal, Spain, and France. A remarkable paleointensity peak is documented around 600 BC with values of 95 μT. High field values for the same period were obtained from the Western USA (Champion, 1980; Hagstrum and Champion, 2002) and the Middle East by Shaar et al. (2009), suggesting the possibility of a global spike. The new data set represents the first paleointensity record for the Atlantic Ocean. New paleomagnetic directions and intensity data from the Azores will contribute to update the existing global dataset, and will help to constrain future global models with real data.

The forth study focused to unravel the Holocene volcanic history of the Capelo Peninsula, the western part of the Faial Island (Azores Archipelago). I used the paleomagnetic method to correlate scoria cones and lava flows. I recognized seven different paleomagnetic clusters (interpreted as volcanic phases) of the pre-historical volcanic activity, whereas fifteen lavas were correlated with eight scoria cones. Subsequently, I dated the volcanic events, by comparing paleomagnetic directions with relocated Holocene reference curves of the paleo-secular variation of the geomagnetic field from France and United Kingdom. By combining paleomagnetic results and stratigraphic evidence, I inferred that the volcanics exposed at the Capelo Peninsula are younger than previously believed. The Peninsula probably formed during the last 4,000 years, with a migration of the volcanic activity from 2,000 to 1,000 BC and then persisted on the western tip of the Peninsula until present (Capelinhos eruption, 1957-58 AD), with the exception of the other historical eruption of Fogo, which occurred in the central area of the Peninsula in 1672-3 AD. Geochronological data will serve to verify these conclusions in the future. The implications of this study are important for a better assessment of the volcanic hazard estimates of this volcanically (and seismically) active island of the Azores.

Summing up, the main contribution of this thesis was to provide new paleomagnetic data (both directions and intensity) for the Atlantic Ocean, where reference data are lacking, thus allowing better constraining the magnetic field behavior of the Holocene (last 10,000 years) with global models. Moreover, this thesis contributed to reconstruct the volcanic history of both Faial and Pantelleria, by dating and correlating volcanic products. These data will be surely important for further studies of future eruptive scenarios, thus to assess local volcanic hazard.

16.1 Concluding remarks and outlooks

This thesis aims at promoting a wider diffusion of the use of PSV analysis for providing original evidence to solve volcanological problems, by correlating and dating volcanic rocks. Indeed, owing to the complexity of volcanic rock geometries, unequivocal diagnostic characteristics and the lack of chronological data, the reconstruction of the eruptive history of a volcano can be problematic.

The paleomagnetic correlation relies on the comparison of paleomagnetic directions from volcanics, as units sharing similar paleomagnetic directions are expected to be correlative. To evaluate similarity using statistical methods, normally the McFadden test (McFadden and Lowes, 1981) is used to establish whether two sites share the same paleomagnetic directions, thus can be considered as correlative. One of the main results of this thesis is that the McFadden and Lowes (1981) test is unsuitable to address correlations of volcanic rocks, probably because the α_{95} values are very low (normally 2°-5°), compared to sites sampled in sediments (α_{95} normally >10°). I applied the paleomagnetic correlation method to ignimbrites, lava flows, and also for correlating volcanic cones with lava flows emplaced during the same eruption.

Paleomagnetic dating is achieved by comparing paleomagnetic directions from the studied volcanics and reference values from PSV curves. The fact that the paleomagnetic dating method requires the availability of regional PSV reference curves is related to the other goal pursued by this thesis: provide new directional and intensity reference data from historically-radiometrically dated volcanics of the Azores. It must be acknowledged that large areas of the Earth and long time intervals of the geomagnetic field still lack paleomagnetic data, leading to an under-determination of the geomagnetic field behavior.

I used paleomagnetism at Pantelleria to correlate ignimbrites, and at Capelo Peninsula to correlate and date volcanic units. Although the method can represent an invaluable contribution for both correlating deposits and yielding absolute ages, it is not a stand-alone method, as paleomagnetic directions can be re-occupied over time; therefore it is recommendable to combine paleomagnetic results with other independent data (e.g., geological mapping, stratigraphic studies, and radiometric age determinations).

The results achieved in this thesis are promising, and hopefully will encourage further studies applying the paleomagnetic method for correlating and dating volcanics, with the final aim of unraveling the geological history of active and quiescent volcanoes. Furthermore, besides the volcanological contribution, the new data will increasingly improve the knowledge of the geomagnetic field during the geological past.

REFERENCES

Abokodair, A. A. (1977). The Accuracy of the Thelliers' Technique for the Determination of Paleointensities of the Earth's Magnetic Field. PhD Thesis, University of California, Santa Cruz.

Aitken, M. J., A. L. Ailsop, G. D. Bussell, and M. B. Winter (1989). Geomagnetic intensity variation during the last 4000 years. Physics of the Earth and Planetary Interiors, 56, 49-58.

Aitken, M. J., A. L. Allsop, G. D. Bussell, and M. B. Winter (1988), Determination of the intensity of the Earth's magnetic field during archeological times: Reliability of the Thellier technique, Rev. Geophys., 26, 3–12.

Arrighi, S., J.-C. Tanguy, V. Courtillot, and M. Le Goff (2005). Reply to comment by F. Speranza et al. on ''Recent eruptive history of Stromboli (Aeolian Islands, Italy) determined from high-accuracy archeomagnetic dating'', Geophys. Res. Lett., 32(23), L23305, doi:10.1029/ 2005GL023768.

Arrighi, S., M. Rosi, J.-C. Tanguy, and V. Courtillot (2004). Recent eruptive history of Stromboli (Aeolian Islands, Italy) determined from high accuracy archeomagnetic dating, Geophys. Res. Lett., 31, L19603, doi:10.1029/2004GL020627.

Baag, C., C. E. Helsley, S. Xu, and B. R. Lienert (1995). Deflection of paleomagnetic directions due to magnetization of the underlying terrain. J. Geophys. Res., 100(B6), 10,013–10,027.

Baloga, S. M., L. S. Glaze, J. A. Crisp, and S. A. Stockman (1998). New statistics for estimating the bulk rheology of active lava flows: Puu Oo examples. J. Geophys. Res., 103(B3), 5133–5142, doi:10.1029/97JB03743.

Barberi, F., F. Innocenti, L. Lirer, R. Munno, T. Pescatore, and R. Santacroce (1978). The campanian ignimbrite: a major prehistoric eruption in the Neapolitan area (Italy). Bulletin Volcanologique, 41(1), 10-31.

Barberi, F., M.L. Carapezza, M. Valenza, and L. Villari (1993). The control of lava flow during the 1991–1992 eruption of Mt. Etna. J. Volcanol. Geotherm. Res, 56, 1–34.

Barbetti M. (1977). Measurements of recent geomagnetic secular variation in southeastern Australia and the question of dipole wobble. Earth Planet. Sci. Lett., 36, 207-218

Beamud, E., M. Gómez-Paccard, G. McIntosh, and J. C. Larrasoaña (2012). New archaeomagnetic data from three roman kilns in northeast Spain: a contribution to the Iberian palaeosecular variation curve. Geophysical Research Abstracts, 14, EGU2012-8232.

Ben-Yosef, E., H. Ron, L. Tauxe, A. Agnon, A. Genevey, T. E. Levy, U. Avner, and M. Najjar (2008b). Application of copper slag in archeointensity research. J. Geophys. Res., 113. doi:10.1029/2007JB005235.

Ben-Yosef, E., L. Tauxe, H. Ron, A. Agnon, A. Avner, M. Najjar, and T. E. Levy (2008a). A new approach for geomagnetic archaeointensity research: insights on ancient metallurgy in the Southern Levant. J. Archaeol. Sci., 35, 2863–2879.

Ben-Yosef, E., L. Tauxe, T. E. Levy, R. Shaar., R. Ron, and M. Najjar (2009). Geomagnetic intensity spike recorded in high resolution slag deposit in Southern Jordan. Earth and Planetary Science Letters, 287, 529–539. doi:10.1016/j.epsl.2009.09.001

Biggin, A. J., and D. N Thomas (2003). Analysis of long-term variations in the geomagnetic poloidal field intensity and evaluation of their relationship with global geodynamics. Geophysical Journal International, 152(2), 392–415.

Biggin, A. J. (2006). First-order symmetry of weak-field partial thermoremanence in multi-domain (MD) ferromagnetic grains. 2. Implications for Thellier-type palaeointensity determination. Earth Planet. Sci. Lett. 245, 454–470.

Biggin, A. J. (2010). Are systematic differences between thermal and microwave Thellier-type palaeointensity estimates a consequence of multidomain bias in the thermal results? Phys. Earth Planet. Inter. 180, 16–40.

Biggin, A.J., and T. Poidras (2006). First-order symmetry of weak-field partial thermoremanence in multi-domain ferromagnetic grains. 1. Experimental evidence and physical implications. Earth Planet. Sci. Lett. 245, 438–453.

Blake, S. (1981). Eruptions from zoned magma chambers. Journal of the Geological Society of London, 138(3), 281-287, doi: 10.1144/gsjgs.138.3.0281.

Blake, S., 1981, Eruptions from zoned magma chambers: Journal of the Geological Society of London, v. 138, no. 3 p. 281-287, doi: 10.1144/gsjgs.138.3.0281

Bleil, U., and M. Dillon (2008). Holocene Earth's magnetic field variations recorded in marine sediments of the NW African continental margin. Stud. Geophys. Geod. , 52(2), 133–155, doi:10.1007/s11200-008-0010-6.

Blong, R.J. (1984). Volcanic hazards. A sourcebook on the effects of eruptions. Academic Press (Sydney and Orlando, Fla.)

Bogue, R.W., and R. S. Coe (1981). Paleomagnetic correlation of Columbia River Basalt using Secular Variation. Journal of Geophysical Research, 86(B12), 883-897.

Booth, B., R. Croasdale, and G.P.L. Walker (1978). A quantitative study of five thousand years of volcanism on São Miguel, Azores. Philos. Trans. R. Soc. London, A, 288, 271–319, doi:10.1098/rsta.1978.0018.

Borges, J.F., M. Bezzeghoud, E. Buforn, C. Pro, and A. Fitas (2007). The 1980, 1997 and 1998 Azores earthquakes and some seismo-tectonic implications: Tectonophysics, 435, 37-54.

Bowles, J., J. S. Gee., D. Kent., E. Bergmanis, and J. Sinton (2005). Cooling rate effects on paleointensity estimates in submarine basaltic glass and implications for dating young flows. Geochem., Geophys., Geosyst., 6, doi:10.1029/2004GC000900.

Brandt, U., N. R. Nowaczyk, A. Ramrath, A. Brauer, J. Mingram, S. Wulf, and J. F. W. Negendank (1999). Palaeom agnetism of Holocene and Late Pleistocene sediments from Lago di Mezzano and Lago Grande di Monticchio (Italy): initial results. Quat. Sci. Rev., 18, 961-976.

Brandt, U., Nowaczyk, N. R., Ramrath, A., Brauer, A., Mingram, J, Wulf, J, and Negendank, J. F. W. (1999). Palaeomagnetism of Holocene and Late Pleistocene sediments from Lago di Mezzano and Lago Grande di Monticchio (Italy): initial results. Quat. Sci. Rev., 18, 961-976.

Branney, M. J., and P. Kokelaar (2002). Pyroclastic density currents and the sedimentation of ignimbrites. Geological Society Memoir, London, 27.

Breed, W. J. (1964). Morphology and lineation of cinder cones in the San Francisco volcanic field, Flagstaff, Arizona: Mus. North. Ariz. Bull., 40, 65–71.

Bucur, I. (1994). The direction of the terrestrial magnetic filed in France during the last 21 centuries. Recent progress. Phyics of the Earth and Planetary Interior, 168, 95-109.

Butler, R. F. (2004). Paleomagnetism: Magnetic Domains to Geological Terranes

Calvo, M., M. Prèvot, M. Perrin, and J. Riisager (2002). Investigating the reasons for the failure of palaeointensity experiments: a study on historical lava flows from Mt. Etna (Italy). Geophys. J. Int., 149, 44–63

Camacho, A. G., J. C. Nunes, E. Ortiz, Z. França, and R. Vieira (2007). Gravimetric determination of an intrusive complex under the Island of Faial (Azores): some methodological improvements. Geophysical Journal International, 171, 478–494, doi: 10.1111/j.1365-246X.2007.03539.x.

Camus, G., P. Boivin, A. De Goër De Herve, A. Gourgaud, G. Kieffer, J. Mergoil, and P.M. Vincent (1981). Le Capelinhos (Faial, Açores) vingt ans apres son éruption: le modele éruptif 'surtseyan' et les anneaux de tufs hyaloclastiques. Bulletin Volcanologique, 44, 31–42.

Carlut, J., and D.V. Kent (2000). Paleointensity record in zero-age submarine basalt glasses: testing a new dating technique for recent MORBs. Earth and Planetary Science Letters, 183, 389-401.

Carlut, J., X. Quidelleur, V. Courtillot, and G. Boudon (2000). Paleomagnetic directions and K/Ar dating of 0 to 1 Ma lava flows from La Guadeloupe Island (French West Indies): Implications for time-averaged field models. Journal of Geophysical Research, 105, 835-849.

Carlut, J., M. H. Cormier, D. V. Kent., K. E. Donnelly, and C. H. Langmuir (2004). Timing of volcanism along the northern East Pacific Rise based on paleointensity experiments on basaltic glasses. J. Geophys. Res., 109, B04104.

Carracedo, J. C., C. Principe, M. Rosi, and V. Soler (1993). Time correlation by palaeomagnetism of the 1631 eruption of Mount Vesuvius. Volcanological and volcanic hazard implications. Journal of Volcanology and Geothermal Research, 58, 203-209.

Carracedo, J. C., E. Rodriguez Badiola, and V. Soler (1992). The 1730-1736 eruption of Lanzarote, Canary Islands: a long, high magnitude basaltic fissure eruption. Journal of Volcanology and Geothermal Research, 53, 539-250.

Casas, L., and A. Incoronato (2007). Distribution analysis of errors due to relocation of geomagnetic data using the 'Conversion via Pole' (CVP) method: implication on archaeomagnetic data. Geophys. J. Int., 169, 448-454.

Castello-Branco, A., G. Zbyzewski, F. Moitinho de Almeida, and O. Veriga Ferreira (1959). Rapport de la première mission geologique sur la volcanisme de l' île de Faial: Servicio Geologico de Portugal, Mem. 4, Nile Sèrie, 9-27.

Catanzariti, G., M. Gòmez-Paccard, G. McIntosh, F.J. Pavòn-Carrasco, A. Chauvin, and M.L. Osete (2012). New archaeomagnetic data recovered from the study of Roman and Visigothic remains from central Spain (3rd–7th centuries). Geophysical Journal International, doi: 10.1111/j.1365-246X.2011.05315.x.

Channell, J. E. T., D. A Hodell, and B. Lehman (1997). Relative geomagnetic paleointensity and d 18O at ODP Site 983_Gardar Drift, North Atlantic/since 350 ka. Earth and Planetary Science Letters, 153, 103-118.

Chauvin, A., P. Roperch, and S. Levi (2005). Reliability of geomagnetic paleointensity data: the effects of the NRM fraction and concave up behaviour on paleointensity determination by Thellier method, Phys. Earth planet. Inter., 150, 265–286

Chauvin, A., Y. Garcia, Ph. Lanos, and F. Laubenheimer (2000). Paleointensity of the geomagnetic field recovered on archaeomagnetic sites from France. Physics of the Earth and Planetary Interiors, 120, 111–136.

Chenet, A. L., F. Fluteau, V. Courtillot, M. Gèrard, and K. V. Subbarao (2008). Determination of rapid Deccan eruptions across the Cretaceous-Tertiary boundary using paleomagnetic secular variation: Results from a 1200-m-thick section in the Mahabaleshwar escarpment. J. Geophys. Res., 113, B04101, doi:10.1029/2006JB004635.

Chenet, A. L., V. Courtillot, F. Fluteau, M. Gérard, X. Quidelleur, S. F. R. Khadri, K. V. Subbarao, and T. Thordarson (2009). Determination of rapid Deccan eruptions across the Cretaceous-Tertiary boundary using

paleomagnetic secular variation: 2. constraints from analysis of eight new sections and synthesis for a 3500-m-thick composite section. J. Geophys. Res., 114, B06103, doi:10.1029/2008JB005644.

Chevallier, R. (1925). L'aimantation des laves de l'Etna et l'orientation du champ terrestre en Sicile du XIIeme au XVIIeme siècle. thèse, 163 pp., Univ. of Paris, Paris.

Chovelon, P. (1982). Évolution volcanotectonique des iles de Faial et de Pico, Archipel des Açores - Atlantique Nord. PhD thesis, Univ. de Paris-Sud, Paris, France.

Christensen, U. R., and J. Wicht (2007). Numerical dynamo simulations. G. Schubert (Ed.), Treatise of Geophysics, 8, Elsevier, Amsterdam, 245–282.

Coe, R. S. (1967). The determination of paleo-intensities of the Earth's magnetic field with emphasis on mechanisms which could cause non-ideal behavior in Thellier's method. J. Geomagn. Geoelectric., 19, 157-179.

Coe, R.S., J. Riisager, G. Plenier, R. Leonhardt, and D. Kràs (2004). Multidomain behavior during Thellier paleointensity experiments: results from the 1915 Mt. Lassen flow. Physics of the Earth and Planetary Interiors, 147, 141–153.

Coe, R.S., S. Grommè, and E.A. Mankinen (1978). Geomagnetic paleointensities from radiocarbon-dated lava flows on Hawaii and the question of the Pacific nondipole low. J. Geophys. Res., 83, 1740–1756.

Cole, P.D., A.M. Duncan, and J.E. Guest (1996). Capelinhos: The disappearing volcano: Geology Today, 12, 68–72, doi:10.1046/j.1365-2451.1996.00010.x.

Cole, P.D., J. E. Guest, A. M. Duncan, and J. M. Pacheco (2001). Capelinhos 1957–1958, Faial, Azores: Deposits formed by an emergent surtseyan eruption: Bulletin of Volcanology, 63, 204–220, doi:10.1007/s004450100136.

Corazzato, C., and A. Tibaldi (2006). Fracture control on type, morphology and distribution of parasitic volcanic cones: An example from Mt. Etna, Italy. Journal of Volcanology and Geothermal Research, 158, 177–194, doi:10.1016/j.jvolgeores.2006.04.018.

Corazzato, C., and A. Tibaldi (2006). Fracture control on type, morphology and distribution of parasitic volcanic cones: An example from Mt. Etna, Italy. Journal of Volcanology and Geothermal Research, 158, 177–194, doi:10.1016/j.jvolgeores.2006.04.018.

Cottrell, R.D., and J. A. Tarduno (2000). In search of high-fidelity geomagnetic paleointensities: a comparison of single plagioclase crystal and whole rock Thellier–Thellier analyses. J. Geophys. Res. 105, 23579–23594

Coutinho, R., D.K. Chester, N. Wallenstein, and A. M. Duncan (2010). Responses to, and the short and long-term impacts of, the 1957/1958 Capelinhos volcanic eruption and associated earthquake activity on Faial, Azores. Journal of Volcanology and Geothermal Research, 196, 265–280.

Crandell, D. R., B. Booth., K. Kusumadinata, D. Shimozuru, G. P. L. Walker, and D. Westercamp (1984). Source Book for Volcanic-Hazard Zonation. UNESCO, Paris, 97.

Crandell, D. R., and D. R. Mullineaux (1975). Technique and rational of volcanic hazards appraisals in the Cascades Range, north-western United States. Environ. Geol., 1, 23–32.

Crisp, J and S. Baloga (1990). A model for lava flows with two thermal components. Journal of Geophysical Research, 95(B2), 1255–1270, doi:10.1029/JB095iB02p01255.

Cromwell, G., L. Tauxe., H. Staudigel, H. Ron, and F.Trusdell (2011). Paleointensity results for 0 and 3 ka from Hawaiian lava flows: a new approach to sampling. American Geophysical Union, Fall Meeting 2011, abstract#GP13A-08.

David, P. (1910). Sur la stabilité de la direction d'aimantation dans quelques roches volcaniques. C. R. Acad. Sci., Paris, 138, 41–42.

Dekkers M.J., and H. N. Boehnel (2006). Reliable absolute palaeointensities independent of magnetic domain state. Earth Planet. Sci. Lett., 248, 508-517.

Demant, A., P. Lestrade, R. T. Lubala, A. B. Kampunzu, and J. Durieux (1994). Volcanological and petrological evolution of Nyiragongo volcano, Virunga volcanic field, Zaire. Bulletin of Volcanology, 56(1), 47-61.

Di Chiara, A., F. Speranza, and M. Porreca (2012), Paleomagnetic secular variation at the Azores during the last 3 ka, J. Geophys. Res., 117, B07101, doi:10.1029/2012JB009285.

Doell, R. R., and A. Cox (1963). The accuracy of the paleomagnetic method as evaluated from historic Hawaiian lava flows. J. Geophys. Res., 68, 1997– 2009.

Doel, R.R., and A. Cox (1965). Paleomagnetism of Hawaiian lava flows: Journal of Geophysical Research, 70, 14, 3377-3405.

Donadini, F., K. Korhonen, P. Riisager, L. J. Pesonen (2006). Database for Holocene geomagnetic intensity information. EOS Trans. Am. Geophys. Union 87 (14), 137.

Donadini, F., M. Kovacheva., M. Kostadinova, Ll. Casas, and L. Pesonen (2007). New archaeointensity results from Scandinavia and Bulgaria. Rock magnetic studies inference and geophysical application. Phys. Earth Planet. Inter., 165, 229-247.

Donadini, F., M. Korte, and C. G. Constable (2009). Geomagnetic field for 0–3 ka: 1. New data sets for global modeling. Geochem. Geophys. Geosyst., 10, Q06007, doi:10.1029/2008GC002295.

Dóniz, J., C. Romero, E. Coello, C. Guillén, N. Sánchez, C. García-Cacho, and C. García (2008). Morphological and statistical characterisation of recent mafic volcanism on Tenerife (Canary Islands, Spain). Journal of Volcanology and Geothermal Research, 173, 185–195.

Druit, T. H. (1998). Pyroclastic density currents. Geological Society, London, Special Publications,145:145-182, doi:10.1144/GSL.SP.1996.145.01.08.

Dunlop, D. J., and Ö. Özdemir (2000). Effect of grain size and domain state on thermal demagnetization tails. Geophys. Res. Lett. 27, 1311–1314.

Dunlop, D. J., and Ö. Özdemir (1997/2001). Rock Magnetism, Fundamentals and Frontiers. Cambridge University Press, New York, p. 573 (paperback ed.).

Ellwood, B. B., N.D. Watkins, C. Amerigian, and S Self (1973). Brunhes Epoch Geomagnetic Secular Variation on Terceira Island, Central North Atlantic. Journal of Geophyisical Research, 78(35), 8699-8710.

Fabian, K. (2001). A theoretical treatment of paleointensity determination experiments on rocks containing pseudo-single or multi domain magnetic particles. Earth and Planetary Science Letters, 188, 45-58.

Favalli, M., E. Boschi, F. Mazzarini, and M. T. Pareschi (2009). Seismic and landslide source of the 1908 Straits of Messina tsunami (Sicily, Italy). Geophysical Research Letters, 36, L16304, doi:10.1029/2009GL039135.

Fedotov, S. A., G. A. Sobolev, S. A. Boldyrev, A. A. Gusev, A. M. Kondratenko, O. V. Potapova, L. B. Slavina, V. D. Theophylaktov, A. A. Khramov, V. A. Shirokov (1977). Long- and short-term earthquake prediction in Kamchatka. Tectonophysics, 37(4), 305–321.

Feraud, G. (1977). Contribution à la datation du volcanisme de l'archipel des Açores par la mèthode Potassium-Argon. Consèquences gèodynamiques: Thesis, Paris.

Feraud, G., I. Kaneoka, and C. J. Allègre (1980). K/Ar ages and stress pattern in the Azores: Geodynamic implications. Earth Planet. Sci. Lett., 46, 275–286, doi:10.1016/0012-821X(80)90013-8.

Ferk, A., R. Leonardht, D. Richard, F. Aulock, K. Hess, and D. Dingwell (2008). Paleointensity study on subaerial volcanic glass. Geophysical Research Abstracts, 10, EGU2008-A-06936.

Fernandes, R. M. S., L. Bastos, J. M. Miranda, N. Laurenço, B. A. C. Ambrosius, R. Noomen, and W. Simons (2006). Defining the plate boundaries in the Azores region. Journal of Vulcanology and Geothermal Research, 156(1-2), 1-9.

Ferreira, T. (2000). Caracterização da actividade vulcânica da ilha de S. Miguel (Açores): Vulcanismo basáltico recente e zonas de desgaseificação. Avaliação de riscos, PhD thesis, 248 pp., Dep. de Geoci., Univ. dos Açores, Ponta Delgada, Portugal.

Feuillard, M., C. J Allegre, G. Brandeis; R. Gaulon, J. L. Le Mouel, J. C. Mercier, J. P. Pozzi, and M.P. Semet (1983). The 1975-1977 crisis of La soufrièr de Guadalupe (F.W.I.): a still-born magmatic eruption. Journal of Volcanoloy and Geothermal Research, 16, 317-334.

Fink, H., and J. R. Zimbelman (1986). Rheology of the 1983 Royal Gardens basalt flows, Kilauea Volcano, Hawaii. Bulletin of Volcanology, 48(2-3), 87-96.

Finlay, C. C.; S. Maus, C. D. Beggan, T. N. Bondar, A. Chambodut, T. A. Chernova, A. Chulliat, V. P. Golovkov, B. Hamilton, M. Hamoudi, R. Holme, G. Hulot, W. Kuang, B. Langlais, V. Lesur, F. J. Lowes, H. Lühr, S. Macmillan, M. Mandea, S. McLean, C. Manoj, M. Menvielle, I. Michaelis, N. Olsen, J. Rauberg, M. Rother, T. J. Sabaka, A. Tangborn, L. Tøffner-Clausen, E. Thébault, A. W. P. Thomson, I. Wardinski, Z. Wei, and T. I. Zvereva (2010). International Geomagnetic Reference Field: the eleventh generation. Geophys. J. Int., 183 (3), 1216-1230.

Finn, D.R., R. S. Coe, F. Spinardi, M. K. Reichow, T. Knott, L. McDonnell, D. Cunningham, and M. Branney (2011). Paleomagnetic correlation of ignimbrites along the southern margin of the central Snake River Plain, Yellowstone hotspot. American Geophysical Union, Fall Meeting 2011, abstract #T51H-2472.

Fisher, R. A. (1953). Dispersion on a sphere: Proceeding of the Royal Society of London Accademy, A., 217, 1130, 295–305, doi: 10.1098/rspa.1953.0064.

Forjaz, V. H. (1965). Observações realizadas no vulcão dos Capelinhos (Açoers) em Agosto e Setembro de 1963: Boletim di Museu e Laboratòrio Mineralògico de Facultate de Cìências, 10, 89-94.

Fornaciai, A., M. Favalli, D. Karátson, S. Tarquini, and E. Boschi (2012). Morphometry of scoria cones, and their relation to geodynamic setting: A DEM-based analysis. Journal of Volcanology and Geothermal Research, 217-218, 56–72.

Fournier d'Albe, E. M. (1979). Objectives of Volcanic Monitoring and Prediction. Journ. Geol. Soc. Lond., 136, 321-326.

Fox, J. M. W., and J. Aitken (1980). Cooling-rate dependence of thermoremanent magnetization. Nature, 283, 462 – 463, doi:10.1038/283462a0.

Fries, Jr. (1953). Volumes and weights of pyroclastic material, lava and water erupted by Paricutin volcano Michoacan, Mexico. Trans. Am. Geophys. Union, 34, 603–616.

Gallet, Y., and M. Le Goff (2006). High-temperature archeointensity measurements from Mesopotamia. Earth Planet. Sci. Lett., 241, 159–173.

Gallet, Y., A. Genevey, and M. Le Goff (2002). Three millennia of directional variation of the Earth's magnetic field in western Europe as revealed by archaeological artefacts. Physic of Earth and Planetary Interior, 131, 81– 89.

Gallet, Y., A. Genevey, M. Le Goff, F. Fluteau, and S.A. Eshraghi (2006). Possible impact of the Earth's magnetic field on the history of ancient civilizations. Earth Planet. Sci. Lett., 246, 17– 26.

Gee, J. S., S. C. Cande, J. A. Hildebrand, K. Donnelly, and R. L. Parker (2000). Geomagnetic intensity variations over the past 780 kyr obtained from near-seafloor magnetic anomalies. Nature, 408, 827–832.

Genevey, A., and Y. Gallet (2002). Intensity of the geomagnetic field inwestern Europe over the past 2000 years: new data from ancient French potteries. J. geophys. Res., 107, doi:10.1029/2001JB000701.

Genevey, A., Y. Gallet, J. Rosen, and M. Le Goff (2009). Evidence for rapid geomagnetic field intensity variations in Western Europe over the past 800 years from new French archaeointensity data. Earth and Plan. Sci. Lett 284, 132–143.

Glatzmaier, G. A., and P. H. Roberts (1996). An anelastic evolutionary geodynamo simulation driven by compositional and thermal convection. Physica D: Nonlinear Phenomena, 97 (1–3), 81–94.

Gómez-Paccard, M., A. Chauvin, P. Lanos, and J. Thiriot (2008). New archeointensity data from Spain and the geomagnetic dipole moment in western Europe over the past 2000 years, J. Geophys. Res., 113, B09103, doi:10.1029/2008JB005582.

Gómez-Paccard, M., A. Chauvin, P. Lanos, G. McIntosh, M. L. Osete, G. Catanzariti, V. C. Ruiz-Martínez, and J. I. Núñez (2006). First archaeomagnetic secular variation curve for the Iberian Peninsula: Comparison with other data from western Europe and with global geomagnetic field models. Geochem. Geophys. Geosyst., 7, Q12001, doi:10.1029/2006GC001476.

Gómez-Paccard, M., G. McIntosh, A. Chauvin, E. Beamud, F.J. Pavòn-Carrasco, and J. Thiriot (2012). Archaeomagnetic and rock magnetic study of six kilns from North Africa (Tunisia and Morocco). Geophys. J. Int., 189, 169–186. doi: 10.1111/j.1365-246X.2011.05335.x.

Granot, R., L. Tauxe, J.S., Gee, and H. Ron (2006). A view into the Cretaceous geomagnetic field from analysis of gabbros and submarine glasses. Earth and Planetary Science Letters, 256(1-2), 1-11.

Griffiths, R. W., and J. H. Fink (1992). Solidification and Morphology of Submarine Lavas' A Dependence on Extrusion Rate. Journal of Geophysical Research, 97(B13), 19,729-19,737.

Grommè, C. S, E. H. McKEE, M. C. and Blake (1972). Paleomagnetic Correlations and Potassium-Argon Dating of Middle Tertiary Ash-Flow Sheets in the Eastern Great Basin, Nevada and Utah. GSA Bulletin, 83, 6, 1619-1638, doi: 10.1130/0016-7606

Hagstrum, J. T., and D. E. Champion (1994). Paleomagnetic correlation of Late Quaternary lava flows in the lowest east rift zone of Kilauea Volcano, Hawaii. Journal of Geophysical Research, 99 (B11), 21679-21690.

Hartmann, G.A., R.I.F. Trindade, A. Goguitchaichvili, C. Etchevarne, J. Morales, and M. C. Afonso (2009). First archeointensity results from Portuguese potteries (1550–1750 AD). Earth Planets Space, 61, 93–100

Hasenaka, T., and I. S. E. Carmichael (1985). The cinder cones of Michoacán—Guanajuato, central Mexico: their age, volume and distribution, and magma discharge rate. Journal of Volcanology and Geothermal Research, 25(1–2), 105–124.

Hayashida, A., H. Kamatat, and T. Danhara (1996). Correlation of widespread tephra deposits based on paleomagnetic directions: link between a volcanic field and sedimentary sequence in Japan. Quaternary International, 34-36, 89-98.

Herrero-Bervera E. and J. P. Valet (2009). Testing determinations of absolute paleointensity from the 1955 and 1960 Hawaiian flows. Earth and Planetary Science Letters, 287, 420–433.

Hewitt, K. (1997). Regions of Risk: A Geographical Introduction to Disasters, Longman, Harlow, Essex.

Hildenbrand, A., F. O. Marques, A. C. G. Costa, A. L. R. Sibrant, P. F. Silva, B. Henry, J. M. Miranda, and P. Madureira (2012). Reconstructing the architectural evolution of volcanic islands from combined K/Ar, morphologic, tectonic, and magnetic data: The Faial Island example (Azores). Journal of Volcanology and Geothermal Research, 241–242, 39–48, doi:10.1016/j.jvolgeores.2012.06.019.

Hill, M. J., and J. Shaw (2000). Magnetic field intensity study of the 1960 Kilauea lava flow, Hawaii, using the microwave palaeointensity technique. Geophys. J. Int., 142, 487–504.

Hoffman, K. A., V. L. Constantine, and D. L. Morse (1989). Determination of absolute paleointensity using a multi-specimen procedure. Nature, 339, 295–297.

Hooper, D. M. (1995). Computer-simulation models of scoria cone degradation in the Colima and Michoacàn-Guanajuato volcanic fields, Mexico. Geofìsica Internacional, 34, 321–340.

Hoye, G. S. (1981). Archeomagnetic secular variation record of Mount Vesuvius. Nature 291, 216 - 218. doi:10.1038/291216a0.

Inbar, M., and C. Risso (2001). A morphological and morphometric analysis of a high density cinder cone volcanic field—Payun Matru, south-central Andes, Argentina. Zeitschrift fuer Geomorphologie, 45, 3, 321–343.

Inbar, M., M. Gilichinsky, I. Melekestsev, D. Melnikov, and N. Zaretskaya (2011). Morphometric and morphological development of Holocene cinder cones: A field and remote sensing study in the Tolbachik volcanic field, Kamchatka. Journal of Volcanology and Geothermal Research, 201, 301–311.

Incoronato, A., A. Angelino, R. Romano, A. Ferrante, R. Sauna, G. Vanacore, and C. Vecchione (2002), Retrieving geomagnetic secular variations from lava flows: Evidence from Mounts Arso, Etna and Vesuvius (southern Italy). Geophysical Journal International, 149, 724–730.

Irving, E. (1964). Paleomagnetism and its application to geological and geophysical problems.

Jackson, A., A. R. T. Jonkers, and M. R. Walker (2000). Four centuries of geomagnetic secular variation from historical records. Royal Society of London Philosophical Transactions, 358, 957-990.

Johnson, C. L., J. R. Wijbrans, C. G. Constable, J. Gee, H. Staudigel, L. Tauxe, V. H. Forjaz, and M. Salgueiro (1998). $^{40}Ar/^{39}Ar$ ages and paleomagnetism of São Miguel lavas, Azores. Earth and Planetary Science Letters, 160, 637–649.

Jones, D. L., and M. W. McElhinny (1966). Paleomagnetic correlation of basic intrusions in the Precambrian of southern Africa. Journal of Geophyical Research, 71(2), 543–552, doi:10.1029/JZ071i002p00543

Jurado-Chichay, Z., J. Urrutia-Fucugauchi, and S. K. Rowland (1996). A paleomagnetic study of the Pohue Bay flow and its associated coastal cones, Mauna Loa volcano, Hawaii: constraints on their origin and temporal relationships. Physics of the Earth and Planetary Interiors, 97(1-4), 269-277.

Kervyn, M., G. G. J. Ernst, J.-C. Carracedo, P. Jacobs (2012). Geomorphometric variability of "monogenetic" volcanic cones: Evidence from Mauna Kea, Lanzarote and experimental cones. Geomorphology, 136, 59–75. doi:10.1016/j.geomorph.2011.04.009.

Kirschvink, J. L. (1980). The least-squares line and plane and the analysis of palaeomagnetic data. Geophysical Journal of the Royal Astronomical Society, 62(3), 699-718.

Kissel, C., and C. Laj (2004). Improvements in procedure and paleointensity selection criteria (PICRIT-03) for Thellier and Thellier determinations: application to Hawaiian basaltic long cores. Physics of the Earth and Planetary Interiors, 147, 155–169.

Kletetschka, G., M. D. Fuller, T. Kohout, P. J. Wasilewski, E. Herrero-Bervera, N. F. Ness, M. H. Acuna (2006). TRM in low magnetic fields: a minimum field that can be recorded by large multi domain grains. Phys. Earth Planet. Inter., 154, 290–298.

Knudsen, N. F., B. H. Jacobsen, and N. Abrahamsen (2003). Palaeomagnetic distortion modelling and possible recovery by inversion. Physics of the Earth and Planetary Interiors, 135, 55–73.

Konigsberger, J. G. (1938). Natural Residual Magnetism of eruptive rocks. Terrestrial magnetism and atmospheric electricity, 43 (3), 299-320, doi:10.1029/TE043i003p00299.

Kono, M. (1978). Reliability of paleointensity methods using alternating field demagnetization and anhysteretic remanence. Geophys. J. Roy. Astron. Soc. 54, 241–261.

Korhonen, K., F. Donadini, P. Riisager, and L. Pesonen (2008). GEOMAGIA50: an archeointensity database with PHP and MySQL. Geochemistry, Geophysics, Geosystems, 9, doi:10.1029/2007GC001,893.

Korte, M., and C. Constable (2005). Continuous geomagnetic field models for the past 7 millennia: 2. CALS7K. Geochemistry, Geophysics, Geosystems, 6, Q02H16. doi:10.1029/2004GC000801.

Korte, M., and C. G. Constable (2011). Improving geomagnetic field reconstruction for 0–3 ka, Phys. Earth Planet. Inter., 188, 247–259, doi:10.1016/j.pepi.2011.06.017.

Korte, M., and R. Holme (2010). On the persistence of geomagnetic flux lobes in global Holocene field models. Phys. Earth Planet. Inter., 182(3–4), 179–186, doi:10.1016/j.pepi.2010.08.006.

Korte, M., C. G. Constable, F. Donadini, and R. Holme (2011). Reconstructing the Holocene geomagnetic field. Earth and Planetary Science Letters, 312(3–4), 497–505.

Krafft, M., and A. Gerente (1977). L'activité du Piton de la Fournaise entre octobre 1972 et mai 1973. (Ile de La Réunion, Océan Indien). C. R. Acad. Sci. Paris, 284, 607–610.

Krasa, D., C. Heunemann, R. Leonhardt, and N. Petersen (2003). Experimental procedure to detect multidomain remanence during Thellier–Thellier experiments. Physics and Chemistry of the Earth, 28, 681–687.

Lanos, P. (2004). Bayesian inference of calibration curves: application to archaeomagnetism. In: Buck, C., Millard, A. (Eds.), Tools for Constructing Chronologies: Crossing Disciplinary Boundaries. Springer-Verlag, London, 177, 43-82.

Lanza, R., and E. Zanella (2003). Paleomagnetic secular variation at Vulcano (Aeolian Islands) during the last 135 kyr. Earth and Planetary Science Letters, 213, 321-336, doi:10.1016/S0012-821X(03)00326-1.

Lanza, R., and E. Zanella (2006). Comments on "Chronology of Vesuvius' activity from A.D. 79 to 1631 based on archeomagnetism of lavas and historical sources" by C. Principe et al.. Bulletin of Volcanology, 68, 394–396.

Lanza, R., A. Meloni, and E. Tema (2005a). Historical measurements of the Earth's magnetic field compared with remanence directions from lava flows in Italy over the last four centuries. Physics of the Earth and Planetary Interiors, 148, 97–107.

Lanza, R., A. Meloni, and E. Tema (2005b). Reply to Comment on "Historical measurements of the Earth's magnetic field compared with remanence directions from lava flows in Italy over the last four centuries", by Tanguy, J.C., Principe C., Arrighi S. Physics of the Earth and Planetary Interiors, 152, 121–124.

Leonardht, R., D. Kràsa, and R.S. Coe (2004). Multidomain behavior during Thellier paleointensity experiments: a phenomenological model. Physics of the Earth and Planetary Interiors, 147, 127–140.

Levi, S. (1977). The effect of Magnetite particle size on paleointensity determinations of the geomagnetic field. Physics of the Earth and Planetary Interiors, 13, 245-259.

Lockwood, J. P, and R. W., Hazlett (2010). Volcanoes: Global Perspectives. Wiley-Blackwell Publications, 204-215.

Lund, S. P., and L. Kleigwin (1994). Measurement of the degree of smoothing in sediment paleomagnetic secular variation records: An example from late Quaternary deep-sea sediments of the Bermuda Rise, western North Atlantic Ocean, Earth Planet. Sci. Lett., 122, 317–330, doi:10.1016/0012-821X(94)90005-1.

Machado, F. (1955). The Fracture Pattern of Azoren Volcanoes. Bulletin of Volcanology, 17, 119-125.

Machado, F. (1958). Actividade vulcanica da Ilha do Faial (1957–58). Atlantida, 2, 225–236. Angra do Heroìsmo.

Machado, F. (1958b). Actividade Vulcânica de Ilha do Faial (1957–1958). Atlantida, 2, 305–315.

Machado, F. (1959a). Actividade Vulcânica de Ilha do Faial (1957–1958). Notícia preliminar relativa aos meses de Maio a Agosto de 1958. Atlantida, 3, 40–55.

Machado, F. (1959). A erupção do Faial em 1672. Serviços Geológicos de Portugal, Memória 4 (Nova Série), Lisboa.

Machado, F. (1960). A erupção dos Capelinhos (Açores) e a energia das regioes vulcanicas: Electricidade, v. 4, p. 344-346.

Machado, F. (1967). Active Volcanoes of the Azores: Catalogue of the Active Volcanoes of the World, 21, Atlantic Ocean. (M. Neumann Van Padang et al.,) Inter. Assoc. Volcan., 9-52.

Machado, F. (1982). Interpretation of ground deformation in the Azores: Arquipèlago, 3, 95-112.

Machado, F., and Forjaz, V. H. (1968). Actividade Vulcanica do Faial, 1957-67. Com. Reg. Turismo da Horta, 151.

Machado, F., and V. H. Forjaz (1978). Actividade vulcanica da Ilha do Faial: Com. Gen. Turismo da Horta. Imp. Porto., 79.

Machado, F., W. H. Parsons, A. F. Richards, J. W. and Mulford (1962). Capelinhos eruption of Fayal Volcano, Azores, 1957–1958. Journal of Geophysical Research, 67, 9, 3519–3529.

Madeira, J. (1998). Estudos de neotectónica nas ilhas do Faial, Pico e S. Jorge: Uma contribuição para o conhecimento geodinâmico da junção tripla dos Açores [PhD thesis]. Departamento De Geologia, Universidad de Lisboa, Lisboa.

Madeira, J., and A. Brum da Silveira (2003). Active tectonics and first paleosismological results in Faial, Pico e S. Jorge islands (Azores, Portugal). Annal of Geophysics, 46(5), 733–761.

Madeira, J. and A. Ribeiro (1990). Geodynamic models for the Azores triple junction: a contribution from tectonics. Tectonophysics, 184(3-4), 405-415.

Madeira, J., A.M.M. Soares, A., Brum da Silveira, and A. Serralheiro (1995). Radiocarbon dating recent volcanic activity on Faial Island (Azores). Radiocarbon, 37(2), 139–147.

Mannen, K., and T. Ito (2007). Formation of scoria cone during explosive eruption at Izu-Osshima volcano, Japan. Geophysical Research Letters, 34, L18302, doi:10.1029/2007GL030874.

Márton, E., T. Zelenka, and P. Márton (2007). Paleomagnetic correlation of Miocene pyroclastics of the Bükk Mts and their forelands. Central European Geology, 50/1, 47–57, doi:10.1556/CEuGeol.50.2007.1.4.

McClelland-Brown, E., (1984). Experiments on the intensity dependence on cooling rate. Geophys. Res. Lett., 11, 205–208.

McClelland, E., and J. C. Briden (1996). An improved methodology for Thellier-type paleointensity determination in igneous rocks and its usefulness for verifying primary thermoremanence. J. Geophys. Res. 101, 21995–22013.

McElhinny, M.W., and J. Lock (1996). IAGA paleomagnetic databases with Access. Surv. Geophys., 17, 575-591.

McFadden P. L., and F. J. Lowes (1981). The discrimination of mean directions drawn from Fisher distributions. Geophys. J. R. Astr. Soc., 67, 19–33.

McElhinny, M. W, and P. L. McFadden (1997). Palaeosecular variation over the past 5 Myr based on a new generalized database. Geophys. J. Int., 131, 240-252.

McElhinny, M. W., and P. L. McFadden (2000). Paleomagnetism: Continents and Oceans. Academic Press.

McElhinny, M. W., N. D. Opdyke,. and S. A. Pisarevsky (1998). Worldwide database for magnetostratigraphy available. EOS, Trans. Amer. Geophys. Union, 79, 167.

McGetchin, T. R., M. Settle, and B. A. Chouet (1974). Cinder cone growth modeled after Northeast Crater, Mount Etna, Sicily. Journal of Geophysical Research, 79, 3257–3272.

McRae, A. (1998). Radiometric Dating and the Geological Time Scale: Circular Reasoning or Reliable Tools? Radiometric Dating and the Geological Time Scale.

Merrill, R. T. (2010). Our Magnetic Earth: The Science of Geomagnetism. University of Chicago Press

Merril R. T., M. W. McElhinny, and P. L. McFadden (1996). The Magnetic field of the Earth, Paleomagnetism,the Core, and Deep Mantle. International geophysics series, 63.

Michalk, D. M., A. R. Muxworthy, H. N. Böhnel, J. Maclennan, and J. N. Nowaczyk (2008). Evaluation of the multispecimen parallel differential pTRM method: a test on historical lavas from Iceland and Mexico. Geophys. J. Int., 173, 409–420.

Michel-Tomè, R. C. (1981). Vulcanicity of Historic Times in the Middle Atlantic Islands. Bulletin of Volcanology, 44-1, 57-69.

Mitra, R., L. Tauxe, and S. K. Mcintosh (in press). Two thousand years of archeointensity from West Africa. Earth and Planetary Science Letters.

Moore, R. B. (1991). Geologic map of São Miguel, Azores. U.S. Geological Survey, Miscellaneous Investigations series, map I-2007, scale 1:50,000.

Moore, R. B., and M. Rubin (1991) Radiocarbon dates for lava flows and pyroclastic deposits on São Miguel, Azores. Radiocarbon, 33, 1, 151-164.

Moore, R. B., and F. A. Trusdell (1991). Geologic map of the lower east rift zone of Kilauea Volcano, Hawaii, U.S. Geol. Sur. Misc. Invest. Ser., Map 1-2225.

Nachasova, I. E., and K. S. Burakov (2009). Variation of the intensity of the Earth's magnetic field in Portugal in the 1st Millennium BC. Physics of the Solid Earth, 45(7), 595–603.

Nagata, T., Y. Arai, and K. Momose (1963). Secular variation of the geomagnetic total force during the last 5000 years. J. Geophys. Res., 68, 5277–5281.

Néel, N. (1955). Some theoretical aspects of rock magnetism. Abv. Phys., 4, 191-242.

Néel, L. (1949). Théorie du traînage magnétique des ferromagnéniques en grains fins avec applications aux terres cuites. Ann. Géophys., 5, 99–136.

Nicolaysen, L. O., J. W. L de Villiers, A. J. Burger, and F. W. E. Strelow (1958). New measurements relating to the absolute age of the Transvaal system and of the Bushveld igneous complex. Trans. Geol. Soc. S. Africa, 61, 137-163.

Noel, M., and C. M. Batt (1990). A method for correcting geographically separated remanence directions for the purpose or archaeomagnetic dating. Geophysical Journal International, 102, 753-756.

Oosthuyzen, E. J. (1964). 'n geochronologiese studie van sekere stollingsgesteentes net ouer en jonger as die sisteem. Waterberg. M.Sc. thesis, University of Pretoria.

Opdyke, N. D., and J. E. T. Channell (1996). Magnetic Stratigraphy. Academic Press.

Pacheco, J. M. (2001). Processos associados ao desenvolvimento de erupções vulcânicas hidromagmáticas explosivas na ilha do Faial e sua interpretação numa perspectiva de avaliação do Hazard e minimização de risco [PhD tesi]. Departamento de Geociências, Universidad dos Açores, Ponta Delgada, Portugal.

Pan, Y., J. Shaw, R. Zhu, and M. J. Hill (2002). Experimental reassessment of the Shaw paleointensity method using laboratory-induced thermal remanent magnetization. Journal of Geophysical Research, 107, B7.

Parrot, J. F. (2007). Tri-dimensional parameterization: an automated treatment to study the evolution of volcanic cones. Gèomorphologie: relief, processus, enviroment, 3, 247-257.

Paterson, G. A. (2010) Decisions, decisions: The selection of paleointensity data American Geophysical Union, Fall Meeting 2011, abstract #GP13A-08.

Pavòn-Carrasco, F. J., and V. Villasante Marcos (2010) Geomagnetic Secular Variation in the Canary Islands: paleomagnetic data, models and application to paleomagnetic dating. Fìsica de la Tierra, 22, 59-80.

Pavòn-Carrasco, F. J., M. L. Osete, J. M. Tor, and L. R. Gaya-Piquè (2009). A regional archeomagnetic model for Europe for the last 3000 years, SCHA.DIF.3K: applications to archeomagnetic dating. Geochemistry, Geophysics, Geosystems 10, Q03013, doi:10.1029/2008GC002244.

Pavòn-Carrasco, F. J., J. Rodríguez-González, M. L. Osete, and M. J. Torta (2011). A Matlab tool for archaeomagnetic dating. Journal of Archaeological Science, 38, 408-419.

Peitersen, M. N., and D. A. Crown (2000). Correlations between topography and intraflow width behavior in Martian and terrestrial lava flows. J. Geophys. Res., 105(E2), 4123–4134, doi:10.1029/1999JE001033.

Perrin, M., and E. Schnepp, (2004). IAGA paleointensity database: distribution and quality of the data set. Physics of the Earth and Planetary Interiors, 147, 255–267.

Perrin, M., E. Schnepp, and V. Shcherbakov (1998). Paleointensity Database Updated. EOS, 79, 198.

Pick, T., and L. Tauxe (1993). Geomagnetic palaeointensities during the Cretaceous normal superchron measured using submarine volcanic glass. Nature, 366, 238–242.

Pressling, N., C. Laj, C. Kissel, D. Champion, D. Gubbins (2006). Palaeomagnetic intensities from ^{14}C-dated lava flows on the Big Island, Hawaii: 0–21 kyr. Earth and Planetary Science Letters, 247, 26–40.

Pressling, N., F. A. Trusdell, and D. Gubbins (2009). New and revised ^{14}C dates for Hawaiian surface lava flows: Paleomagnetic and geomagnetic implications. Geophys. Res. Lett., 36, L11306, doi:10.1029/2009GL037792.

Prévot, M., and M. McWilliams (1989). Paleomagnetic correlation of Newark Supergroup volcanics. Geology, 17, 11, 1007-1010.

Priest, S. S., W. A. Duffield, K. Malis-Clark, J. W. Hendley, and P. H. Stauffer (2001). The San Francisco Volcanic Field, Arizona. U.S. Geological Survey Fact Sheet 017-01.

Principe, C., J. C. Tanguy , S. Arrighi , A. Paiotti, M. Le Goff, and U. Zoppi (2004). Chronology of Vesuvius activity from A.D. 79 to 1631 based on archeomagnetism of lavas and historical sources. Bull Volcanol, 66, 703–724. doi 10.1007/s00445-004-0348-8.

Quartau, R., F. Tempera, N. C. Mitchell, L. M. Pinheiro, H. Duarte, P. O. Brito, C. R. Bates, and J. H. Monteiro (2012). Morphology of the Faial Island shelf (Azores): The interplay between volcanic, erosional, depositional, tectonic and mass-wasting processes. Geochemistry, Geophysics, Geosystems, 13, 4, Q04012, doi:10.1029/2011GC003987.

Quidelleur, X., J. Carlut, P.-Y. Gillot and V. Soler (2002). Evolution of the geomagnetic field prior to the Matuyama–Brunhes transition: radiometric dating of a 820 ka excursion at La Palma. Geophys. J. Int., 151, F6–F10.

Quidelleur, X., P.-Y. Gillot, G. Filoche, and J.-C. Lefèvre (2005). Fast geochemical changes and rapid lava accumulation at Stromboli Island (Italy) inferred from K-Ar dating and paleomagnetic variations recorded at 60 and 40 ka. J. Volcanol. Geotherm. Res., 141, 177–193.

Riedel, C., G. G. J. Ernst, and M. Riley (2003). Controls on the growth and geometry of pyroclastic constructs. Journal of Volcanology and Geothermal Research, 127, 121–152, doi: 10.1016/S0377-0273(03)00196-3.

Riisager, P., and J. Riisager (2001). Detecting multidomain magnetic grains in Thellier palaeointensity experiments. Physics of the Earth and Planetary Interiors, 125, 111–117.

Riisager, J., P. Riisager, and A. K. Pedersen (2003). Paleomagnetism of large igneous provinces: case-study from West Greenland, North Atlantic igneous province. Earth and Planetary Science Letters, 214, 409-425.

Rolph, T. C., and J. Shaw (1986). Variations of the geomagnetic field in Sicily. Journal of geomagnetism and geoelectricity, 38, 1269– 1277.

Rolph, T. C., J. Shaw, and J. E. Guest (1987). Geomagnetic field variations as a dating tool: application to Sicilian lavas. Journal of Archaeological Science, 14 (2), 215-225, doi:10.1016/0305-4403(87)90008-2.

Rotolo, S. G., S. Scaillet, S. La Felice and G. Vita-Scaillet (2013). A revision of the structure and stratigraphy of pre-Green Tuff ignimbrites at Pantelleria (Strait of Sicily). Journal of Volcanology and Geothermal Research, 250, 61-74. http://dx.doi.org/10.1016/j.jvolgeores.2012.10.009,

Rutten, M. G., and H. Wensink (1960). Paleomagnetic dating, glaciations and the chronology of the Plio-Pleistocene in Iceland. Int. Geol. Congr., XXI Sess., Norden, Part IV 62.

Salgueiro, M. A. O. (1991). Estudo paleomagnètico e cronologia stratigrafica da fornações volcanicas da ilha de Santa Maria, Açores. Life and Earth Sciences, 9, 83-99.

Scaillet, S., S. G. Rotolo, S. La Felice, and G. Vita (2011). High-resolution $^{40}Ar/^{39}Ar$ chronostratigraphy of the post-caldera (b20 ka) volcanic activity at Pantelleria, Sicily Strait. Earth and Planetary Science Letters, 309, 280–290.

Scherbakova V. V., and V. P. Scherbakov (2000). Properties of partial thermoremanent magnetization in pseudosingle domain and multidomain magnetite grains. J. Geophys. Res., 105, 767–781.

Schweitzer, C., and H. C. Soffel (1980). Paleointensity measurements on postglacial lavas from Iceland. J. Geophys., 47, 57-60.

Self, S., R. S. J. Sparks, B. Booth and G. P. L. Walker (1974). The 1973 Heimaey Strombolian Scoria deposit, Iceland. Geological Magazine, 111, 539-548, doi:10.1017/S0016756800041583.

Selkin and L. Tauxe (2000). Long-term variations in palaeointensity. Phil. Trans. R. Soc. Lond. A 2000 358, 1065-1088, doi: 10.1098/rsta.2000.0574.

Selkin, P. A., J. S. Gee, and L. Tauxe (2007) Non linear thermoremanence acquisition and implications for paleointensity data. Earth and Planetary Science Letters, 256, 81–89.

Selkin, P. A., J. S. Gee, L. Tauxe, W. P. Meurer, and A. J. Newell (2000). The effect of remanence anisotropy on paleointensity estimates: a case study from the Archean Stillwater Complex. Earth Planet. Sci. Lett., 183, 403–416.

Sella, G., T. H. Dixon, and A. Mao (2002). REVEL: a model for recent plate velocities from space geodesy. Journal of Geophysical Research, 107(B4), 2081, doi:10.1029/2000JB000033.

Serralheiro, A., V. H. Forjaz, C. M. A. Alves, and B. Rodrigues (1989). Carta Vulcanológica dos Açores – Ilha do Faial, Scale 1:15 000, Sheets 1, 2, 3, and 4. Centro de Vulcanologia do INIC, Serviço Regional de Protecção Civil dos Açores and Univ. of Azores (Ed.), Ponta Delgada.

Shaar, R., H. Ron, L. Tauxe, R. Kessel, A. Agnon, E. Ben-Yosef, and J. M. Feinberg (2010). Testing the accuracy of absolute intensity estimates of the ancient geomagnetic field using copper slag material. Earth and Planetary Science Letters, 290 (1–2), 15, 201–213.

Shaar, R., H. Ron, L. Tauxe, R. Kessel, and A. Agnon (2011). Paleomagnetic field intensity derived from non-SD: Testing the Thellier IZZI technique on MD slag and a new bootstrap procedure. Earth and Planetary Science Letters, 310, 213–224.

Shaw, J. (1974). A new method of determining the magnitude of the palaeomagnetic field, application to five historic lavas and five archaeological samples. Geophys. J. R. Astron. Soc., 39, 133– 141.

Shaw, J., D. Walton, S. Ang, T.C. Rolph, and J.A. Share (1996). Microwave archaeointensity from Peruvian ceramics. Geophys. J. Int., 124, 241–244.

Shcherbakov, V.P., and V. V. Shcherbakova (2001). On the suitability of the Thellier method of paleointensity determination on pseudo-single-domain and multidomain grains. Geophys. J. Int. 146, 20–30.

Shcherbakova, V. V., V. P. Shcherbakov, and F. Heider (2000). Properties of partial thermoremanent magnetization in pseudosingle domain and multidomain magnetite grains. J. Geophys. Res., 105(B1), 767–781, doi:10.1029/1999JB900235.

Sherwood, G. J. (1991). Evaluation of a multi-specimen approach to paleointensity determination. J. Geomag. Geoelectr., 43, 341–349.

Silva, J. L. M. P. (2008). The arrival of the immigrants and how they were received. In: Goulart, T. (Ed.), Capelinhos, a Volcano of Synergies. Azorean Emigration to America. San Jose CA, Portuguese Heritage Publications of California, p. 137–144.

Silva, P. F., B. Henry, F. O. Marques, A. Hildenbrand, P. Madureira, C. A. Mèriaux and Z. Kratinovà (2012). Palaeomagnetic study of a subaerial volcanic ridge (São Jorge Island, Azores) for the past 1.3 Myr: evidence for the Cobb Mountain Subchron, volcano flank instability and tectonomagmatic implications. Geophys. J. Int, 1-20, doi: 10.1111/j.1365-246X.2011.05320.x.

Silva, P. F., B. Henry, A. Hildenbrand, P. Madureira, F. O. Marques, Z. Kratinová, and J. C. Nunes (2010). Spatial/temporal evolution of Faial's onshore volcanism (Azores Archipelago). Joint AGU Meeting, Foz de Iguassu.

Smirnov, A. V., J. A. Tarduno and B. N. Pisakin (2003). Paleointensity of the early geodynamo (2.45 Ga) as recorded in Karelia: A single-crystal approach. Geology, 31, 415-418.

Snowball, I., L. Zillén, A. Ojala, T. Saarinen, and P. Sandgren (2007). FENNOSTACK and FENNORPIS: Varve dated Holocene palaeomagnetic secular variation and relative palaeointensity stacks for Fennoscandia. Earth and Planetary Science Letters, 255, 106–116, doi:10.1016/j.epsl.2006.12.009.

Soler, V., Carracedo, J.C., and Heller, F. (1984). Geomagnetic secular variation in historical lavas from the Canary Islands: Geophysical Journal of the Royal Astronomical Society, 78, 313-318, doi:10.1111/j.1365-246X.1984.tb06487.x.

Sparks, R. S. J., S. Self, and G. P. L. Walker (1973). Products of ignimbrite eruptions. Geology, 1, 115-118.

Speranza, F., M. Pompilio, and L. Sagnotti (2004). Paleomagnetism of spatter lava from Stromboli volcano (Aeolian Islands, Italy): Implications for the age of paroxysmal eruption. Geophysical Research Letters, 31, L02607, doi:10.1029/2003GL018944.

Speranza, F., A. Di Chiara, and S. Rotolo (2012). Correlation of welded ignimbrites on Pantelleria (Strait of Sicily) using paleomagnetism. Bull. Volcanol., 74, 341-357.

Speranza, F., S. Branca, M. Coltelli, F. D'Ajello Caracciolo, and L. Vigliotti (2006). How accurate is ''paleomagnetic dating''? New evidence from historical lavas from Mount Etna. Journal of Geophysical Research, 111, B12S33, doi:10.1029/2006JB004496.

Speranza, F., Pompilio, M., D'Ajello Caracciolo, F., and Sagnotti, L. (2008). Holocene eruptive history of the Stromboli volcano: constraints from paleomagnetic dating. Journal of Geophysical Research, 113, B09101, doi:10.1029/2007JB005139.

Speranza, F., P. Landi, F. D'Ajello Caracciolo, and A. Pignatelli (2010). Paleomagnetic dating of the most recent silicic eruptive activity at Pantelleria (Strait of Sicily). Bulletin of Volcanology, 72, 847-858, doi: 10.1007/s00445-010-0368-5.

Stanton, T., P. Riisager, M.F. Knudsen, and T. Thoardrson, (2011). New paleointensity data from Holocene Icelandic lavas. Phys. Earth Planet. Inter., 186(1–2), 1–10, doi:10.1016/j.pepi.2011.01.006.

Stoner, J. S., J. E. T. Channell, C. Hillaire-Marcel, and C. Kissel (2000). Geomagnetic paleointensity and environmental record from Labrador Sea core MD95-2024: Global marine sediment and ice core chronostratigraphy for the last 110 kyr. Earth Planet. Sci. Lett., 183, 161–177.

Stoner, J. S., A. Jennings, G. B. Kristjánsdóttir, G. Dunhill, J. T. Andrews, and J. Hardardottir (2007). A paleomagnetic approach toward refining Holocene radiocarbon-based chronologies: Paleoceanographic records from the north Iceland (MD99–2269) and the east Greenland (MD99–2322) margins. Paleoceanography, 22, PA1209, doi:10.1029/ 2006PA001285.

Strong, M., and J. Wolff (2003). Compositional variations within scoria cones. Geology, 31, 2, 143–146.

Stuiver, M., Reimer, P.J., and Reimer, R.W. (2009). CALIB 6.0 program and documentation: http://calib.qub.ac.uk/calib (March 2012).

Tanaka, H., and M. Kono (1991). Preliminary results and reliability of palaeointensity studies on historical and ^{14}C dated Hawaiian lavas. J. Geomagn. Geoelect., 43, 375–388.

Tanaka, H., Kono, M., and Kaneko, S. (1995). Paleosecular variation of direction and intensity from two Pliocene-Pleistocene lava sections in Southwestern Iceland. J. Geomag. Geoelectr., 47, 89–102.

Tanaka H., Y. Hashimoto, and N. Morita, (2012). Palaeointensity determinations from historical and Holocene basalt lavas in Iceland. Geophys. J. Int., 189, 833–845 doi: 10.1111/j.1365-246X.2012.05412.x

Tanguy, J.C., and M. Le Goff (2004). Distorsion of the geomagnetic field in volcanic terrains: an experimental study of the Mount Etna stratovolcanos. Physic of the Earths and Planetary Interiors, 141, 59-70.

Tanguy, J. C., I. Bucur, and J. F. C Thompson (1985). Geomagnetic secular variation in Sicily and revised ages of historic lavas from Mount Etna. Nature, 318, 453-455.

Tanguy, J. C., M. Le Goff, C. Principe, S. Arrighi, V. Chillemi, A. Paiotti, S. La Delfa, and G. Patanè (2003). Archeomagnetic dating of Mediterranean volcanics of the last 2100 years: validity and limits. Earth and Planetary Science Letters, 211(1–2), 111–124.

Tanguy, J. C., M. Le Goff, S. Arrighi, C. Principe, S. La Delfa, and G. Patanè (2009), The History of Italian Volcanoes Revised by Archeomagnetism. Eos Trans. AGU, 90(40), 349, doi:10.1029/2009EO400001.

Tarduno, J. A., R. D., Cottrell, and A. V. Smirnov (2001). High geomagnetic field intensity during the mid-Cretaceous from Thellier analyses of single plagioclase crystals. Science, 291, 1779-1783.

Tarduno, J. A., R. D. Cottrell, and A. V. Smirnov (2006). The paleomagnetism of single silicate crystals: recording geomagnetic field strength during mixed polarity intervals, superchrons, and inner core growth. Rev. Geohys. 44, RG1002. doi:10.1029/2005RG000189.

Tarling, D. H. (1983). Palaeomagnetism: Principles and applications in geology, geophysics, and archaeology.

Tauxe, L. (1998). Paleomagnetic principles and practice, Kluwer acad., pp. 312.

Tauxe, L. (2009). Essentials of Paleomagnetism, University of California Press, Berkeley.

Tauxe, L., and H. Staudigel (2004). Strenght of the geomagnetic field in the Cretaceous Normal Superchron: New data from submarine basaltic glass of the Troodos Ophiolite. Geoch. Geoph. Geosyst., 5, 5, Q02H06. doi:10.1029/2003GC000635.

Tauxe, L., and T. Yamazaki (2007). Paleointensities, in Treatise on Geophysics, edited by M. Kono, Treatise on Geophysics, 5, 509– 563, Elsevier, New York.

Tauxe, L., H. Staudigel, and J. R. Wijbrans (2000). Paleomagnetism and $^{40}Ar/^{39}Ar$ ages from La Palma in the Canary Islands. Geochem. Geophys. Geosyst., 1(9), 1038, doi:10.1029/2000GC000063.

Tazieff, H. (1959). L 'èruption de 1957-1958 et la tectonique de Faial: Servicio Gèologico Portugal, Mem. n. 4, NIle Sèrie, p. 71-88.

Tazieff, H. (1977). An exceptional eruption: Mt. Nyiragongo, Jan. 10th,1977, Bull. Volcanol., 40, 189–200.

Thellier, E., and O. Thellier (1959). Sur l'intensité du champ magnétique terrestre dans la passé historique et géologique. Ann. Géophys., 15, 285 – 376.

Thompson, R., and G. Turner (1985). Icelandic Holocene paleomagnetism. Physics of the Earth and Planetary Interiors, 38, 250-261.

Thouret, L. C. (1999). Volcanic geomorphology – an overview. Earth-Sci. Rev., 47, 95–131.

Tilling, R. I. (1989). Volcanic hazards and their mitigation: progress and problems. Rev. Geophys., 27, 237–269.

Torsvik, T. H., R. D. Muller, R. Van der Voo, B. Steinberger, and C. Gaina (2008). Global plate motion frames: Toward a unified model. Rev. Geophys., 46, RG3004, doi:10.1029/2007RG000227.

Trippanera D., M. Porreca, J. Ruch, A. Pimentel, V. Acocella, J.M. Pacheco, Salvatore M. (in press). Relationships between tectonics and magmatism in a transtensive/transform setting: an example from Faial Island (Azores, Portugal). The Geological Society of America Bulletin.

Tsunakawa, H., and J. Shaw (1994). The Shaw method of paleointensity determinations and its application to recent volcanic rocks. Geophys. J. Int., 118, 781–787.

Turner, G., and R. Thompson (1981). Lake sediment record of the geomagnetic secular variation in Britain during Holocene times. Geophysical Journal of Royal Astronomical Society, 65, 703–725.

Turner, G., and R. Thompson (1982). Detransformation of the British geomagnetic secular variation record for Holocene times. Geophysical Journal of Royal Astronomical Society, 70, 789–792.

Urrutia-Fucuguachi, J., L. M. Alva-Valdivia, A. Goguitchaichvili, M. L. Rivas, and J. Morales (2004). Paleomagnetic, rock-magnetic and microscopy studies of historic lava flows from the Paricutin volcano, Mexico: implication for the deflection of paleomagnetic directions. Geophysical Journal International, 156, 431-442, doi:10.1111/j.1365- 246X.2004.02166.x.

Urrutia-Fucugauchi, J., A. Trigo-Huesca, and L. Pérez-Cruz, (2012). Magnetic links among lava flows, tuffs and the underground plumbing system in a monogenetic volcano, derived from magnetic and paleomagnetic studies. Physics of the Earth and Planetary Interiors, 212-213, 10–18.

Valentine, G.A., D. Krier, F.V. Perry, and G. Heiken (2005). Scoria cone construction mechanisms, Lathrop Wells volcano, southern Nevada, USA. Geology, 33, 8, 629–632, doi: 10.1130/G21459.1.

Valet, J. P., and V. Soler (1999). Magnetic anomalies of lava fields in the Canary Islands. Possible consequences for paleomagnetic records. Phys. Earth Planet. Inter., 115(2), 109–118.

Valet, J. P., and E. Herrero-Barvera (2000). Paleointensity experiments using alternating field demagnetization. Earth and Planetary Science Letters, 177, 43-58.

Valet, J. P. (2003). Time variations in geomagnetic intensity. Rev. Geophys., 41, 1–43.

Vezzoli, L., C. Principe, J. Malfatti, S. Arrighi, J. C. Tanguy, and M. Le Goff, (2009). Modes and times of caldera resurgence: The <10 ka evolution of Ischia Caldera, Italy, from high-precision archaeomagnetic dating. Journal of Volcanology and Geothermal Research, 186, 305-319.

Wadge, G. (1977). The storage and release of magma on Mount Etna. Journal of Volcanology and Geothermal Research, 2(4), 361–384.

Wadge, G., and R. M. C. Lopes (1991). The lobes of lava flow son Earth and Olympus Mons, Mars. Bull. Volcanol., 54,10–24.

Walker, G. P. L., R. F. Heming, and C. J. N. Wilson (1980). Low-aspect ratio ignimbrites. Nature, 283, 286-287.

Walker, G. P. L., Self, and P.C. Froggatt (1981). The ground layer of the Taupo Ignimbrite: a striking example of sedimentation from a Pyroclastic flow. Journal of Volcanology and Geothermal Research, 10, 1-11.

Walton, D., J. Shaw, J. Share, and J. Hakes (1992). Microwaved demagnetization. J. Appl. Phys., 7(1), 1549-1551.

Water, A. C., and Fisher, R. V. (1971). Base surges and their deposits: Capelinhos and Taal Volcanoes. Journal of Geophysical Research, 76, 23.

Wilson, C. J. N. (1986). Reconnaissance stratigraphy and volcanology of ignimbrites from Mangakino volcano. In: Smith, I. E. M. ed. Late Cenozoic volcanism in New Zealand. Royal Society of New Zealand Bulletin, 23, 179-193.

Wilson, C. J. N. (1993). Stratigraphy, chronology, styles and dynamics of late Quaternary eruptions from Taupo volcano, New Zealand. Philosophical Transactions of the Royal Society of London, A343, 205-306.

Wood, C. A. (1980). Morphometric evolution of cinder cones: Journal of Volcanology and Geothermal Research, 7, 387-413.

Xu, S., and D. J. Dunlop (1995). Theory of partial thermoremanent magnetization in multidomain grains. 2. Effect of microcoercivity distribution and comparison with experiment. J. Geophys. Res. 99, 9025–9033.

Xu, S., and D .J. Dunlop (2004). Thellier paleointensity theory and experiments for multidomain grains. J. Geophys. Res. 109, B07103. doi:10.1029/2004JB003024.

Yamamoto, Y., H. Tsunakawa, H. Shibuya, (2003). Palaeointensity study of the 1960 Hawaiian lava: implications for possible causes of erroneously high intensities. Geophys. J. Int. 153, 263–276.

York, D. (1966). Least-squares fitting of a straight line. Can. J. Phys., 44, 1079-1086.

Yu, Y., and L. Tauxe. (2005). Testing the IZZI protocol of geomagnetic field intensity determination. Geoch. Geoph. Geosyst., 6(5), Q05H17, doi: 10.1029/2004GC000840

Yu, Y., L. Tauxe, and A. Genevey (2004). Toward an optimal geomagnetic field intensity determination technique. Geoch. Geoph. Geosyst., 5(2), Q02H07, doi: 10.1029/2003GC000630.

Zanella, E. (1998). Paleomagnetism of Pleistocene volcanic rocks from Pantelleria Island (Sicily Channel), Italy. Physics of the Earth and Planetary Interiors, v. 108, p. 291-303.

Zbyszewski, G. (1960). L' eruption du Volcan de Capelinhos (Ille de Faial, Acores): Bulletin Volcanologique, 2, 23, 78–100.

Zbyszewski, G. (1963). Les phénomènes volcaniques modernes dans l'archipel des Açores: Comunicações dos Serviços Geológicos de Portugal, 47.

Zbyszewski, G., and O. da Veiga Ferreira (1959). Rapport de la deuxième mission gèologique sur le volcanisme de l'île de Faial: Servicio Geologico de Portugal, Mem., 4, NIle Sarie, 30-55.

Zijderveld, J. D. A. (1967). AC demagnetization of rocks: analysis of results: Runcorn SK, Creer KM, Collinson DW (eds). Methods in palaeomagnetism, Elsevier, Amsterdam, 254–286.

ACKNOWLEDGMENTS

First of all, I want to thank my advisor Dr. Fabio Speranza for the patience and dedication to my scientific growing up, he handed down his decennial experience in the field and the accuracy thoroughness to work.

A special thanks goes to Valentina B. for being a wonderful partner of my life since 2010 and lovely supporting me always, even when it was really hard to, waiting for me patiently during many work fields and helping me during (numerous) existential crisis and discouragement, thanks.

A special thanks goes also to my family; my grandmother who taught me to "fly", to love the nature and mountains, that "the attention is the base of the love", that "the night will pass throughout", and remembering every time that "exams do not finish ever, also at 95 years old". My father supported and supports me with special love and carefulness, I owe all to him; my mother noiselessly and with few straightforward words walks nearby and intermediates with whom I cannot see but they say He is very powerful. My two "little" brothers Cosimo and Guglielmo for loving me as a sister, for supporting and following me every time, also in my "bizarre idea" to try the way of the Research, looking at me as a benchmark (they did not understand that indeed it is the opposite!). Thanks to my aunts Giovanna and Matteo Collura for support me. I will never forget my extended part of the family, Ida La Porta, with her involving passion of school, militancy politic, and courage of the choice. A thought goes to Vita Lala. She left recently this Planet leaving here the vivid memory of her love for the deepest side of this life: the research of the truth.

During these three years of my PhD Studies, I had the opportunity to met very special collaborators and friends.

I would like to thank Silvio Rotolo for introducing me to the magic world of the Volcanology; during a immemorial field work at Pantelleria (June 2005) where I had the pleasure to meet and work also with my best friends Michela Costa and Andrea Di Piazza, with Sonia La Felice, and with Elisa Falcone and many other colleagues and friends from the University of Palermo, my hometown, working hard and drinking even harder (unforgivable Passito). A special thought goes to the Pantelleria Island, that with its magic atmosphere and beautiful outcrops influenced my scientific and personal life after the working field of June 2005, March and May 2009. Many thank to my friend Sergio Meraviglia who helped me studying outcrops and Helena A. M. for infecting me with her all-involving enthusiasm for science and life. From Palermo I also want to mention my friend Martina Oddo who always has interesting arguments on science and life, and passion for the nature, and with whom I share many memorable trekking as at Etna Volcano, Stromboli volcano, and Ragusa (south of Sicily).

During the work field in São Miguel (July 2010) in collaboration with CVARG and Massimiliano Porreca, I had the pleasure to share part of the work with my partner Valentina B.; she helped for sampling as also Andrea and Adriano Pimentel.

On January 2011, I met my new mentor, Prof. Lisa Tauxe, who taught me a lot about science, but above all she taught me the passion and the importance to be self-independent. During the period spent in San Diego, I had the chance to meet my new friends, Atreey and Ritayan, with whom I share the passion of red wines, coffees, good food and science.

I would like to thank Domenico D'Elia who gave an important help in sampling during the work field in Faial (July 2011) and also Francesca Mariani a very good friend of mine since the University years. Annamaria P. also collaborated with her accuracy in collecting data and field clue. During the years of the Roma Tre University I owe my outliving to my friends Giuditta Radeff, Francesca Mariani and Andrea Di Piazza, as well as all my climbing partners.

I also want to thank all the friend from the "pollaio": Enkelejda (Leda) Qamili and F. Javier Pavón-Carrasco two good friends and good scientists, which introduced me (bravely) to the mysterious (to me) world of the global geomagnetic field models and some letters indicating…, ehy guys what was the meaning of…?, and of course I cannot forget to mention and thank specially Catalina Hernandez Moreno, who started the PhD last years; we worked together during the dangerous work field in central Chile (March 2012), surrounded by active volcanoes, fearful mega-faults and super-hard rocks (augh!).

I want to dedicate this thesis to the memory of Dr. Nancy Romengo, colleague and friend, and to the Prof. Renato Funicello, passed away in August 2009, for be a mentor of my advisor Fabio. S, and the first to have introduced the paleomagnetism in Roma Tre.